ZooKeys 1048: 1–21 (2021)
doi: 10.3897/zookeys.1048.57493
https://zookeys.pensoft.net

RESEARCH ARTICLE

A peer-reviewed open-access journal
ZooKeys
Launched to accelerate biodiversity research

# A new species of *Procambarus* (Decapoda, Cambaridae) from the State of Querétaro, Mexico

Carlos Pedraza-Lara[1], Pedro Joaquín Gutiérrez-Yurrita[2], Vladimir Salvador De Jesus-Bonilla[1]

**1** *Ciencia Forense, Facultad de Medicina, Universidad Nacional Autónoma de México, Circuito de la Investigación Científica s/n, Ciudad Universitaria, Coyoacán, México City, México* **2** *Instituto Politécnico Nacional – Centro Interdisciplinario de Investigaciones y Estudios sobre Medio Ambiente y Desarrollo, México City, México*

Corresponding author: Carlos Pedraza-Lara (pedrazal@gmail.com)

Academic editor: L. E. Bezerra | Received 11 August 2020 | Accepted 21 October 2020 | Published 6 July 2021

*http://zoobank.org/B55DEC1A-6C1D-40CF-BB59-3BA3F84C3F6E*

**Citation:** Pedraza-Lara C, Gutiérrez-Yurrita PJ, De Jesus-Bonilla VS (2021) A new species of *Procambarus* (Decapoda, Cambaridae) from the State of Querétaro, Mexico. ZooKeys 1048: 1–21. https://doi.org/10.3897/zookeys.1048.57493

## Abstract

With a Nearctic distribution, the family Cambaridae harbors a high species richness in Mexico, which is also evident along the Pánuco River catchment. A series of surveys carried on in five populations from the Sierra Gorda Biosphere Reserve in the State of Querétaro resulted in localizing a putative new species for science. A molecular phylogenetic study and species delimitation analyses including all the known *Procambarus* species from the Pánuco River catchment were conducted based on three mitochondrial genes (16S rDNA, 12S rDNA, and COI; 2,462 bp in total). Phylogeny recovered all species as monophyletic, including the populations under study. All delimitation results based on barcoding, ABGD, GMYC, bPTP, and gonopod differentiation agree in the recognition of a new taxon, to which the name *Procambarus xihui* **sp. nov.** is given, and its diagnosis and description are provided. The new species can be distinguished from the remaining species in the genus, among other characters, by a unique configuration of the terminal elements of the first pleopod of form I male, which includes a central projection lamellate, hood-like, forming a concave blade-like structure mesially directed, as well as a caudal process crest-like, mesiodistally directed, forming a lateral side of the concavity.

## Keywords

Astacidea, Crayfish, integrative taxonomy, species delimitation, systematics

## Introduction

The genus *Procambarus* Ortmann, 1905 encompass 45 native species and subspecies occurring in Mexico, inhabiting both Atlantic and Pacific coasts. An important part of the species richness in Mexico inhabits the Pánuco water basin, along the Sierra Madre Oriental and north of the Trans Mexican Volcanic Belt. To date, seven species have been recorded from that region: *Procambarus cuevachicae* (Hobbs, 1941), *P. hidalgoensis* López-Mejía, Álvarez & Mejía-Ortíz, 2005, *P. roberti* Villalobos & Hobbs, 1974, *P. strenthi* Hobbs, 1977, *P. toltecae* Hobbs, 1943, *P. villalobosi* Hobbs, 1969, and *P. xilitlae* Hobbs & Grubbs, 1982. In a survey of the diversity of the genus, previous studies located a series of populations from the aforementioned basin, in the Sierra Gorda Biosphere Reserve, at the northern side of the State of Querétaro, whose specific identity could not be confirmed (Gutiérrez-Yurrita et al. 2002). Analyses by the authors found a degree of morphological distinctiveness compared to other species of the genus from nearby regions while additional studies obtained the 16S rDNA gene from several of them. Later, a study using Random Amplification of Polymorphic DNA and morphological information agreed with the conclusion that several populations from the Sierra Gorda Biosphere Reserve could correspond to an undescribed species (Pedraza-Lara et al. 2004). It is necessary to verify such findings, and to formalize the taxonomic status of such populations (see Materials and methods). Consequently, this article aims to clarify this taxonomic situation using an integrative approach, including molecular markers commonly used for the delimitation of crayfish species in addition to traditional morphology.

## Materials and methods

### Sampling

A series of collections were made in the Sierra Gorda Biosphere Reserve (**SGBR**) for 20 years, beginning in 2002 (Table 1; Fig. 1). This study includes the following populations assigned to the new species from the counties Jalpan de Serra and Landa de Matamoros in the state of Querétaro: Arroyo Álamos, Arroyo Camelinas, Río Verdito, San Juanito and Saldiveña. All were sampled in 2002, 2007, and 2019 by the collectors mentioned in Systematics. For the localities of San Juanito and Saldiveña we failed to obtain any crayfish in 2019. Other populations sampled more than once were Palitla (2002, 2019), Media Luna (2007, 2015, 2019), Santa Anita spring (2012, 2018), and Xicotepec (two occasions in 2019). Specimens were collected by hand and identified using the available keys (Hobbs 1972a), original descriptions, and reviews (Hobbs 1941, 1943, 1977; Villalobos 1944, 1955, 1958; Villalobos-Figueroa 1954; Villalobos Figueroa and Hobbs 1974; López-Mejía et al. 2005). Details of the collection sites are provided in Table 1. Type material was deposited at the following Institutions: National Collection of Crustaceans, Institute of Biology, Universidad Nacional

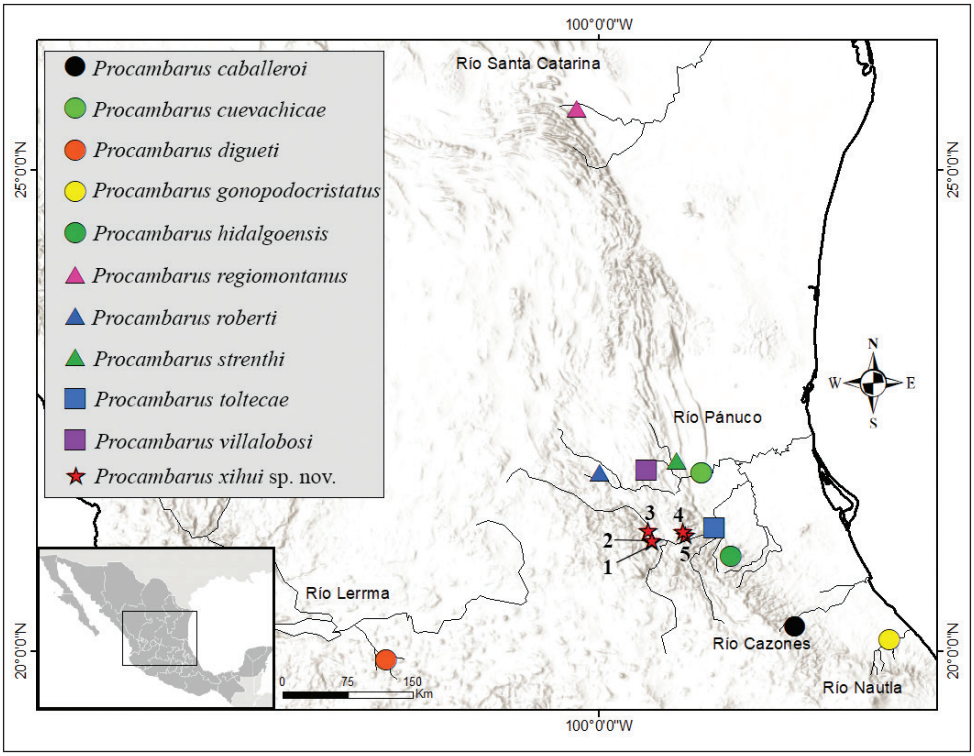


**Figure 1.** Map of localities. Populations from SGBR are depicted as stars, and numbers correspond to the following sites: 1. Arroyo Los Álamos; 2. Arroyo Camelinas; 3. Saldiveña; 4. Río Verdito; 5. San Juanito.

Autónoma de México (**CNCR**); National Museum of Natural History, Smithsonian Institution, USA (**NMNH**) and Arthropod Collection of Forensic Reference at Forensic Program, UNAM, Mexico (**CARF**). The holotype (CNCR 35721), allotype (CNCR 35723), and morphotype (CNCR 35722) were deposited at CNCR. Paratype series (one male form I, and one female, under catalog number USNM 1638484 and USNM 1638485, respectively) were deposited at NMNH. Additional paratypes were deposited at CARF under catalog numbers CARF – CPLC45 – CARF – CPLC47. Measurements of the types are provided in Table 2.

Aiming to account for an accurate representation of Mexican species of *Procambarus*, except for the troglobitic *Procambarus xilitlae*, all the species previously assigned to the subgenus *Ortmannicus* (Hobbs 1972b) were included: *P. acutus*, *P. caballeroi*, *P. cuevachicae*, *P. gonopodocristatus*, *P. hidalgoensis*, *P. toltecae*, and *P. villalobosi*. In addition, *P. digueti* and *P. regiomontanus* were included as outgroups for phylogenetic analysis and reference in species delimitation (Table 1). Voucher numbers were assigned to all specimens and included in CARF (UNAM). Laboratory work was carried on in the Forensic Entomology Lab, Forensics Program, at UNAM.

Specimens were identified using the appropriate taxonomic keys (Hobbs 1972a; Bezerra et al. 2020), as well as the respective taxonomic descriptions. Measurements

of type specimens were made on standard morphological characters used in crayfish taxonomy (Pedraza-Lara and Doadrio 2015). For paired characters, measurements were taken from the left side of the specimen with a digital caliper (Mitutoyo's Absolute Series 500, resolution: 0.01 mm) and a stereoscopic microscope (Leica M60 APO). A validation procedure was done by measuring the same randomly chosen individuals three times. A Pearson correlation between replicates was done in which values above 0.8 were considered as indicatives of low measurement error. This was verified and all measurements, which showed values above 0.8. Drawings from type series for description were prepared by direct observations using a caliper and a stereoscopic microscope (Leica M60 APOP) by Aslam Narvaez. Additionally, SEM pictures were taken from gonopods, epistome, and antennal scale of holotype, as well as annulus ventralis from allotype, at the Electronic Microscopy Laboratory, IBUNAM.

## Phylogenetic and species delimitation analysis

Specimens were preserved in ethanol and a piece of abdominal muscle was taken for DNA purification, which was carried on using a phenol-chloroform protocol (Sambrook et al. 1989). Three mitochondrial genes were sequenced: 16S rDNA (16S), 12S rDNA (12S), and Cytochrome Oxidase subunit I (COI). These genes have accurate phylogenetic signal in crustaceans and are considered optimal choices to characterize the genetic variation and species delimitation in crustacean groups (Toon et al. 2009; Matzen da Silva et al. 2011; Pedraza-Lara et al. 2012). PCR amplifications using gene-specific primers were done using primers and following conditions previously standardized on cambarid species delimitation (Pedraza-Lara and Doadrio 2015) (see Table 3 for details on amplifications and genes analyzed). Amplifications were carried out in 10 mL reactions containing: 1X PCR buffer, 0.5 mM of each primer, 0.2 mM of each dNTP, 1.5 mM MgCl2, 1 U Platinum Taq polymerase (Thermo), and 10–50 ng of template DNA.

To investigate the species limits between the putatively undescribed taxon and other *Procambarus* species with molecular information we used the following approaches: genetic divergence of the barcoding COI gene (Hebert et al. 2003), the Automatic Barcode Gap Discovery (ABGD) (Puillandre et al. 2012), Bayesian Tree Poisson Process (bPTP) (Zhang et al. 2013), and the General Mixed Yule Coalescent model (GMYC) (Pons et al. 2006). Barcoding and ABGD analyses were carried using the COI gene; input for bPTP and GMYC was a concatenated matrix with the three mitochondrial markers.

The uncorrected *P*-distances and standard error of the COI marker between putative species were calculated in Mega 10.1.8, estimating standard error based on bootstrapping (Kumar et al. 2018). To determine the barcode gap, the ABGD analysis was run online (https://bioinfo.mnhn.fr/abi/public/abgd/abgdweb.html) setting the simple distance (relative gap width) to 0.5, and default values for the remaining parameters.

For the GMYC approach, an ultrametric tree was reconstructed in Beast 2.6.2 (Bouckaert et al. 2014) using the GTR + Γ + I model, a relaxed clock lognormal, and Yule model prior. Bayesian Markov chain Monte Carlo was run for 25 million

generations, sampling trees every 1,000 generations. The log file was inspected in Tracer 1.7.1 (Rambaut et al. 2018) to confirm convergence and Effective Sample Size (ESS) ≥ 200. A single maximum credibility tree was summarized with TreeAnnotator v2.6.2 after removing 15% of the trees as burn-in. The resulting tree was used as input to delimit species with the single threshold GMYC approach in the package 'splits' implemented in R (http://r-forge.r-project.org/projects/). The bPTP analysis was performed online (https://species.h-its.org/ptp/) using a ML phylogenetic tree as input (see below), the analysis was run 100,000 MCMC generations with burn-in of 15%.

A phylogenetic hypothesis regarding the included specimens of *Procambarus* species was reconstructed with Maximum Likelihood (ML) and Bayesian Inference (BI) methods. These analyses were carried out to evaluate the congruence of the delimitation analyses previously mentioned with the formation of monophyletic clades at the terminals and evaluate its clade support. Conformation to monophylly is also another way to assist during taxon recognition (Rosen 1979; Donoghue 1985). The ML reconstruction was conducted in RAxML 8.2.12 (Stamatakis 2014) with a rapid bootstrap algorithm (-f a) with 1000 bootstrap replicates. For the BI method, the appropriate substitution model for each marker was inferred with Partition Finder 2 (Lanfear et al. 2017). The BI reconstruction was conducted in MrBayes 3.2.7a (Ronquist and Huelsenbeck 2003). We ran two runs with four MCMC chains with 50,000,000 generations, sampling every 1000 generations and setting a burn-in of 10%. Convergence of chains and ESS (> 200) were confirmed in Tracer 1.7.1 (Rambaut et al. 2018).

It has been described that habitats in the SGBR face important threats like increasing drying (Mendoza-Villa et al. 2018), the cutting of forests, introduction of exotic species, destruction of habitat for agriculture and grazing, pollution of water and the alteration of river channels for human activities (Gutiérrez-Yurrita 2014). Considering this, an assessment of the extinction risk was done using the International Union for Conservation of Nature (IUCN) Red List of Threatened Species Categories and Criteria (IUCN Standards and Petitions Committee 2019). IUCN criteria were applied to the crayfish populations inhabiting the SGBR.

The data underpinning the analysis reported in this paper are deposited at GBIF, the Global Biodiversity Information Facility, and are available at https://doi.org/10.15468/3hu4bh.

## Results

In all cases, morphological features were congruent and stable when several form I male specimens were available for one species. No issues were evident when separating and identifying species according to the literature. As usual in *Procambarus*, the morphology of the first pair of pleopods of male form I was useful to identify and distinguish the new species, as the structure of terminal elements was always congruent with what was originally described and allowed robust species identification. Accordingly, a series of unique traits were observed for the populations from the SGBR.

**Table 1.** Species, locality data, and GenBank accession numbers of specimens used in the phylogenetic and species delimitation analyses.

| Species | Locality | Specimen | Collection year | GenBank accession numbers | | |
|---|---|---|---|---|---|---|
| | | | | 16S | 12S | cox1 |
| *Procambarus xihui* sp. nov. | Arroyo de Los Álamos, Yerbabuena, Jalpan de Serra, Querétaro * | CPLC1† | 2019 | MW280269 | MW280231 | MW266807 |
| | Arroyo de Los Álamos, Yerbabuena, Jalpan de Serra, Querétaro * | CPLC23‡ | 2019 | MW280277 | MW280238 | MW266814 |
| | Arroyo Camelinas, Yerbabuena, Querétaro | CPLC27 | 2002 | MW280280 | MW280242 | MW266816 |
| | San Juanito, Landa de Matamoros, Querétaro | CPLC24 | 2002 | – | MW280239 | – |
| | Río Verdito, Landa de Matamoros, Querétaro | CPLC25 | 2019 | MW280278 | MW280240 | – |
| | Saldiveña, Jalpan de Serra, Querétaro | CPLC26 | 2007 | MW280279 | MW280241 | MW266815 |
| *P. toltecae* | Stream 1 Km Soutwest of Palitla, San Luis Potosí* | CPLC3 | 2019 | MW280270 | MW280246 | MW266808 |
| | Stream 1 Km Soutwest of Palitla, San Luis Potosí* | CPLC28 | 2019 | MW280281 | MW280243 | MW266817 |
| | Huichihuayán, San Luis Potosí** | PopHui | 2012 | JX127823 | JX127687 | JX127966 |
| *P. hidalgoensis* | Stream on driveway from Tlanchinol-Olotla, Hidalgo | CPLC5 | 2019 | MW280272 | MW280233 | MW266810 |
| | Stream on driveway from Tlanchinol-Olotla, Hidalgo | CPLC29 | 2019 | MW280282 | MW280244 | – |
| *P. villalobosi* | Cave East of Rayón, San Luis Potosí* | CPLC11 | 2019 | MW280274 | MW280235 | MW266812 |
| *P. villalobosi* | Cave East of Rayón, San Luis Potosí* | CPLC33 | 2019 | MW280285 | – | MW266820 |
| *P. gonopodocristatus* | María de la Torre, Veracruz* | CPLC30 | 2019 | MW280283 | – | MW266818 |
| | María de la Torre, Veracruz* | CPL2474 | 2019 | MW280268 | MW280230 | – |
| *P. roberti* | Creek coming from La Media Luna, 0.5 Km East, San Luis Potosí* | CPLC13 | 2019 | MW280276 | MW280237 | – |
| *P. roberti* | Creek coming from La Media Luna, 0.5 Km East, San Luis Potosí* | CPLC32 | 2007 | MW280284 | MW280245 | MW266819 |
| *P. roberti* | –*** | roberti1 | – | KX238070 | – | – |
| *P. strenthi* | Santa Anita spring, San Luis Potosí* | CPLC10 | 2018 | MW280273 | MW280234 | MW266811 |
| | –*** | strenthi1 | 2017 | KX238078 | – | – |
| *P. caballeroi* | Stream southern of Xicotepec de Juárez, Puebla* | 2419 | 2019 | MW280265 | MW280226 | MW266803 |
| | Stream southern of Xicotepec de Juárez, Puebla* | 2420 | 2019 | MW280266 | MW280227 | MW266804 |
| | –*** | Pcb302 | – | KX238005 | – | – |
| *P. cuevachicae* | La Cueva Chica, Ciudad Valles, San Luis Potosí* | 2424 | 2020 | – | MW280228 | MW266805 |
| | La Cueva Chica, Ciudad Valles, San Luis Potosí* | 2425 | 2020 | MW280267 | MW280229 | MW266806 |
| *P. acutus* | Canal en Ciudad Mante, Tamaulipas | 3952 | 2007 | MW280264 | – | MW266802 |
| | Canal en Ciudad Mante, Tamaulipas** | PopMan | 2007 | JX127827 | – | JX127970 |
| *P. digueti* | Camécuaro River, Michoacán | CPLC12 | 2012 | MW280275 | MW280236 | MW266813 |
| *P. regiomontanus* | Guadalupe, Nuevo León | CPLC4 | 2018 | MW280271 | MW280232 | MW266809 |
| | *** | DJ43 | 2018 | KX238068 | KX238138 | KX238224 |

* Type locality; ** from Pedraza-Lara et al. 2012; *** from Stern et al. 2017; † holotype; ‡ allotype.

## Species delimitation and phylogenetic analyses

The following gene fragments were obtained: 16S (559 bps), 12S (397 bps), and COI (1506 bps), resulting in 2462 characters and giving a series of substitution models (Table 3). The resulting sequences were deposited in GenBank (Table 1), no signs of numts were found. The most variable fragment was 16S, followed by 12S and COI (variable sites: COI = 221/1506, 16S = 169/559 12S = 71/397); besides this, COI showed the highest proportion of parsimony-informative (PI) sites: COI = 138, 16S = 82, 12S = 51 (Table 3).

All delimitation analyses recovered a congruence between morphological identifications and molecular information for all species (Fig. 2; Suppl. material 1). The populations from SGBR are delimited as one distinct species according to all delimitation criteria, including the morphological observations carried on over specimens sampled. The COI genetic *P*-distance between all localities of the SGBR and the other species

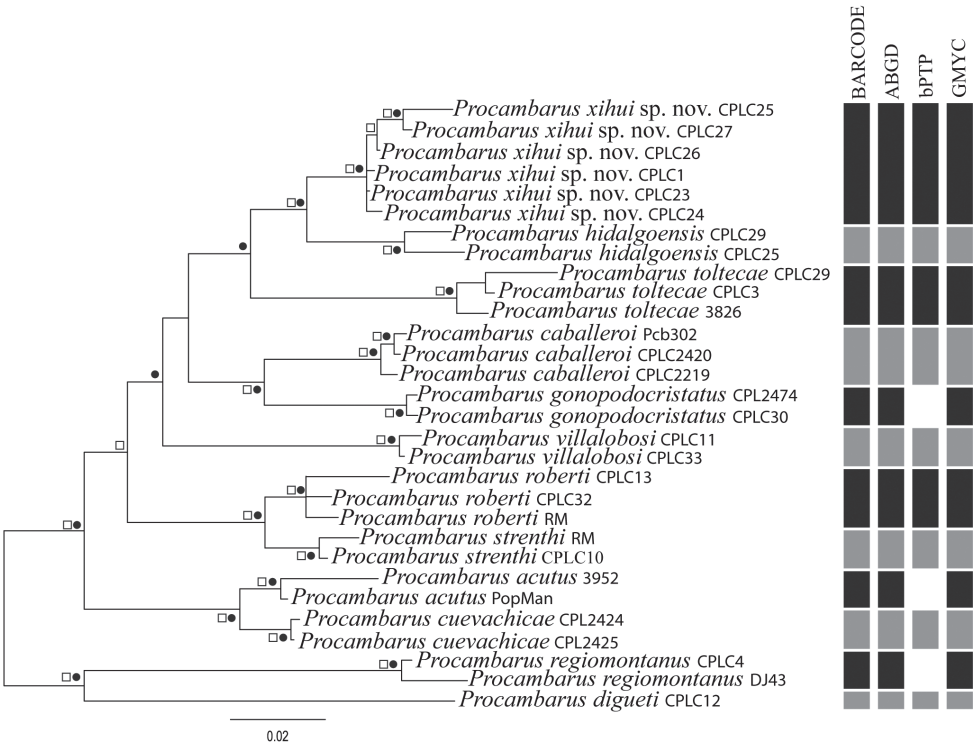


**Figure 2.** Phylogenetic tree of species analyzed. Codes are referred to in Table 1. BI and ML topologies were completely congruent. Support values of 95 or more (BI) and of 70 or more (ML) are depicted with figures above nodes; circles = posterior probabilities, squares = bootstrap support. At right, recovery of species delimited according to each of the four delimitation criteria used.

of *Procambarus* ranges from a minimum of $D_p$ = 3% for that observed with *Procambarus hidalgoensis*, and a maximum of $D_p$ = 10.6% of with *Procambarus regiomontanus* (Suppl. material 2: Table S1). Such values are above D = 1% and above what is common for between-species distances in crustaceans and crayfish (Fetzner and Crandall 2002; da Silva et al. 2011).

Congruently, the ABGD analysis recovered the undescribed taxon as a separate species from other *Procambarus* species. The bPTP and GMYC species delimitation analyses separate sequences of such populations as a distinct taxon; GMYC confirms the latter observation as well as the specific status of the remaining *Procambarus* species (Fig. 2). With the most supported partition scheme of bPTP analysis, all specimens assigned to *Procambarus gonopodocristatus*, *P. acutus*, and *P. regiomontanus* were not supported as forming one species each; however, the estimated number of species considered by bPTP is between 10 and 26, which includes the scheme of species delimited by the other methods. Bayesian inference and maximum likelihood topologies were congruent (Fig. 2). Topology recovered all species as monophyletic in highly supported clades. One clade included *Procambarus acutus* and *Procambarus cuevachicae*; next, a

clade is recovered containing the remaining species from the Pánuco basin except for *Procambarus caballeroi* and *Procambarus gonopodocristatus*, inhabitants of distinct basins south of the Trans Mexican Volcanic Belt (TMVB). Inside this clade, the populations from SGBR were included in a clade in a sister relationship to *P. hidalgoensis*. These both form a clade close to populations of *P. toltecae*. In the light of these results, a new species is described which includes populations analyzed from the SGBR.

Regarding the conservation assessment, in total, five populations for the species were recorded: populations from Álamos and Camelinas fall into one single 5–10 km$^2$ quadrant, and Saldiveña, Río Verdito, and San Juanito each falls into their own 5 km$^2$ quadrant. This resulted in a maximum area of occupancy of 25–35 km$^2$. However, this would be extremely inaccurate, as the available area of habitat (small streams, probably fragmented by large-magnitude creeks) is much more reduced inside each quadrant. Consequently, we consider that a gross estimation of area of occupancy for the species would fall in less than 5 km$^2$. Considering the factors aforementioned, we found a conservation status for *Procambarus xihui* of Critically Endangered (CR) based on the following criteria: B.2.*a* (habitat severely fragmented), B.2.*b.ii* (continuing decline in area of occupancy), and B.2.*b.iv* (continuing decline in number of locations).

## Systematics

**Cambaridae Hobbs, 1942**
**Genus *Procambarus* Ortmann, 1905**

***Procambarus xihui* sp. nov.**
http://zoobank.org/DCFCDB8F-896F-4071-8CB6-12D6241FE9DB
Figures 3, 4, Table 2

**Material examined. *Holotype*:** male from I (CNCR 35721), 21°8.548'N, 99°17.106'W, ca 1210 m; stream Los Álamos, Yerbabuena, Jalpan de Serra, Querétaro State, Mexico. A small headwater first-magnitude stream, which keep water in shallow ponds along the year. leg. Heriberto Pedraza Rodríguez, Patricia Ornelas-García, Carlos Pedraza-Lara, Ma. Guadalupe Lara Zúñiga, Guadalupe Gracia, Regina Pedraza Lara, May 22, 2019. ***Allotype*:** female (CNCR 35723), same data as holotype. ***Morphotype*:** male (CNCR 35722), same data as holotype.

**Diagnosis.** Body pigmented, eyes well developed. Rostrum lanceolate, concave, without lateral spines; antennal scale width 0.50–0.54 × in its length; areola of moderate width (0.22–0.23 × wide in length) with 2–4 large punctations in narrowest part; cervical spine absent, single, shallow branchiostegal spine; chela shorter than cephalothorax length, long and thin, length 0.87–0.89 × the length of cephalothorax and 0.28–0.31 × wide than long, narrow-ovate. Dactyl forming a concave profile in mesial margin, palm of chela with scattered tubercles, mesial surface with row of seven or eight tubercles, palm length 0.55–0.66 × in dactyl length; no lateral spines on carapace; postrostral ridges very strong and wide, forming a strong tubercle, provided with longitudinal groove along its

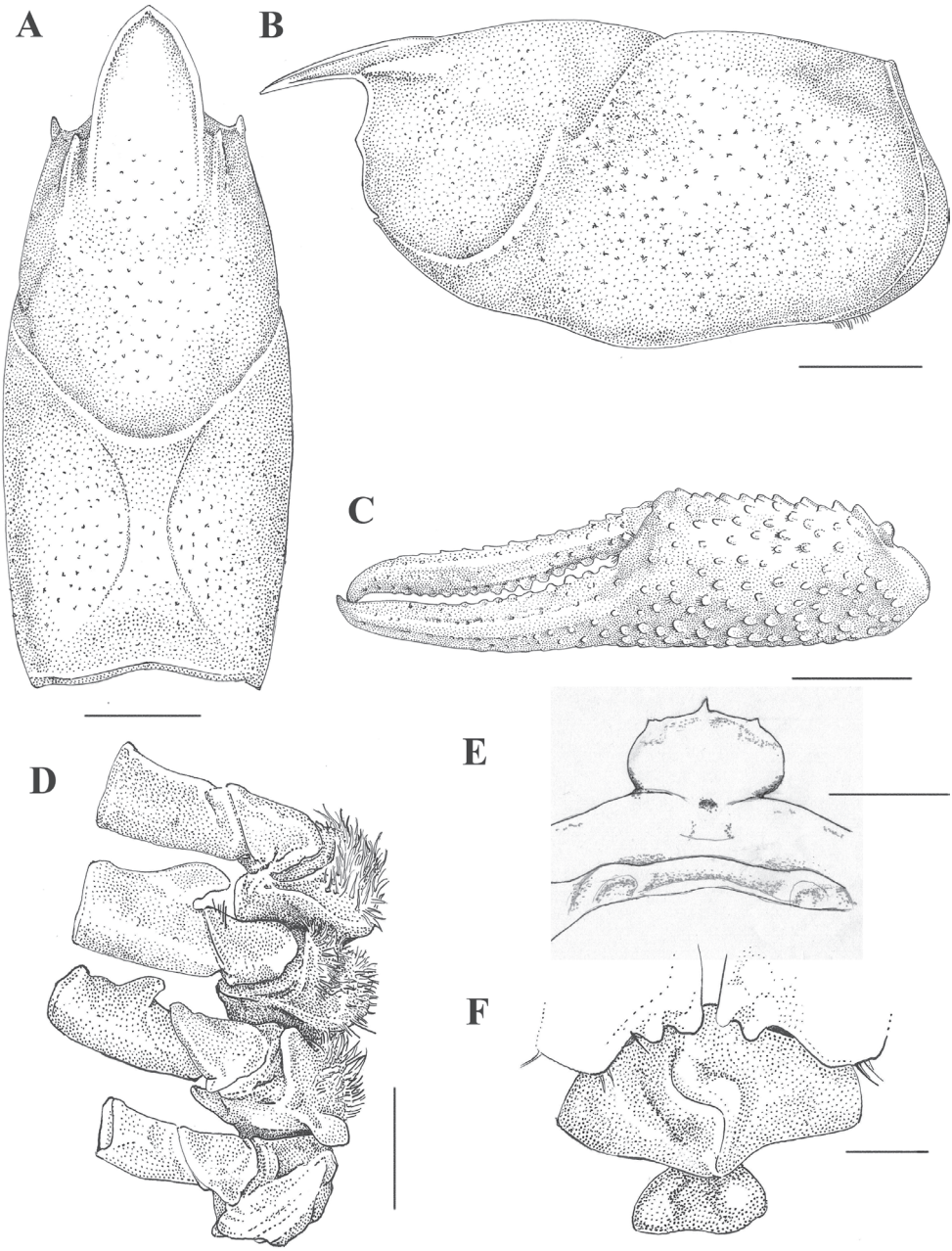


**Figure 3.** *Procambarus xihui*. All illustrations from holotype except for F which is from allotype **A** dorsal view of cephalothorax **B** lateral view of cephalothorax **C** lateral view of cheliped **D** basal podomeres of second to fifth pereiopods **E** Epistome **F** caudal view of annulus ventralis. Scale bars: 5 mm (**A–C**); 2 mm (**D–F**).

laterodorsal margin, its apical extreme slightly overreaching carapace surface, not forming evident apical spine. Male with hooks on ischiopodites of the third and fourth pairs of pereiopods, those on third ischiopodite extending beyond basioischial articulation.

First pair of pleopods slightly asymmetrical, reaching coxopodite of third pereiopod, with shoulder on cephalic margin beginning at distal fifth; a row of setae from base to second third of pleopod, a second row of setae along mesial surface starting at mid-length and third row of setae along mesial surface starting on last quart and extending laterally to base of terminal processes, where it forms a tuft of plumose setae; mesial process spiniform, directed caudally and slightly mesially, cephalic process spiniform, acute, hood-like, directed caudomedial, upon central projection and hidden beneath apical tuft; central projection corneous, lamellate, hood-like, tip decidedly projecting mesially, forming a concave blade-like structure, distally folded in mesial direction and reaching beyond the remaining terminal elements; caudal process corneous, crest-like, running on caudomesial surface of pleopod tip, along longitudinal pleopod axis, mesiodistally directed, forming a lateral side of the concavity formed distally by the central projection, reaching bellow point of mesial process position in lateral view.

Preanular plate with strong tubercles in caudal margin, and with setae along its margin, both well projecting over annulus cephalic area. Annulus ventralis rather fusiform, with depression along median surface and sinus in shallow Z-shape. Endopodite and exopodite of uropods with strong distolateral spines and median ridge ending in small spine, not reaching endopodite margin.

**Description of holotypic male, Form I.** (Figs 3, 4, Table 2). Body pigmented, eyes well developed. Body subovate, abdomen narrower than thorax. At cervical groove carapace slightly higher than wide (0.99 × height). Areola moderate in width (0.22 × length) with three or four punctations in narrowest part; length of areola ca. 0.32 × that of entire carapace length. Rostrum lanceolate, dorsally excavated, reaching distal third of second basal segment of antennule, its width 0.69 × in length; margins raised slightly thickened, acumen not sharped, dorsal surface of rostrum punctuated at its base, row of setiferous punctations along base of marginal ridges, subrostral ridges poorly developed, and not evident from dorsal view.

Postrostral ridges conspicuous and wide, forming a strong tubercle, provided with longitudinal groove along its laterodorsal side, its apical edge slightly overreaching carapace surface, not forming evident apical spine. Suborbital angle obtuse, one branchiostegal spine present. Surface of the carapace deeply punctuate.

Epistome broadly triangular, subsymmetrical, with cephalomedian projection well defined. Antennule with ventral spine on basal segment well developed. Antennal scale width 0.5 × its length, maximum width at ca. 0. 5 × length, with a ridge along lateral margin ending in a strong spine.

Chela long and thin, 0.89 × the length of carapace and 0.31 × wide as long, narrow-ovate, dactyl forming a concave profile in mesial margin. Chela scattered with numerous setose tubercles and crowded with numerous denticles. Mesial margin of palm with row of seven tubercles, opposable sides of both fingers with strong tubercles, seven stronger on proximal half of dactyl. Fingers gaping along their length. Lateral margin of dactyl with weak ridge of acute tubercles proximally and punctations distally. Tip of fingers forming strong pencils. Opposable margin of fixed finger with four tubercles on basal one-quarter and five punctations along second and third distal quarters.

**Table 2.** Measurements of types. Morphometric measurements (mm) of holotype, allotype, and morphotype of *P. xihui* sp. nov.

| Measurements | Holotype | Allotype | Morphotype |
|---|---|---|---|
| Total Length (TL) | 59.80 | 61.41 | 65.68 |
| Cephalothorax | | | |
| Length (CL) | 28.89 | 28.99 | 32.15 |
| Height (CH) | 13.91 | 14.11 | 15.63 |
| Width (CW) | 13.71 | 13.99 | 15.26 |
| Cephalon length (CEL) | 18.95 | 19.75 | 21.29 |
| Abdomen width (AW) | 12.08 | 11.82 | 13.21 |
| Rostrum | | | |
| Length (RL) | 7.26 | 7.18 | 8.60 |
| Width (RW) | 4.85 | 5.59 | 5.65 |
| Acumen length (AL) | 1.39 | 1.03 | 1.77 |
| Antennal scale length (ASL) | 6.11 | 6.41 | 6.86 |
| Cheliped | | | |
| Chela length (CHL) | 25.75 | 19.22 | 27.82 |
| Chela width (CHW) | 8.02 | 5.98 | 7.84 |
| Dactyl length (DL) | 14.50 | 11.30 | 16.01 |
| Palm length (PL) | 9.56 | 7.12 | 8.81 |
| Merus length (ML) | 13.13 | 11.38 | 13.32 |
| Areola | | | |
| Areola width (ARW) | 9.12 | 8.79 | 10.56 |
| Areola length (ARL) | 2.00 | 2.05 | 2.51 |

**Table 3.** Variability parameters of analyzed gene fragments and the most accurate substitution models.

| Gene | Primers* | bp | V | PI | Model** |
|---|---|---|---|---|---|
| 16S | 1471 | 559 | 169 | 82 | GTR+G |
| | 16S-1472 | | | | |
| 12S | 12sf | 397 | 71 | 51 | GTR+I+G |
| | 12sr | | | | |
| COI | ORCO1F | 1506 | 221 | 138 | GTR+I+G |
| | ORCO1R | | | | |

bp = length in base pairs; V = variable sites; PI = parsimony informative sites; * amplification conditions followed Pedraza-Lara et al. 2012; ** most appropriate substitution model selected using Partition Finder 2.

Width of carpus of first pereiopod ca. 0.63 × in its length. Merus length 0.45 × in cephalothorax length, with scattered punctations in lateral surface, two rows of spike-like tubercles on mesial surface, stronger at distal half, apical spine present. Hooks on ischiopodites of third and fourth pereiopods, former well exceeding basioischial articulation, latter reaching it. Bases of coxopodites of fourth and fifth pereiopods with caudomesial boss projection, the former extending on wide prominence on caudoventrally surface, caudomedial oriented, setose around margin, the latter blade-like, mesially oriented, bare.

**First pleopods as described in diagnosis.** Abdomen slightly narrower than carapace, width 0.88 × in cephalothorax width. Protopodite of uropods with distolateral spines, endopodite and exopodite with strong distolateral spines and median ridge ending in small spine, not reaching endopodite margin. Dorsal side of telson with one median spine on each caudolateral corner.

**Description of allotypic female.** (Fig. 3, Table 2). Differing from holotype in following respects: areola of moderate width (0.23 × length) with two or three

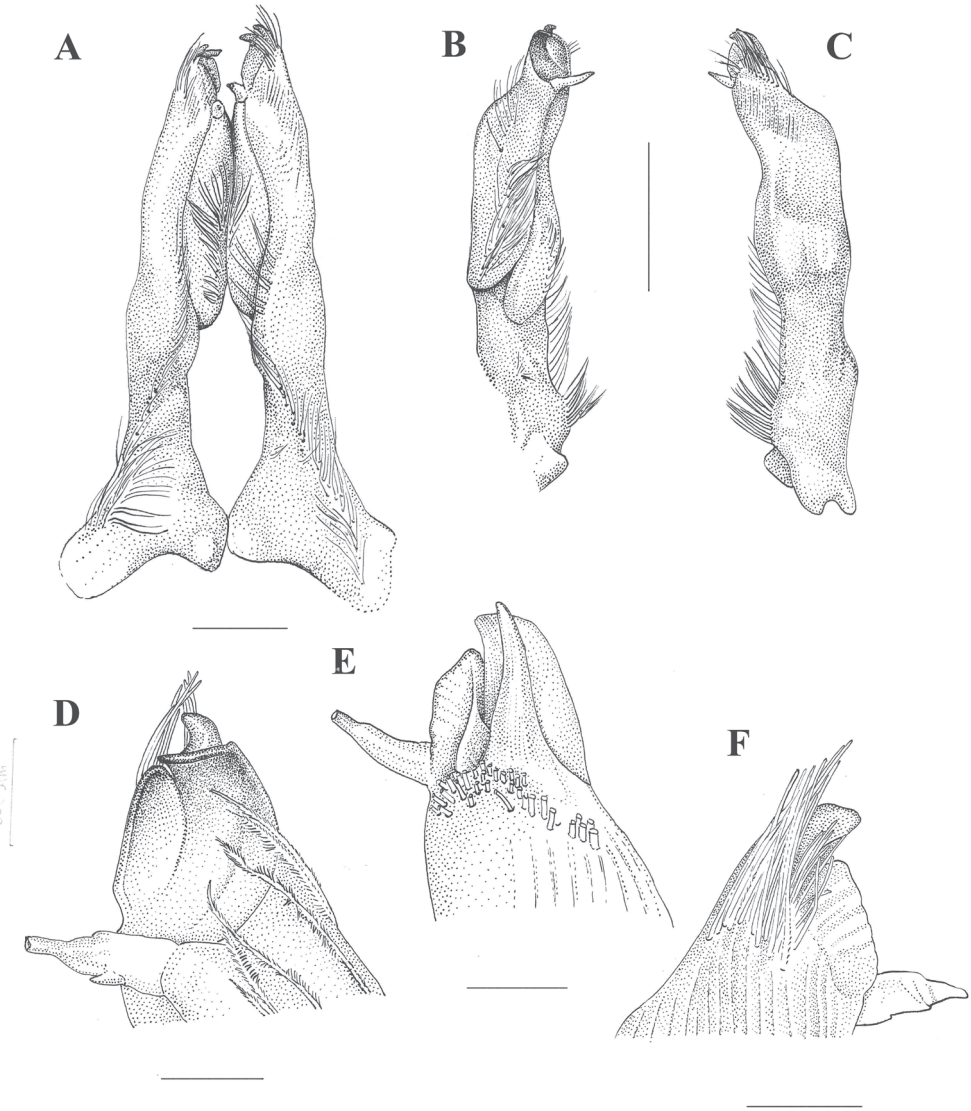


**Figure 4.** *Procambarus xihui*, holotype **A** caudal view of the first pair of pleopods **B** mesial view of left gonopod **C** lateral view of left gonopod **D** detail of apex, mesial view **E** detail of apex, latero-cephalic view **F** detail of apex, lateral view. Scale bars: 2 mm (**A**); 0.5 mm (**B, C**); 0.1 mm (**D–F**).

punctations in narrowest part, areola length 0.3 × carapace length. Rostrum wide (0.78 × rostrum length).

Shorter and smaller chela, 0.66 × length of carapace and width 0.31 × length, mesial profile of dactyl straight. Four strong tubercles on proximal half of opposable side of dactyl. Two conspicuous tubercles on opposable side of fixed finger, one on distal third. Width of carpus of first pereiopod ca. 0.63 × its length. Shorter merus, 0.39 × cephalothorax length. Left dactyl abnormally small, shorter than fixed finger.

No hooks on ischiopodites of pereiopods. Caudomesial boss only evident on fifth coxopodite, mesially projected.

Annulus ventralis as described in diagnosis (Fig. 3). First pleopods uniramous, reaching cephalic region of annulus ventralis when abdomen is flexed.

**Description of morphotypic male, form II.** (Table 2). Differing from holotype in the following respects: areola of moderate width (0.24 × length) with punctations (two or three in narrowest part).

Left chela 0.87 × the length of cephalothorax and width 0.28 × in its length, mesial surface of chela with a row of ten tubercles, palm 0.55 × in dactyl length. Right chela abnormally smaller. Opposable side of dactyl with five stronger tubercles on proximal side, lateral margin of dactyl with ridge of punctations. Opposable margin of fixed finger with five tubercles on basal quarter, two of them stronger, and punctate along distal half.

Carpus of first pereiopod ca. 1.35 × longer than wide. Shorter merus (0.41 × cephalothorax length). Shallow hooks on ischiopodites of third and fourth pereiopods, the former longer, none exceeding basioischial articulation.

Terminal elements of first pleopods not stylized, certain incipient development in mesial process and central projection, the latter together with caudal and cephalic processes mesially oriented.

The new species depicts certain variability in coloration among populations, but most individuals show a general brownish body background with lighter scattered spots along thorax and abdomen (Fig. 5). For most individuals, the chela is brown to reddish, with scattered darker or yellowish punctations. Color become lighter to the base of pereiopods. In some individuals, a diffuse darker band is visible on the sides of thorax, which become darker posteriorly, but it is not apparent in others.

**Etymology.** The specific epithet *-xihui* comes from the term used by natives from the region, (also known as the Pame people), to refer to themselves. The term also means 'indigenous' in the Pame language.

**Phylogenetic relationships and remarks.** Except for *Procambarus digueti* and *P. regiomontanus*, which are clearly distinctive among the crayfish fauna of Mexico and used here as outgroups, the new species shares some traits with the remaining species included, most of them inhabiting the Pánuco River basin. Among those are the possession of hooks on the ischiopodites of third and fourth pereiopods and the first pair of pleopods reaching the coxa of third pereiopods. However, the new species can be readily distinguished from two other species included inhabiting the Pánuco basin, *P. strenthi* and *P. roberti*, based in the following characters (among others): in *P. roberti*, the first pleopods are asymmetrical and lack a cephalic shoulder, and it possess a subtriangular, laterally grooved caudal process abutting the caudal base of central projection, which is notably more reduced than the shown by *P. xihui*. In *P. strenthi*, the first pleopods of the male form I are also strongly asymmetrical, bearing a strong angular shoulder in the cephalic surface, a cephalic process broad and lamellate, a dentiform central projection and a smaller subtriangular caudal process.

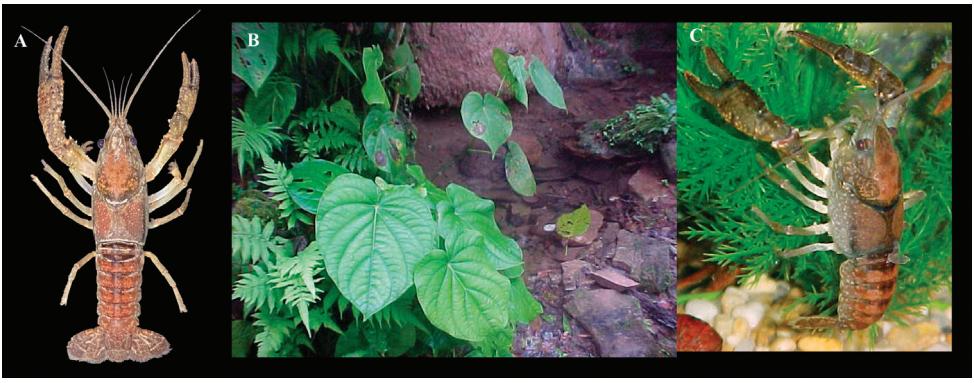


**Figure 5.** *Procambarus xihui* **A** photograph of form I male alive showing coloration **B** general habitat in type locality **C** photograph of live specimen in aquarium. Photographs by CPL.

More specifically, the new species is morphologically related to a group of species placed in the subgenus *Ortmannicus* by Hobbs (1972), although subgeneric groupings in *Procambarus* have not been recognized recently (Crandall and De Grave 2017). Still, such grouping allows us to identify some morphological similarities among *P. xihui* and the species morphologically most like it. Such species are *P. acutus*, *P. caballeroi*, *P. cuevachicae*, *P. gonopodocristatus*, *P. hidalgoensis*, *P. toltecae*, and *P. villalobosi*. Several traits are shared among the new species and the remaining Mexican species assigned to *Ortmannicus* sensu Hobbs (1972) such as the lack of caudal knob. In general, the new species can readily be distinguished from the remaining species by the configuration of terminal elements of the first pair of pleopods. In addition, it can be distinguished from *P. acutus* and *P. cuevachicae* as these show a distally directed mesial process, a cephalic process somewhat rounded distally, an acute caudal process, a somewhat twisted central projection, and an almost obliterated areola. *P. acutus* and *P. cuevachicae* also lack a cephalic shoulder in the first pleopod. The new species can be readily separated from *P. villalobosi*, among several other traits, by the conspicuous arrangement of all apical elements of the first pleopod in *P. villalobosi*, which has a singularly long mesial process far exceeding the other elements caudally.

Among other differences, the new species can be separated from *P. caballeroi* as the latter possess a wider rostrum, a laminated, laterally flattened cephalic process, a crest-like caudal process whose apex ends in a spine-like structure that is caudodistally directed. Among the main differences with *P. gonopodocristatus* are that the latter possesses a caudal process in the form of a long blade arced along the caudolateral surface, when in *P. xihui* this process is longer and situated along the caudomesial surface of the pleopod. *Procambarus caballeroi* and *P. gonopodocristatus* inhabit other river basins, south of the TMVB. The two species that most resemble *P. xihui* are *P. toltecae* and *P. hidalgoensis*.

The new species can easily be differentiated from *P. toltecae* because the latter shows a different arrangement of the terminal elements of the first pleopod: most conspicuous are the caudal orientations of the cephalic and caudal processes as well as the central

projection, the latter two forming a triangular projection which extends in caudally and forms a right angle to the longitudinal axis of the appendix. In *P. toltecae*, the central projection is the longest among the related species, while in *P. xihui*, the three most apical elements are directed mesially and the caudal process is blade-like and runs along the mesial side of the pleopod. We find that the new species is most similar to *P. hidalgoensis*, from which, however, clear differences can be noticed. In the latter, the mesial process is latero-distally oriented, while in *P. xihui* its orientation is caudal and slightly mesial; both show a central projection that is corneous and flattened, but its division in two elements in *P. hidalgoensis* is clear, one larger and distally projected and the other shorter, straight, and mesially projected, while in *P. xihui* the two elements are fused and no clear delimitation exists between them unless observed on electron microscopy; they form one concave blade-like structure, distally folded in a mesial direction. The caudal process is laminated in both species, but in *P. hidalgoensis* it is located mesiocaudally to central projection, while in *P. xihui* it is more laterally located, becoming the lateral side of the concavity formed by the central projection, also mesially directed. In vivo, a distinctive red coloration was recorded in the male form I of *P. hidalgoensis* with a contrasting blackish stripe running laterally of cephalothorax. In *P. xihui*, a dark stripe can be present, but it does not contrast as the body color is brownish (Fig. 5).

The phylogenetic analysis partially agrees with deductions from morphological similarities. The new species is grouped in a clade with *P. hidalgoensis*: these two species inhabit small, first-order springs of the Pánuco basin, although *P. xihui* inhabits higher altitude parts of three different sub-basins (between 1,000 m and ca. 1,200 m): the Jalpan River (later a tributary of the Santa María sub-basin), the Tancuilín sub-basin, and Extoraz sub-basin (both tributaries of the Moctezuma River). On the other side, *P. hidalgoensis* inhabits similar habitats (at an altitude of 1,485 m) but from the Río Hule sub-basin, a southern component of the Moctezuma sub-basin. This clade is grouped with *P. toltecae*, which inhabits much lower altitudes (here collected from 273 m). Similarly, the Pánuco system is inhabited by the remaining species here included except for *P. digueti* and *P. regiomontanus*, but most of them are from distinct sub-basins or altitudes. Results shown here support that this region is a depositary of distinct clades of crayfish diversity in Mexico, which possibly reflects a complex biogeographic history for the genus in northeast Mexico, from which *P. xihui* is one additional component. Additional phylogenetic and biogeographic inferences are surely complex and beyond the scope of the present manuscript and will be treated in further work.

**Habitat and conservation notes.** The new species inhabits an entirely included area in the SGBR. With certain variation among populations, habitats are headwater stream ecosystems, less than 1.5 meters wide, showing surface water intermittently along their course for most of the year, especially in small ponds that are 0.5–3 m wide with reduced water flow (Fig. 5). These are very sensitive habitats, reduced in area and characterized by a high quality of riparian vegetation and pristine water conditions (Meyer et al. 2007). During the rainy season they can occasionally join the next water course, where crayfish populations have not been found; consequently it is possible

that a high degree of habitat fragmentation can exist between locations. They are characterized by oligotrophic water conditions (elevated oxygen concentration, low temperatures and low nutrients) and substrates composed of bedrock, rocks, pebbles, cobbles, leaf litter, tree branches (Pedraza-Lara et al. 2004), and other elements that provide shadow, refuge, and high habitat heterogeneity. The riparian vegetation, rocks, and gravels are of special importance for crayfish survival since they are nocturnal and usually spend most of the day hidden in these substrates.

The characteristic physical and chemical parameters of their habitats are temperatures between 20 and 28 °C, dissolved oxygen content between 8 and 12 mg $l^{-1}$, pH 7–8 , and water hardness 90–350 mg CaCO3 $l^{-1}$. The terrestrial vegetation of the riverside where the crayfish populations were found is composed by riparian vegetation of *Platanus mexicana*, *Taxodium mucronatum*, and *Salix* species.

Headwater streams might be more vulnerable to disturbances in the surrounding catchment than other aquatic habitats, which relate to a higher risk of biodiversity loss (Lowe and Likens 2005). Populations inhabiting headwater stream ecosystems are especially sensitive to rainy conditions, as short and severe periods of drought could represent a high risk of extinction of their populations (Boulton 2003). The last decade in central and northern Mexico has been dryer than preceding decades (Seager et al. 2009): the most severe drought recorded from the BRSG was during 2010–2015, with the year 2012 being the most intense (Mendoza-Villa et al. 2018). Climatic predictions at a regional scale indicate that naturally occurring sub-decadal droughts will be made more frequent and widespread by anthropogenic climate change (Seager et al. 2009). Locally, water from the localities of the new species is intensively used for human consumption, crops, and livestock activities. Impacts driven by climate change are expected to be substantial on headwater streams ecosystems, which makes diagnosing and planning for conservation an urgent task (Durance and Ormerod 2007). From this perspective, the conservation of the headwaters of the rivers, as well as the maintenance of seasonal water regimes is of utmost importance to preserve endemic species, especially those that have very narrow distributions, such as *P. xihui*. Human actions also induce climate change to be faster in these areas, affecting the general ecological functioning of the Sierra and with it, also human activities (pers. obs.).

Collections for populations from the new species were made in the year 2002 and attempted in 2019, covering nearly 20 years. The climatic conditions and intense use of water described above has probably been related to the dramatic change observed by us at the visited sites, in which three of the five streams were almost dry or completely modified. In June 2019, an attempt to collect with the same sampling effort used in 2002 was carried out at all sites. We failed to find any crayfish at Las Camelinas, Saldiveña, and San Juanito, and in the remainder, crayfish were at much lower abundances than previously recorded. Additionally, several mass mortalities of crayfish were recorded from some sites, produced by the use of pesticides in crops surrounding the small streams.

As seen by their location, most populations were found in separated streams which were not in contact with each other for most of the year or even for several years. Most of individuals were found in such small populations and face situations

of high dryness, in which they are limited to a small number of pools, representing a high risk of local extinctions. If crayfish diversity is one of the most endangered among freshwater fauna in the world (Richman et al. 2015), cambarids have the most threatened species in Mexico concerning freshwater Crustacea (Alvarez and Villalobos 2016). The new species is an especially sensitive case derived from its peculiar habitat and narrow distribution ranges, which emphasizes an urgent need to design and fulfill conservation measures in the short term to avoid extinction of most of its populations. Consequently, efforts to include the species into the Mexican law NOM-059-SEMARNAT-2010: Environmental Protection-Native species of Mexico of wild flora and fauna will be conducted.

## Acknowledgements

We thank Patricia Ornelas, Heriberto Pedraza R., Ma. Guadalupe Lara, Sandra Pedraza, Heriberto Pedraza L., Regina Pedraza, and Gael Pedraza for their guidance and help collecting several of the populations. Halan Ortíz-Herrera made took some of the measurements, Aslam Narváez made the illustrations. This work was financed by project 257263 granted by CONACyT and project IA205020 by DGAPA – PAPIIT, UNAM both granted to the first author. This work was also supported by a post-doctoral fellowship to VJB by DGAPA, UNAM. Micrographs were taken by Berenit Mendoza-Garfias at the Lab of Electron Microscopy of Biology Institute, UNAM. Some lab work was assisted by Christian Cárdenas Monroy. Some species were collected with the help of Leonardo García-Vázquez, Stephany Rodríguez, Sharif Rodríguez, and Carlos Garita; some populations from SGBR were sampled on previous occasions with the help of Alfredo Morales-Ortíz and Carlos Ramírez.

## References

Alvarez F, Villalobos JL (2016) Freshwater decapod diversity and conservation in Mexico. In: Kawai T, Cumberlidge N (Eds) A global overview of the conservation of freshwater decapod crustaceans. Springer, Cham, 237–266. https://doi.org/10.1007/978-3-319-42527-6_8

Bezerra F, Rudolph E, Pedraza-Lara C (2020) Decapoda: Astacidea. In: Damborenea C, Rogers C, Thorp JH (Eds) Thorp and Covich's Freshwater Invertebrates. Volume V. Keys to Neotropical and Antarctic Fauna. Elsevier, London, 874–901.

Bouckaert R, Heled J, Kühnert D, Vaughan T, Wu C-H, Xie D, Suchard MA, Rambaut A, Drummond AJ (2014) BEAST 2: A Software Platform for Bayesian Evolutionary Analysis. PLoS Computational Biology 10: e1003537. https://doi.org/10.1371/journal.pcbi.1003537

Boulton AJ (2003) Parallels and contrasts in the effects of drought on stream macroinvertebrate assemblages. Freshwater Biology 48: 1173–1185. https://doi.org/10.1046/j.1365-2427.2003.01084.x

Crandall KA, De Grave S (2017) An updated classification of the freshwater crayfishes (Decapoda: Astacidea) of the world, with a complete species list. Journal of Crustacean Biology 37: 615–653. https://doi.org/10.1093/jcbiol/rux070

Donoghue MJ (1985) A critique of the biological species concept and recommendations for a phylogenetic alternative. Bryologist: 172–181. https://doi.org/10.2307/3243026

Durance I, Ormerod SJ (2007) Climate change effects on upland stream macroinvertebrates over a 25-year period. Global change biology 13: 942–957. https://doi.org/10.1111/j.1365-2486.2007.01340.x

Fetzner JJ, Crandall KA (2002) Genetic variation. In: Holdich DM (Ed.) Biology of freshwater crayfish. Blackwell Science, Oxford, 291–326.

Gutiérrez-Yurrita PJ (2014) Holistic management of temporary watersheds in Central Mexico: an improved easy mathematical model for decision-makers. International Journal of Ecology and Environmental Sciences 40: 95–110.

Gutiérrez-Yurrita PJ, Morales-Ortiz A, Oviedo A, Ramírez-Pérez C (2002) Distribution, spread, habitat characterization and conservation of freshwater crayfish species (Cambaridae) in Querétaro, Central México. Freshwater Crayfish 13: 349–358.

Hebert PDN, Cywinska A, Ball SL, DeWaard JR (2003) Biological identifications through DNA barcodes. Proceedings of the Royal Society B – Biological Sciences 270: 313–321. https://doi.org/10.1098/rspb.2002.2218

Hobbs HHJ (1941) A new crayfish from San Luis Potosi, Mexico (Decapoda, Astacidae). Zoologica 26: 1–4. https://doi.org/10.2307/2420759

Hobbs HHJ (1943) Two new crayfishes of the genus Procambarus from Mexico (Decapoda, Astacidae). Lloydia 6: 198–206.

Hobbs HHJ (1972a) Biota of Freshwater Ecosystems, Identification Manual no. 9, Crayfishes (Astacidae) of North and Middle America. EPA project # 18050 ELD.

Hobbs HHJ (1972b) The subgenera of the crayfish genus Procambarus (Decapoda, Astacidae). Smithsonian Contributions to Zoology 117: 1–22. https://doi.org/10.5479/si.00810282.117

Hobbs HHJ (1977) A new crayfish (Decapoda: Cambaridae) from San Luis Potosí, Mexico. Proceedings of the Biological Society of Washington 90: 412–419.

IUCN Standards and Petitions Committee (2019) Guidelines for using the International Union for Conservation of Nature Red List categories and criteria.

Kumar S, Stecher G, Li M, Knyaz C, Tamura K (2018) MEGA X: Molecular evolutionary genetics analysis across computing platforms. Molecular Biology and Evolution 35: 1547–1549. https://doi.org/10.1093/molbev/msy096

Lanfear R, Frandsen PB, Wright AM, Senfeld T, Calcott B (2017) PartitionFinder 2: New methods for selecting partitioned models of evolution for molecular and morphological phylogenetic analyses. Molecular Biology and Evolution 34: 772–773. https://doi.org/10.1093/molbev/msw260

López-Mejía M, Alvarez F, Mejía-Ortíz LM (2005) *Procambarus* (*Ortmannicus*) *hidalgoensis* (Crustacea: Decapoda: Cambaridae), a new species of crayfish from Mexico. Proceedings of the Biological Society of Washington 118: 558–565. https://doi.org/10.2988/0006-324X(2005)118[558:POHCDC]2.0.CO;2

Lowe WH, Likens GE (2005) Moving headwater streams to the head of the class. BioScience 55: 196–197. https://doi.org/10.1641/0006-3568(2005)055[0196:MHSTTH]2.0.CO;2

Matzen da Silva J, Creer S, Dos Santos A, Costa AC, Cunha MR, Costa FO, Carvalho GR (2011) Systematic and evolutionary insights derived from mtDNA COI barcode diversity in the Decapoda (Crustacea: Malacostraca). PLoS ONE 6(5): e19449. https://doi.org/10.1371/journal.pone.0019449

Mendoza-Villa ON, Cambrón-Sandoval VH, Cerano-Paredes J, Cervantes-Martínez R, Soto-Correa JC (2018) Reconstruction of historical precipitation (1877–2014) for the southwest of the Sierra Gorda Biosphere Reserve, Querétaro, Mexico. Revista Chapingo Serie Ciencias Forestales 24: 371–386. https://doi.org/10.5154/r.rchscfa.2018.01.008

Meyer JL, Strayer DL, Wallace JB, Eggert SL, Helfman GS, Leonard NE (2007) The contribution of headwater streams to biodiversity in river networks 1. JAWRA Journal of the American Water Resources Association 43: 86–103. https://doi.org/10.1111/j.1752-1688.2007.00008.x

Pedraza-Lara C, Doadrio I (2015) A new species of dwarf crayfish (Decapoda: Cambaridae) from central México, as supported by morphological and genetic evidence. Zootaxa 3963: 583–594. https://doi.org/10.11646/zootaxa.3963.4.5

Pedraza-Lara C, López-Romero A, Gutiérrez-Yurrita PJ (2004) Preliminary studies concerning phenotype and molecular differences among freshwater crayfish from the sub-genus *Procambarus* (*Ortmannicus*) in Sierra Gorda Biosphere Reserve, Mexico. Freshwater crayfish 14: 129–139.

Pedraza-Lara C, Doadrio I, Breinholt JW, Crandall KA (2012) Phylogeny and Evolutionary Patterns in the Dwarf Crayfish Subfamily (Decapoda: Cambarellinae). Castresana J (Ed.) PLoS ONE 7: e48233. https://doi.org/10.1371/journal.pone.0048233

Pons J, Kamoun S, Barraclough TG, Duran DP, Vogler AP, Cardoso A, Sumlin WD, Gomez-Zurita J, Hazell S (2006) Sequence-Based Species Delimitation for the DNA Taxonomy of Undescribed Insects. Systematic Biology 55: 595–609. https://doi.org/10.1080/10635150600852011

Puillandre N, Lambert A, Brouillet S, Achaz G (2012) ABGD, Automatic Barcode Gap Discovery for primary species delimitation. Molecular Ecology 21: 1864–1877. https://doi.org/10.1111/j.1365-294X.2011.05239.x

Rambaut A, Drummond AJ, Xie D, Baele G, Suchard MA (2018) Posterior summarization in Bayesian phylogenetics using Tracer 1.7. Systematic biology 67(5): 901–904. https://doi.org/10.1093/sysbio/syy032

Richman NI, Bohm M, Adams SB, Alvarez F, Bergey EA, Bunn JJS, Burnham Q, Cordeiro J, Coughran J, Crandall KA, Dawkins KL, DiStefano RJ, Doran NE, Edsman L, Eversole AG, Fureder L, Furse JM, Gherardi F, Hamr P, Holdich DM, Horwitz P, Johnston K, Jones CM, Jones JPG, Jones RL, Jones TG, Kawai T, Lawler S, Lopez-Mejia M, Miller RM, Pedraza-Lara C, Reynolds JD, Richardson AMM, Schultz MB, Schuster GA, Sibley PJ, Souty-Grosset C, Taylor CA, Thoma RF, Walls J, Walsh TS, Collen B (2015) Multiple drivers of decline in the global status of freshwater crayfish (Decapoda: Astacidea). Philosophical Transactions of the Royal Society B – Biological Sciences 370: 20140060–20140060. https://doi.org/10.1098/rstb.2014.0060

Ronquist F, Huelsenbeck JP (2003) MrBayes 3: Bayesian phylogenetic inference under mixed models. Bioinformatics 19: 1572–1574. https://doi.org/10.1093/bioinformatics/btg180

Rosen DE (1979) Fishes from the uplands and intermontane basins of Guatemala: revisionary studies and comparative geography. Bulletin of the AMNH vol. 162, article 5.

Sambrook J, Fritsch EF, Maniatis T (1989) Molecular cloning: a laboratory manual, 2nd edn. Cold Springs Harbor Laboratory Press, New York, 1626 pp.

Seager R, Ting M, Davis M, Cane M, Naik N, Nakamura J, Li C, Cook E, Stahle DW (2009) Mexican drought: an observational modeling and tree ring study of variability and climate change. Atmósfera 22: 1–31.

Stamatakis A (2014) RAxML version 8: a tool for phylogenetic analysis and post-analysis of large phylogenies. Bioinformatics (Oxford, England) 30: 1312–1313. https://doi.org/10.1093/bioinformatics/btu033

Toon A, Finley M, Staples J, Crandall KA (2009) Decapod phylogenetics and molecular evolution. In: Martin JW, Crandall KA, Felder DL (Eds) Decapod crustacean phylogenetics. Taylor and Francis Group, LLC, Boca Raton, FL, 15–29. https://doi.org/10.1201/9781420092592-c2

Villalobos-Figueroa A (1954) Estudios de los cambarinos mexicanos XI. Una nueva subespecie de Procambarus simulans del Edo. de Nuevo León. Anales del Instituto de Biologia, Universidad Nacional Autonoma de Mexico 25: 289–298.

Villalobos A (1944) Estudios de los cambarinos Mexicanos, III. Una especie nueva de Procambarus, Procambarus caballeroi n. sp. Anales del Instituto de Biología, Universidad Nacional Autónoma de México 15: 175–184.

Villalobos A (1955) Cambarinos de la fauna mexicana (Crustacea Decapoda). PhD Tesis. Universidad Nacional Autónoma de México.

Villalobos A (1958) Estudios de los cambarinos mexicanos, XIII. Descripción de una nueva especie de cambarinos del estado de Veracruz (Crustacea, Decapoda). Anales del Instituto de Biologia, Universidad Nacional Autónoma de México 28: 279–288.

Villalobos Figueroa A, Hobbs HHJ (1974) Three new crustaceans from La Media Luna, San Luis Potosí, Mexico. Smithsonian Contributions to Zoology 174: 1–18. https://doi.org/10.5479/si.00810282.174

Zhang J, Kapli P, Pavlidis P, Stamatakis A (2013) A general species delimitation method with applications to phylogenetic placements. Bioinformatics 29: 2869–2876. https://doi.org/10.1093/bioinformatics/btt499

## Supplementary material 1

**Results of the ABGD, bPTP and GMYC species delimitation analysis**

Authors: Carlos Pedraza-Lara, Pedro Joaquín Gutiérrez-Yurrita, Vladimir Salvador De Jesus-Bonilla

Data type: Delimitation analyses



Link: https://doi.org/10.3897/zookeys.1048.57493.suppl1

## Supplementary material 2

**Table S1**

Authors: Carlos Pedraza-Lara, Pedro Joaquín Gutiérrez-Yurrita, Vladimir Salvador De Jesus-Bonilla

Data type: Genetic distances

Explanation note: Uncorrected *P*-distances for the COI fragment between species included in this study (in bold) and standard error.



Link: https://doi.org/10.3897/zookeys.1048.57493.suppl2

ZooKeys 1048: 23–47 (2021)
doi: 10.3897/zookeys.1048.65650
https://zookeys.pensoft.net

RESEARCH ARTICLE

A peer-reviewed open-access journal
ZooKeys
Launched to accelerate biodiversity research

# A sheep in wolf's clothing: *Elaphe xiphodonta* sp. nov. (Squamata, Colubridae) and its possible mimicry to *Protobothrops jerdonii*

Shuo Qi[1,2*], Jing-Song Shi[2,3*], Yan-Bo Ma[2,4], Yi-Fei Gao[2,4], Shu-Hai Bu[4], L. Lee Grismer[5], Pi-Peng Li[2], Ying-Yong Wang[1]

**1** *State Key Laboratory of Biocontrol/ The Museum of Biology, School of Life Sciences, Sun Yat-sen University, Guangzhou, Guangdong 510275, China* **2** *Institute of Herpetology, Shenyang Normal University, Shenyang 110034, China* **3** *Key Laboratory of Vertebrate Evolution and Human Origins of Chinese Academy of Sciences, Institute of Vertebrate Paleontology and Paleoanthropology, Chinese Academy of Sciences, Beijing 100044, China* **4** *College of Life Sciences, Northwest Agriculture and Forestry University, Yangling, 712100, China* **5** *Herpetology Laboratory, Department of Biology, La Sierra University, Riverside, California 92515, USA*

Corresponding authors: Jing-Song Shi (shijingsong@ivpp.ac.cn); Ying-Yong Wang (wangyy@mail.sysu.edu.cn)

Academic editor: Robert Jadin | Received 8 March 2021 | Accepted 26 May 2021 | Published 6 July 2021

*http://zoobank.org/06E23984-0C12-4A8F-ACC4-E80EB102DE18*

**Citation:** Qi S, Shi J-S, Ma Y-B, Gao Y-F, Bu S-H, Grismer LL, Li P-P, Wang Y-Y (2021) A sheep in wolf's clothing: *Elaphe xiphodonta* sp. nov. (Squamata, Colubridae) and its possible mimicry to *Protobothrops jerdonii*. ZooKeys 1048: 23–47. https://doi.org/10.3897/zookeys.1048.65650

## Abstract

Based on combined morphological and osteological characters and molecular phylogenetics, we describe a new species of the genus *Elaphe* that was discovered from the south slope of the Qinling Mountains, Shaanxi, China, namely *Elaphe xiphodonta* **sp. nov.** It is distinguished from the other congeners by a combination of the following characters: dorsal scales in 21-21-17 rows, the medial 11 rows keeled; 202–204 ventral scales, 67–68 subcaudals; two preoculars (including one subpreocular); two postoculars; two anterior temporals, three posterior temporals; reduced numbers of maxillary teeth (9+2) and dentary teeth (12); sharp cutting edges on the posterior or posterolateral surface of the rear maxillary teeth and dentary teeth; dorsal head yellow, three distinct markings on the head and neck; a distinct black labial spot present in supralabials; dorsum yellow, 46–49 complete (or incomplete) large black-edged reddish brown blotches on the body and 12–19 on the tail, two rows of smaller blotches on each ventrolateral side; ventral scales yellow with mottled irregular black blotches, a few irregular small red spots dispersed on the middle of the ventral. Based on molecular phylogenetic analyses, the new species forms the sister taxon to *E. zoigeensis*. The discovery of this new species increases the number of the recognized species in the genus *Elaphe* to 17.

* Contributed equally as the first authors.

**Keywords**
Colubrid, morphology, osteology, Qinling Mountains, taxonomy

## Introduction

The colubrid genus *Elaphe* sensu lato Fitzinger (in Wagler), 1833, once contained approximately forty species ranging throughout temperate, subtropical, and tropical zones in both the eastern and western hemispheres (Schulz 1996). Most of the members of this genus have a slender body, partially or completely keeled dorsal scales, and round pupils. The head is distinguishable from the neck, the trunk vertebra lack a hypapophysis, and the posterior maxillary teeth are not significantly differentiated from the others. With the rise of molecular taxonomy in the last decades of the 20$^{th}$ century, a series of major taxonomic changes occurred at generic and species levels, resulting in the establishment or resurrection of several genera and species (Helfenberger 2001; Lenk Joger and Wink 2001; Utiger et al. 2002; Huang et al. 2012; Jablonski et al. 2019). Recent molecular phylogenetic studies suggest that the genus *Orthriophis* should be subsumed within the genus *Elaphe*, because the generic status of *Orthriophis* renders *Elaphe* paraphyletic, where *E. zoigeensis* Huang, Ding, Burbrink, Yang, Huang, Ling, Chen & Zhang, 2012 is sister to all the other *Elaphe* plus *Orthriophis* (Chen et al. 2017; Li et al. 2020; but see Figueroa et al. 2016). Currently, the genus *Elaphe* sensu stricto is comprised of 16 species of which most, are widely distributed in eastern Asia and the south slopes of the Himalaya, although the range of the genus extends east to eastern Russia, south to the Indonesia-Malayan region, and west to as far as Italy (Helfenberger 2001; Zhao 2006; Huang et al. 2012; Jablonski et al. 2019; Uetz et al. 2021). Previous biogeographic, phylogenetic, and phylogenomic studies support the hypothesis that *Elaphe* originated in the Eastern Palearctic (Lenk, Joger and Wink 2001; Utiger et al. 2002; Burbrink and Lawson 2007; Burbrink and Pyron 2010; Chen et al. 2017). In regards to China, 11 species of *Elaphe* are recognized: *E. anomala* (Boulenger, 1916), *E. bimaculata* Schmidt, 1925, *E. carinata* (Günther, 1864), *E. cantoris* (Boulenger, 1894), *E. davidi* (Sauvage, 1884), *E. dione* (Pallas, 1773), *E. hodgsonii* (Günther, 1860), *E. moellendorffi* (Boettger, 1886), *E. taeniura* (Cope, 1861), *E. schrenckii* (Strauch, 1873), and *E. zoigeensis*, two of which (*E. bimaculata* and *E. zoigeensis*) are endemic to China (Wang et al. 2020).

The main part of Qinling Mountains, lies on the south of Shaanxi Province, having an average elevation of approximately 2000 m and have long been regarded as the geographical, biological and climatological boundary between North (Palaearctic Realm; warm temperate monsoon climate) and South China (Oriental Realm; subtropical monsoon climate, Zhang 1999). Due to the unique environment and climate, the Qinling Mountains are the habitat of many rare animals (e.g., *Ailuropoda melanoleuca*, *Budorcas bedfordi*, and *Rhinopithecus roxellana qinlingensis*). Additionally, the herpetological diversity of that area is high. To date, more than 10 species of amphibians and 20 species of reptiles have been reported in this area, some of which are endemic to the Qinling Mountains and adjacent areas (e.g., *Scutiger ningshanensis*, *Hyla tsinlingensis*,

*Batrachuperus taibaiensis*, *Stichophanes ningshaanensis*, *Scincella tsinlingensis*, *Protobothrops jerdonii* and *Gloydius qinlingensis* (Bu and Zheng 2015).

Bates (1862) discovered a spectacular type of adaptation known as "mimicry", building on Charles Darwin's views on evolution. This phenomenon, now called "Batesian mimicry", which is defined as an edible species (mimic) evolving to resemble a conspicuous inedible species (model), thereby gaining protection from predation, its efficiency relying on confusing the mimic with the model (Carpenter and Ford 1933; Ruxton et al. 2004). Batesian mimicry is observed among a wide variety of animals, ranging from invertebrates to vertebrates, including several non-venomous snakes mimicking the color pattern, head shape or behavior of sympatric venomous snakes to avoid predation (Brodie 1993).

During our recent herpetological surveys in the south slope of the Qinling Mountains, Shaanxi, China, two colubrid specimens were collected, which look quite different to any of the known species but similar to *Protobothrops jerdonii* (Figs 1–3). Detailed morphological examinations and further molecular analyses revealed that these specimens represent a separately evolving lineage within the genus *Elaphe* and can be distinguished from all congeners by morphological characters. We herein describe this overlooked *Elaphe* population as a new species. Furthermore, we suspect this new species is able to avoid predation by mimicking the syntopic pit-viper (*P. jerdonii*).

## Materials and methods

### Morphometrics

Morphological examinations were performed on two specimens collected from Chengguan Town, Ningshaan County, Shaanxi Province, China (Fig. 4). Both specimens were fixed in 10% buffered formalin after taking the tissue samples (liver or muscle), and then transferred to 70% ethanol for permanent preservation. The specimens are deposited in the Museum of Biology, Sun Yat-sen University (SYS r002534, Figs 1, 2, 3A) and Institute of Vertebrate Paleontology and Paleoanthropology, Chinese Academy of Sciences (IVPP OV 2721, Fig. 3C).

Morphological descriptions follow Dowling (1951) and Zhao (2006). The following measurements were taken with digital calipers (Neiko 01407A Stainless Steel 6-Inch Digital Caliper, USA) to the nearest 0.1 mm: **TL** total length (from tip of snout to tip of tail); **SVL** snout-vent length (from tip of snout to posterior margin of cloacal plate); **TaL** tail length (from posterior margin of cloacal plate to tip of tail); **HL** head length (from tip of snout to posterior margin of the mandible); **HW** maximum head width; **ED** eye horizontal diameter; **RW** = maximum rostral width; **RH** maximum rostral height.

Scalation features and their abbreviations are as follows: **DSR** dorsal scale rows, counted at one head length behind head, at midbody, and at one head length before vent; **SPL** supralabials; **IFL** infralabials; **CS** chin shields; **PrO** preoculars; **PtO** postoculars; **LoR** loreal; **aTMP** anterior temporals; **pTMP** posterior temporals; **PrV** preventral scales; **V** ventral scales; **PrC** precloacal plate; **SC** and subcaudals. Gender

was determined by dissection or by the presence/absence of everted hemipenes. The numbers of maxillary teeth (**MT**) were counted based on the three-dimensional reconstructed model.

Other morphological characters (e.g., coloration, scalation, and size) for *Elaphe* taxonomy were obtained from Boulenger (1894), Stejneger (1907), Wen and Ji (1997), Zhao (2006), Huang et al. (2012), Jablonski et al. (2019), Shi et al. (2019) and Che et al. (2020).

The following abbreviations for museum collections are used throughout the paper:

**AMNH** American Museum of Natural History;
**BFU** Beijing Forest University;
**BM** British Museum;
**CAS** Chinese Academic of Sciences;
**IVPP** Institute of Vertebrate Paleontology and Paleoanthropology;
**MHNG** Muséum d'Histoire Naturelle, Genève;
**SYS** Sun Yat-sen University.

## X-ray scanning and three-dimensional reconstructions

The X-ray scanning was carried out with Nano-computerized tomography. Specimens were scanned using a GE v|tome|x m dual tube 300/180kV system in the Key Laboratory of Vertebrate Evolution and Human Origins, Institute of Vertebrate Paleontology and Paleoanthropology (IVPP), Chinese Academy of Sciences. The specimen was scanned with an energy beam of 80 kV and a flux of 80*μA using a 360° rotation and then reconstructed into the 4096*4096 matrix of 1536 slices. The final CT reconstructed skull images were exported with a minimum resolution of 6.099 μm. The skull images were exported from the virtual 3D model which was reconstruct by Volume Graphics Studio 3.0.

The dataset of the 3D model included in this study is available online in the repository (ADMorph, Hou et al. 2020) at http://www.admorph.org/; https://doi.org/10.12112/R.0005 (IVPP OV 2721, paratype).

## DNA Extraction, Polymerase Chain Reaction (PCR) and sequencing

For the molecular analyses, two tissue samples of the new species were included, which were taken prior to fixation, preserved in 99% alcohol, and stored at -40 °C.

Genomic DNA was extracted from muscle or liver tissue samples, using a DNA extraction kit from Tiangen Bio-tech (Beijing) Co., Ltd. Partial segments of the mitochondrial genes, 16S ribosomal RNA gene (16S), cytochrome C oxidase 1 gene (CO1) and Cytochrome b gene (cytb) were amplified. Nested PCR experiments were performed as described in Li et al. (2017). Primers used for PCR and sequencing followed Li et al. (2020), see Table 1 for details. The first PCR procedure was performed with an

initial denaturation at 94 °C for 4 min, 35 cycles of 94 °C for 45 s, 45 °C for 40 s and 72 °C for 2 min, followed by a final extension at 72 °C for 10 min. The second PCR procedure was performed with an initial denaturation at 94 °C for 4 min, 30 cycles of 94 °C for 45 s, 50 °C for 40 s and 72 °C for 1.5 min, followed by a final extension at 72 °C for 10 min. PCR products were purified with spin columns and then sequenced using BigDye Terminator Cycle Sequencing Kit as per the guidelines on an ABI Prism 3730 automated DNA sequencer by Guangzhou Tianyi Huiyuan Bio-tech Co., Ltd.

## Phylogenetic analyses

Fifty-nine sequences from 16 known *Elaphe* species plus six outgroup sequences from *Euprepiophis mandarinus* (Cantor, 1842) used to root the tree, were obtained from GenBank, and composed the dataset (Table 2).

DNA nucleotide sequences were aligned in the ClustalW algorithm with default parameters (Thompson et al. 1997) in MEGA 6 (Tamura et al. 2013). The aligned 16S, CO1 and cytb datasets were partitioned by codons with no gap positions allowed and applying default parameters in Gblocks version 0.91b (Castresana 2000). Three gene segments, with 1329 base pairs (bp) of 16S, 657 bp of CO1, and 585 bp of cytb, were concatenated seriatim into a 2571 bp sequence. With respect to the different evolutionary characters of each molecular marker, the dataset was split into seven partitions by gene and codon positions taking advantage of PartitionFinder 2.1.1 (Lanfear et al. 2012). The evolution models of each partition selected by PartitionFinder 2.1.1 were as follows: partition 1: 16S, GTR+I+G, 1287 bp; partition 2: COI\1, SYM+G, 219 bp; partition 3: COI\2, HKY+I, 219 bp; partition 4: COI\3, TVM+G, 219 bp; partition 5:;cytb\1, GTR+G, 195 bp; partition 6: cytb\2, HKY+I+G, 195 bp; partition 7:cytb\3, GTR+G 195 bp. General time-reversible (GTR) model. Sequence data were analyzed using Bayesian inference (BI) in MrBayes 3.2.4 (Ronquist et al. 2012), and maximum likelihood (ML) in RaxmlGUI 1.3 (Silvestro and Michalak 2012). Two independent runs were conducted in the BI analysis with 10,000,000 generations each and sampled

**Table 1.** Nested PCR primers for this study (Li et al. 2020).

| Gene | Primer name | Assay | Sequence |
|---|---|---|---|
| 16S | 12S-16S_Phe_F1 | 1st PCR | AAGCDYDGCRCTGAAAATGC |
| | 12S-16S_ND1_R1 | | AANGCNACNGCDATNAR |
| | S12S902L2 | 2nd PCR | YACACACCGCCCGTCA |
| | S16S2984H2 | | GACCTGGATTDCTCCGGTCTGAACTC |
| COI | COI_Asn_F1 | 1st PCR | GDTTRGRYKDYTARYTGTTAAYTA |
| | COI_Asp_R1 | | GTDATTYRRYYDYGACA |
| | COI_25_F2 | 2nd PCR | TCRACHAAYCAYAAAGAYATYGG |
| | COI_706_R2 | | TADACTTCWGGRTGDCCRAARAATCA |
| cytb | Scytb15025F | 1st PCR | TGGTGGAAYTTYGGNWSNATGYT |
| | Scytb15726R | | TANGCRAANARRAARTACCAYTC |
| | Scytb15082F | 2nd PCR | TTYTTYYTRGCNRTHCAYTAYAC |
| | Scytb15692R | | GCYTTDVWRAARTTKTCNGGRTC |

**Table 2.** Localities, specimen vouchers and GenBank accession numbers of the specimens included in this study.

| No. | Species name | Locality | Specimen voucher | Genbank accession number | | | References |
|---|---|---|---|---|---|---|---|
| | | | | 16S rRNA | CO1 | Cytb | |
| 1 | *Elaphe xiphodonta* sp. nov. | Ningshaan, Shaanxi, China | SYS r002534 | MZ242100 | MZ19164 | MZ19166 | This study |
| 2 | | Ningshaan, Shaanxi, China | IVPP OV 2721 | MZ242101 | MZ19165 | MZ19167 | This study |
| 3 | *Elaphe anomala* | Huangshan, Anhui, China | HS11075 | MK193929 | MK064632 | MK201281 | Li et al. 2020 |
| 4 | *Elaphe bimaculata* | Huangshan, Anhui, China | HS15168 | MK193931 | MK064634 | MK201283 | Li et al. 2020 |
| 5 | *Elaphe cantoris* | Pailong, Tibet, China | JK201705 | MK194263 | MK064913 | MK201564 | Li et al. 2020 |
| 6 | *Elaphe carinata* | Guangze, Fujian, China | HS13055 | MK193932 | MK064635 | MK201284 | Li et al. 2020 |
| 7 | | Longyou, Zhejiang, China | HS13062 | MK193934 | MK064637 | MK201286 | Li et al. 2020 |
| 8 | *Elaphe climacophora* | Abashiri, Hokkaido, Japan | KUZ R64481 | N/A | LC328423 | LC327534 | Moriyama et al. 2018 |
| 9 | | Deshikutsu, Hokkaido, Japan | KUZ R68813 | N/A | LC328426 | LC327537 | Moriyama et al. 2018 |
| 10 | *Elaphe davidi* | Taishan Mt., Shandong, China | N/A | KM401547 | KM401547 | KM401547 | Xu et al. 2015 |
| 11 | *Elaphe dione* | Taibai, Shaanxi, China | HS11036 | MK193928 | MK064631 | MK201280 | Li et al. 2020 |
| 12 | *Elaphe hodgsonii* | Jilong, Tibet, China | HS13004 | MK193983 | MK064680 | MK201335 | Li et al. 2020 |
| 13 | *Elaphe moellendorffi* | Yunlin, Guangxi, China | S-113 | N/A | KF698944 | KF913314 | Cao et al. 2014 |
| 14 | *Elaphe quadrivirgata* | N/A | N/A | AB738958 | AB738958 | AB738958 | Direct Submission |
| 15 | | Ashiu, Kyoto, Kansai, Japan | As1352 | N/A | N/A | HQ122007 | Kuriyama et al. 2010 |
| 16 | *Elaphe quatuorlineata* | Crkvino, Northern Macedonia | 1509 | MK334307 | MK334307 | MK334307 | Jablonski et al. 2019 |
| 17 | | Galatas, Argolida, Greece | ZMUP 60 | N/A | N/A | MH444348 | Thanou et al. 2020 |
| 18 | *Elaphe sauromates* | Taganrogskyi Gulf, Russia | ZISP 26197 | N/A | MK640250 | N/A | Jablonski et al. 2019 |
| 19 | | Solenoe Ozero, "Crimea" | 1179 | MK070315 | MK070315 | MK070315 | Jablonski et al. 2019 |
| 20 | *Elaphe schrenckii* | Changbai, Jilin, China | HS16031 | MK193935 | MK064638 | MK201287 | Li et al. 2020 |
| 21 | *Elaphe taeniura* | Zhouzhi, Shaanxi, China | HS2010025 | MK193982 | MK064679 | MK201334 | Li et al. 2020 |
| 22 | | Heishiding, Guangdong, China | SYS r001057 | MK194113 | MK064790 | MK201445 | Li et al. 2020 |
| 23 | *Elaphe urartica* | Kısıklı, Süphan Mts., Bitlis, Turkey | ZDEU 26/2012 | N/A | MK640299 | N/A | Jablonski et al. 2019 |
| 24 | | Guzdak, Qobustan, Azerbaijan | IZANAS T17 | N/A | MK640269 | N/A | Jablonski et al. 2019 |
| 25 | *Elaphe zoigeensis* | Zoige, Sichuan, China | HS11251 | MK193927 | MK064630 | MK201279 | Li et al. 2020 |
| 26 | | Zoige, Sichuan, China | HS2010015 | MK193930 | MK064633 | MK201282 | Li et al. 2020 |
| 27 | *Euprepiophis mandarinus* | HuangShan, Anhui, China | HS12062 | MK193939 | MK064643 | MK201291 | Li et al. 2020 |
| 28 | | HuangShan, Anhui, China | HS14017 | MK193940 | MK064644 | MK201292 | Li et al. 2020 |

every 1000 generations with the first 25% of samples discarded as burn-in, resulting in a potential scale reduction factor (PSRF) of < 0.005. In the ML analysis, a bootstrap consensus tree inferred from 1000 replicates was generated. Nodes with Bayesian posterior probabilities (BPP) ≥0.95 and ML support values of ≥70 were considered strongly supported (Huelsenbeck et al. 2001; Wilcox et al. 2002). Pairwise distances (*p*-distance) were calculated in MEGA6 using the uncorrected model. Gaps/Missing Data Treatment use the complete-deletion option, Substitutions to Include *d*: Transitions + Transversions option.

## Taxonomic accounts

### *Elaphe xiphodonta* sp. nov.

http://zoobank.org/AEA2D68D-5621-4B08-A4AE-BD99FA2192B9

**Material examined.** ***Holotype*.** SYS r002534, adult female (Figs 1, 2, 3A), collected by Yan-Bo Ma, Yi-Fei Gao on 4 September 2020 from Chengguan Town (33.58°N,

**Figure 1.** General view of the holotype (SYS r002534) of *Elaphe xiphodonta* sp. nov. in life. Photo by Shuo Qi.

108.46°E (DD); ca 1731 m a.s.l.), Ningshaan County, Shaanxi Province, China. ***Paratypes.*** IVPP OV 2721, juvenile female (Fig. 3C), collected by Jing-Song Shi on 7 September 2020 from Chengguan Town (33.56°N, 108.50°E (DD); ca 1751 m a.s.l.), Ningshaan County, Shaanxi Province, China (Fig. 4).

**Etymology.** The specific epithet "*xiphodonta*" of the new species comes from the Ancient Greek "ξίφοσ (ksίfos, refer to 'knife' or 'blade')" and "δοντι (dónti, refer to 'tooth')", meaning "blade-shaped teeth", indicating that the new species has unique blade-shaped MT and DT (Figs 5, 6), which differs from the inconspicuous dental specializations (all teeth are cone-shaped) in its congeners. We suggest the Chinese formal name as "秦皇锦蛇" (Qín Huáng Jǐn Shé), which derived from Qin Shi Huang (personal name: Ying Zheng or Zhao Zheng; 259 BC–210 BC), the founder of the Qin dynasty and the first emperor of unified China, whose territory including the distribution range of *Elaphe xiphodonta* sp. nov. The English name is suggested as "Qin Emperor Rat Snake" or "Blade-teethed Rat Snake".

**Diagnosis.** *Elaphe xiphodonta* sp. nov. can be differentiated from its congeners by the combination of the following morphological characters: (1) medium body size , SVL 785 mm in single adult female; (2) dorsal scales in 21-21-17 rows, the medial 11 rows keeled; (3) supralabials seven or eight, third/fourth (right) or fourth/fifth (left) in contact with eye, infralabials 9 or 10; (4) ventral scales 202–204; (5) subcaudals 67–68; (6) loreal single, not in contact with eye, not in contact with internasals; (7) two preoculars (including one subpreocular), two postoculars; (8) two anterior temporals, three posterior temporals; (9) precloacal plate divided; (10) reduced teeth number in maxilla and dentary bones (MT 9+2, DT 12; (11) sharp edges on the posterior or posterolateral surface of the rear MT and DT; (12) top of head yellow, three distinct

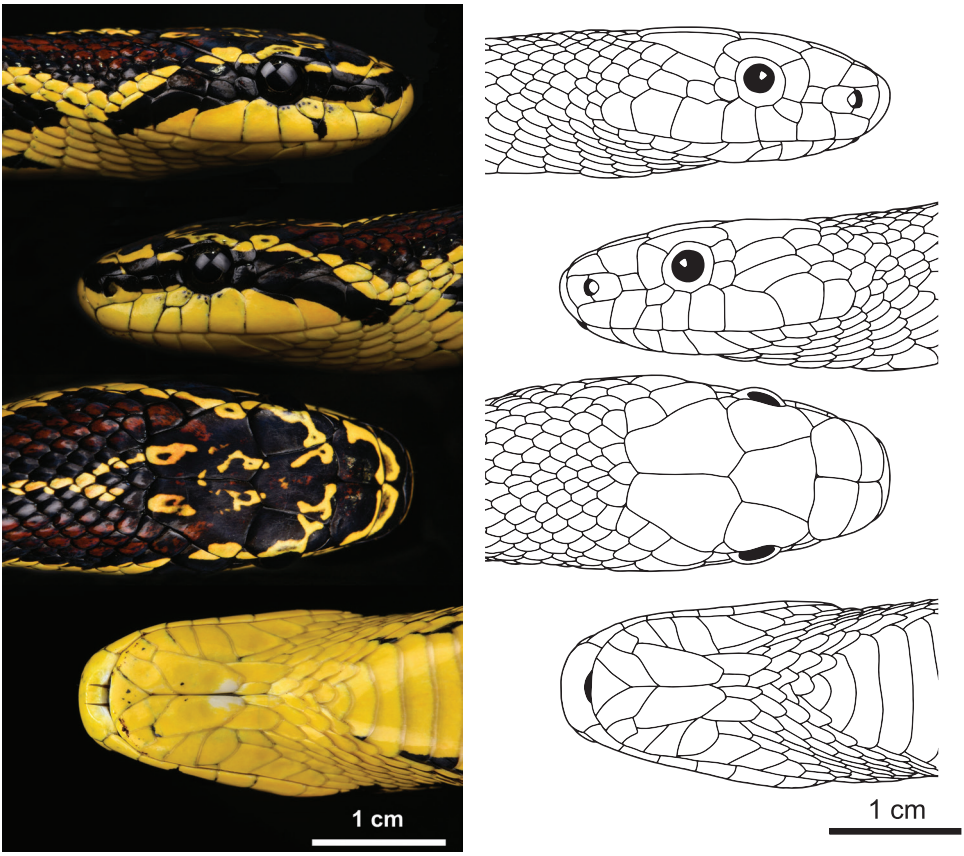


**Figure 2.** Detailed pholidosis of the head of the holotype (SYS r002534) of *Elaphe xiphodonta* sp. nov. Photos by Shuo Qi, illustrated by Xue-Man Zheng.

markings on head and neck; (13) a distinct black labial spot present on supralabials; (14) ground color of dorsum yellow, 46–49 entire (or incomplete) reddish brown blotches with black edges on body and 12–19 similarly colored spots on tail; (15) ventral surface of body yellow with mottled irregular black blotches, a few irregular small red spots dispersed on middle of ventral scales.

**Description of holotype.** Adult female (Figs 1, 2, 3A). Body and tail slender, TL 967.5 mm (SVL 785.2 mm, TaL 182.3 mm, TaL/TL: 0.19); dorsal scales in 21–21–17 rows, the medial 11 rows keeled, the vertebral scales not enlarged; head elongate, moderately distinct from neck, longer than width and narrow anteriorly, HL 26.5 mm, HW 18.1 mm (HW/HL: 0.68); eye medium, ED 3.2 mm, pupil elliptic; rostral triangular, broader than high, RW 7.1 mm, RH 4.5 mm (RW/RH: 1.58; RW/HW: 0.39), visible from dorsum; nostril laterally pointed, located in the middle of nasal; nasal divided into two scales by nostril; two internasals, anteriorly rounded, bordered by two large prefrontals posteriorly; frontal single and enlarged, narrowed posteriorly; parietals paired, longer than width, in contact with each other medially, with upper


**Figure 3.** Comparison between *Elaphe xiphodonta* sp. nov. and sympatric *Protobothrops jerdonii* in different age stages **A** adult *Elaphe xiphodonta* sp. nov. (SYS r002534, holotype) **B** adult *Protobothrops jerdonii* **C** juvenile *E. xiphodonta* sp. nov. (IVPP OV 2721, paratype), road-killed specimen **D** juvenile *P. jerdonii* specimen in preservative. The black arrow points to the labial spot. Photos **A, B, D** by Shuo Qi, photo **C** by Liang Sun.

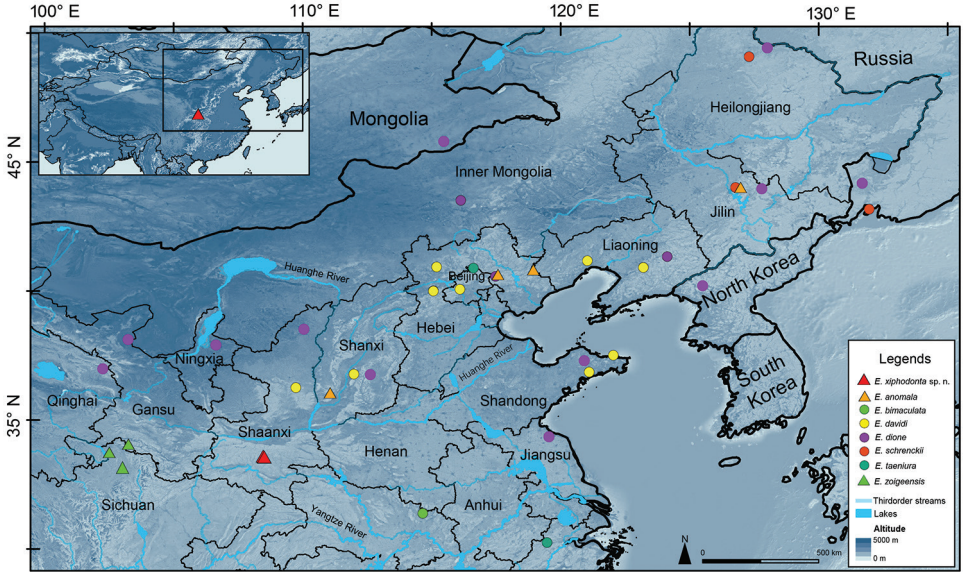


**Figure 4.** Type terra of *Elaphe xiphodonta* sp. nov (marked with red triangles), with the collection localities of some other Chinese species of *Elaphe*.

anterior and posterior temporals laterally; one loreal on each side, in contact with nasal anteriorly, preocular posteriorly, prefrontals dorsally and the second supralabial ventrally; one enlarged preocular in contact with eye and supraocular posteriorly, pre-

**Table 3.** Uncorrected *P*-distance of CO1 gene among 17 *Elaphe* species used in this study.

| | | 1 | 2 | 3 | 4 | 5 | 6 | 7 | 8 | 9 | 10 | 11 | 12 | 13 | 14 | 15 | 16 | 17 |
|---|---|---|---|---|---|---|---|---|---|---|---|---|---|---|---|---|---|---|
| 1 | *Elaphe xiphodonta* sp. nov. | 0.0 | | | | | | | | | | | | | | | | |
| 2 | *E. anomala* | 12.2 | / | | | | | | | | | | | | | | | |
| 3 | *E. bimaculata* | 16.4 | 12.9 | / | | | | | | | | | | | | | | |
| 4 | *E. cantoris* | 14.2 | 17.9 | 18.4 | / | | | | | | | | | | | | | |
| 5 | *E. carinata* | 13.9 | 11.3 | 13.4 | 17.9 | 0.3 | | | | | | | | | | | | |
| 6 | *E. climacophora* | 15.7 | 16.0 | 15.7 | 19.1 | 14.4 | 0.0 | | | | | | | | | | | |
| 7 | *E. davidi* | 14.4 | 12.2 | 11.5 | 19.5 | 13.5 | 13.5 | / | | | | | | | | | | |
| 8 | *E. dione* | 15.3 | 16.0 | 10.9 | 18.2 | 14.3 | 13.9 | 14.2 | / | | | | | | | | | |
| 9 | *E. hodgsonii* | 13.8 | 17.1 | 16.7 | 13.7 | 16.2 | 17.3 | 14.8 | 16.4 | / | | | | | | | | |
| 10 | *E. moellendorffi* | 14.6 | 16.4 | 17.1 | 13.7 | 16.6 | 16.1 | 17.4 | 16.8 | 12.2 | / | | | | | | | |
| 11 | *E. quadrivirgata* | 10.7 | 8.7 | 12.5 | 17.9 | 8.5 | 14.9 | 11.4 | 12.6 | 13.4 | 16.6 | / | | | | | | |
| 12 | *E. quatuorlineata* | 17.1 | 14.1 | 12.5 | 18.4 | 13.8 | 17.9 | 12.5 | 13.6 | 16.1 | 15.8 | 12.5 | / | | | | | |
| 13 | *E. sauromates* | 15.5 | 13.9 | 14.1 | 19.1 | 15.5 | 14.7 | 14.5 | 13.4 | 17.3 | 16.6 | 15.6 | 8.5 | 0.3 | | | | |
| 14 | *E. schrenckii* | 12.2 | 0.0 | 12.9 | 17.9 | 11.3 | 16.0 | 12.2 | 16.0 | 17.1 | 16.4 | 8.7 | 14.1 | 13.9 | / | | | |
| 15 | *E. taeniura* | 15.2 | 16.3 | 16.7 | 16.0 | 16.0 | 15.5 | 15.6 | 15.3 | 13.2 | 16.2 | 13.8 | 14.7 | 16.1 | 16.3 | 6.8 | | |
| 16 | *E. urartica* | 14.1 | 14.0 | 13.9 | 16.8 | 12.7 | 13.7 | 13.3 | 11.8 | 15.2 | 15.6 | 12.5 | 9.4 | 8.9 | 14.0 | 16.5 | 0.0 | |
| 17 | *E. zoigeensis* | 8.4 | 13.3 | 14.9 | 16.9 | 15.0 | 16.4 | 13.3 | 15.5 | 13.5 | 14.6 | 12.3 | 16.0 | 14.2 | 13.3 | 16.3 | 14.0 | 0.0 |

**Table 4.** Uncorrected *P*-distance of cytb gene among 16 *Elaphe* species used in this study.

| | | 1 | 2 | 3 | 4 | 5 | 6 | 7 | 8 | 9 | 10 | 11 | 12 | 13 | 14 | 15 | 16 |
|---|---|---|---|---|---|---|---|---|---|---|---|---|---|---|---|---|---|
| 1 | *Elaphe xiphodonta* sp. nov. | 0.0 | | | | | | | | | | | | | | | |
| 2 | *E. anomala* | 17.1 | / | | | | | | | | | | | | | | |
| 3 | *E. bimaculata* | 13.7 | 17.0 | / | | | | | | | | | | | | | |
| 4 | *E. cantoris* | 17.2 | 16.6 | 18.2 | / | | | | | | | | | | | | |
| 5 | *E. carinata* | 18.7 | 14.1 | 14.6 | 19.1 | 0.0 | | | | | | | | | | | |
| 6 | *E. climacophora* | 17.9 | 11.0 | 16.2 | 19.4 | 12.9 | 0.4 | | | | | | | | | | |
| 7 | *E. davidi* | 18.8 | 15.2 | 12.1 | 17.2 | 14.8 | 15.9 | / | | | | | | | | | |
| 8 | *E. dione* | 19.6 | 19.0 | 15.0 | 15.2 | 18.6 | 17.6 | 16.1 | / | | | | | | | | |
| 9 | *E. hodgsonii* | 16.7 | 15.5 | 17.1 | 14.5 | 17.7 | 15.0 | 14.1 | 19.6 | / | | | | | | | |
| 10 | *E. moellendorffi* | 21.7 | 18.5 | 21.8 | 16.3 | 16.4 | 17.6 | 18.6 | 20.7 | 14.8 | / | | | | | | |
| 11 | *E. quadrivirgata* | 19.7 | 13.1 | 15.4 | 16.9 | 12.6 | 13.3 | 13.8 | 15.5 | 15.8 | 18.9 | 0.9 | | | | | |
| 12 | *E. quatuorlineata* | 16.7 | 13.0 | 16.5 | 14.5 | 13.7 | 11.0 | 13.7 | 15.5 | 17.4 | 17.1 | 11.7 | 0.0 | | | | |
| 13 | *E. sauromates* | 20.0 | 15.3 | 18.6 | 14.3 | 16.0 | 15.5 | 15.4 | 20.8 | 17.2 | 17.5 | 15.6 | 6.8 | / | | | |
| 14 | *E. schrenckii* | 17.7 | 0.4 | 17.6 | 17.2 | 14.7 | 11.6 | 15.2 | 18.3 | 16.1 | 19.1 | 12.5 | 13.5 | 15.9 | / | | |
| 15 | *E. taeniura* | 16.3 | 17.8 | 15.4 | 12.8 | 16.1 | 17.1 | 15.0 | 16.6 | 12.9 | 15.9 | 14.7 | 14.0 | 15.0 | 18.4 | 5.4 | |
| 16 | *E. zoigeensis* | 13.3 | 16.3 | 16.4 | 17.1 | 20.4 | 16.5 | 18.3 | 15.4 | 12.5 | 20.0 | 16.6 | 14.3 | 16.0 | 16.9 | 15.7 | 0.0 |

frontal and loreal anteriorly, a smaller subpreocular ventrally, and not in contact with frontal; subpreocular in contact with eye and the third supralabial posteriorly, the second supralabial anteriorly, and preocular dorsally; two postoculars, upper one in contact with eye anteriorly, supraocular and parietal dorsally, and upper anterior temporal posteriorly, bottom one in contact with eye anteriorly, with upper and lower anterior temporals posteriorly, fifth and sixth supralabials below on left, and with fourth and fifth supralabials below on right; eight supralabials on left, seven supralabials on right (the third and the forth merged relative to left), first and second in contact with nasal, fourth and fifth reaching orbit on left, third and fourth reaching orbit on right; ten infralabials on left, nine infralabials on right, first pair in broad contact with each other, first to fifth in contact with anterior pair of chin shields, fifth in contact with posterior chin shields, fifth infralabial bipartitioned, lower part obviously larger than upper one;

two pairs of chin shields, elongate, anterior pair larger, first pair meeting in midline, posterior pair is separated by three small scales; two similarly sized anterior temporals on left, lower one divided into two small scales on the right; three similarly sized posterior temporals on each side; 204 ventrals, excluding two preventrals; 67 pairs of subcaudals, excluding tail tip; precloacal plate divided.

**Coloration in life.** Dorsal surface of head yellow, three distinct markings on head and neck; the anterior transverse black stripe, somewhat reddish medially, extends from the posterior margin of rostral and through the each eye to last two supralabials and adjacent small scales; interorbital arcuate cross-band, covering anterior part of frontals, most part of prefrontals, top of supraoculars, bottom half of upper postoculars, intact bottom postoculars, bottom half of upper temporals, most of bottom of temporals, dorsal edge of sixth left supralabials (fifth on the right), dorsal half of seventh supralabials (sixth) and bottom half of posterior-most supralabials, not reaching internasals, connected to largest posterior marking from mediolateral part; largest marking is a distinct black "M"-shaped marking that is reddish medially, covering the posteromedial part of the frontals, posterior part of supraoculars, most of parietals, dorsal margin of upper temporals, posteriorly extended, forming two thick black-edged reddish brown stripes on nape. Lateral surface of head yellow, a few small black spots dispersed on supralabials (2, 4 and 5 on left and 2, 3 and 4 on right) and subpreocular, a distinct scutellate black labial spot on the junction of the 2, 3 and right subpreocular (absent on left). Ventral surface of head consistently light-yellow, a few small black spots dispersed on the mental, infralabials, and anterior chin shields. An irregular spot occurs on the posterior edge of the junction of two anterior chin shields. Mouth lining is pale-heather and tongue is black.

Ground color of dorsal surface yellow, 49 complete or incomplete, black-edged reddish brown blotches on body and 12 similarly colored spots on tail; dorsal blotches on body approximately three to five scales in length, and eight to eleven scales rows in width; each blotch is usually composed of reddish brown scale with dark-brown edges. Two rows of smaller, black-edged reddish brown blotches on both side of the larger mid-body blotches, alternating with the mid-body blotches, each blotch covers 2–4 dorsal scales and separated from ventral scales by two rows of the dorsolateral scales. Ground color of ventral surface is yellow, mottled with irregular black blotches, a few irregular small red spots scattered midventrally.

**Intraspecific variation.** Measurements, body proportions and scale and pattern counts of the two specimens are listed in Table 5. The third and fourth supralabials are merged on right in holotype, which leads to the different supralabial counts. Regardless of the slight variation in scalation among the type series of *E. xiphodonta* sp. nov., the color pattern varies considerably between the juvenile and the adult: In adult one (SYS r002534, holotype), the color of the rostral, top and side of head, and chin, as well as dorsal and ventral sections of body are consistently light-yellow, whereas in the juvenile (IVPP OV 2721), the color of head and dorsal body is greyish to olive-green; the ventral scales and subcaudal scales are oyster white, with irregular greyish black spots. The juvenile has a similar dorsal pattern as the adult.

**Table 5.** Measurements and scale counts and body proportions of *Elaphe xiphodonta* sp. nov.

| Voucher | SYS r002534 | IVPP OV 2721 |
|---|---|---|
| **Sex** | female | female |
| **SVL** | 785.2 | 307.5 |
| **TaL** | 182.3 | 62.5 |
| **TL** | 967.5 | 370.1 |
| **TaL/TL** | 0.19 | 0.17 |
| **HL** | 26.5 | 17.64 |
| **HW** | 18.1 | 11.14 |
| **HW/HL** | 0.68 | 0.63 |
| **ED** | 3.2 | 2.8 |
| **RW** | 7.1 | 3.4 |
| **RH** | 4.5 | 2.0 |
| **RW/RH** | 1.58 | 1.70 |
| **RW/HW** | 0.39 | 0.31 |
| **DSR** | 21-21-17 | 21-21-17 |
| **SPL** | 8/7 | 8/8 |
| **IFL** | 10/9 | 11/11 |
| **CS** | 4 (2 pairs) | 4 (2 pairs) |
| **V** | 204 | 202 |
| **SC** | 67 | 67/68 |
| **MT** | 11 (9+2) | 11 (9+2) |
| **Dorsal blotches** | 61 (49+12) | 65(46+19) |

**Skull.** The osteological description is based on a road-killed juvenile individual (Paratype, IVPP OV 2721, Figs 5, 6). The skull is nearly completely preserved except for the slightly crushed parietal, and basioccipital bones.

**Snout (Fig. 5).** The premaxilla is short and blunt. The ascending process is laterally expanded and slanted posteriorly as in many borrowers (e.g., *Euprepiophis* and *Archelaphe*), rendering it hourglass-shaped in anterior view. The transverse process of premaxilla is flat, triangular-shaped in dorsal view. The posterior end of vomerine process of premaxilla contacts the tip of both vomer and septomaxilla. The posteromedial surface of vomerine process is expanded and oval shaped. The anterior section of the dorsal plate of nasal is tapered while the posterior section is expanded as oval shaped. The dorsal surface is slightly bulged.

**Braincase (Fig. 5).** The parietal is blunt and rounded, lacks a lateral crest on each side. The prefrontal is slender, somewhat rectangular. The anterolateral process is blunt. The anterior margin of frontal presents as trapezium-shaped. The lateral margin slightly concave. The postorbital is crescent-shaped, the anterodorsal process does not contact the frontal. The ventral process of postorbital is tapered, not furcated. The supraoccipital is rectangular and compressed, bearing a trifurcated dorsal ridge. The basisphenoid is wide and flat, with no conspicuous ridges on the ventral surface. The rostrum of parasphenoid is not divided. The angular surface between the basisphenoid and basioccipital is smooth. The columella is stubby, the shaft of columella quite short, approximately 1.2 times as length as the diameter of foot plate. The foramina for maxillary branch of trigeminal (f5b) and mandibular branch of trigeminal (f5c) nerves are oval shaped, not reaching the margin of prootic. The f5b is approximately 1/2 the width of f5c.

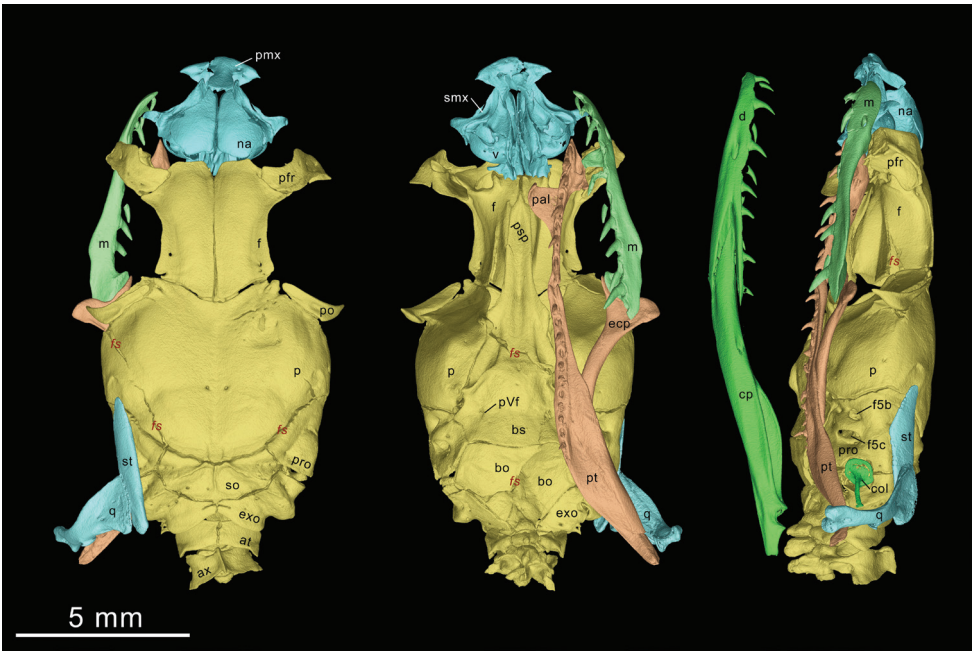


**Figure 5.** Three-dimensional model of the skull of *Elaphe xiphodonta* sp. nov. (IVPP OV 2721, paratype). Left, dorsal view; middle, ventral view; right, lateral view. (Right palatomaxillary arch, mandible and suspensorium are not shown). Implemented by Peng-Fei Yin, Ye-Mao Hou and Jing-Song Shi.

**Palatomaxillary arch (Fig. 6)** The maxilla is slender. The maxillary nutrient foramen is transversely elongate, oval shaped and opens on the anterolateral side at the level of the third maxillary tooth and perforates the maxilla laterally. The anterior portion of maxilla curves slightly inward. The palatine process of maxilla is elongate while the ectopterygoid process is short and bunt.

The maxilla has 11 teeth on each side, with one or two rows of replacement teeth on the lingual side. In contrast to other species of *Elaphe*, the maxillary dentition of the new species is conspicuously differentiated. The anterior five MT have inconspicuous posterolateral ridges, while the posterior six teeth have a sharply edged ridge on their posterior margin (which could be also described as: the posterolateral ridge gradually moved posteriorly by the MT row, forming a sharp cutting edge on the posterior MT), forming blade-like teeth. The MT increase in size posteriorly, the posterior-most two being the largest, not separated from the anterior teeth by a diastema. The cutting edges of the posterior four MT slightly posteriorly convex, rendering them kukri shaped.

The palatine bears nine teeth, with one row of replacement teeth on the labial side. The choanal process of palatine (chp) forms a right triangular in dorsal view. The anterolateral margin of the maxillary process forms an approximate 30° angle with the medial line. The posterior margin of maxillary process is perpendicular to the medial line and collinear with the anterior margin of the choanal process. The pterygoid is slender and lanceolate in shape, 1.8 times the length of palatine, bearing 12 solid teeth

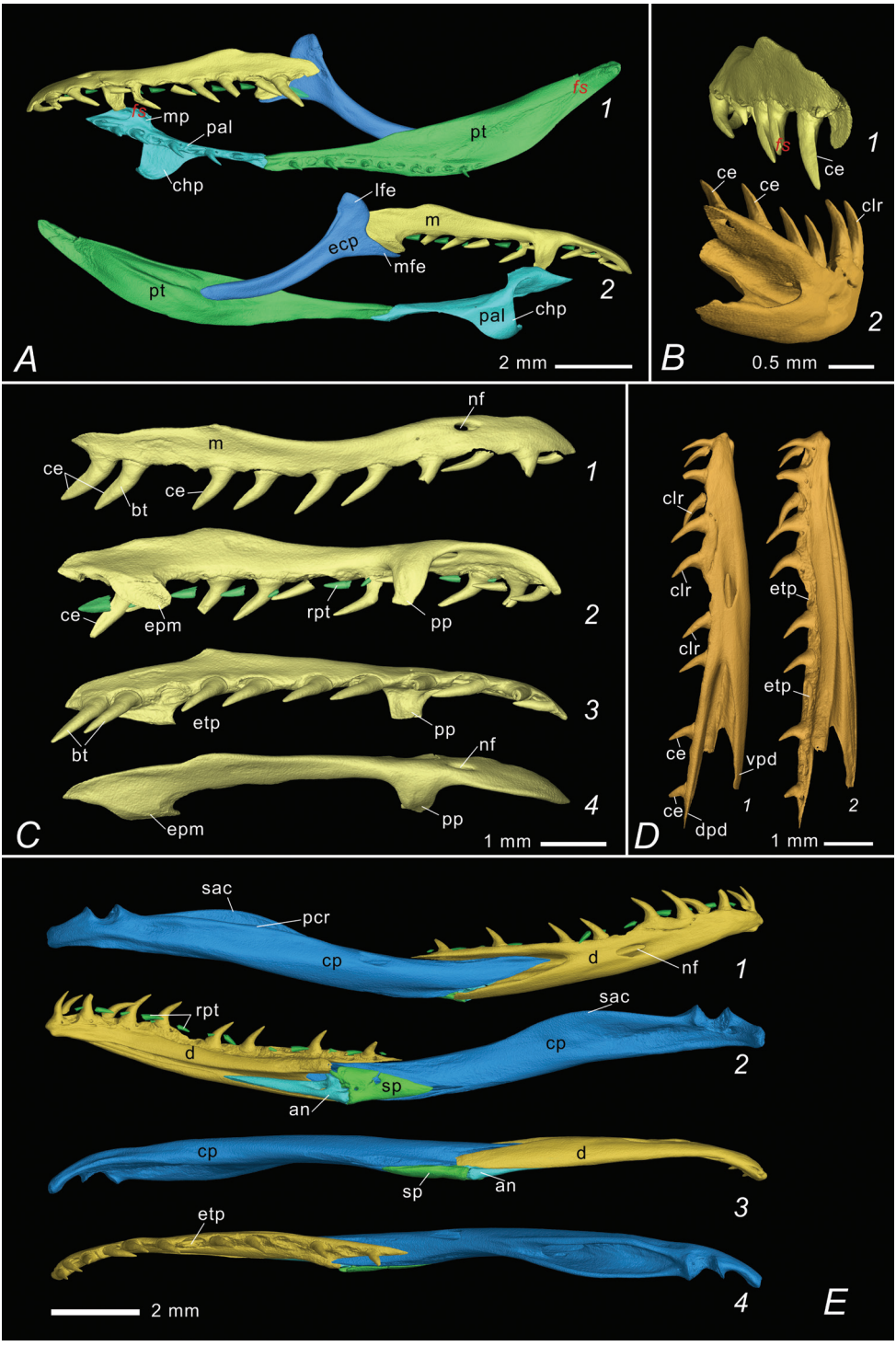
A
fs
mp
pal
chp
pt
fs
1
lfe
m
ecp
mfe
pt
pal
chp
2
2 mm
B
fs
ce
ce
1
ce
ce
clr
2
0.5 mm
C
nf
m
ce
ce
bt
1
ce
epm
rpt
pp
2
bt
etp
pp
3
nf
epm
pp
4
1 mm
D
clr
clr
etp
clr
etp
ce
vpd
ce
dpd
1
2
1 mm
E
sac
pcr
cp
d
nf
1
rpt
sac
d
cp
2
sp
an
cp
d
sp
an
3
etp
4
2 mm

**Figure 6.** Palatomaxillary apparatus and mandibles of *Elaphe xiphodonta* sp. nov. (IVPP OV 2721, paratype). Implemented by Peng-Fei Yin, Ye-Mao Hou and Jing-Song Shi **A** ventral (A1) and dorsal (A2) view of left palatomaxillary apparatus **B** posterolateral view of left maxilla (B1) and right dentary (B2), with cutting edges (ce) and caudolateral ridges indicated **C** labial (C1, right), ventrolateral (C2, left), ventral (C3, right, mirrored) and dorsal (C4, left) view of maxilla **D** Labial (D1) and lingual (D2) view of right dentary **E** labial (E1), lingual (E2), ventral (E3) and dorsal (E4) view of right mandible. Abbreviations: an. angular, at. atlas, ax. axis, bo. basioccipital, bs. basisphenoid, bt. blade teeth ("xiphodont"), ce. Posterior cutting edge of the blade teeth, chp. choanal process of palatine, clr. caudolateral ridge of the teeth, cp. compound bone, d. dentary, dpd. dorsal process of dentary, ecp. ectopterygoid, epm. ectopterygoid process of maxilla, etp. empty tooth position, exo. exoccipital, f. frontal, f5b. foramen for maxillary branch of trigeminal, f5c. foramen for mandibular branch of trigeminal, lf. lacrimal foramen, lfe. lateral furcula of ectopterygoid, m. maxilla, na. nasal, mfe. mesial furcula of ectopterygoid, mp. maxillary process of palatine, nf, nutrient foramen, p. parietal, pcr. prearticular crest of compound bone, pfr. prefrontal, pmx. premaxilla, po. postorbital, pp. palatine process of maxilla, pro. prootic, psp. parasphenoid rostrum, pt. pterygoid, pVf. posterior Vidian foramen, rpt. replacement teeth, sac. surangular crest of compound bone, smx, septomaxilla, so. supraoccipital, sp. splenial, st. supratemporal, v. vomer, vpd. ventral process of dentary, *fs.* fracture surface.

(with one row of replacement teeth on the labial side). The ectopterygoid process and the medial transverse process of pterygoid are very small and difficult to see. The ectopterygoid is horizontally expanded, and outwardly curved in dorsal view. The labial furcula of ectopterygoid is oval, and distinct from the lingual process. The medial furcula (medial process) is elongate and spiculate, slightly curved ventrally.

**Suspensorium and mandible (Figs 5, 6)** The mandible is slender and moderately curved. The supratemporal is flat and slender, fusiform, and the anteroventral margin is slightly angulated upward. The quadrate is triangulated in lateral view, and approximately the same length as supratemporal. The supratemporal angular surface of the quadrate is expanded, elongated and oval shaped. The prearticular crest (pcr) of the compound bone is prominent while the surangular crest (sac) is absent. The angular is slender and triangular. The splenial is triangular, coracoid shaped and shorter than angular. The dental bone bears 13 teeth, decreasing in size at the fifth tooth, with one or two rows of replacement teeth on the lingual side. The posterior tip of dorsal process of dentary extends farther posteriorly than the ventral process. The largest dentary nutrient foramen is elongated-oval shaped and lies below the seventh tooth.

**Dentition (IVPP OV 2721, paratype)** Maxilla: 11/11 (9+2); pterygoid: 12/12; palatine: 9/9; dentary: 13/13. Dentitional comparisons within the genus *Elaphe* and some related colubrid groups are listed in Table 6.

**Comparisons.** Detailed comparisons among *Elaphe* species are given in Table 7 and Fig. 7.

*Elaphe xiphodonta* sp. nov. is distinct from all of its congeners by having fewer MT, enlarged posterior MT, cutting edges on both MT and DT, and three rows of large, black-bordered reddish brown dorsal blotches.

Additionally, *Elaphe xiphodonta* sp. nov. can be distinguished from *E. cantoris*, *E. climacophora* (Boie, 1826), *E. hodgsoni*, *E. moellendorffi*, and *E. taeniura* by having

**Table 6.** Dentition comparison of the *Elaphe* species and related colubrid species.

| Taxon (*n*) | Maxillary | Blade teeth | Palatine | Pterygoid | Dentary | Reference |
|---|---|---|---|---|---|---|
| ***Elaphe*** | | | | | | |
| *E. xiphodonta* sp. nov. (1) | 11/11 | Y | 9/9 | 12/12 | 13/13 | this study |
| *E. bimaculata* (1) | 19/20 | N | 9/10 | 15/16 | 18/19 | this study |
| *E. carinata* (5) | 17 | N | 9–11 | 13–16 | 19–21 | this study |
| *E. climacophora* (2) | 17 | N | 11 | 17–20 | 23–25 | Helfenberger and Schätti 1998 |
| *E. dione* (2) | 16–20 | N | 7–9 | 12–13 | 18–23 | this study |
| *E. davidi* (3) | 16–17 | N | 9–12 | 12–16 | 16–19 | Helfenberger and Schätti 1998 |
| *E. moellendorffi* (2) | 22–23 | N | 11 | 19–22 | 27–29 | this study |
| *E. schrenckii* (2) | 16–17 | N | 10–11 | 12–13 | 19–21 | this study |
| *E. taeniura* (3) | 17–23 | N | 10–11 | 16–19 | 19–23 | this study |
| *E. zoigeensis* (2) | 14–17 | Y | 10–10 | 10–13 | 16–17 | this study |
| ***Euprepiophis*** | | | | | | |
| *Eu. mandarinus* (2) | 16–19 | Y | 10–11 | 19–24 | 19–22 | this study |
| *Eu. perlaceus* (2) | 20–20 | Y | 12–12 | 18–21 | 21–22 | this study |
| ***Coelognathus*** | | | | | | |
| *C. flavolineatus* (1) | 23 | N | 11/13 | 25/26 | 27/28 | this study |
| *C. philippinus* (1) | 25 | N | 12/13 | 26/27 | 29/28 | this study |
| *C. radiatus* (5) | 20–23 | Y | 10–12 | 18–24 | 23–27 | this study |
| ***Oligodon*** | | | | | | |
| *Ol. ornatus* (1) | 8/8 | Y | 4/4 | 5/5 | 13/13 | this study |
| ***Oocatochus*** | | | | | | |
| *Oo. rufodorsatus* (2) | 18–19 | Y | 10–11 | 17–18 | 21–23 | this study |
| ***Gonyosoma*** | | | | | | |
| *G. oxycephalum* (1) | 23/23 | N | 10/10 | 14/13 | 26/26 | this study |
| ***Ptyas*** | | | | | | |
| *P. carinata* (2) | 24–25 | Y | 17–15 | 19–20 | 22 | this study |
| *P. dhumnades* (1) | 26 | Y | 21/20 | 23 | 26 | this study |
| ***Dasypeltis*** | | | | | | |
| *D. scabra* (2) | 7–6 | N | 8–9 | 0 | 3–3 | Helfenberger and Schätti 1998 |
| ***Thermophis*** | | | | | | |
| *T. zhaoermii* (2) | 19–21 | Y | 12–16 | 18–23 | 21/24 | this study |

Abbreviations: *n.* number of referenced specimens (if $N = 1$, the dentition count are listed as: left/right; $N > 1$: minimum – maximum).

**Table 7.** Diagnostic characters separating all 17 species of the *Elaphe*, with distinguishing characters marked in bold. *: Counts of PrO contain subpreocular.

| Species | maximum SVL (in mm) | DSR | SPL | IFL | PrO* | PtO | TMP | V | SC |
|---|---|---|---|---|---|---|---|---|---|
| *Elaphe xiphodonta* sp. nov. | 785 | 21-21-17 | 8 (7) | 9 (10) | 2 | 2 | 2+3 | 202–204 | 67–68 |
| *Elaphe anomala* | **1925** | 23 (21–25)-23 (19–23)-19 (17–19) | 8 | 9–11 | 2 (1) | 2 (1) | 2 (3)+3 (2) | 203–225 | 45–77 |
| *Elaphe bimaculata* | 760 | **23 (23–25)-23 (21–25)-19 (21)** | 8 (7) | 9–12 | 2 (1) | 2 | 2+3 | 170–209 | 61–81 |
| *Elaphe cantoris* | **1158** | 19 (20, 21)-19 (21–23)-17 | 8 | 9–10 | 2 | 2 | 2+3 (2) | **226–239** | **78–87** |
| *Elaphe carinata* | **> 2000** | 23 (21–25)-23 (21–25)-19 (17) | 8 (9) | 9–12 | 2 (1) | 2 | 2+3 | 186–227 | **69–102** |
| *Elaphe climacophora* | **> 1500** | **NA-23 (25)-NA** | 8 (9) | 11 | 2 | 2 | 2+3 (2) | **222–236** | **97–116** |
| *Elaphe davidi* | **1227** | **25 (22–27)-23 (22–25)-19 (17–21)** | 8 (7) | **11–13** | 2 (1, 3) | 2 (1–4) | 2 (1, 3)+4 (2–3) | **155–183** | 53–72 |
| *Elaphe dione* | 893 | 25 (21–27)-25 (21–27)-19 (17–21) | 8 (9) | 9–11 | 2 (1) | 2 | 2+3 | 168–206 | 51–84 |
| *Elaphe hodgsoni* | **1190** | 23 (21–25)- 23 (21–25)-17 | 8 (9) | 9–12 | 2 (1) | 2 | 2 (1, 3)+3 (2, 4) | **228–247** | **72–92** |
| *Elaphe moellendorffi* | **1602** | **25 (23–27)-27 (5)-19 (21)** | **9 (10)** | 10–13 | 2 | 2 | 2 (3)+3 (4) | **270–278** | **92–102** |
| *Elaphe quadrivirgata* | **>1000** | **NA-19-NA** | 8 | **11** | 2 | 2 | 2 (1)+3 (2) | 195–215 | **70–96** |
| *Elaphe quatuorlineata* | **> 2000** | **25-25 (23–27)-19** | 8 (9) | 11 | 2 (3) | 2 (3) | 2 (3)+3 (4) | 187–234 | 56–90 |
| *Elaphe sauromates* | **1250** | **25 (21–27)-25 (23, 24)-19 (18–21)** | 8 (7–10) | 11 (9–12) | 2 (1, 3) | 2 (1) | 2(1, 3)+ 4 (2–5) | 199–222 | 61–79 |
| *Elaphe schrenckii* | **1335** | **23 (21)-23 (21)-19** | 8 (7) | 8–11 | 2 (1) | 2 | 2+3 (2) | **208–224** | 57–75 |
| *Elaphe taeniura* | **> 2000** | **25 (23)-23 (21, 25)-19 (17)** | 9 (6–10) | 9–13 | 2 (1) | 2 (3) | 2 (1, 3)+3 (2–5) | **223–261** | **73–121** |
| *Elaphe urartica* | 970 | **25 (23, 24)- 25 (23, 24)-19 (18)** | 8 (9) | 11 (10–13) | 2 (1, 3) | 2 (1, 3) | 2 (3)+ 4 (2, 3) | 154–211 | 60–74 |
| *Elaphe zoigeensis* | 722 | 21-19(21)-17 | 7–8 | 9 | **3** | 2 | 2+3(2) | 202–212 | 68–79 |


**Figure 7.** Comparisons of general morphological characteristics with its congeners in China **A** *Elaphe xiphodonta* sp. nov. (SYS r002534, holotype), Ningshaan, Shaanxi, by Shuo Qi **B** *E. anomala*, Benxi, Liaoning, by Shuo Qi **C** *E. bimaculata*, Hong'an, Hubei, by Chong-Jian Zhou **D** *E. cantoris*, Bomê, Tibet, by Jing-Song Shi **E** *E. carinata*, Mentougou, Beijing, by Jing-Song Shi **F** *E. davidi*, Benxi, Liaoning, by Jing-Song Shi **G** *E. dione*, Yongdeng, Gansu, by Shuo Qi **H** *E. hodgsonii*, Gyirong, Tibet, by Shuo Qi **I** *E. moellendorffi*, Chongzuo, Guangxi, by Jia-Jun Zhou **J** *E. schrenckii*, Baishan, Jilin, by Shuo Qi **K** *E. taeniura* from Hangzhou, Zhejiang, by Wei-Liang Xie **L** *E. zoigeensis*, Jiuzhaigou, Sichuan, by Jin-Wang.

fewer ventral scales (202–204 vs. 226–239 in *E. cantoris*, 222–236 in *E. climacophora*, 228–247 in *E. hodgsoni*, 270–278 in *E. moellendorffi*, and 223–261 in *E. taeniura*), fewer subcaudals (67–68 vs. 78–87 in *E. cantoris*, 97–116 in *E. climacophora*, 72–92 in *E. hodgsoni*, 92–102 in *E. moellendorffi*, and 73–121 in *E. taeniura*), smaller body size (SVL 785 mm in single adult female vs. maximum SVL 1158 mm in *E. cantoris*, > 2000 mm in *E. climacophora*, 1190 mm in *E. hodgsoni*, 1602 mm in *E. moellendorffi*, and > 2000 mm in *E. taeniura*), and vastly different color pattern (Table 7).

*Elaphe xiphodonta* sp. nov. can be differentiated from *E. quatuorlineata* Lacepede, 1789, *E. sauromates* (Pallas, 1811) and *E. urartica* (Jablonski, Kukushkin, Avci, Bunyatova, Ilgaz, Tuniyev & Jandzik, 2019) by having fewer dorsal scale rows (21-21-17

vs. 25-25 (23–27)-19 in *E. quatuorlineata*, 25 (21–27)-25 (23, 24)-19 (18–21) in *E. sauromates* and 25 (23, 24)- 25 (23, 24)-19 (18) in *E. urartica*) and a vastly different color pattern. Beyond that, *E. xiphodonta* sp. nov. can be further differentiated from *E. quatuorlineata* and *E. sauromates* by its smaller body size (SVL 785 mm in single adult female vs. maximum SVL > 2000 mm in *E. quatuorlineata* and 1250 mm in *E. sauromates*).

*Elaphe xiphodonta* sp. nov. can be differentiated from *Elaphe carinata*, *E. davidi* and *E. quadrivirgata* (Boie, 1826) by its smaller body size (SVL 785 mm in single adult female vs. maximum SVL > 2000 mm in *E. carinata*, 1227 mm in *E. davidi*, and > 1000 mm in *E. quadrivirgata*), having fewer subcaudals (67–68 vs. 69–102 in *E. carinata*, 70–96 in *E. quadrivirgata*), and a vastly different color pattern.

Despite the morphological similarities to *E. bimaculata*, *E. dione*, and *E. zoigeensis*, *Elaphe xiphodonta* sp. nov. differs from them by having different dorsal scale row counts (21-21-17 vs. 23 (23–25)-23 (21–25)-19 (21) in *E. bimaculata*), fewer preoculars (2 vs. 3 in *E. zoigeensis*), fewer MT (11/11 vs. 19/20 in *E. bimaculata*, 16–20 in *E. dione*, and 14–17 in *E. zoigeensis* (Table 6), blade-like posterior MT and the unique color pattern within the genus *Elaphe*.

**Molecular phylogeny.** The ML and BI analyses produced identical topologies, which were integrated in Fig. 8. The pairwise distances based on CO1 and cytb genes among all species are given in the Tables 3, 4, respectively.

The phylogenetic analyses recovered a strongly supported monophyletic lineage containing all *Elaphe* (BS 100; BPP 1.00) which can be divided into three strongly supported clades (BS 95–97; BPP 1.00). Clade 1 includes all species previously in the genus "*Orthriophis*" with strong nodal support (BS 95; BPP 1.00). Notable intraspecific genetic differentiation within *E. taeniura* (mean *p*-distances 6.8% in CO1, 5.4% in cytb), pertains to different geographical clades.

The two samples from Chengguan Town, Shaanxi are clustered together with strong support (BS 100; BPP 1.00) with nearly no molecular divergence (mean *p*-distances 0% in CO1, 0% in cytb) between them. The clade of the above-mentioned specimens constitutes a sister clade with *E. zoigeensis* (Clade2, mean *p*-distances 8.4% in CO1, 13.3% in cytb).

Within Clade 3, the relationship between *Elaphe anomala* and *E. schrenckii* are worth noting. These two species form a strongly supported monophyletic group (BS 100; BPP 1.00) bearing low interspecific molecular divergence (mean *p*-distances 0.0% in CO1, 0.4% in cytb), suggesting they may be different color morphs of the same species, as mention before (An et al. 2010). However, given their distinctive color pattern differences and obvious geographical separation, we follow the current taxonomy.

Based on their phylogenetic relationships, genetic differentiation, and morphological distinctiveness (see Taxonomic accounts below), we hypothesize that the population from Chengguan Town, Shaanxi represents a separately evolving lineage and should be described as a new species.

**Distribution, ecology and habit.** *Elaphe xiphodonta* sp. nov. is currently known only from the Chengguan Town, Ningshaan County, Shaanxi Province, China. The

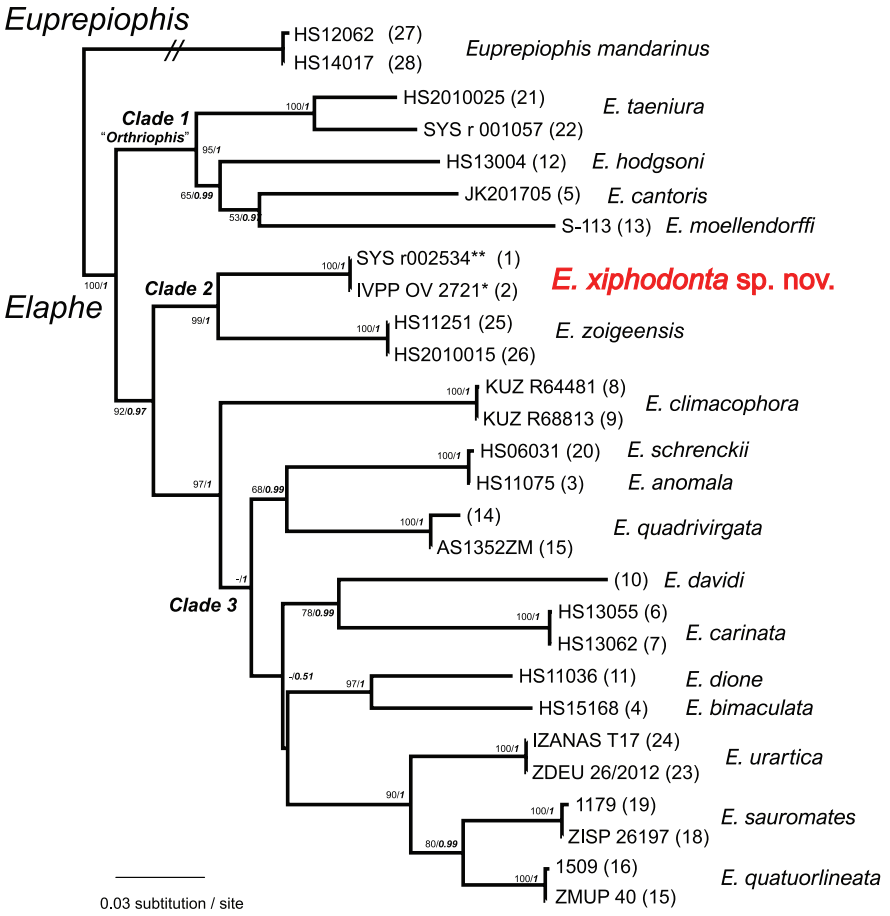


**Figure 8.** Bayesian inferenced topology of 13 *Elaphe* species, based on the four partial mitochondrial DNA sequences (12S rRNA, 16S rRNA, CO1 and Cytb genes). BPP and BS values, respectively, occur at the nodes.

new species inhabits sunny or semi-sunny gravels and bushes on slopes of less than 20°, along Chang'an River with an average width of 3 m. Elevation of the habitat ranges from 1700 to 1900 m. The vegetation types are *Abies fargesii* forest with artificial *Picea asperata*, *Salix fargesii*, *Rubus koereana*, *Betula albosinensis* and *Fargesia qinlingensis*. The canopy density is 0.75 (Bu and Zheng 2015). The new species is sympatric with *Nanorana unculuanus*, *Scutiger ningshanensis*, *Euprepiophis perlaceus*, *Rhabdophis nuchalis*, *Stichophanes ningshaanensis*, *Gloydius qinlingensis* and *Protobothrops jerdonii* (Fig. 9). When being captured, the new species flattens its head triangular and releases scent from the cloacal scent glands with smells a bit similar to *P. jerdonii*.

In feeding habits, the fecal samples from the holotype were checked and contained only feathers, indicating that this species is at least a bird-eater. The holotype was observed to prey on captive nesting quail and quail egg.

**Figure 9.** Habitats of *Elaphe xiphodonta* sp. nov. (Ningshaan County, Shaanxi), Provide by Shu-Hai Bu.

## Discussion

This study described a new *Elaphe* species which has a unique coloration and specialized teeth and had been overlooked for a long time during previous surveys. The new species was mistaken for *P. jerdonii*, which it mimics, at first glance during the field work. Nevertheless, the mimicry in *E. xiphodonta* is not unique within *Elaphe*. The coloration and head shape of *E. davidi* mimics that of the sympatric *Gloydius* spp. (Zhao 2006). *Gloydius qinlingensis* and *Protobothrops jerdonii* are sympatric with *E. xiphodonta*. *Elaphe xiphodonta* is similar to *P. jerdonii* in body shape, coloration, pattern and cloacal gland odor. Therefore, we hypothesize that *E. xiphodonta* is mimicking the model *P. jerdonii* as a means to avoid predation. Additional observations concerning the potential mimic-model relationship between *E. xiphodonta* and *P. jerdonii* are necessary.

*Elaphe dione* was previously widely recorded from northern China (Zhao 2006). Its distribution is currently restricted to Qinling Mountains-Huaihe River Line, and the records from other localities may belong to different taxa (e.g., *E. zoigeensis*, Huang et al. 2012). Previously collected specimens designated as *E. dione* (e.g., Fang and Song 1981) from Ningshaan County and surrounding areas are worth carefully re-examining.

Based on the dentition comparison in Table 6, it is clear that *E. xiphodonta* has far fewer MT and DT than most other species of *Elaphe*, which have more than 14 MT and DT. The tooth morphology of *E. xiphodonta* is similar to that of the genus

*Oligodon* in a number of ways. Their reduced number and the specialized shape might relate to their unusual diet, since the morphology of the teeth in snakes have yet to be correlated with diet and prey-handling behaviors (Cundall and Irish 2008; Shi 2020). Some lizard-eating snakes tend to have numerous and closely spaced teeth (e.g., *Scaphiodontophis*, *Sibynophis* and *Liophidium* Zaher et al., 2012) while many oophagous snakes have reduced numbers of MT and DT (e.g., *Dasypeltis*). Blade-like rear teeth (sickle or kukri in shape, with sharp cutting edges on the posterior margins of two or more posterior MT) occur widely in many clades of the superfamily Colubroidea (e.g., Colubridae, Dipsadidae, Natricidae and Pseudoxenodontidae), most of which are anuran predators (e.g., *Heterodon*, *Hydrodynastes* and *Rhabdophis*) while some of the others tend to feed on eggs (e.g., *Oligodon*, *Prosymna* and *Cemophora*) or lizards (e.g., *Orientocoluber* and *Hemorrhois*). The diet and prey behaviors of the above-mentioned snakes have been widely reported in previous studies (Henderson 1984; Cundall and Greene 2000; Cundall and Irish 2008; Zaher et al. 2012), whereas far fewer comprehensive studies have focused on the function of blade-like teeth. A recent study indicated that a large proportion of anuran predators have blade-like rear teeth. Some snakes have been observed to deflate their anuran prey by puncturing and slicing their skin (e.g., *Pseudoagkistrodon rudis*; Shi 2020) or to consume the egg liquid (or embryos) of reptile eggs by cutting through their shells (e.g., *Oligodon*, *Prosymna* and *Cemophora*). Hence, we speculate that *E. xiphodonta* preys on frogs or eggs in the wild. In view of the limited numbers of the specimens in the present study, further field observation is needed to verify the above-mentioned hypothesis.

## Acknowledgements

We are grateful to Li Ding for sharing important specimens for osteological comparison, to Fan Yang, Shi-Chao He, Zi-Chuan Wei, Jun Yan, Liang Sun, Jun-Dong Deng, Zong-Chang Yang, Bo Tan, Zhao-Chi Zeng and Zhi-Tong Lyu for their help in the field and the preparation of the manuscript; to Jin-Wang, Jia-Jun Zhou, Wei-Liang Xie, Chong-Jian Zhou and Liang Sun for providing important photographs; to Ye-Mao Hou, Peng-Fei Yin and Hao Ding for their assistance with CT scanning and three-dimensional reconstruction; to Xue-Man Zheng for the help with illustrations, and to Sheng Zheng for providing priceless literature references. We thank Dr. Luis Ceríaco, Dr. Robert Jadin and an anonymous reviewer for their helpful comments and suggestions on the manuscript.

This study is supported by "the Second Tibetan Plateau Scientific Expedition and Research Program" (Grant No. 2019QZKK0705), "the Specimen Platform of Ministry of Science and Technology, China, teaching specimen's sub-platform" (No. 2005DKA21403-JK) and "the National Park Project of Central Financial Subsidy" (No. ZX2020-09-43).

## References

An JH, Park DS, Lee JH, Kim KS, Lee H, Min MS (2010) No Genetic Differentiation of *Elaphe schrenckii* Subspecies in Korea Based on 9 Microsatellite Loci. Animal Systematics Evolution and Diversity 26(1): 15–19. https://doi.org/10.5635/KJSZ.2010.26.1.015

Burbrink FT, Lawson R (2007) How and when did Old World rat snakes disperse into the New World? Molecular Phylogenetics and Evolution 43(1): 173–189. https://doi.org/10.1016/j.ympev.2006.09.009

Bates HW (1862) Contributions to an Insect Fauna of the Amazon Valley. Lepidoptera: Heliconidae. Transactions of the Linnean Society 23(3): 495–566. https://doi.org/10.1111/j.1096-3642.1860.tb00146.x

Boulenger GA (1894) Catalogue of the Snakes in the British Museum (Natural History) (Vol. II) Containing the Conclusion of the Colubridae Aglyphae. Trustees of the British Museum (Natural History). Taylor and Francis, London.

Brodie III ED (1993) Differential avoidance of coral snake banded patterns by free-ranging avian predators in Costa Rica. Evolution 47(1): 227–235. https://doi.org/10.1111/j.1558-5646.1993.tb01212.x

Bu S, Zheng X (2015) An illustrated guide to wildlife in Huoditang forest region of Qinling Mountain. Science Press, Beijing, 71–79. [in Chinese]

Burbrink FT, Pyron RA (2010) How does ecological opportunity influence rates of speciation, extinction, and morphological diversification in New World rat snakes (tribe Lampropeltini)? Evolution 64: 934–943. https://doi.org/10.1111/j.1558-5646.2009.00888.x

Carpenter GDH, Ford EB (1933) Mimicry. Methuen, London.

Castresana J (2000) Selection of conserved blocks from multiple alignments for their use in phylogenetic analysis. Molecular Biology and Evolution 17: 540–552. https://doi.org/10.1093/oxfordjournals.molbev.a026334

Che J, Jiang K, Yan F, Zhang YP (2020) Amphibians and Reptiles in Tibet: Diversity and Evolution. Science Press, Beijing, 648–659. [In Chinese]

Chen X, Lemmon AR, Lemmon EM, Pyron AR, Burbrink FT (2017) Using phylogenomics to understand the link between biogeographic origins and regional diversification in rat snakes. Molecular Phylogenetics and Evolution 111: 206–218. https://doi.org/10.1016/j.ympev.2017.03.017

Cundall D, Greene HW (2000) Feeding in snakes. In: Schwenk K (Ed.) Feeding: Form, Function and Evolution in Tetrapod Vertebrates. Academic Press, San Diego. https://doi.org/10.1016/B978-012632590-4/50010-1

Cundall D, Irish F (2008) The Snake Skull. Biology of the Reptilia. Contributions to Herpetology, New York.

Dowling HG (1951) A proposed standard system of counting ventral in snakes. Journal of Herpetology 1: 97–99. https://doi.org/10.2307/1437542

Fang RS, Song MT (1981) A preliminary survey of snakes from southern slope of Eastern Qinling Mountains. Journal of Shaanxi Normal University (Natural Science Edition): 263–272.

Figueroa A, Mckelvy AD, Grismer LL, Bell CD, Lailvaux SP (2016) A species-level phylogeny of extant snakes with description of a new Colubrid subfamily and genus. PLoS ONE 11(9): e0161070. https://doi.org/10.1371/journal.pone.0161070

Helfenberger N (2001) Phylogenetic relationships of Old-World rat snakes based on visceral organ topography, osteology, and allozyme variation. Russian Journal of Herpetology 8: 1–62.

Helfenberger N, Schätti B (1998) Morphological adaptations for egg-eating in the snake *Elaphe davidi* Sauvage 1884. Russian Journal of Herpetology 5(1): 36–42.

Henderson RW (1984) The Diet of the Hispaniolan Snake *Hypsirhynchus ferox* (Colubridae). Amphibia Reptilia5: 367–371. https://doi.org/10.1163/156853884X-005-03-17

Hou YM, Cui XD, Canul-Ku M, Jin SC, Hasimoto-Beltran R, Guo QH, Zhu M (2020) AD-Morph: a 3D Digital Microfossil Morphology Dataset for Deep Learning. IEEE Access 8: 148744–148756. https://doi.org/10.1109/ACCESS.2020.3016267

Huang S, Ding L, Burbrink FT, Yang J, Huang J, Ling C, Chen X, Zhang Y (2012) A new species of the genus *Elaphe* (Squamata: Colubridae) from Zoige County, Sichuan, China. Asian Herpetological Research 3(1): 38–45. https://doi.org/10.3724/SP.J.1245.2012.00038

Huelsenbeck JP, Ronquist F, Nielsen R, Bollback JP (2001) Bayesian Inference of Phylogeny and Its Impact on Evolutionary Biology. Science 294: 2310–2314. https://doi.org/10.1126/science.1065889

Jablonski D, Kukushkin OV, Avcı A, Bunyatova S, Kumlutaş Y, Ilgaz Ç, Polyakova E, Shiryaev K, Tuniyev B, Jandzik D (2019) The biogeography of *Elaphe sauromates* (Pallas, 1814), with a description of a new rat snake species. PeerJ 7: e6944. https://doi.org/10.7717/peerj.6944

Jablonski D, Soltys K, Kukushkin OV, Simonov E (2019) Complete mitochondrial genome of the Blotched snake, *Elaphe sauromates* (Pallas, 1814). Mitochondrial DNA Part B 4(1): 468–469. https://doi.org/10.1080/23802359.2018.1551083

Kuriyama T, Brandley MC, Katayama A, Mori A, Honda M, Hasegawa M (2011) A time-calibrated phylogenetic approach to assessing the phylogeography, colonization history and phenotypic evolution of snakes in the Japanese Izu Islands. Journal of Biogeography 38: 259–271. https://doi.org/10.1111/j.1365-2699.2010.02403.x

Lanfear R, Calcott B, Ho SY, Guindon S (2012) PartitionFinder: combined selection of partitioning schemes and substitution models for phylogenetic analyses. Molecular Biology and Evolution 29(6): 1695–1701. https://doi.org/10.1093/molbev/mss020

Lenk P, Joger U, Wink M (2001) Phylogenetic relationships among European rat snakes of the genus *Elaphe* Fitzinger based on mitochondrial DNA sequence comparisons. Amphibia-Reptilia 22(3): 329–339. https://doi.org/10.1163/156853801317050124

Li JN, He C, Guo P, Zhang P, Liang D (2017) A workflow of massive identification and application of intron markers using snakes as a model. Ecology and Evolution 7: 10042–10055. https://doi.org/10.1002/ece3.3525

Li JN, Liang D, Wang YY, Guo P, Huang S, Zhang P (2020) A large-scale systematic framework of Chinese snakes based on a unified multilocus marker system. Molecular phylogenetics and evolution 148: e106807. https://doi.org/10.1016/j.ympev.2020.106807

Moriyama J, Takeuchi H, Ogura-Katayama A, Hikida T (2018) Phylogeography of the Japanese rat snake, *Elaphe climacophora* (Serpentes: Colubridae): impacts of Pleistocene climatic oscillations and sea-level fluctuations on geographical range. Biological Journal of the Linnean Society 124: 174–187. https://doi.org/10.1093/biolinnean/bly066

Ronquist F, Teslenko M, Van Der Mark P, Ayres DL, Darling A, Höhna S, Larget B, Liu L, Suchard MA, Huelsenbeck JP (2012) MrBayes 3.2: efficient Bayesian phylogenetic in-

ference and model choice across a large model space. Systematic Biology 61: 539–542. https://doi.org/10.1093/sysbio/sys029

Ruxton GD, Sherratt TN, Speed MP (2004) Avoiding Attack: The Evolutionary Ecology of Crypsis, Warning Signals and Mimicry. Oxford University Press, Oxford. https://doi.org/10.1093/acprof:oso/9780198528609.001.0001

Schulz K-D (1996) A monograph of the colubrid snakes of the genus *Elaphe*, Fitzinger. Koeltz Scientific Books, Hessen, 439 pp.

Silvestro D, Michalak I (2012) RaxmlGUI: a graphical front-end for RAxML. Organisms Diversity and Evolution 12: 335–337. https://doi.org/10.1007/s13127-011-0056-0

Shi JS, Jiang ZW, Zhao W, Shi Y (2019) *Elaphe zoigeensis* Found in Tewo Country, Gansu Province. Chinese Journal of Zoology 54(5): 769–770.

Shi JS (2020) Morphological diversity and character evolution of the maxillary teeth in Colubroidea (Reptilia: Serpentes). University of Chinese Academy of Sciences.

Stejneger L (1907) Herpetology of Japan and adjacent territory. Bulletin of the United States National Museum 58: 1–577. https://doi.org/10.5479/si.03629236.58.i

Tamura K, Stecher G, Peterson D, Filipski A, Kumar S (2013) MEGA6: molecular evolutionary genetics analysis, version 6.0. Molecular Biology and Evolution 30: 2725–2729. https://doi.org/10.1093/molbev/mst197

Thanou E, Kornilios P, Lymberakis P, Leaché AD (2020) Genomic and mitochondrial evidence of ancient isolations and extreme introgression in the four-lined snake. Current Zoology 66(1): 99–111. https://doi.org/10.1093/cz/zoz018

Thompson JD, Gibson TJ, Plewniak F, Jeanmougin F, Higgins DG (1997) The CLUSTAL_X windows interface: flexible strategies for multiple sequence alignment aided by quality analysis tools. Nucleic Acids Research 25: 4876–4882. https://doi.org/10.1093/nar/25.24.4876

Uetz P, Freed P, Hošek J [Eds] (2021) The Reptile Database. http://www.reptile-database.org [accessed March 2, 2021]

Utiger U, Helfenberger N, Schätti B, Schmidt C, Ruf M, Ziswiler V (2002) Molecular systematics and phylogeny of Old World and New World ratsnakes, *Elaphe auct*., and related genera (Reptilia, Squamata, Colubridae). Russian Journal of Herpetology 9(2): 105–124.

Wang K, Ren JL, Chen HM, Lyu ZT, Guo XG, Jiang K, Chen JM, Li JT, Guo P, Wang YY, Che J (2020) The updated checklists of amphibians and reptiles of China. Biodiversity Science 28(2): 189–218.

Wen SS, Ji DM (1997) The study of *Elaphe davidi* from China. Chinese Journal of Zoology 32(2): 16–19.

Wilcox TP, Zwickl DJ, Heath TA., Hillis DM (2002) Phylogenetic relationships of the Dwarf Boas and a comparison of Bayesian and bootstrap measures of phylogenetic support. Molecular Phylogenetics and Evolution 25: 361–371. https://doi.org/10.1016/S1055-7903(02)00244-0

Xu CZ, Mu YS, Kong QR, Xie GL, Guo ZR, Zhao S (2016) Sequencing and analysis of the complete mitochondrial genome of *Elaphe davidi* (Squamata: Colubridae). Mitochondrial DNA Part A 27(4): 2383–2384. https://doi.org/10.3109/19401736.2015.1028041

Zaher H, Grazziotin FG, Graboski R, et al. (2012) Phylogenetic relationships of the genus Sibynophis. Papéis Avulsos de Zoologia 52: 141–149. https://doi.org/10.1590/S0031-10492012001200001

Zhang RZ (1999) Zoogeography of China. Science Press, Beijing, 502 pp. [In Chinese]
Zhao EM (2006) Snakes of China. I. Anhui Science and Technology Publishing House, Hefei, 197–211. [In Chinese]

## Appendix 1

Details of the osteological specimens examined for dentition comparisons in this study.

**Colubridae**

*Elaphe*

*E. xiphodonta* sp. nov. IVPP OV 2721, 3D model of impregnated specimens, IVPP.
*E. zoigeensis* IVPP OV 2672, 3D model of impregnated specimens, IVPP.
*E. carinata* IVPP OV 2296, osteological specimens, IVPP.
*E. climacophora* SH 530, lateral and dorsal views of skull (Helfenberger and Schätti 1998).
*E. davidi* BM 1916.1.15.17, lateral and dorsal views of skull, BM (Helfenberger and Schätti 1998).
*E. dione* IVPP OV 2302, osteological specimen, IVPP.
*E. moellendorffi* IVPP OV 2686, osteological specimen, IVPP.
*E. schrenckii* IVPP OV 2295, osteological specimen, IVPP.
*E. taeniura* IVPP OV 2298, osteological specimen, IVPP.

*Coelognathus*

*C. flavolineatus* IVPP OV 2687, osteological specimen, IVPP.
*C. radiatus* IVPP OV 2411–2415, osteological specimens, IVPP.

*Euprepiophis*

*Eu. mandarinus* IVPP OV 2675, osteological specimen, IVPP.

*Oligodon*

*Ol. ornatus* SYS r001297, 3D model of Impregnated specimens, SYS.

*Oocatochus*

*Oo. Rufodorsatus* IVPP OV 2691, osteological specimen, IVPP.

*Ptyas*

*P. dhumnades* IVPP OV 2686, osteological specimen, IVPP.

**Dipsadidae**

*Dasypeltis*

*D. scabra* MHNG 1362.78, lateral and dorsal views of skull (Helfenberger and Schätti 1998). MHNG; AMNH r-31638, 3D model of impregnated specimens, AMNH.

*Thermophis*

*T. zhaoermii* BFU R_Th_001. 3D model of impregnated specimen, BFU.

ZooKeys 1048: 49–67 (2021)
doi: 10.3897/zookeys.1048.65620
https://zookeys.pensoft.net

RESEARCH ARTICLE

A peer-reviewed open-access journal
ZooKeys
Launched to accelerate biodiversity research

# A new species of *Nanorana* Günther, 1896 (Anura, Dicroglossidae) from Yunnan, China

Shuo Liu[1], Peisong Zhang[2], Dingqi Rao[3]

**1** *Kunming Natural History Museum of Zoology, Kunming Institute of Zoology, the Chinese Academy of Sciences, 32 Jiaochang Donglu, Kunming, Yunnan 650223, China* **2** *Research Institute of Xishuangbanna National Nature Reserve, No. 6 North Galan Road, Jinghong, Yunnan 666100, China* **3** *Kunming Institute of Zoology, the Chinese Academy of Sciences, No. 17 Longxin Road, Kunming, Yunnan 650201, China*

Corresponding authors: Dingqi Rao (raodq@mail.kiz.ac.cn); Shuo Liu (liushuo@mail.kiz.ac.cn)

Academic editor: A. Ohler | Received 7 March 2021 | Accepted 14 June 2021 | Published 7 July 2021

*http://zoobank.org/EC587B49-FB7F-4C3A-9E9D-D11DA6BF3E91*

**Citation:** Liu S, Zhang P, Rao D (2021) A new species of *Nanorana* Günther, 1896 (Anura, Dicroglossidae) from Yunnan, China. ZooKeys 1048: 49–67. https://doi.org/10.3897/zookeys.1048.65620

## Abstract

A new species of *Nanorana* Günther, 1896 is described from Yunnan Province, China, based on morphological and molecular evidence. Morphologically, *Nanorana xuelinensis* **sp. nov.** is distinguished from its congeners by a combination of the following diagnostic characters: body size large; adult males with keratinized spines on chest, belly, lateral body, posterior dorsum, buttocks, outer side of the fore limbs, the inner metacarpal tubercle, fingers I and II, and upper eyelids; no spines on the inner side of the lower and upper arm; forelimbs strongly hypertrophied in adult males; anterior dorsum skin smooth; dorsolateral folds absent; finger I longer than finger II; webbing deeply incurved between tips of toes; present outer metacarpal tubercle and absent outer metatarsal tubercle. The new species is separated from all other congeners by uncorrected genetic distances ranging from 5.2% to 7.3% based on mitochondrial 16S rRNA gene and ranging from 3.9% to 7.6% based on mitochondrial 12S rRNA gene.

## Keywords

12S, 16S, morphology, phylogeny, spiny frog, systematic, taxonomy

## Introduction

The tribe Paini is a widespread, complex taxon, and there are many different views on the classification of this taxon. Dubois (1992) first proposed the tribe Paini to include the genera *Paa* Dubois, 1975 and *Chaparana* Bourret, 1939. Roelants et al. (2004) suggested that *Nanorana* Günther, 1896 is imbedded within *Paa* on the basis of molecular data. Jiang et al. (2005) presented that *Quasipaa* Dubois, 1992 is a distinct genus in the tribe Paini. Chen et al. (2005) placed *Chaparana*, *Paa*, and *Nanorana* into *Nanorana* on the basis that *Paa* is paraphyletic with respect to *Nanorana* and *Chaparana*. Ohler and Dubois (2006) described two new genera in the tribe Paini, namely *Allopaa* Ohler & Dubois, 2006 and *Chrysopaa* Ohler & Dubois, 2006. Che et al. (2010, 2020) considered that the high elevation species of *Nanorana* represent dwarfed and degraded ones derived from lower elevation *Paa* on the basis of evidence of molecular phylogeny. Dubois et al. (2021) presented a different classification of the tribe Paini that included more genera, namely *Chaparana*, *Diplopaa* Dubois, Ohler & Pyron, 2021, *Feirana* Dubois, 1992, *Gynandropaa* Dubois, 1992, *Nanorana*, *Ombropaa* Dubois, Ohler & Pyron, 2021, and *Paa*.

To reduce confusion, we currently use the classification system on the "Amphibian Species of the World" website (Frost 2021). In this classification system, the genus *Nanorana* now contains 30 species (Frost 2021), of which 21 species were recorded in China (AmphibiaChina 2021).

During a field survey in Yunnan, China in 2019, some specimens of the genus *Nanorana* were collected. Morphological and molecular analyses indicated that these frogs were distinctive, differing from all known species of genus *Nanorana*. Therefore, we described them here as a new species.

## Materials and methods

### Sample collection

Specimens were collected by hand from Lancang County, Yunnan, China, euthanized, tissue samples taken, then preserved in 75% ethanol. Tissue samples were taken from liver and placed in 99% ethanol and subsequently stored at –80 °C. All specimens were deposited at Kunming Natural History Museum of Zoology, Kunming Institute of Zoology, the Chinese Academy of Sciences (**KIZ**).

### Laboratory methods

Genomic DNA extracted from 99% ethanol-preserved liver tissues, using DNA extraction kit from Beijing Dingguo Changsheng Biotechnology Co. Ltd. Two mitochondrial genes, 12S and 16S, were amplified. Primers used for 12S were FS01:

5'-AACGCTAAGATGAACCCTAAAAAGTTCT-3' and R16: 5'-ATAGTGGGG-TATCTAATCCCAGTTTGTTTT-3' (Qi et al. 2019) and for 16S were 16Sar: 5' -CGCCTGTTTACCAAAAACAT-3' and 16Sbr: 5'-CCGGTYTGAACTCAGAT-CAYGT-3' (Palumbi et al. 1991). PCR conditions followed Qi et al. (2019). Amplifications were processed with the cycling conditions that initial denaturing step at 94 °C for 5 min, 35 cycles of denaturing at 94 °C for 30 sec, annealing at 55 °C for 30 sec and extending at 72 °C for 1 min, and final extending step at 72 °C for 5 min. PCR products were isolated through electrophoresis using 1% agarose gels, and further purified using Millipore Microcon Kits. Purified PCR products were sequenced by Davis Sequencing using BigDye terminator 3.1 and sequences were edited and manually managed using SeqMan in Lasergene 7.1 (DNASTAR Inc., Madison, WI, USA) and MEGA X (Kumar et al. 2018). All sequences were deposited in GenBank (Table 1).

## Phylogenetic analyses

Total genomic DNA was isolated from the tissue samples of three individuals. *Quasipaa boulengeri* (Günther, 1889) and *Limnonectes fragilis* (Liu & Hu, 1973) were used as outgroups according to Qi et al. (2019). The mitochondrial genes 12S ribosomal RNA (12S) and 16S ribosomal RNA (16S), and the nuclear genes recombination activating protein 1 (Rag1), rhodopsin (Rhod), and tyrosinase (Tyr) of 19 known *Nanorana* species and two outgroup species were obtained from GenBank. Detail information of these materials are given in Table 1.

Sequences were aligned using ClustalW (Thompson et al. 1994) integrated in MEGA X (Kumar et al. 2018) with default parameters. The genetic divergences (uncorrected *p*-distance) were calculated in MEGA X (Kumar et al. 2018). 12S, 16S, Rag1, Rhod, and Tyr gene segments were concatenated seriatim into a single partition. Bayesian inference (BI) was performed in MrBayes 3.2.7 (Ronquist et al. 2012) and used the Akaike information criterion (AIC) in ModelFinder (Kalyaanamoorthy et al. 2017) to calculate that GTR+F+I+G4 was the best-fit model of evolution for 12S and 16S; HKY+F+I was the best-fit model of evolution for Rag1, Rhod, and Tyr. Two runs were performed simultaneously with four Markov chains starting from a random tree. The chains were run for 1,000,000 generations and sampled every 100 generations. The first 25% of the sampled trees was discarded as burn-in after the standard deviation of split frequencies of the two runs was less than a value of 0.01, and then the remaining trees were used to create a 50% majority-rule consensus tree and to estimate Bayesian posterior probabilities. Maximum likelihood (ML) analysis was performed in IQ-TREE (Nguyen et al. 2015) and used the Akaike information criterion (AIC) in ModelFinder (Kalyaanamoorthy et al. 2017) to calculate that GTR+F+R3 was the best-fit model of evolution for 12S and 16S, and that TPM3+F+I was the best-fit model for Rag1, Rhod, and Tyr. 1000 bootstrap pseudoreplicates via the ultrafast bootstrap (UFB; Hoang et al. 2018) approximation algorithm were used to construct a final consensus tree.

**Table 1.** Information of samples used in molecular analysis.

| Species name | Locality | Specimen voucher | 12S | 16S | Rag1 | Rhod | Tyr |
|---|---|---|---|---|---|---|---|
| *Nanorana aenea* | Sa Pa, Lao Cai, Vietnam | ROM37984 | EU979693 | EU979830 | HM163609 | EU979895 | EU979986 |
| *Nanorana aenea* | Sa Pa, Lao Cai, Vietnam | MNHN 1999.5818 | AY880456 | AY880443 | – | – | – |
| *Nanorana blanfordii* | Yatung, Tibet, China | SYNU-1507011 | MH315954 | MH315963 | – | – | – |
| *Nanorana chayuensis* | Zayü, Tibet, China | SYNU-XZ64 | EU979709 | DQ118509 | – | EU979853 | EU979944 |
| *Nanorana chayuensis* | Zayü, Tibet, China | SYNU-XZ67 | EU979708 | DQ118510 | – | EU979852 | EU979943 |
| *Nanorana conaensis* | Cona, Tibet, China | KIZ-YP152 | EU979703 | EU979834 | – | EU979874 | EU979965 |
| *Nanorana liebigii* | Janakpur, Nepal | A17_12_NME | MN011989 | MN012104 | MN032528 | MN012368 | MN012518 |
| *Nanorana liebigii* | Janakpur, Nepal | R18_12_NME | – | MN012105 | MN032529 | MN012369 | MN012519 |
| *Nanorana maculosa* | Jingdong, Yunnan, China | YNU-HU2002308 | EU979706 | EU979835 | – | EU979859 | EU979950 |
| *Nanorana maculosa* | Jingdong, Yunnan, China | YNU-HU2002322 | EU979707 | DQ118512 | – | EU979860 | EU979951 |
| *Nanorana medogensis* | Medôg, Tibet, China | SYNU-XZ35 | EU979705 | DQ118506 | – | EU979862 | EU979953 |
| *Nanorana medogensis* | Medôg, Tibet, China | SYNU-XZ75 | EU979704 | DQ118507 | – | EU979861 | EU979952 |
| *Nanorana parkeri* | – | N7_06_NME | MN012006 | MN012126 | MN032549 | MN012391 | MN012540 |
| *Nanorana parkeri* | Dangxiong, Tibet, China | – | KP317482 | KP317482 | – | – | – |
| *Nanorana phrynoides* | Yimen, Yunnan, China | YNU-HU20024012 | EU979686 | EU979825 | – | EU979877 | EU979968 |
| *Nanorana pleskei* | – | KQ47_14_NME | MN012019 | MN012156 | MN032562 | MN012422 | MN012570 |
| *Nanorana pleskei* | Shiqu, Sichuan, China | CIB20080515-1 | HQ324232 | HQ324232 | – | – | – |
| *Nanorana polunini* | Pangum, Nepal | K1553 | – | KR827957 | – | – | – |
| *Nanorana quadranus* | An, Sichuan, China | SCUM20030031GP | EU979694 | EU979831 | – | EU979886 | EU979977 |
| *Nanorana quadranus* | Maowen, Sichuan, China | SCUM20045195CJ | EU979695 | DQ118514 | – | EU979887 | EU979978 |
| *Nanorana rostandi* | Kyirong, Tibet, China | SYNU-1507058 | MH315955 | MH315964 | – | – | – |
| *Nanorana sichuanensis* | Huili, Sichuan, China | SCUM20030091GP | EU979685 | EU979824 | – | EU979880 | EU979971 |
| *Nanorana taihangnica* | Jiyuan, Henan, China | KIZ-HN0709001 | EU979724 | EU979842 | – | EU979893 | EU979984 |
| *Nanorana taihangnica* | Jiyuan, Henan, China | KIZ-HN0709002 | EU979725 | EU979843 | – | EU979894 | EU979985 |
| *Nanorana unculuanus* | Jingdong, Yunnan, China | YNU-HU2002502601 | EU979699 | DQ118490 | – | DQ458262 | DQ458277 |
| *Nanorana unculuanus* | Jingdong, Yunnan, China | YNU-HU2002502702 | EU979700 | DQ118491 | HM163585 | EU979865 | EU979956 |
| *Nanorana ventripunctata* | – | SH050538_NME | MN012066 | MN012208 | MN032610 | MN012478 | MN012626 |
| *Nanorana ventripunctata* | Xianggelila, Yunnan, China | SCUM045887WD | EU979717 | DQ118501 | HM163585 | EU979868 | EU979959 |
| *Nanorana yunnanensis* | Yongde, Yunnan, China | YNU-HU20011102 | EU979691 | EU979829 | – | EU979884 | EU979975 |
| *Nanorana zhaoermii* | Lhünzê, Tibet, China | SYNU-1706049 | MH315947 | MH315956 | – | – | – |
| *Nanorana zhaoermii* | Lhünzê, Tibet, China | SYNU-1706058 | MH315948 | MH315957 | – | – | – |
| *Nanorana xuelinensis* sp. nov. | Lancang, Yunnan, China | KIZL2019012 | MZ410625 | MZ410628 | – | – | – |
| *Nanorana xuelinensis* sp. nov. | Lancang, Yunnan, China | KIZL2019013 | MZ410624 | MZ410627 | – | – | – |
| *Nanorana xuelinensis* sp. nov. | Lancang, Yunnan, China | KIZL2019014 | MZ410623 | MZ410626 | – | – | – |
| *Limnonectes fragilis* | Hainan, China | ZNAC11006 | AY899241 | AY899241 | – | – | – |
| *Quasipaa boulengeri* | Yichang, Hubei, China | KIZ-HUB292 | KX645665 | KX645665 | – | – | – |

## Morphology

All measurements were taken with digital calipers to the nearest 0.1 mm. Morphological characters used and their measurement methods followed Qi et al. (2019). The morphometrics and character terminology include:

**AG** axilla to groin, distance from posterior base of forelimb at its emergence from body to anterior base of hindlimb at its emergence from body;

**EHD** eye horizontal diameter;
**END** eye to nostril distance, distance from anterior corner of eye to nostril;
**FL** foot length, from proximal end of inner metatarsal tubercle to tip of toe IV;
**FML** femur length;
**HAL** hand length, from proximal end of outer metacarpal tubercle to tip of the finger III;
**HH** head height, greatest height of head;
**HL** head length, from posterior corner of mandible to tip of snout;
**HW** head width, at the greatest cranial width;
**ID** internasal distance, distance between nostrils;
**IOD** interorbital distance, least distance between upper eyelids;
**LAD** diameter of lower arm;
**LAL** length of lower arm, from proximal end of outer metacarpal tubercle to elbow joint;
**SL** snout length, from tip of snout to the anterior corner of eye distance;
**SND** snout to nostril distance, distance from tip of snout to nostril;
**SVL** Snout–vent length, from tip of snout to vent;
**TDH** horizontal diameter of tympanum;
**TDV** vertical diameter of tympanum;
**TFL** length of tarsus and foot, from proximal end of tarsus to tip of the toe IV;
**TIL** tibia length;
**UEW** upper eyelid width, maximum width of upper eyelid.

All measurements were taken on the left side of the examined specimen. It should be noted that because the limbs of our specimens cannot be spread, the characters FLL (length of forelimb, from axilla to tip of finger III) and HLL (length of hindlimb, from tip of disk of toe IV to vent) in Qi et al. (2019) are not provided here.

## Results

### Genealogical relationships

The results of BI and ML phylogenetic trees were constructed based on the concatenated DNA sequences and resulted in approximately identical topologies (Fig. 1). The phylogenetic tree showed that the newly discovered population from Xuelin Township, Lancang County is a member of *Nanorana*; however, its phylogenetic position in the genus was not clearly resolved. The newly discovered population formed a unique clade sister to the clade consisting of *Nanorana aenea* (Smith, 1922), *N. phrynoides* (Boulenger, 1917), *N. quadranus* (Liu, Hu & Yang, 1960), *N. sichuanensis* (Dubois, 1987), *N. taihangnica* (Chen & Jiang, 2002), *N. unculuanus* (Liu, Hu & Yang, 1960), and *N. yunnanensis* (Anderson, 1879), but the node supports were very low.

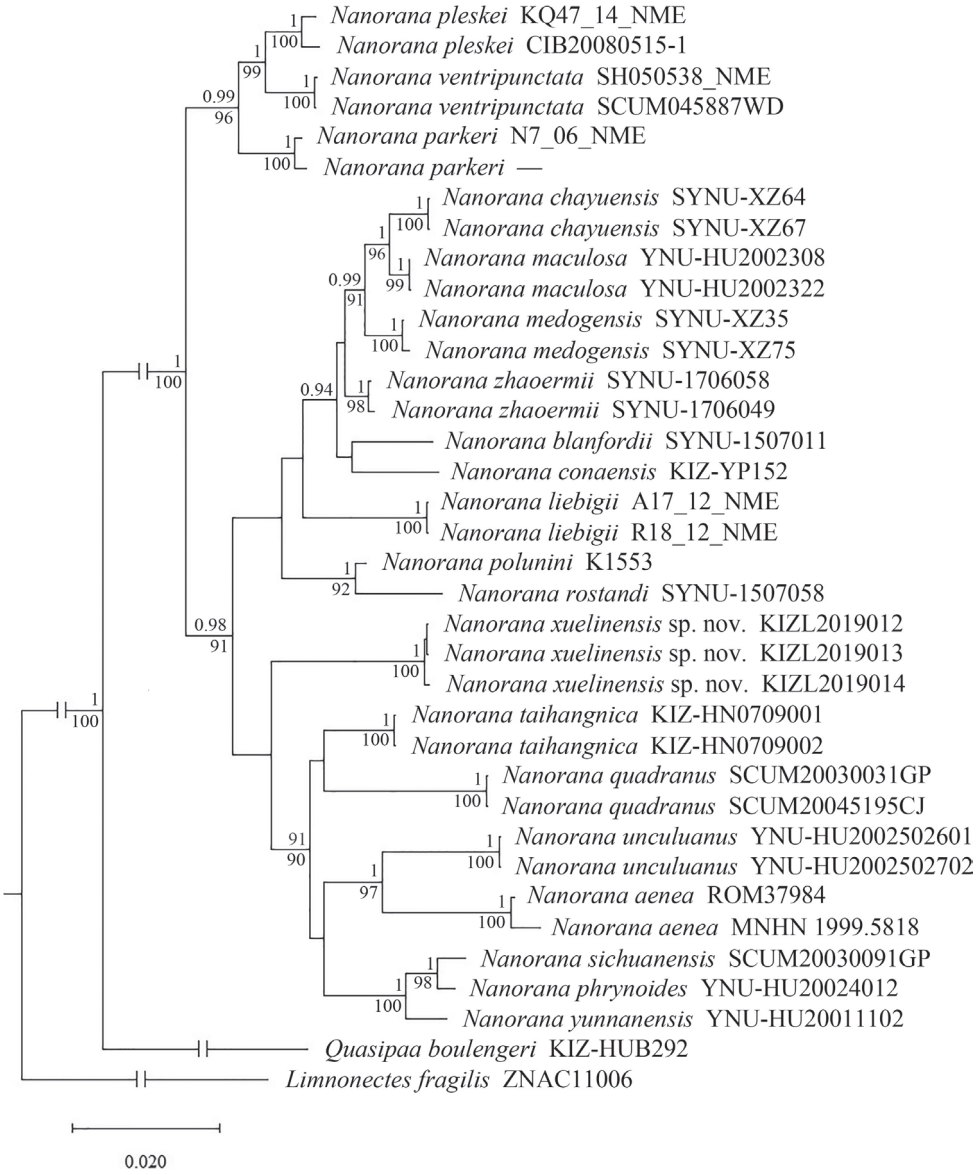


**Figure 1.** Bayesian inference tree of the genus *Nanorana* based on the sequences of the mitochondrial 12S and 16S, and the nuclear Rag1, Rhod, and Tyr gene. *Limnonectes fragilis* and *Quasipaa boulengeri* were included as outgroup. Numbers above branches indicate Bayesian posterior probabilities (≥0.9 retained) and numbers below branches indicate the ML ultrafast bootstrap (UFB) (≥90 retained).

## Genetic distances

The uncorrected *p*-distances calculated from 12S rRNA and 16S rRNA gene fragment sequences of the examined species are shown in Tables 2 and 3, respectively. The observed

**Table 2.** Mean uncorrected pairwise genetic distances (%) among the species of *Nanorana* and outgroups based on partial 12S gene.

| | 1 | 2 | 3 | 4 | 5 | 6 | 7 | 8 | 9 | 10 | 11 | 12 | 13 | 14 | 15 | 16 | 17 | 18 | 19 | 20 |
|---|---|---|---|---|---|---|---|---|---|---|---|---|---|---|---|---|---|---|---|---|
| 1 *Nanorana aenea* | | | | | | | | | | | | | | | | | | | | |
| 2 *N. blanfordii* | 7.8 | | | | | | | | | | | | | | | | | | | |
| 3 *N. chayuensis* | 6.9 | 5.0 | | | | | | | | | | | | | | | | | | |
| 4 *N. cuonaensis* | 7.7 | 5.3 | 6.6 | | | | | | | | | | | | | | | | | |
| 5 *N. liebigii* | 6.9 | 5.8 | 5.6 | 6.3 | | | | | | | | | | | | | | | | |
| 6 *N. maculosa* | 7.2 | 4.8 | 2.0 | 5.8 | 4.9 | | | | | | | | | | | | | | | |
| 7 *N. medogensis* | 6.1 | 3.9 | 3.3 | 4.0 | 4.5 | 2.8 | | | | | | | | | | | | | | |
| 8 *N. parkeri* | 6.8 | 6.9 | 5.3 | 7.1 | 5.9 | 4.9 | 4.5 | | | | | | | | | | | | | |
| 9 *N. phrynoides* | 6.6 | 7.3 | 7.1 | 8.3 | 7.3 | 7.1 | 6.0 | 8.8 | | | | | | | | | | | | |
| 10 *N. pleskei* | 6.0 | 5.1 | 5.3 | 6.7 | 5.7 | 5.3 | 4.8 | 3.6 | 7.6 | | | | | | | | | | | |
| 11 *N. quadranus* | 7.5 | 8.1 | 7.2 | 8.1 | 7.4 | 7.9 | 7.0 | 8.4 | 7.9 | 7.6 | | | | | | | | | | |
| 12 *N. rostandi* | 6.1 | 6.3 | 5.5 | 7.5 | 5.6 | 5.8 | 5.4 | 5.9 | 7.3 | 5.5 | 7.6 | | | | | | | | | |
| 13 *N. sichuanensis* | 6.8 | 7.5 | 7.3 | 9.5 | 7.3 | 7.4 | 6.7 | 9.1 | 1.2 | 7.8 | 8.1 | 7.5 | | | | | | | | |
| 14 *N. taihangnica* | 5.2 | 5.3 | 5.1 | 6.3 | 4.4 | 4.9 | 4.0 | 6.1 | 5.4 | 4.6 | 5.4 | 5.3 | 5.6 | | | | | | | |
| 15 *N. unculuanus* | 5.5 | 5.0 | 5.4 | 7.1 | 5.4 | 5.2 | 4.3 | 7.3 | 5.4 | 5.9 | 7.4 | 4.8 | 6.1 | 3.7 | | | | | | |
| 16 *N. ventripundata* | 8.4 | 6.3 | 6.7 | 8.3 | 6.4 | 6.6 | 6.3 | 5.4 | 8.2 | 3.4 | 8.6 | 7.4 | 8.9 | 6.7 | 6.7 | | | | | |
| 17 *N. yunnanensis* | 4.5 | 6.5 | 5.2 | 8.1 | 6.8 | 5.7 | 5.6 | 6.0 | 1.9 | 5.2 | 7.4 | 5.7 | 2.2 | 4.9 | 5.4 | 6.6 | | | | |
| 18 *N. zhaoermii* | 6.0 | 3.2 | 3.2 | 3.5 | 4.1 | 2.1 | 1.4 | 5.0 | 5.9 | 4.1 | 6.3 | 4.4 | 6.8 | 3.5 | 3.5 | 5.1 | 5.8 | | | |
| 19 *Nanorana xuelinensis* sp. nov. | 6.3 | 5.6 | 6.0 | 6.6 | 4.0 | 5.4 | 4.6 | 5.9 | 6.8 | 6.0 | 7.1 | 6.0 | 7.1 | 3.9 | 6.1 | 7.6 | 6.5 | 4.5 | | |
| 20 *Quasipaa boulengeri* | 11.9 | 12.8 | 12.5 | 14.1 | 11.8 | 12.4 | 12.5 | 12.8 | 14.7 | 12.7 | 13.5 | 11.9 | 14.9 | 12.0 | 12.9 | 14.8 | 13.6 | 14.0 | 11.8 | |
| 21 *Limnonectes fragilis* | 18.1 | 16.0 | 17.8 | 20.0 | 17.5 | 18.0 | 17.8 | 17.8 | 18.5 | 17.0 | 18.7 | 18.4 | 17.5 | 17.5 | 18.0 | 19.1 | 17.3 | 18.0 | 17.4 | 15.9 |

distances calculated from 12S gene between the sequences of the specimens collected from Xuelin Township, Lancang County and the homologous sequences obtained from GenBank ranged from 3.9% to 7.6%. The observed distances calculated from 16S gene between the sequences of the specimens collected from Xuelin Township, Lancang County and the homologous sequences obtained from GenBank ranged from 5.2% to 7.3%.

## Systematics

***Nanorana xuelinensis* sp. nov.**

http://zoobank.org/3BB0CC31-8B68-4EA7-BC7C-DDF7D78C977F

Figures 2–6

**Holotype.** KIZL2019016, adult male, collected on 13 July 2019 by Shuo Liu from Xuelin Township, Lancang County, Puer City, Yunnan Province, China (23°2'38"N, 99°32'35"E; at an elevation of 1840 m asl).

**Paratypes.** KIZL2019012 and KIZL2019015, two subadult males; KIZL2019013 and KIZL2019014, two subadult females; and KIZL2019017, adult female. All with same collection information as for the holotype.

**Diagnosis.** Large body size, SVL 101.7–107.3 mm in adults; adult males with keratinized spines on chest, belly, lateral body, posterior dorsum, buttocks, outer side of the fore limbs, the inner metacarpal tubercle, fingers I and II, and upper eyelids; no spines on the inner side of the lower and upper arm; forelimbs strongly hypertrophied

**Table 3.** Mean uncorrected pairwise genetic distances (%) among the species of *Nanorana* and outgroups based on partial 16S gene.

| | 1 | 2 | 3 | 4 | 5 | 6 | 7 | 8 | 9 | 10 | 11 | 12 | 13 | 14 | 15 | 16 | 17 | 18 | 19 | 20 | 21 |
|---|---|---|---|---|---|---|---|---|---|---|---|---|---|---|---|---|---|---|---|---|---|
| 1 *Nanorana aenea* | | | | | | | | | | | | | | | | | | | | | |
| 2 *N. blanfordii* | 5.1 | | | | | | | | | | | | | | | | | | | | |
| 3 *N. chayuensis* | 5.2 | 2.4 | | | | | | | | | | | | | | | | | | | |
| 4 *N. cuonaensis* | 5.5 | 2.8 | 3.6 | | | | | | | | | | | | | | | | | | |
| 5 *N. liebigii* | 6.2 | 4.1 | 4.1 | 5.3 | | | | | | | | | | | | | | | | | |
| 6 *N. maculosa* | 5.4 | 2.5 | 0.9 | 4.0 | 3.8 | | | | | | | | | | | | | | | | |
| 7 *N. medogensis* | 5.9 | 3.0 | 2.5 | 4.4 | 4.0 | 2.2 | | | | | | | | | | | | | | | |
| 8 *N. parkeri* | 5.5 | 2.9 | 3.3 | 3.5 | 4.4 | 3.2 | 3.8 | | | | | | | | | | | | | | |
| 9 *N. phrynoides* | 4.7 | 4.5 | 5.3 | 4.0 | 4.6 | 5.3 | 5.4 | 4.4 | | | | | | | | | | | | | |
| 10 *N. pleskei* | 5.2 | 2.9 | 4.1 | 4.4 | 4.3 | 3.6 | 4.3 | 3.1 | 4.7 | | | | | | | | | | | | |
| 11 *N. polunini* | 6.0 | 3.6 | 4.1 | 4.4 | 6.3 | 4.1 | 3.8 | 4.1 | 6.4 | 5.2 | | | | | | | | | | | |
| 12 *N. quadranus* | 6.1 | 4.2 | 5.8 | 5.7 | 6.8 | 5.8 | 5.3 | 5.5 | 5.1 | 6.1 | 6.2 | | | | | | | | | | |
| 13 *N. rostandi* | 6.6 | 3.4 | 4.5 | 4.1 | 5.3 | 4.3 | 4.3 | 5.1 | 5.8 | 5.3 | 2.3 | 5.5 | | | | | | | | | |
| 14 *N. sichuanensis* | 5.2 | 4.4 | 5.5 | 4.2 | 5.3 | 5.5 | 5.6 | 4.5 | 1.1 | 4.2 | 6.6 | 4.5 | 5.6 | | | | | | | | |
| 15 *N. taihangnica* | 4.6 | 3.2 | 4.5 | 3.6 | 4.4 | 4.2 | 4.2 | 3.0 | 3.8 | 3.1 | 5.1 | 6.3 | 4.9 | 4.0 | | | | | | | |
| 16 *N. unculuanus* | 4.6 | 5.3 | 6.1 | 6.6 | 6.4 | 6.2 | 6.1 | 5.9 | 6.0 | 5.7 | 8.3 | 6.9 | 6.8 | 5.8 | 5.4 | | | | | | |
| 17 *N. ventripundata* | 4.9 | 2.5 | 3.4 | 3.9 | 3.9 | 3.3 | 3.9 | 2.3 | 3.7 | 2.0 | 4.9 | 5.0 | 4.5 | 3.5 | 3.9 | 5.5 | | | | | |
| 18 *N. yunnanensis* | 5.3 | 4.5 | 5.4 | 4.4 | 5.3 | 5.5 | 5.6 | 4.5 | 2.2 | 4.8 | 6.1 | 5.1 | 5.4 | 2.2 | 4.2 | 6.0 | 4.3 | | | | |
| 19 *N. zhaoermii* | 5.5 | 2.4 | 2.1 | 3.1 | 4.3 | 2.2 | 2.6 | 2.9 | 4.6 | 3.0 | 3.2 | 4.0 | 4.7 | 4.0 | 3.6 | 6.0 | 2.9 | 4.4 | | | |
| 20 *Nanorana xuelinensis* sp. nov. | 6.7 | 5.8 | 5.8 | 5.6 | 6.5 | 5.4 | 5.2 | 6.0 | 5.6 | 6.0 | 6.6 | 6.6 | 5.9 | 6.2 | 5.3 | 7.3 | 5.7 | 6.2 | 5.3 | | |
| 21 *Quasipaa boulengeri* | 8.4 | 7.8 | 7.5 | 6.7 | 8.0 | 7.2 | 7.4 | 6.5 | 7.6 | 7.3 | 8.8 | 8.7 | 9.4 | 8.0 | 7.1 | 9.2 | 7.7 | 7.8 | 6.1 | 8.3 | |
| 22 *Limnonectes fragilis* | 12.0 | 11.8 | 12.0 | 11.7 | 12.2 | 11.6 | 11.8 | 11.1 | 12.4 | 12.2 | 16.2 | 13.3 | 14.3 | 12.6 | 11.5 | 12.2 | 12.5 | 12.8 | 11.4 | 12.3 | 10.3 |

in adult males; tympanum big but indistinct, ca 2/3 of eye diameter; anterior dorsum skin smooth; dorsolateral folds absent; finger I longer than finger II; webbing deeply incurved between tips of toes; no tarsal fold; present outer metacarpal tubercle and absent outer metatarsal tubercle; vomerine teeth distinct.

The living specimens were yellowish brown with distinct or indistinct black spots on the dorsum and sides of the body and the dorsal side of limbs; no band on arms and legs. Ventral surface white with no spots, throat yellow in adult males.

**Description of holotype.** Adult male, habitus very stout, SVL 107.3 mm, large size in genus *Nanorana*; head flat and broader than long (HL/HW 0.85, HH/HL 0.53); snout blunt and rounded in both dorsal and lateral views; canthus rostralis obtuse; tympanum large and very indistinct (TDH/EHD 0.76); supratympanic fold extending from eye over tympanum to shoulder; transversal fold behind eyes; eye relatively large (EHD/HL 0.26), pupil slightly rhombic; vomerine teeth distinct; tongue large and cordiform, deeply notched posteriorly.

Forelimbs short and strongly hypertrophied (LAD 18.8 mm); relative finger length: II < I < IV < III; inner metacarpal tubercle enlarged, dorsal surface of inner metacarpal tubercle, fingers I, and finger II with black keratinized nuptial spines, no spine on inner side of fore limbs, and a few spines on outer side of fore limbs; finger tips rounded but not dilated, fingers free, without webbing, no circum-marginal groove or lateroventral groove; subarticular tubercles distinct, outer metacarpal tubercle indistinct.

**Figure 2.** Dorsal and ventral views of the specimens of the type series of *Nanorana xuelinensis* sp. nov. in preservative.

**Figure 3.** Various views of the male holotype (KIZL2019016) of *Nanorana xuelinensis* sp. nov. in preservative.

**Figure 4.** Various views of the female paratype (KIZL2019017) of *Nanorana xuelinensis* sp. nov. in preservative.

**Figure 5.** Different views of the male holotype (KIZL2019016) of *Nanorana xuelinensis* sp. nov. in life.

Hindlimbs rather long and stout; relative toe length: I < II < V < III < IV; tips of toes rounded but not dilated; subarticular tubercles oval and distinct, formula is 1, 1, 2, 3, 2; inner metatarsal tubercles elongated and pronounced; outer metatarsal tubercle absent; webbing deeply incurved between tips of toes, formula I 0-0$^{-}$ II 0-0$^{-}$ III 0$^{-}$-0$^{-}$ IV 0$^{-}$-0 V; lateral fringe on the outer side of toe V developed; no circum-marginal groove or lateroventral groove; tarsal fold absent.

Anterior dorsum skin smooth; keratinized spines present on chest, belly, lateral body, posterior dorsum, buttocks, and upper eyelids; spines most dense on axilla and each side of chest.

**Coloration of holotype in life.** The coloration of dorsum is yellowish brown with very indistinct black spots in dorsum, and no band on arms and legs. Ventral surface white with no spots. The throat is yellow. The pupil is black, and the iris is light yellow with many black radial strips around the pupil.

**Sexual dimorphism.** The forelimbs of adult males are strongly hypertrophied; in addition, adult males have keratinized spines on chest, belly, lateral body, posterior dorsum, buttocks, outer side of the fore limbs, the inner metacarpal tubercle, fingers I and II, and upper eyelids. The forelimbs of adult females are not hypertrophied, and adult females have distinct black spots on the dorsum, lateral body, and the dorsal side of limbs, no keratinized spines on chest, belly, lateral body, posterior dorsum, buttocks, and upper eyelids, and only some keratinized spines on finger I and a few small spines on finger II.

**Figure 6.** Different views of the female paratype (KIZL2019017) of *Nanorana xuelinensis* sp. nov. in life.

**Table 4.** Morphological measurements (mm) of the type series of *Nanorana xuelinensis* sp. nov.

| | KIZL2019016 Holotype Adult male | KIZL2019017 Paratype Adult female | KIZL2019012 Paratype Subadult male | KIZL2019013 Paratype Subadult female | KIZL2019014 Paratype Subadult female | KIZL2019015 Paratype Subadult male |
|---|---|---|---|---|---|---|
| SVL | 107.3 | 101.7 | 60.3 | 79.2 | 75.1 | 66.9 |
| AG | 36.2 | 40.6 | 15.9 | 29.1 | 29.7 | 20.1 |
| HL | 35.9 | 36.4 | 23.7 | 27.0 | 27.7 | 25.8 |
| HW | 42.1 | 38.1 | 23.6 | 28.8 | 28.9 | 27.0 |
| HH | 19.1 | 18.9 | 11.6 | 14.1 | 15.4 | 13.1 |
| SL | 16.4 | 14.4 | 9.7 | 11.3 | 11.6 | 11.2 |
| ID | 7.3 | 7.4 | 4.6 | 5.7 | 5.6 | 5.5 |
| IOD | 4.1 | 4.7 | 2.5 | 3.3 | 3.9 | 3.3 |
| UEW | 7.0 | 7.2 | 4.3 | 5.6 | 5.7 | 5.1 |
| EHD | 9.5 | 10.8 | 6.6 | 8.4 | 8.3 | 8.4 |
| TDH | 7.2 | 7.7 | 4.5 | 5.6 | 5.7 | 4.6 |
| TDV | 6.6 | 4.8 | 3.5 | 4.4 | 4.2 | 3.6 |
| SND | 8.4 | 7.1 | 4.5 | 6.4 | 5.1 | 4.9 |
| END | 7.9 | 7.3 | 4.6 | 5.6 | 5.8 | 5.4 |
| LAl | 22.5 | 19.9 | 11.7 | 15.3 | 13.9 | 14.1 |
| LAD | 18.8 | 10.3 | 7.9 | 8.8 | 8.2 | 9.4 |
| HAL | 22.7 | 19.0 | 14.6 | 17.8 | 15.9 | 15.6 |
| FML | 45.4 | 41.8 | 26.8 | 34.6 | 33.5 | 29.5 |
| TIL | 42.5 | 39.2 | 25.7 | 33.2 | 31.1 | 28.9 |
| TFL | 65.9 | 63.1 | 41.9 | 54.2 | 49.9 | 45.8 |
| FL | 44.3 | 42.7 | 29.1 | 36.0 | 33.6 | 33.1 |

**Etymology.** The name refers to Xuelin Township, the locality where the new species was found. We propose "Xuelin Paa Frog" or "Xuelin Spiny Frog" for the common English name and "雪林棘蛙" (Xuě Lín Jí Wā) for the common Chinese name of the new species.

**Figure 7.** Habitat of *Nanorana xuelinensis* sp. nov. at the type locality.

**Distribution.** *Nanorana xuelinensis* sp. nov. is recorded in Lancang County (Pu'er City), Shuangjiang County (Lincang City), and Jinghong City (Xishuangbanna Prefecture), Yunnan Province, China.

**Habitat.** The type series was found in a still-water pond. At the type locality we found three other species of amphibians: *Chirixalus* cf. *doriae* Boulenger, 1893; *Raorchestes hillisi* Jiang Ren, Guo, Wang & Li, 2020; *Tylototriton verrucosus* Anderson, 1871a; and three species of reptiles: *Calotes emma* Gray, 1845; *Pareas xuelinensis* Liu & Rao, 2021; and *Pseudocalotes microlepis* (Boulenger, 1887).

**Comparisons.** *Nanorana xuelinensis* sp. nov. differs from *N. aenea*, *N. annandalii* (Boulenger, 1920), *N. gammii* (Anderson, 1871b), *N. liebigii* (Günther, 1860), *N. polunini* (Smith, 1951), *N. rarica* (Dubois, Matsui & Ohler, 2001), *N. rostandi* (Dubois, 1974), and *N. unculuanus* by the absence of dorsolateral fold (vs presence).

*Nanorana xuelinensis* sp. nov. differs from *N. arnoldi* (Dubois, 1975), *N. maculosa* (Liu, Hu & Yang, 1960), *N. yunnanensis*, and *N. zhaoermii* Qi, Zhou, Lu & Li, 2019 by the spines present only on finger I and finger II in adult males (vs present on finger I–III).

*Nanorana xuelinensis* sp. nov. differs from *N. arunachalensis* (Saikia, Sinha & Kharkongor, 2017), *N. blanfordii* (Boulenger, 1882), *N. chayuensis* (Ye, 1977), *N. conaensis* (Fei & Huang, 1981), *N. minica* (Dubois, 1975), and *N. mokokchungensis* (Das & Chanda, 2000) by its larger body size.

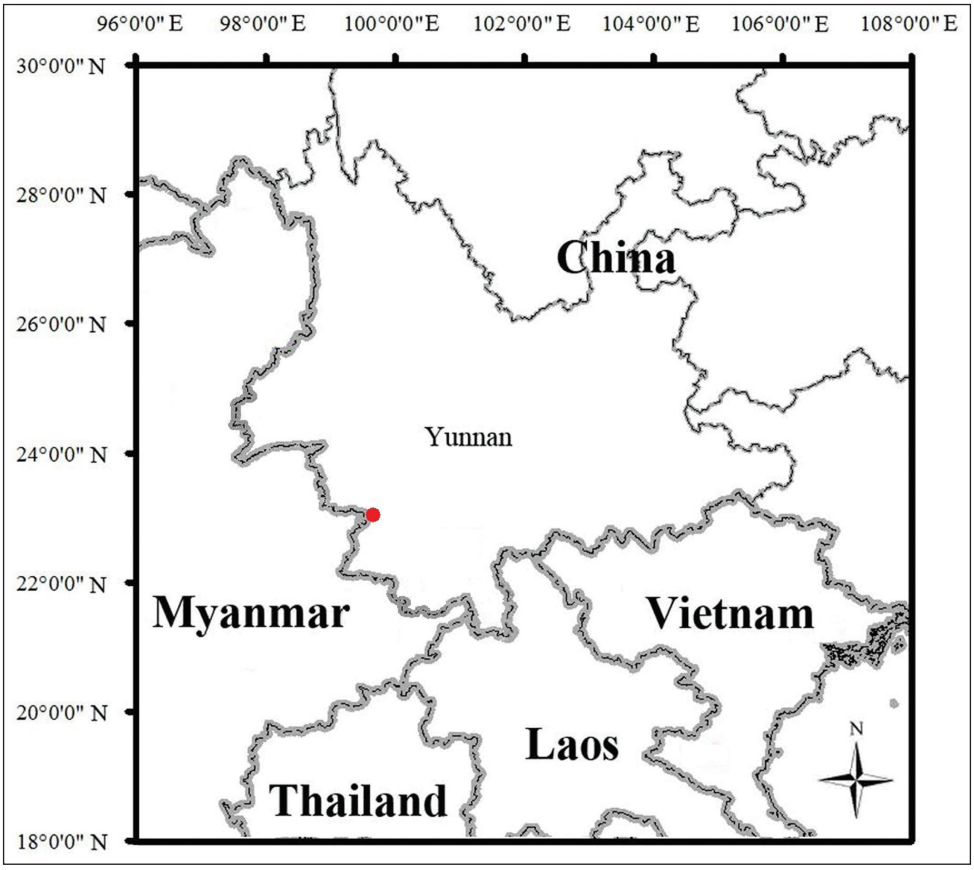


**Figure 8.** Map showing the type locality of *Nanorana xuelinensis* sp. nov. (red dot).

*Nanorana xuelinensis* sp. nov. differs from *N. feae* (Boulenger, 1887) by the absence of spines on the inner side of the fore limbs in adult males (vs. presence).

*Nanorana xuelinensis* sp. nov. differs from *N. kangxianensis* (Yang, Wang, Hu & Jiang, 2011), *N. quadranus*, *N. taihangensis* by the strongly hypertrophied forelimbs in adult males (vs not hypertrophied), and by the presence of nuptial spines on the chest and fingers in adult males (vs absence).

*Nanorana xuelinensis* sp. nov. differs from *N. medogensis* (Fei & Ye, 1999), *N. phrynoides*, and *N. sichuanensis* by smooth anterior dorsum skin (vs many warts present).

*Nanorana xuelinensis* sp. nov. differs from *N. parkeri* (Stejneger, 1927), *N. pleskei* Günther, 1896, and *N. ventripunctata* Fei & Huang, 1985 by the shape of the nuptial spines (large and conical spines vs tiny and compact spines).

*Nanorana xuelinensis* sp. nov. differs from *N. vicina* (Stoliczka, 1872) by its toes ca 2/3 webbed (vs fully webbed) and by the absence of bands on the hind limbs (vs presence).

## Discussion

Most species of *Nanorana* live in running waters, especially in swiftly running waters (Dubois and Ohler 2005; Ohler and Dubois 2006) such as rivers or streams, except for *N. parkeri*, *N. pleskei*, and *N. ventripunctata*, which have produced a series of specialized adaptations to high-altitude habitats (Che et al. 2020). However, the habitat of the *Nanorana xuelinensis* sp. nov. is distinctive. All specimens of *Nanorana xuelinensis* sp. nov. were found in still waters in different seasons. Why this species lives in still waters needs further study.

Morphologically, *Nanorana xuelinensis* sp. nov. is obviously different from all other known species of the genus *Nanorana*. The skins of most species of *Nanorana* are rough with more or less tubercles or warts (Che et al. 2020). However, the skin of *Nanorana xuelinensis* sp. nov. is quite smooth on most areas of the body. Most males of the tribe Paini have spines on the fingers, arms, or breast. The presence of these spines is an adaptation to breeding in swiftly running waters, helping the males grasp of the females (Ohler and Dubois 2006). Although *Nanorana xuelinensis* sp. nov. does not live in running waters, the males still may need spines to help grasp females due to their smoother skins. But why the males of *Nanorana xuelinensis* sp. nov. have so many keratinized spines on the other areas of the body except for the fingers and breast we do not yet know, and the reason for this feature also needs further study.

The genus *Nanorana* contains 30 species, of which 22 species are recorded in China (Frost 2021); however, *N. arnoldi* is not recorded from China according to AmphibiaChina (2021), which lists only 21 species. This is probably due to an erroneous synonymy: *N. chayuensis* was placed into the synonymy of *N. arnoldi* by Dubois (1980), which subsequently was rejected by Hu (1985). In the phylogenetic analyses of Che et al. (2009), the gene sequences of *N. arnoldi* and *N. chayuensis* clustered together, but these sequences of *N. arnoldi* were from Yunnan, China, which were possibly wrongly identified and probably belong to *N. chayuensis*. We speculate that the true *N. arnoldi* is distributed in northern Myanmar, and not in China. Because we do not have specimens from northern Myanmar, whether *N. chayuensis* and *N. arnoldi* are the same species remains to be solved, but for the time being, we support AmphibiaChina (2021) in treating *N. chayuensis* as valid and considering that *N. arnoldi* is not distributed in China. Further collections from both countries will clarify this taxonomic conundrum.

## Acknowledgements

We thank Decai Ouyang, Lei Ouyang, and Zhongqiang Yang for assistance in the field. Thanks are also due to our workmates for their help and advice. We also thank the reviewers for their valuable comments on the manuscript. This work was supported by Science-Technology Basic Condition Platform from the Ministry of Science and

Technology of the People's Republic of China (grant no. 2005DKA21402), and the project of Ministry of Ecology and Environment of China: Investigation and assessment of amphibians and reptiles in Lancang County, and Investigation and assessment of amphibians and reptiles in Jinghong City, Menghai County, and Mengla County.

## References

AmphibiaChina (2021) The database of Chinese amphibians. Electronic Database. http://www.amphibiachina.org [accessed on 6 March 2021]

Anderson J (1871a) Description of a new genus of newts from western Yunan. Proceedings of the Zoological Society of London 1871: 423–425.

Anderson J (1871b) A list of the reptilian accession to the Indian Museum, Calcutta from 1865 to 1870, with a description of some new species. Journal of the Asiatic Society of Bengal 40: 12–39.

Anderson J (1879) Anatomical and Zoological Researches: Comprising an Account of the Zoological Results of the Two Expeditions to Western Yunnan in 1868 and 1875; and a Monograph of the Two Cetacean Genera Platanista and Orcella. 2 Volumes. Bernard Quaritch, London, 985 pp. https://doi.org/10.5962/bhl.title.55401

Boulenger GA (1882) Catalogue of the Batrachia Salientia s. Caudata in the Collections of the British Museum. (Natural History). 2nd edn. Taylor and Francis, London, 503 pp.

Boulenger GA (1887) An account of the batrachians obtained in Burma by M.L. Fea of the Genoa Civic Museum. Annali del Museo Civico di Storia Naturale di Genova 5: 418–424.

Boulenger GA (1888) An account of the reptiles and batrachians obtained in Tenasserim by M. L. Fea, of the Genova Civic Museum. Annali del Museo Civico di Storia Naturale di Genova 5: 474–486.

Boulenger GA (1893) Concluding report on the reptiles and batrachians obtained in Burma by Signor L. Fea dealing with the collection made in Pegu and the Karin Hills in 1887–88. Annali del Museo Civico di Storia Naturale di Genova 13: 304–347.

Boulenger GA (1917) Descriptions of new frogs of the genus *Rana*. Annals and Magazine of Natural History (Series 8) 20: 413–418. https://doi.org/10.1080/00222931709487029

Boulenger GA (1920) A monograph of the South Asian, Papuan, Melanesian and Australian frogs of the genus *Rana*. Records of the Indian Museum 20: 1–226. https://doi.org/10.5962/bhl.title.12471

Bourret R (1939) Notes herpétologiques sur l'Indochine française. XVII. Reptiles et batraciens reçus au Laboratoire des Sciences Naturelles de l'Université au cors de l'année 1938. Descriptions de trois espèces nouvelles. Annexe au Bulletin Général de l'Instruction Publique. Hanoi 1939: 13–34.

Che J, Hu JS, Zhou WW, Murphy RW, Papenfuss TJ, Chen MY, Rao DQ, Li PP, Zhang YP (2009) Phylogeny of the Asian spiny frog tribe Paini (Family Dicroglossidae) sensu Dubois. Molecular Phylogenetics and Evolution 50: 59–73. https://doi.org/10.1016/j.ympev.2008.10.007

Che J, Zhou WW, Hu JS, Yan F, Papenfuss TJ, Wake DB, Zhang YP (2010) Spiny frogs (Paini) illuminate the history of the Himalayan region and Southeast Asia. Proceedings of the National Academy of Sciences 107: 13765–13770. https://doi.org/10.1073/pnas.1008415107

Che J, Jiang K, Yan F, Zhang YP (2020) Amphibians and Reptiles in Tibet – Diversity and Evolution. Science Press, Beijing, 803 pp.

Chen LQ, Murphy RW, Lathrop A, Ngo A, Orlov NL, Ho CT, Somorjai ILM (2005) Taxonomic chaos in Asian ranid frogs: an initial phylogenetic resolution. Herpetological Journal 15: 231–243.

Chen XH, Jiang JP (2002) A new species of the genus *Paa* from China. Herpetologica Sinica 9: 231.

Das I, Chanda SK (2000) A new species of *Scutiger* (Anura: Megophryidae) from Nagaland, north-eastern India. Herpetological Journal 10: 69–72.

Dubois A (1974) Diagnoses de trois espèces Nouvelles d'amphibiens du Népal. Bulletin de la Société Zoologique de France 98: 495–497.

Dubois A (1975) Un nouveau sous-genre (*Paa*) et trois nouvelles espèces du genre *Rana*. Remarques sur la phylogenies des ranidés (Amphibiens, Anoures). Bulletin du Museum National d'Histoire Naturelle 324: 1093–1115.

Dubois A (1980) Notes sur la systématique et la répartition des amphibiens anoures de Chine et des régions avoisinantes. 3. *Rana maculata* Liu, Hu & Yang, 1970, *Rana* (*Paa*) *arnoldi* Dubois, 1975 et *Rana maculosa chayuensis* Ye, 1977. Bulletin Mensuel de la Société Linnéenne de Lyon 49: 142–147. https://doi.org/10.3406/linly.1980.10415

Dubois A (1987) Miscellanea taxinomica batrachologica (I). Alytes 5: 7–95.

Dubois A (1992) Notes sur la classification des Ranidae (Amphibiens, Anoures). Bulletin mensuel de la Société linnéenne de Lyon 61: 305–352. https://doi.org/10.3406/linly.1992.11011

Dubois A, Matsui M, Ohler A (2001) A replacement name for *Rana* (*Paa*) *rara* Dubois & Matsui, 1983 (Amphibia, Anura, Ranidae, Raninae). Alytes 19: 2–4. https://doi.org/10.2307/1445091

Dubois A, Ohler A (2005) Taxonomic notes on the Asian frogs of the tribe Paini (Ranidae, Dicroglossinae): 1. Morphology and synonymy of *Chaparana aenea* (Smith, 1922), with proposal of a new statistical method for testing homogeneity of small samples. Journal of Natural History 39: 1759–1778. https://doi.org/10.1080/00222930400023735

Dubois A, Ohler A, Pyron RA (2021) New concepts and methods for phylogenetic taxonomy and nomenclature in zoology, exemplified by a new ranked cladonomy of Recent amphibians (Lissamphibia). Megataxa 5: 1–738. https://doi.org/10.11646/megataxa.5.1.1

Fei L (1999) Atlas of Amphibians of China. Henan Press of Science and Technology, Zhengzhou, 432 pp.

Fei L, Huang YZ (1985) A new species of the genus *Nanorana* (Amphibia: Ranidae) from northwestern Yunnan, China. Acta Biologica Plateau Sinica 4: 71–75.

Frost DR (2021) Amphibian Species of the World: an Online Reference. Version 6.1. Electronic Database. https://amphibiansoftheworld.amnh.org/index.php [accessed on 6 March 2021]

Gray JE (1845) Catalogue of the Specimens of Lizards in the Collection of the British Museum. Trustees of the British Museum/Edward Newman, London, 289 pp.

Günther ACLG (1860) Contribution to the knowledge of the reptiles of the Himalaya mountains. Proceedings of the Zoological Society of London 1860: 148–175.

Günther ACLG (1889) Third contribution to our knowledge of reptiles and fishes from the upper Yangtze-Kiang. Annals and Magazine of Natural History 4: 218–229. https://doi.org/10.1080/00222938909460506

Günther ACLG (1896) Report on the collections of reptiles, batrachians and fishes made by Messrs Potanin and Berezowski in the Chinese provinces Kansu and Sze-chuen. Annuaire du Musée Zoologique de l'Academie Impériale des Sciences de St. Pétersbourg 1: 199–219.

Hoang DT, Chernomor O, von Haeseler A, Minh BQ, Vinh LS (2018) UFBoot2: improving the ultrafast bootstrap approximation. Molecular Biology and Evolution 35: 518–522. https://doi.org/10.1093/molbev/msx281

Hu SQ (1985) Raninae (China). In: Frost DR (Ed.) Amphibian Species of the World: A Taxonomic and Geographical Reference. Allen Press, Kansas, 451–521.

Huang YZ, Fei L (1981) Two new species of amphibians from Xizang. Acta Zootaxonomica Sinica 6: 211–215.

Jiang JP, Dubois A, Ohler A, Tillier A, Chen XH, Xie F, Stöck M (2005) Phylogenetic relationships of the tribe Paini (Amphibia, Anura, Ranidae) based on partial sequences of mitochondrial 12S and 16S rRNA genes. Zoological Science 22: 353–362. https://doi.org/10.2108/zsj.22.353

Jiang K, Ren JL, Wang J, Guo JF, Wang Z, Liu YH, Jiang DC, Li JT (2020) Taxonomic revision of *Raorchestes menglaensis* (Kou, 1990) (Amphibia: Anura), with descriptions of two new species from Yunnan, China. Asian Herpetological Research 11: 263–281. https://doi.org/10.16373/j.cnki.ahr.200018

Kalyaanamoorthy S, Minh BQ, Wong TKF, von Haeseler A, Jermiin LS (2017) ModelFinder: fast model selection for accurate phylogenetic estimates. Nature Methods 14: 587–589. https://doi.org/10.1038/nmeth.4285

Kumar S, Stecher G, Li M, Knyaz C, Tamura K (2018) MEGA X: Molecular Evolutionary Genetics Analysis across computing platforms. Molecular Biology and Evolution 35: 1547–1549. https://doi.org/10.1093/molbev/msy096

Liu CZ, Hu SQ, Fei L, Huang CC (1973) On collections of amphibians from Hainan Island. Acta Zoologica Sinica 19: 385–404.

Liu CZ, Hu SQ, Yang FH (1960) Amphibia of Yunnan collected in 1958. Acta Zoologica Sinica 12: 149–174.

Liu S, Rao DQ (2021) A new species of the genus *Pareas* (Squamata, Pareidae) from Yunnan, China. ZooKeys 1011: 121–138. https://doi.org/10.3897/zookeys.1011.59029

Nguyen LT, Schmidt HA, von Haeseler A, Minh BQ (2015) IQ-TREE: a fast and effective stochastic algorithm for estimating maximum-likelihood phylogenies. Molecular Biology and Evolution 32: 268–274. https://doi.org/10.1093/molbev/msu300

Ohler A, Dubois A (2006) Phylogenetic relationships and generic taxonomy of the tribe Paini (Amphibia, Anura, Ranidae, Dicroglossinae), with diagnoses of two new genera. Zoosystema 28: 769–784.

Palumbi SR, Martin A, Romano S, McMillan W, Stice L, Grabowski G (1991) The Simple Fool's Guide to PCR. University of Hawaii Press, Honolulu, 94 pp.

Qi S, Zhou ZY, Lu YY, Li JL, Qin HH, Hou M, Zhang Y, Ma JZ, Li PP (2019) A new species of *Nanorana* (Anura: Dicroglossidae) from southern Tibet, China. Russian Journal of Herpetology 26: 159–174. https://doi.org/10.30906/1026-2296-2019-26-3-159-174

Roelants K, Jiang JP, Bossuyt F (2004) Endemic ranid (Amphibia: Anura) genera in southern mountain ranges of the Indian subcontinent represent ancient frog lineages: evidence from molecular data. Molecular Phylogenetics and Evolution 31: 730–740. https://doi.org/10.1016/j.ympev.2003.09.011

Ronquist F, Teslenko M, Van Der Mark P, Ayres DL, Darling A, Höhna S, Larget B, Liu L, Suchard MA, Huelsenbeck JP (2012) MrBayes 3.2: efficient Bayesian phylogenetic inference and model choice across a large model space. Systematic Biology 61: 539–542. https://doi.org/10.1093/sysbio/sys029

Saikia B, Sinha B, Kharkongor I (2017) *Odorrana arunachalensis*: a new species of Cascade Frog (Anura: Ranidae) from Talle Valley Wildlife Sanctuary, Arunachal Pradesh, India. Journal of Bioresources 4: 30–41.

Sichuan Institute of Biology Herpetology Department (1977) A survey of amphibians in Xizang (Tibet). Acta Zoologica Sinica 23: 54–63.

Smith MA (1922) Notes on reptiles and batrachians from Siam and Indo-China (no. 1). Journal of the Natural History Society of Siam 4: 203–214.

Smith MA (1951) On a collection of amphibians and reptiles from Nepal. Annals and Magazine of Natural History (Series 12) 6: 726–728. https://doi.org/10.1080/00222935308654472

Stejneger L (1927) A new genus and species of frog from Tibet. Journal of the Washington Academy of Sciences 17: 317–319.

Stoliczka F (1872) Notes on some new species of Reptilia and Amphibia, collected by Dr. W. Waagen in north-western Punjab. Proceedings of the Asiatic Society of Bengal 1872: 124–131.

Thompson JD, Higgins DG, Gibson TJ (1994) CLUSTAL W: improving the sensitivity of progressive multiple sequence alignment through sequence weighting, position-specific gap penalties and weight matrix choice. Nucleic Acids Research 22: 4673–4680. https://doi.org/10.1093/nar/22.22.4673

Yang X, Wang B, Hu JH, Jiang JP (2011) A new species of the genus *Feirana* (Amphibia: Anura: Dicroglossidae) from the western Qinling Mountains of China. Asian Herpetological Research 2: 72–86. https://doi.org/10.3724/SP.J.1245.2011.00072

ZooKeys 1048: 69–78 (2021)
doi: 10.3897/zookeys.1048.66920
https://zookeys.pensoft.net

SHORT COMMUNICATION

A peer-reviewed open-access journal
ZooKeys
Launched to accelerate biodiversity research

# The first queen-worker association for Cretaceous Formicidae: the winged caste of *Haidomyrmex cerberus*

Yuanyuan Guo[1], Chungkun Shih[1,2], De Zhuo[3], Dong Ren[1], Yunyun Zhao[1], Taiping Gao[1]

**1** *College of Life Sciences and Academy for Multidisciplinary Studies, Capital Normal University, 105 Xisanhuanbeilu, Haidian District, Beijing 100048, China* **2** *Department of Paleobiology, National Museum of Natural History, Smithsonian Institution, Washington, DC, 20013–7012, USA* **3** *Beijing Xiachong Amber Museum, 9 Shuanghe Middle Road, Beijing, 100023, China*

Corresponding authors: Yunyun Zhao (zhaoyy@cnu.edu.cn); Taiping Gao (tpgao@cnu.edu.cn)

Academic editor: Brian Lee Fisher | Received 4 April 2021 | Accepted 2 June 2021 | Published 7 July 2021

*http://zoobank.org/66461E6D-860D-4709-82BC-23936836C805*

**Citation:** Guo YY, Shih CK, Zhuo D, Ren D, Zhao YY, Gao TP (2021) The first queen-worker association for Cretaceous Formicidae: the winged caste of *Haidomyrmex cerberus*. ZooKeys 1048: 69–78. https://doi.org/10.3897/zookeys.1048.66920

## Abstract

Two queen ant specimens, one alate and one dealate, from mid-Cretaceous (Late Albian–Early Cenomanian) Burmese amber are herein reported as belonging *Haidomyrmex cerberus* Dlussky, 1996. This is the first discovery and documentation of an alate queen in *Haidomyrmex*. Compared with workers of *Haidomyrmex cerberus*, alate and dealate queens are larger in body size, have smaller compound eyes, a longer antennal scape, more complex mandibles, and a relatively large-sized metasoma. It is hypothesized that these differences are due to caste differences.

## Keywords

Alate queen, dealate queen, Haidomyrmecine, Myanmar, queen ant, workers

## Introduction

Mandibles, as the main structures used for foraging, predation, food handling, defense and brood care (Hölldobler and Wilson 1990), are vital to the biology, taxonomy and evolutionary development of ants. For example, haidomyrmecine and zigrasimeciine

ants with unique mandibles have been reported in mid-Cretaceous amber deposits from Myanmar (Dlussky 1996; Barden and Grimaldi 2012, 2013; Perrichot 2014; Perrichot et al. 2016, 2020; Miao and Wang 2019; Cao et al. 2020a, b, c; Lattke and Melo 2020). To date, ten genera and sixteen species of haidomyrmecine ants from Cretaceous amber deposits from France, Canada and Myanmar have been described. *Haidomyrmex*, as the type genus of the extinct subfamily Haidomyrmecinae, has been frequently discussed in relation to the other genera. In 1996, *Haidomyrmex cerberus* Dlussky, 1996, with a peculiar cranio-mandibular morphology, was found in Burmese amber and described. The combination of its bizarre mandibles and head capsule suggested that this ant might have been a specialized predator (Dlussky 1996). However, parts of the antennae, legs and gaster were not preserved in the type specimen whereas some key characters, especially those of the head, were obscured due to the turbidity of the amber piece. Cao et al. (2020a) provided a more detailed description of this species based on two additional worker specimens, including some characters of the antennae, head, legs and gaster. Based on some key characters, such as antennal length, size of compound eyes, location of trigger hairs, and mandible morphology, Lattke and Melo (2020) provided a key for identifying species of *Haidomyrmex*. Unfortunately, until now there was no description of alate queens in *Haidomyrmex*. Barden and Grimaldi (2012) described the only previously-known dealate queen, for the species *Haidomyrmex scimitarus* Barden & Grimaldi. In this study, we report two queen ant specimens of *Haidomyrmex cerberus*: one dealate and one alate, which represents the first discovery of a winged caste in *Haidomyrmex*. Comparing their morphological characters with those of the known dealate queen and workers provides insights into caste differences in *Haidomyrmex* ants.

## Material and methods

This study is based on two new amber specimens from the Hukawng Valley in the Kachin State of northern Myanmar, at the north end of Noije Bum at 26°15'N, 96°34'E, some 18 km south-west of the town of Tanai (Grimaldi et al. 2002; Cruickshank and Ko 2003). The deposit is dated to 98.79 ± 0.62 Mya based on radiometric uranium-lead dating (Shi et al. 2012). The recent finding of an ammonite embedded in amber and assignable to *Puzosia* (*Bhimaites*) supports a Late Albian–Early Cenomanian age of the amber (Yu et al. 2019). The newly-reported amber specimens are housed in the Key Lab of Insect Evolution and Environmental Changes, College of Life Sciences and Academy for Multidisciplinary Studies, Capital Normal University (**CNUB**), Beijing, China.

Specimens No. CNU-HYM-MA2015010 and No. CNU-HYM-MA2015011 are separately preserved in two yellow amber pieces with organic particles, tiny bubbles and dust covering the cuticle in places. Specimens were examined and photographed by using a Nikon SMZ 25 microscope equipped with a Nikon DS-Ri 2 digital camera. The line drawing and figure plates were prepared by using the Adobe Illustrator CC

**Table 1.** Measurements, including abbreviations, used in the descriptions.

| Measurement | Explanation |
|---|---|
| Body length (BL) | in lateral view, from anteriormost point of head capsule excluding mandibles to posteriormost point of abdomen excluding sting. |
| Head length (HL) | in lateral view, from basal insertion of mandibles to the posteriormost point of head capsule. |
| Head height (Hh) | in lateral view, vertical distance from lowermost to highermost point of head capsule. |
| Scape length (SL) | maximum length of scape excluding condylar neck. |
| Eye length (EL) | maximum diameter of compound eye. |
| Mandible length (ML) | in lateral view, straight distance of mandible from basal insertion to apex. |
| Weber's length (WL) | diagonal length of mesosoma in lateral view, from anteriormost point of pronotum to posteriormost point of propodeum. |
| Petiole height (PH) | maximum height of petiole excluding subpetiolar process in lateral view. |
| Petiole length (PL) | maximum length of petiole in lateral view. |
| Gaster length (GL) | maximum length of gaster (abdominal segments III–VII) in lateral view. |

and Adobe Photoshop CC graphics software. Measurements were obtained using the measurement tool of the Nikon software. All measurements are provided in millimeters (mm). Measurements used in the descriptions, including their abbreviations, are detailed in Table 1.

## Taxonomy

**Family Formicidae Latreille, 1809**
**Subfamily Haidomyrmecinae Bolton, 2003**
**Genus *Haidomyrmex* Dlussky, 1996**

***Haidomyrmex cerberus* Dlussky, 1996**
Figs 1–3

**Specimens examined.** CNU-HYM-MA2015011, an alate queen, and CNU-HYM-MA2015010, a dealate queen, both housed in Capital Normal University, Beijing, (CNUB). ***Holotype*** NHM.In.20182, in Natural History Museum, London, UK.

**Diagnosis.** Alate and dealate queens. Antenna with scape distinctly longer than pedicel and the two following flagellomeres combined, FII (second flagellomere) longer than each of the other flagellomeres. Labrum with two long setae curved upward. Mandibles long, internal surface of curved portion with a row of longitudinal serrations on the apical quarter; apical portion tapered to a blunt tip, external margin of apex each with a short erect and suberect seta. Maxillary palps distinctly elongate, formed of 6 segments; labial palps relatively short, formed of 4 segments. Propleuron well developed, with dorsal portion exposed and visible dorsally.

**Description of alate and dealate queens.** Based on CNU-HYM-MA2015011, alate queen, with differential characters from CNU-HYM-MA2015010, dealate queen in square brackets.

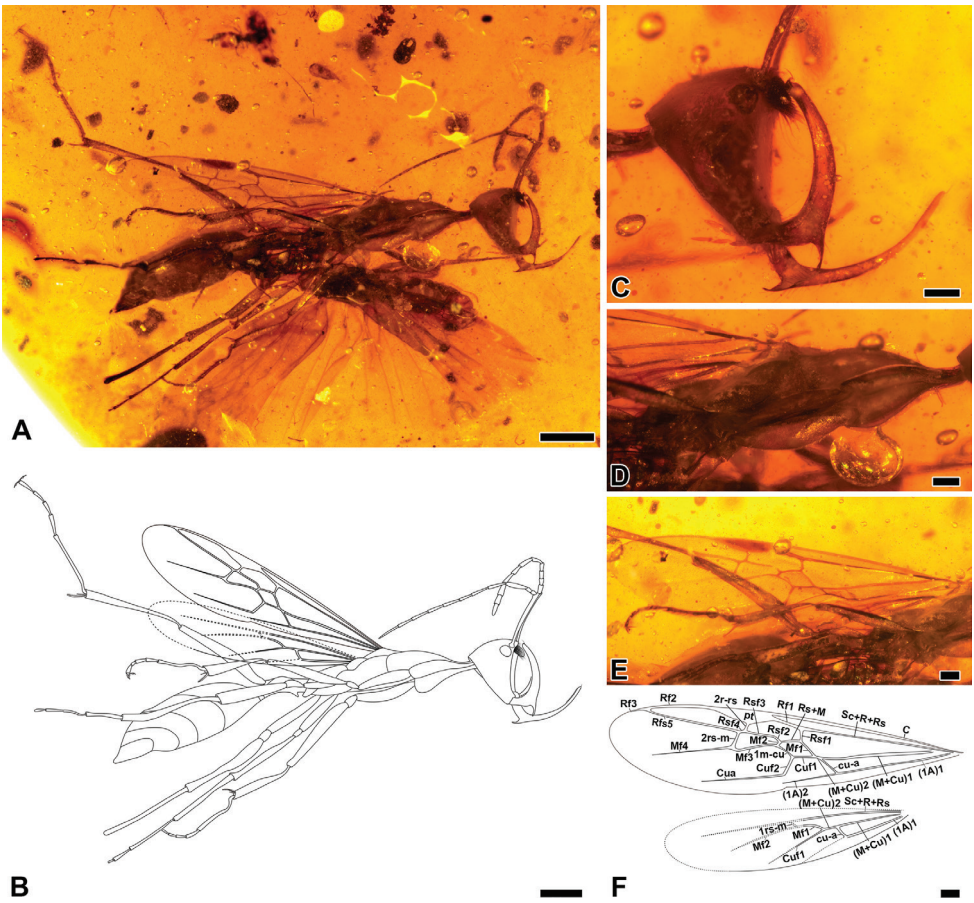


**Figure 1.** *Haidomyrmex cerberus*, alate queen specimen CNU-HYM-MA2015011 **A** photo of right lateral habitus **B** line drawing of habitus **C** photo of head in lateral view **D** photo of mesosoma in lateral view **E** photo of right forewing venation **F** line drawing of right forewing and right hind wing. Scale bars: 1 mm (**A, B**); 0.25 mm (**C–F**).

***Head*:** Vertex broad, evenly rounded, in lateral view approximately as high as long, shaped as an upside-down isosceles triangle; with sparsely thin erect setae [vertex in lateral view severely shrunken, glabrous]. No ocelli. Compound eyes situated high on head capsule, in lateral view ovoid and strongly convex [reniform and weakly convex]. Antennae inserted between compound eyes and flanking clypeal lobe, bases exposed and frontal lobes absent. Antenna geniculate, formed of 12 segments; scape ca. 8 times as long as pedicel [ca. 6 times], FI (first flagellomere) ca. 1.3 times as long as pedicel [ca. 1.2 times]; FII ca. 3 times as long as pedicel. Apex of scape slightly broadened, its margin bearing short and erect setae; FI with a long and curved seta on median ventral surface. Clypeal process a small lobe moderately protruding between bases of antennae, with short peg-like denticles above and longer, dense, stiff

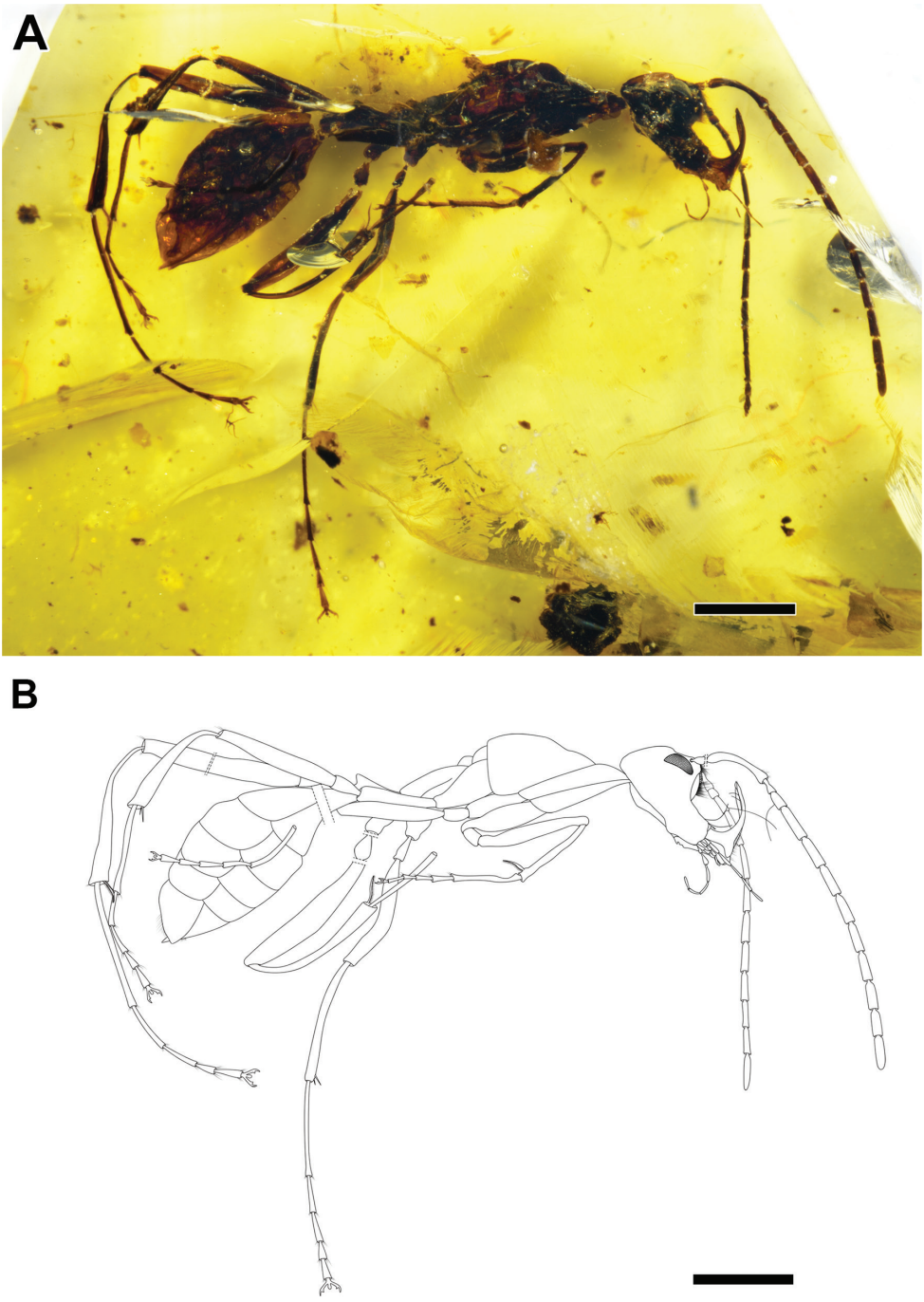


**Figure 2.** *Haidomyrmex cerberus*, dealate queen specimen CNU-HYM-MA2015010 **A** photo of right lateral habitus **B** line drawing of habitus. Scale bars: 1 mm.

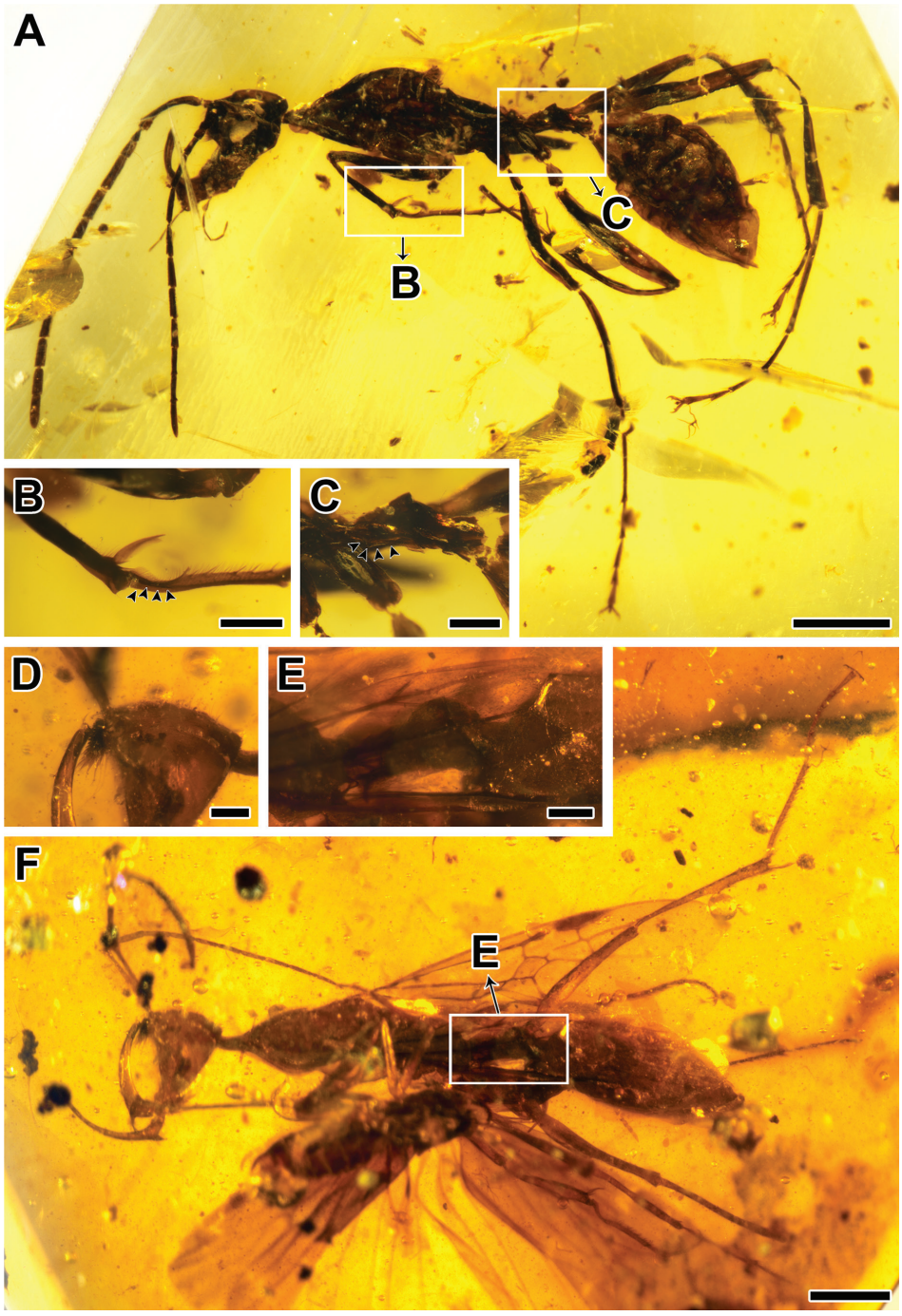


**Figure 3.** *Haidomyrmex cerberus*, specimens CNU-HYM-MA2015010 (**A–C**) and CNU-HYM-MA2015011 (**D–F**) **A** photo of left lateral habitus **B** photo of protibial apex and associated tarsus **C** photo of petiole in lateral view **D** photo of clypeal lobe in lateral view **E** photo of petiole in lateral view **F** photo of left lateral habitus. Scale bars: 1 mm (**A, F**); 0.25 mm (**B–E**).

spine-like setae arranged in longitudinal rows on ventral half. Ventral surface of clypeus with one visible pair of long, fine trigger hairs [trigger hairs invisible]. Labrum with two long setae curved upward. Mandible long, scythe-shaped, internal surface of curved portion with 1–2 short setae near apex and a row of longitudinal serrations on apical quarter; apical portion tapered to a blunt tip, apex reaching clypeal lobe and each with one short, erect and suberect seta; ventral corner between basal and curved portion bearing a triangular blade, apparently symmetrical and with a single tooth; ventral margin of corner with sparsely fine setae from base to apex, becoming gradually shorter and thinner [with dense fine setae from base to one third of external surface of curved portion]. Maxillary palp exposed length 0.53, with 4 visible segments [length 0.86, with 6 obvious segments]. Labial palp is invisible [length 0.30, with 4 segments].

***Mesosoma*:** Long, slender, with sparsely thin erect setae [no visible setae]. Neck narrow and short, pronounced in lateral view. Propleuron well developed and visible in lateral view. Pronotum well developed, convex in anterior two thirds, gradually flattened in posterior third, extending laterally to anterior level of procoxa. Sulcus between pronotum and propleuron and between pronotum and mesonotum present, complete. Mesoscutum shorter than pronotum, mesoscutal dorsal outline slightly convex, with parapsidal furrows converging posteriorly to reach anterior mesonotal margin. Mesoscutellum posteriorly expanded, dorsal and posterior mesoscutellar surfaces concave. Dorsal level of metanotum and propodeum nearly at same level; propodeum slightly lower in elevation and dorsal surface gradually sloping posteriorly [metanotum and propodeum gradually sloping posteriorly]. Metapleural gland opening oval-shaped, slightly depressed. Legs long. Length of procoxa: 1.24 [0.70]; mesocoxa: 1.03 [0.38]; metacoxa:1.32 [0.47]; protrochanter: 0.20 [0.17]; meso- and metatrochanters: 0.27 [0.20]; profemur: 1.65 [1.17]; meso- and metafemora: ca. 1.78 [1.40]; protibia: 1.23 [0.94]; mesotibia: 1.32 [1.25]; metatibia: 1.92 [1.47]. Protibia apex with one large pectinate spur and two short spine-like setae, pecten of probasitarsus with fine hairs of uniform length. Mesotibia with two simple spurs, metatibia with one large pectinate spur and one short simple spur. Protarsus length 1.80 [1.40]; mesotarsus incompletely preserved, part of tarsomeres absent [complete, length 2.09]; metatarsus length 2.65 [2.55]. Ventral surface of tarsomeres with fine setulae and apex of tarsomeres I–V with two pairs of fine, long setae. Pretarsal claws with distinct subapical teeth; arolium small.

***Metasoma*:** Petiole ca. 2.5 times as long as height [ca. 2.2 times], petiolar tergite a broadly convex node, with anterior surface approximately twice as long as posterior surface, with short anterior peduncle; small subpetiolar process projecting ventrally as a small triangle. Gaster with five segments, gastral segments I and II (abdominal segments III and IV) ca. 0.50 of total gaster length. Pygidium and hypopygium setulose. Sting very well developed.

***Right forewing*:** Venation almost complete, anterior margin slightly folded. Cell 1R1C/SMC1 hexagonal; cell 1MC/DC1 with five sides, Rsf2 and Rsf3 distinguished, Rsf4 very short, almost as long as Mf2; (M+Cu)1 branched into (M+Cu)2 and cu-a;

(M+Cu)2 short, nearly half of Rsf1; Rs+M almost as long as Mf1 and almost parallel to Cuf1; Mf2 present to juncture of Rs+M and 1m-cu; cross-vein 2rs-m slightly oblique. Nearly whole right hind wing folded over itself. (M+Cu)2 nearly as long as cross-vein cu-a; Mf1 aligned with Mf2 [wings not preserved].

**Measurements (in mm).** (CNU-HYM-MA2015011, alate queen), [CNU-HYM-MA2015010, dealate queen]. BL (7.75) [6.31]; HL (1.15) [1.17]; Hh (1.24) [0.96]; EL (0.24) [0.28]; length of antennomeres (total 4.41, scape 1.12, pedicel 0.13, FI 0.18, FII 0.39, FIII 0.34, FIV 0.33, FV 0.31, FVI 0.32, FVII 0.34, FVIII 0.33, FIX 0.29, FX 0.30) [total 3.91, scape 0.75, pedicel 0.12, FI 0.15, FII 0.39, FIII 0.35, FIV 0.33, FV 0.28, FVI 0.31, FVII 0.31, FVIII 0.30, FIX 0.28, FX 0.33]; ML (0.98) [0.64]; WL (3.01) [2.45]; PL (0.79) [0.51]; PH (0.31) [0.23]; GL (2.78) [2.24].

**Remarks.** Assignment of these two new specimens to *H. cerberus* is based on most of the characters used by Barden and Grimaldi (2012) and Cao et al. (2020a). This species is most similar to *H. scimitarus*, but the two new specimens could be assigned to *H. cerberus* by having 1) a slightly longer scape, longer than the pedicel and the two following flagellomeres combined (vs. scape visibly shorter in *H. scimitarus*); 2) labrum with two long setae curved upward (vs. labrum with four fine setae); 3) ventral corner of mandible between basal and curved portion with a triangular blade, apparently symmetrical and with a single tooth (vs. 3–4 fine mesal teeth on left mandible, 2–3 slightly larger teeth on right mandible); and 4) head with sparse thin and erect setae (vs. glabrous in *H. scimitarus*).

## Conclusion

Most workers and queens of modern ants are known and the castes can be differentiated by body size and by minor aspects of the mandibular morphology (Hölldobler and Wilson 1990). It is highly probable that all the differences between the two queens described herein and the workers of *H. cerberus* revised by Cao et al. (2020a) are simply due to the difference in caste. The two queens can be differentiated from workers of *H. cerberus* by 1) the larger body of 6.3–7.8 mm (vs. 4.5–5.0 mm body lengths for workers); 2) the obviously longer scape, distinctly longer than the pedicel and two following flagellomeres combined (vs. scape as long as the pedicel and two following flagellomeres combined) and ca. 6–9 times as long as pedicel (vs. ca. 4 times as long as pedicel); 3) the more complex shape of the mandibles, with inner surface with a row of longitudinal serrations near the apex, and triangular blade clearly longer and sharper; 4) metasoma relatively large in proportion to total body size (ca. 0.36 times as long as body vs. ca. 0.32 times as long as body), because of flight muscles. Queens of modern species usually have larger eyes relative to head size compared to workers. Surprisingly, the queens of *H. cerberus* have smaller compound eyes (diameters of 0.24 mm and 0.28 mm) than those of workers (0.30 mm). Documentation of these differences con-

tributes to a better understanding of the Cretaceous Formicidae and shows differences among castes of *Haidomyrmex cerberus* for the first time.

## Acknowledgements

We appreciate Dr. Vincent Perrichot for his helpful advice. We thank the Editorial Board of Zookeys, in particular Dr. Brian Fisher, and two anonymous reviewers for their critical review of the manuscript, with valuable input and guidance. D.R. was supported by grants from the National Natural Science Foundation of China (No. 31730087 and 32020103006). T.P.G. was supported by the Fok Ying-Tong Education Foundation for Young Teachers in the Higher Education Institutions of China (No. 171016).

## References

Barden P, Grimaldi DA (2012) Rediscovery of the bizarre Cretaceous ant *Haidomyrmex* Dlussky (Hymenoptera: Formicidae), with two new species. American Museum Novitates 3755: 1–16. https://doi.org/10.1206/3755.2

Barden P, Grimaldi DA (2013) A new genus of highly specialized ants in Cretaceous Burmese amber (Hymenoptera: Formicidae). Zootaxa 3681(4): 405–412. https://doi.org/10.11646/zootaxa.3681.4.5

Cao HJ, Perrichot V, Shih CK, Ren D, Gao TP (2020a) A revision of *Haidomyrmex cerberus* Dlussky (Hymenoptera: Formicidae: Sphecomyrminae) from mid-Cretaceous Burmese amber. Cretaceous Research 106: 104226. https://doi.org/10.1016/j.cretres.2019.104226

Cao HJ, Boudinot BE, Wang Z, Miao XF, Shih CK, Ren D, Gao TP (2020b) Two new iron maiden ants from Burmese amber (Hymenoptera: Formicidae: †Zigrasimeciini). Myrmecological News 30: 161–173.

Cao HJ, Boudinot BE, Shih CK, Ren D, Gao TP (2020c) Cretaceous ants shed new light on the origins of worker polymorphism. SCIENCE CHINA Life Sciences 63: 1085–1088. https://doi.org/10.1007/s11427-019-1617-4

Cruickshank RD, Ko K (2003) Geology of an amber locality in the Hukawng valley, northern Myanmar. Journal of Asian Earth Sciences 21: 441–455. https://doi.org/10.1016/S1367-9120(02)00044-5

Dlussky GM (1996) Ants (Hymenoptera: Formicidae) from Burmese amber. Paleontological Journal 30: 449–454.

Grimaldi D, Engel MS, Nascimbene PC (2002) Fossiliferous Cretaceous amber from Myanmar (Burma): its rediscovery, biotic diversity, and paleontological significance. American Museum Novitates 3361: 1–71. https://doi.org/10.1206/0003-0082(2002)361%3C0001:FCAFMB%3E2.0.CO;2

Hölldobler B, Wilson EO (1990) The Ants. The Belknap Press of Harvard University Press, Cambridge.

Lattke JE, Melo GAR (2020) New haidomyrmecine ants (Hymenoptera: Formicidae) from mid-Cretaceous amber of northern Myanmar. Cretaceous Research 114: 104502. https://doi.org/10.1016/j.cretres.2020.104502

Miao Z, Wang M (2019) A new species of hell ants (Hymenoptera: Formicidae: Haidomyrmecini) from the Cretaceous Burmese amber. Journal of Guangxi Normal University 37: 139–142. https://doi.org/10.16088/j.issn.1001-6600.2019.02.017

Perrichot V (2014) A new species of the Cretaceous ant *Zigrasimecia* based on the worker caste reveals placement of the genus in the Sphecomyrminae (Hymenoptera: Formicidae). Myrmecological News 19: 165–169. https://doi.org/10.1097/TA.0b013e31821517c5

Perrichot V, Wang B, Engel MS (2016) Extreme morphogenesis and ecological specialization among Cretaceous basal ants. Current Biology 26: 1468–1472. https://doi.org/10.1016/j.cub.2016.03.075

Perrichot V, Wang B, Barden P (2020) New remarkable hell ants (Formicidae: Haidomyrmecinae stat. nov.) from mid-Cretaceous amber of northern Myanmar. Cretaceous Research 109: 104381. https://doi.org/10.1016/j.cretres.2020.104381

Shi GH, Grimaldi DA, Harlow GE, Wang J, Wang J, Yang MC, Lei WY, Li QL, Li XH (2012) Age constraint on Burmese amber based on U-Pb dating of zircons. Cretaceous Research 37: 155–163. https://doi.org/10.1016/j.cretres.2012.03.014

Yu TT, Kelly R, Lin M, Ross A, Kennedy J, Broly P, Xia FY, Zhang HC, Wang B, Dilcher D (2019) An ammonite trapped in Burmese amber. Proceedings of the National Academy of the Sciences of the United States of America 116: 11345–11350. https://doi.org/10.1073/pnas.1821292116

ZooKeys 1048: 79–89 (2021)
doi: 10.3897/zookeys.1048.66477
https://zookeys.pensoft.net

RESEARCH ARTICLE

A peer-reviewed open-access journal
ZooKeys
Launched to accelerate biodiversity research

# A new record of odd-scaled snake (Serpentes, Xenodermidae) from Vietnam: expanded description of *Parafimbrios vietnamensis* based on integrative taxonomy

Nikolai L. Orlov[1], Oleg A. Ermakov[2], Tao Thien Nguyen[3], Natalia B. Ananjeva[1]

**1** *Zoological Institute, Russian Academy of Sciences, Universitetskaya nab. 1, St. Petersburg, 199034, Russia* **2** *Penza State University, Krasnaya ul. 40, Penza, 440026, Russia* **3** *Vietnam National Museum of Nature, Vietnam Academy of Science and Technology, 18 Hoang Quoc Viet Road, Cau Giay, Hanoi, Vietnam*

Corresponding author: Nikolai L.Orlov (azemiops@zin.ru)

Academic editor: Robert Jadin | Received 25 March 2021 | Accepted 26 May 2021 | Published 8 July 2021

*http://zoobank.org/45A68220-4E3D-41E1-9E11-3CE42204FFD0*

**Citation:** Orlov NL, Ermakov OA, Nguyen TT, Ananjeva NB (2021) A new record of odd-scaled snake (Serpentes, Xenodermidae) from Vietnam: expanded description of *Parafimbrios vietnamensis* based on integrative taxonomy. ZooKeys 1048: 79–89. https://doi.org/10.3897/zookeys.1048.66477

## Abstract

Based on the combination of molecular and morphological data, we herein report the second known finding of the xenodermid snake species *Parafimbrios vietnamensis* Ziegler, Ngo, Pham, Nguyen, Le & Nguyen, 2018. The male individual was found in the Yen Bai Province of northwestern Vietnam, more than 200 km from the type locality in Lai Chau Province. Genetic divergence between the newly-collected male and the holotype was low (1.7%), and is in agreement with morphological data that supports that they are conspecific. We give a detailed description of the morphological characters and coloration of the new record and provide an expanded diagnosis of *P. vietnamensis*. *Parafimbrios* is a poorly-understood genus, and our recent discovery brings the total number of known specimens of the genus to nine, 1/3 of them having been found in Vietnam (one specimen of *P. lao* and now two specimens of *P. vietnamensis*).

## Keywords

Distribution, molecular identification, morphology, odd-scaled snake, *Parafimbrios*, Xenodermidae, Vietnam

## Introduction

The snake family Xenodermidae is one of the most poorly-known groups of Asian reptiles. The family is composed of five genera and 23 recognized species that are distributed throughout South, Southeast, and East Asia (Uetz et al. 2020). Many species are only known from a single or a few specimens from a limited number of localities. Among these five genera, *Parafimbrios* Teynié, David, Lottier, Le & Vidal, 2015 only has two recognized species, which are endemic to Indochina and occur across Laos, Vietnam, Thailand and south China (Nguyen et al. 2015; Teynié et al. 2015; Teynié and Hauser 2017; Ziegler et al. 2018; Cai et al. 2020) (Fig. 1).

The genus was originally described as monotypic, including only *Parafimbrios lao* Teynié, David, Lottier, Le & Vidal, 2015 from Louangphabang and Houaphan provinces in northeastern Laos, based on a unique set of morphological characters and high levels of genetic divergence (Teynie et al. 2015). Three years later, the second species was described as *Parafimbrios vietnamensis* Ziegler, Ngo, Pham, Nguyen, Le & Nguyen, 2018 from Lai Chau Province in northwestern Vietnam. Until recently, *P. vietnamensis* was only known from the holotype male. However, during a recent herpetological survey in Yen Bai Province in northern Vietnam, another male specimen was collected that had the unique set of morphological characteristics and color pattern typical for *P. vietnamensis*. Subsequent molecular analysis confirmed the morphological findings and we herein provide a detailed description of the second known specimen of *P. vietnamensis* and an expanded diagnosis of the species.

This discovery brings the total number of known specimens of *Parafimbrios* to nine and of *P. vietnamensis* to two. This work highlights the difficult nature of discovering specimens of this snake family and the need for further surveys in these areas of Vietnam and Eastern Laos.

## Material and methods

This study is based on a single male specimen of *Parafimbrios vietnamensis* (ZISP 31426) from Che Tao Village, Che Tao Commune, of the Mu Cang Chai Species and Habitat Conservation Area (SHCA) (21.5435°N, 104.0364°E, elevation 1300 m) in Yen Bai Province, Vietnam. The specimen was collected on November 30$^{th}$, 2019, by Nikolai Orlov and Larissa Ioganssen and was fixed and subsequently stored in 75% ethanol. A tissue sample was preserved separately in 95% ethanol. The specimen was deposited in the herpetological collection of the Zoological Institute, Russian Academy of Sciences (ZISP), St. Petersburg, Russia.

### Morphological examination

Sex was determined by inspection of the presence or absence of hemipenes. Measurements were taken to the nearest mm with digital calipers. Paired meristic characters are given as left/right. The methodology of measurements and meristic counts followed

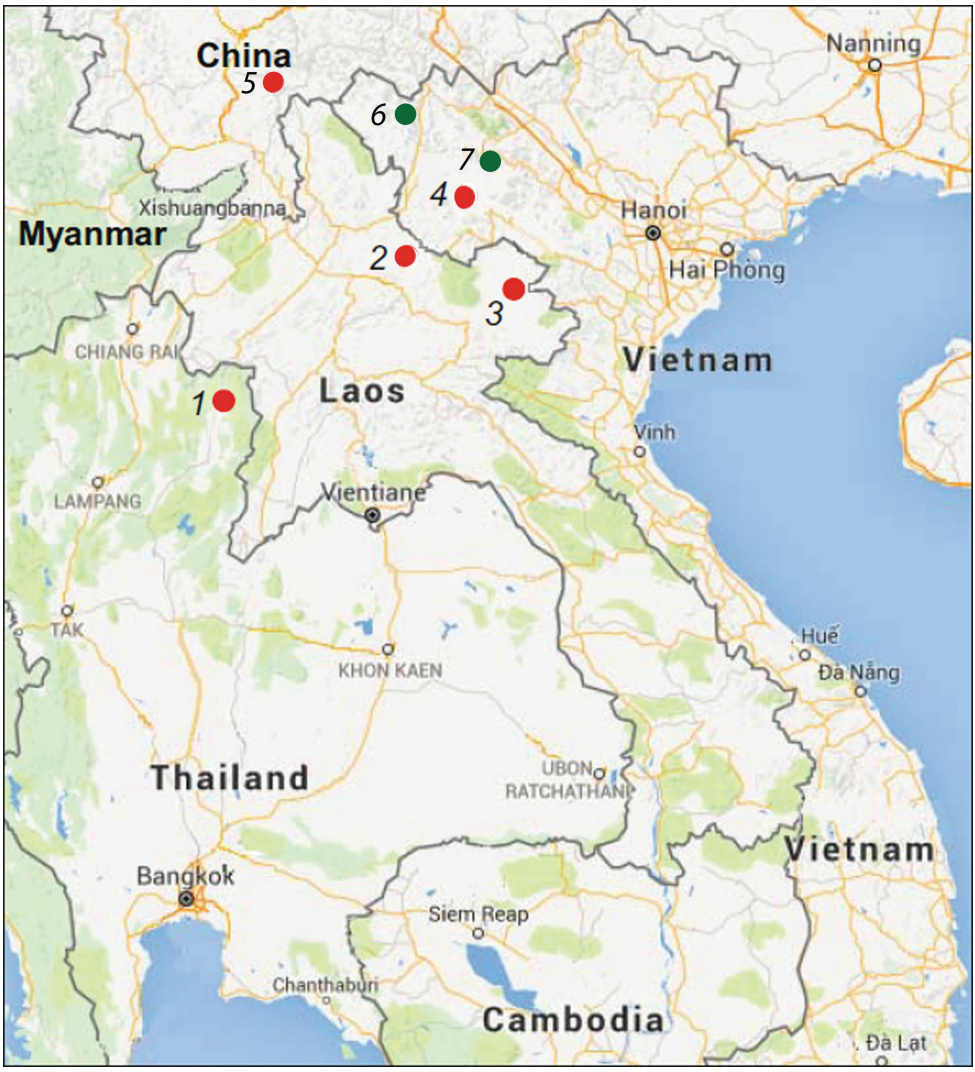


**Figure 1.** Map of Indochina showing the known localities of *Parafimbrios lao* (red dots) and *P. vietnamensis* (green dots) (after Teynié et al. 2015; Nguyen et al. 2015; Teynié and Hauser. 2017; Ziegler et al. 2018; Bo et al. 2020) ***1*** Pua district, Nan Province, Thailand ***2*** Ngoi District, Luangphrabang Province, Laos (type locality of *P.lao*) ***3*** Vieng Xai District, Houaphan Province, Laos ***4*** Thuan Chau District, Son La Province, Vietnam ***5*** Jiangcheng County, Yunnan Province, Southwestern China; *P. vietnamensis* ***6*** Hoang Ho Village, Phang So Lin Commune, Sin Ho District, Lai Chau Province, Vietnam, 22.4167°N, 103.3681°E (type locality of *P. vietnamensis*) ***7*** ZISP 31426, Che Tao Village, The Mu Cang Chai Species and Habitat Conservation Area (SHCA), Yen Bai Province, Vietnam, 21.5435°N, 104.0364°E (new record of *P. vietnamensis*).

Teynié et al. (2015) and Ziegler et al. (2018). The following characters and ratios were evaluated and calculated (Table 1): snout-vent length measured from tip of snout to anterior margin of cloaca (SVL); tail length measured from posterior margin of cloaca to tip of tail (TaL); total length, corresponding to SVL + TaL (TL); ratio of tail length to to-

**Table 1.** Measuremements (in mm), dentition and scalation of *Parafimbrios vietnamensis* compared to *P. lao*.

| Characters | *Parafimbrios lao* male holotype MNHN 2013.1002 | *P. lao* male not collected | *P. lao* male TBU PAR.127 | *P. lao* male QSMI 1381 | *P. lao* male QSMI 1382 | *P. lao* male not collected | *P. lao* female CIB2019090746 | *Parafimbrios vietnamensis* male holotype IEBR A.2018.7 | *P. vietnamensis* ZISP 31426 subadult male |
|---|---|---|---|---|---|---|---|---|---|
| Country | Laos | Laos | Vietnam | Thailand | Thailand | Thailand | China | Vietnam | Vietnam |
| Province | Luangphrabang | Houaphan | Son La | Nan | Nan | Nan | Yunnan | Lai Chau | Yen Bai |
| Snout-vent length mm | 236 | 298 | 310 | 294 | 333 | ? | 256 | 222 | 298 |
| Tail length (TaL) mm | 49 | 55 | 56.5 | 66 | ~72 | ? | 53 | 44 | 56 |
| Total length (TL) mm | 285 | 353 | 366.5 | 360 | ~405 | ~350 | 309 | 266 | 354 |
| TaL / TL | 0.172 | 0.156 | 0.150 | 0.183 | 0.177 | | 0.171 | 0.165 | 0.163 |
| Maxillary teeth | 27 | - | - | - | - | - | - | 27 | 27 |
| Dorsal scale rows | 27–25–23* | 27–25–23* | 27–27–25 | 25 | 25? | 25? | 29-27-24 | **35–33–29** | **31-35-27** |
| Ventrals | 177+2 | 189+1 | 185 | 179 | 171+ | ? | 168 | **164** | 172+2 |
| Subcaudals | 56 | 55 | 53 | 61 | ? | ? | 52 | **49** | **48** |
| Cloacal | 1 | 1 | 1 | - | - | - | - | 1 | 1 |
| Supralabials | 8/8 | 7/7 | 8/8 | - | - | - | - | 8/8 | 8/8 |
| Infralabials | 8/8 | 7/7 | 8/7 | - | - | - | - | 7/7 | 7/7 |
| Subocular | 1/1 | 1/1 | 1/1 | 1/? | 1/? | 1/? | 1/1 | 1/1 | 1/1 |
| Loreal | 1/1 | 1/1 | 1/1 | | | | | 1/1 | 1/1 |
| Preocular | 1/1 | 1/1 | 1/1 | 1/1 | 1/? | 1/? | 1/1 | 1/1 | 1/1 |
| Postoculars | 2/2 | 2/2 | 2/2 | 2/2 | 2/? | 2/? | 2/2 | 2/2 | 2/2 |
| Temporals | 2+2/2+2 | 2+2/2+1 | 2+2/2+2- | - | - | - | - | **4+4/4+5** | 2+3/2+3 |
| Source | Teynie et al. 2015 | Teynie et al. 2015 | Nguyen et al. 2015 | Teynie, Hauser 2017 | Teynie, Hauser 2017 | Teynie, Hauser 2017 | Cai et al. 2020 | Ziegler et al. 2018 | Our data |

tal length (TaL/TL); number of maxillary teeth, counted by investigating the right maxilla for teeth/sockets. The pholidosis characters taken or counted are as follows: dorsal scale rows counted at one head length behind head, at midbody, and at one head length before vent, respectively. The number of ventrals, subcaudals, supralabials, infralabials, suboculars, loreals, preoculars, postoculars, temporals and cloacal scales were counted. Morphological comparisons were based on data from Teynié et al. (2015), Nguyen et al. (2015), Teynié and Hauser (2017), Ziegler et al. (2018), and Cai et al. (2020).

Museum abbreviations are as follows:

**ZISP** Zoological Institute, Russian Academy of Sciences, St. Petersburg, Russia;
**IEBR** Institute of Ecology and Biological Resources, Vietnamese Academy of Science and Technology, Hanoi, Vietnam;
**MNHN** Muséum National d'Histoire Naturelle, Paris, France;
**TBU PAR** Faculty of Biology and Chemistry, Tay Bac University, Son La Province, Vietnam;
**QSMI** Queen Saovabha Memorial Institute, Thai Red Cross Society, Bangkok, Thailand;
**CIB** Museum of Herpetology, Chengdu Institute of Biology, Chinese Academy of Sciences, Chengdu, China.

## Molecular data and phylogenetic analyses

Molecular data were generated for the specimen reported herein from Yen Bai Province, Vietnam. Homologous sequences were obtained from GenBank. DNA was extracted using the standard salt-extraction method (Aljanabi and Martinez 1997), combined with lysis by proteinase K. The cytochrome *c* oxidase subunit 1 (*COI*) gene fragment (660 bp) was amplified using the primer pair UTF 5'-TGT AAA ACG ACG GCC AGT TCT CAA CCA AYC AYA ARG AYA TYG G-3' and UTR 5'-CAG GAA ACA GCT ATG ACT ARA CTT CTG GRT GKC CRA ARA AYC A-3', following the protocol of Lissovsky et al. (2010). PCR products were cleaned by elution with a concentrated saline solution from 6% polyacrylamide gel. Sequencing was performed using an ABI 3500 automatic sequencer (Applied Biosystems) and BigDyeTerminator 3.1 kits 103 (Applied Biosystems). The nucleotide sequence was aligned with the BioEdit software (Hall 1999) and further edited manually. The final sequences were deposited in GenBank (MW542529).

We combined the sequence of the new specimen of *Parafimbrios* reported here with nine sequences downloaded from GenBank. We selected two outgroups, *Xenopeltis unicolor* Reinwardt, 1827 AB179620, *Acrochordus granulatus* Schneider, 1799 AB177879 (Dong and Kumazawa 2005), and five species for our ingroup, *P. vietnamensis* Ziegler, Ngo, Pham, Nguyen, Le & Nguyen, 2018 MH884515 (Ziegler et al. 2018), *P. lao* Teynié, David, Lottier, Le & Vidal, 2015 KT374005 (Nguyen et al. 2015), KP410746, *Fimbrios klossi* Smith, 1921 KP410744–45, *Xenodermus javanicus* Reinhardt, 1836 KP410747 (Teynie et al. 2015), and *Achalinus spinalis* Peters, 1869 MK064591 (Peng et al. 2017; Li et al. 2020) of the family Xenodermidae (Table 2). We used MEGA v. 7.0. (Kumar et al. 2016) for phylogenetic analyses using the Maximum Likelihood (ML) method. The HKY+G+I model was selected as the most appropriate DNA substitution model for the dataset using jModelTest 2.1.10 (Posada 2008). Minimum evolution (ME) and neighbor-joining (NJ) analyses were used as a complement to our maximum likelihood analyses. Node support was estimated using 1000 bootstrap replicates. Lastly, we calculated uncorrected pairwise divergences between all samples in MEGA v. 7.0.

**Table 2.** In-group samples used in molecular analyses.

| Species name | GenBank No. | Locality | Voucher | Reference |
|---|---|---|---|---|
| *Parafimbrios lao* | KP410746 | Louangphabang Province, Laos | MNHN 2013.1002 | Teynie et al. 2015 |
| *Parafimbrios lao* | KT374005 | Son La, Vietnam | TBU PAR.127 | Nguyen et al. 2015 |
| *Parafimbrios vietnamensis* | MH884515 | Lai Chau, Vietnam | IEBR A.2018.7 | Ziegler et al. 2018 |
| *Parafimbrios vietnamensis* | MW542529 | Yen Bai, Vietnam | ZISP | This study |
| *Fimbrios klossi* | KP410745 | Gia Lai, Vietnam | IEBR A.2013.56 | Teynié et al. 2015 |
| *Fimbrios klossi* | KP410744 | Quang Ngai Province, Vietnam | IEBR 3275 | Teynié et al. 2015 |
| *Xenodermus javanicus* | KP410747 | Maninjau Lake, Sumatera Barat Province, Sumatra, Indonesia | – | Teynié et al. 2015 |
| *Achalinus spinalis* | NC032084 | Shaanxi, China | HS12093 | Peng et al. 2017 |
| *Xenopeltis unicolor* | AB179620 | – | NUM-Az0378 | Dong, Kumazawa 2005 |
| *Acrochordus granulatus* | AB177879 | – | NUM-Az0375 | Dong, Kumazawa 2005 |

## Results and discussion

### Description of the second specimen from Vietnam (Figs 2, 3).

Morphological characters of the second male specimen are concordant with those in the original description of *Parafimbrios vietnamensis* by Ziegler et al. (2018). The specimen has a cylindrical and slender body (Figs 2, 3). Head not distinct from neck, dorsally covered with large shields; eyes middle-sized, with a vertically subelliptic pupil.

Snout-vent length 298 mm; tail length 56 mm; total length 354 mm; ratio of tail length to total length 0.163. Dorsal scale rows 31-35-27; laterally rounded ventral scales 172+2; subcaudals 48; postoculars 2/2; preoculars 1/1; suboculars 1/1; supralabials 8/8; infralabials 7/7 (Fig. 3A, B). Rostral triangular, its upper edge separating it from the internasals; nasal in contact zone with rostral with curved raised edge; suture between the internasals much longer than that between the prefrontals; 8 supralabials, the first four bearing raised edges; temporals 2+3/2+3 (Fig. 3A, B); 48 unpaired subcaudals; total length 354 mm; tail length 56 mm; TaL/TL ratio 0.163.

Dorsal scales small, cycloid, keeled from region behind the neck onwards, every second scale of outermost row distinctly enlarged; 31 scales around the anterior part of the body; two dorsal scale rows corresponding to a ventral plate; distinct, laterally-rounded ventrals; single subcaudal scales; cloacal shield entire (Figs 2D, 3C, D). Left hemipenis basally everted.

Morphological data of this new specimen, the holotype of *P. vietnamensis*, and comparative data on seven specimens of *P. lao* are summarized in Table 1. The second male specimen from Vietnam differs from the male holotype of *P. vietnamensis* in having a larger size (SVL 298 mm vs. 222 mm), a higher number of ventrals (172+2 vs. 164), and fewer temporals (2+3/2+3 vs. 4+4/4+5). The pholidosis characteristics of the number of ventrals and temporals look more similar to those seen in *P. lao*.

**Phylogenetic analysis.** Molecular analyses corroborate the morphological data. The new specimen is significantly genetically divergent from *P. lao* by at least 10%. The new sample was strongly supported as the sister lineage to the holotype of *Parafimbrios vietnamensis* (bootstrap support = 100%) (Fig. 5). Genetic divergence between the newly-collected specimen and the holotype was low (1.7%), and thus supports that they are conspecific. The mean uncorrected pairwise genetic distance between the two species within the genus *Parafimbrios* was 7.7±0.8%.

**Coloration.** The color of the dorsum is gray-brown, with varying intensity of brown depending on the angle of the light, and with iridizing sequins. The head is separated from the neck by a wide, light-colored nuchal collar extending to the ventral surface and to the chin; the collar does not completely cover the ventral part of the chin but stops at the ventral scales. The dorsal surface of the head is reddish-brown from the lateral edge of the head to the parietal scale and frontal scales. The gular region is brown; the two huge mandibular plates are brown anteriorly, lightening posteriorly. The color of the nuchal collar is a light cream, slightly white-pinkish. The color of the belly is smoky gray with lightened lateral edges of the abdominal scales.


**Figure 2.** *Parafimbrios vietnamensis* ZISP 31426 **A** dorsal view in life **B** ventrolateral view in life **C** dorsal view in life **D** ventral view of the preserved specimen.

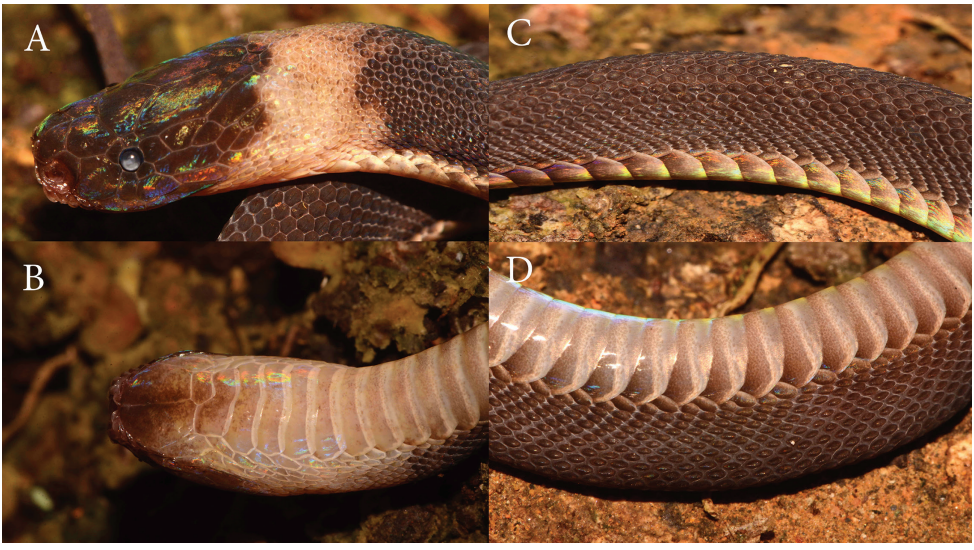


**Figure 3.** *Parafimbrios vietnamensis* ZISP 31426 in life **A** dorsal view of head **B** ventral view of head **C** dorsolateral view of midbody **D** ventrolateral view of midbody.

**Distribution.** *Parafimbrios vietnamensis* is only known from two provinces (Lai Chau Province, Yen Bai Province) in northwestern Vietnam (Fig. 1). The second species, *P. lao*, is only known from northern Vietnam in the Son La Province, but has a much

**Figure 4.** Habitat of *P. vietnamensis* in the primary polydominant forest in Yen Bai Province, Vietnam.

wider distribution in Laos, Thailand, Vietnam and southern China. This area of Vietnam is the highland region associated with Hoang Lien Son ridge (Lai Chau, Lao Cai, and part of Yen Bai). Biogeographically, the species inhabits the south-eastern part of the Sikang-Yunnan floristic Province of the Holarctic floristic kingdom (Takhtajan 1978).

**Ecology and habitat.** The specimen was collected on November 30, 2019 after an overnight rain, at midnight. The specimen was found in the leaf litter in primary polydominant forest (Fig. 4) at an elevation of 1300 m a.s.l.

The second male specimen from Vietnam differs from the male holotype of *P. vietnamensis* in having a larger size (SVL 298 mm vs. 222 mm), a higher number of ventrals (172+2 vs. 164), and fewer temporals (2+3/2+3 vs. 4+4/4+5). The number of ventrals and temporals are similar to those reported from *P. lao*. Morphological data from our new finding, the holotype of *P. vietnamensis*, and comparative data for seven specimens of *P. lao* are summarized in Table 1.

Due to the only minor morphological differences between the holotype of *Parafimbrios vietnamensis* and the new specimen described in this paper, and to the very low genetic divergence, we consider the new specimen conspecific with the holotype of *P. vietnamensis*. The expanded diagnosis of the species is as follows:

A species of the genus *Parafimbrios*, characterized by the following combination of characters: 1) rostral laterally with two raised, curved edges; the upper one, together with a horizontal curved ridge of tissue, separates the rostral from the internasals; 2) nasal in contact zone with rostral with curved, raised edge; 3) nasal in contact zone with supralabials with two small oblique, curved raised edges located above first and second as well as above second and third supralabials; 4) suture between the internasals much longer than that between the prefrontals; 5) supralabials 8, the first four bearing

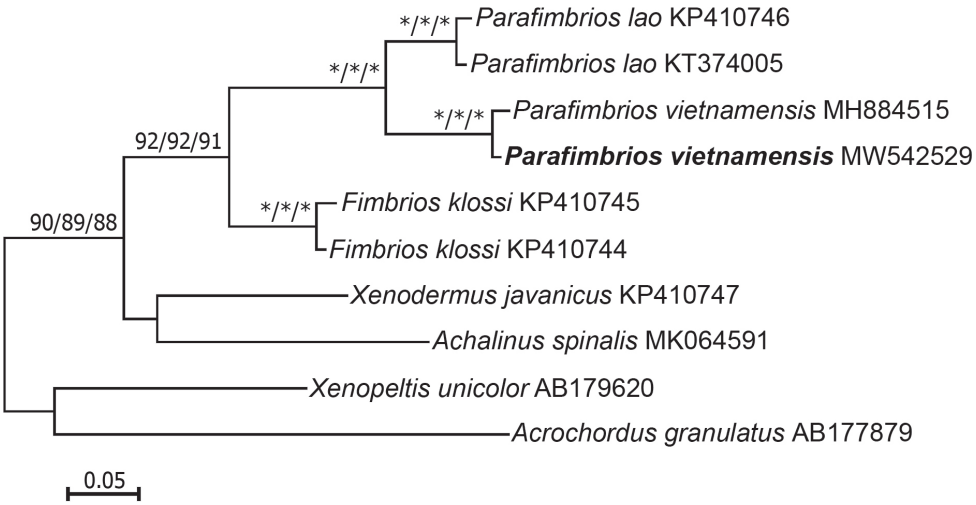


**Figure 5.** ML phylogenetic tree (HKY+G+I model) based on the mitochondrial *COI* gene. Numbers near the branches denote percentage bootstrap resampling support from 1000 replications (ML/ME/NJ). Bootstrap support is only shown for values exceeding 80%. Asterisks represent 100% values. Scale bar shows substitutions/site.

raised edges; 6) infralabials 7; mental and anterior three to four infralabials with raised edges; 7) temporals 2+3.2+3–4+4–5; 8) (31–35)-(33–35)-(27–29) dorsal scale rows; 9) laterally rounded ventrals 164–172+2; 10) unpaired subcaudals 48–49; 11) total length at least 266–354 mm in males (with a tail length of 44–56 mm and a TaL/TL ratio of 0.16). The coloration corresponds to that given in the original description (Ziegler et al. 2018): brownish-black above, with a broad yellow neckband widening towards the venter and stretching to the chin region; dorsal head surface in part reddish-brown, in particular in the middle of the parietals and frontal; venter grayish-brown, lighter anteriorly, darker towards tail region; ventrals anteriorly and laterally darker. It should be noted that we are most likely dealing with subadult specimens, with a pronounced whitish-pinkish nuchal collar. For example, in the related species *Parafimbrios lao*, the nuchal collar dims and disappears with age, which can be seen in Teynié et al. (2015: fig. 4). More findings of this rare snake will add information to this species' diagnosis.

*Parafimbrios vietnamensis* was previously known only from Hoang Ho Village, Phang So Lin Commune, Sin Ho District, Lai Chau Province in northern Vietnam (Ziegler et al. 2018). Although the new locality in Yen Bai Province is more than 200 km southeast of the type locality, the samples exhibit a relatively low amount of genetic divergence from each other.

The mountain systems in this area are composed of magmatic silicate rocks, particularly granite and quartzite, which were formed as extensive intrusions of late Paleozoic and Mesozoic age (Dovzikov et al. 1965). Tertiary tectonic movements uplifted these mountain terrains up to the present-day elevations, and subsequent erosion processes formed the present-day characteristic rocky landscape of this highland area, with very steep slopes, numerous rocky cliffs and deep and narrow river canyons (Fridland 1961;

Averyanov et al. 2003). This area is extremely humid, with warm rainy summers and cold foggy and misty winters and without a distinct dry period. The peak of rainfall arrives in the summer months. Morning dew is very common throughout the mountain zone, as well as frequent heavy fog. Humid, cold, northeast monsoon winds that bring heavy fog, mist and drizzle are very common in the winter and early spring (Averyanov et al. 2003). Zonal types of vegetation in the studied area belong to a group of closed evergreen tropical monsoon (seasonal) submontane forests (Averyanov et al. 2003).

There are now three known specimens of genus *Parafimbrios* recorded in Vietnam: one of *P. lao* and two of *P. vietnamensis*. The discovery highlights the difficulty of finding specimens of Xenodermidae and the need for further surveys in these areas of Vietnam and Eastern Laos.

So far, the following snake species were reported from Che Tao Village, Che Tao Commune, Mu Cang Chai District, Yen Bai Province in Vietnam: *Oreocryptophis porphyraceus* (Cantor, 1839), *Hebius bitaeniatus* (Wall, 1925), *H. boulengeri* (Gressitt, 1937), *Pararhabdophis chapaensis* Bourret, 1934, *Sinonatrix percarinata* (Boulenger, 1899), *Pareas hamptoni* (Boulenger, 1905) (Le et al. 2018). This new record of the rare snake species *Parafimbrios vietnamensis* is an important supplement to the list of snakes recorded from Yen Bai Province, and highlights its conservation needs.

## Acknowledgements

We are grateful to the directorate of the The Mu Cang Chai Species and Habitat Conservation Area (SHCA) for supporting our fieldwork. We would like to thank Larissa Lohanssen for assistance in the field and Svetlana Lukonina for her contribution to laboratory work. Many thanks to John Murphy, Thomas Ziegler and an anonymous reviewer for providing valuable comments on the manuscript. This study was supported by projects of the Russian Foundation of Basic Research #19-54-54003 and #19-04-00119 and by State Research Topic AAAA-A19-119082990107-3. We appreciate Alexandre Teynié for providing a distribution map of *P. lao* and Jesse L. Grismer for his kind help editing the manuscript. Field work in northern Vietnam was funded by The Ministry of Science and Technology (ĐTĐLCN.38/21) to Tao Thien Nguyen.

## References

Aljanabi S, Martinez I (1997) Universal and rapid salt-extraction of high genomic DNA for PCR-based techniques. Nucleic Acids Research 25: 4692–4693. https://doi.org/10.1093/nar/25.22.4692

Averyanov LV, Phan KL, Nguyen TH, Do TD (2003) Highland vegetation and flora of Van Ban District, Lao Cai Province in northern Vietnam. Turczaninowia 6(4): 47–86.

Dong S, Kumazawa Y (2005) Complete mitochondrial DNA sequences of six snakes: phylogenetic relationships and molecular evolution of genomic features. Journal of Molecular Evolution 6: 12–22. https://doi.org/10.1007/s00239-004-0190-9

Cai B, Chen Z, Gao J, Ding L, Dai R (2020) New record of a genus and species of odd-scaled snake (Serpentes: Xenodermidae) from China. Russian Journal of Herpetology 27(6): 348–352. https://doi.org/10.30906/1026-2296-2020-27-6-348-352

Dovzikov AE (1965) Geological map of Vietnam 1:500000. In: Dovzikov AE (Ed.) Hanoi, Main Geological Department of DRV.

Dong S, Kumazawa Y (2005) Complete mitochondrial DNA sequences of six snakes: phylogenetic relationships and molecular evolution of genomic features. Journal of Molecular Evolution 61: 12–22. https://doi.org/10.1007/s00239-004-0190-9

Fridland BM (1961) Nature of the North Vietnam. USSR Academy of Science Editorial House, Moscow, 175 pp. [in Russian]

Hall TA (1999) BioEdit: a user friendly biological sequence alignment editor and analysis program for Windows 95/98/NT. Nucleic Acids Symposium Series 41: 95–98.

Kumar S, Stecher G, Tamura K (2016) MEGA7: Molecular Evolutionary Genetics Analysis Version 7.0 for Bigger Datasets. Molecular Biology and Evolution 33(7): 1870–1874. https://doi.org/10.1093/molbev/msw054

Le DT, Dao AN, Pham DT, Ziegler T, Nguyen TQ (2018) New records and an updated list of snakes from Yen Bai Province, Vietnam. Herpetology Notes 11: 101–108.

Li J, Liang D, Wang Y, Guo P, Huang S, Zhang P (2020) A large-scale systematic framework of Chinese snakes based on a unified multilocus marker system. Molecular Phylogenetics and Evolution 148: e106807. https://doi.org/10.1016/j.ympev.2020.106807

Lissovsky AA, Obolenskaya EV, Abramson NI, Dokuchaev NE, Yakimenko VV, Mal'kova MG, Bogdanov AS, Ivanova NV (2010) Geographic variation of *Microtus middendorffii* (Cricetidae, Arvicolinae, Rodentia) sensu lato studied by craniometrical and mitochondrial features. Russian Journal of Theriology 9: 71–81. https://doi.org/10.15298/rusjtheriol.09.2.03

Nguyen TQ, Pham AV, Nguyen SLH, Le MD, Ziegler T (2015) First country record of *Parafimbrios lao* Teynié, David, Lottier, Le, Vidal et Nguyen, 2015 (Squamata: Xenodermatidae) for Vietnam. Russian Journal of Herpetology 22(4): 297–300.

Peng L, Yang D, Duan Sh, Huang S (2017) Mitochondrial genome of the Common burrowing snake *Achalinus spinalis* (Reptilia: Xenodermatidae), Mitochondrial DNA Part B, 2: 571–572. https://doi.org/10.1080/23802359.2017.1365643

Posada D (2008) jModelTest: Phylogenetic Model Averaging. Molecular Biology and Evolution 25: 1253–1256. https://doi.org/10.1080/23802359.2017.1365643

Takhtajan A (1978) The floristic regions of the world. Nauka, Leningrad, 248 pp. [in Russian]

Teynié A, David P, Lottier A, Le MD, Vidal N, Nguyen TQ (2015) A new genus and species of xenodermatid snake (Squamata: Caenophidia: Xenodermatidae) from northern Lao People's Democratic Republic. Zootaxa 3926(4): 523–540. https://doi.org/10.11646/zootaxa.3926.4.4

Teynié A, Hauser S (2017) First record of *Parafimbrios lao* Teynié, David, Lottier, Le, Vidal et Nguyen 2015 (Squamata: Caenophidia: Xenodermatidae) for Thailand. Russian Journal of Herpetology 24(1): 41–48. https://doi.org/10.30906/1026-2296-2019-24-1-41-48

Ziegler T, Ngo HN, Pham AV, Nguyen TT, Le MD, Nguyen TQ (2018) A new species of *Parafimbrios* from northern Vietnam (Squamata: Xenodermatidae). Zootaxa 4527(2): 269–276. https://doi.org/10.11646/zootaxa.4527.2.7

Uetz P, Freed P, Hošek J (2020) The Reptile Database. http://www.reptile-database.org [Accessed 25 December 2020]

ZooKeys 1048: 91–107 (2021)
doi: 10.3897/zookeys.1048.66250
https://zookeys.pensoft.net

RESEARCH ARTICLE

A peer-reviewed open-access journal
ZooKeys
Launched to accelerate biodiversity research

# New records of nudibranchs and a cephalaspid from Kuwait, northwestern Arabian Gulf (Mollusca, Heterobranchia)

Manickam Nithyanandan[1], Manal Al-Kandari[1], Gopikrishna Mantha[1]

1 *Ecosystem Based Management of Marine Resources, Environment and Life Sciences Research Center, Kuwait Institute for Scientific Research, P.O. Box.1638, Salmiya 22017, Kuwait*

Corresponding author: Manickam Nithyanandan (nandan.ocean@gmail.com)

Academic editor: Nathalie Yonow | Received 21 March 2021 | Accepted 24 June 2021 | Published 13 July 2021

*http://zoobank.org/84376509-9450-4B55-AFAB-D7414079B51D*

**Citation:** Nithyanandan M, Al-Kandari M, Mantha G (2021) New records of nudibranchs and a cephalaspid from Kuwait, northwestern Arabian Gulf (Mollusca, Heterobranchia). ZooKeys 1048: 91–107. https://doi.org/10.3897/zookeys.1048.66250

## Abstract

In this study five new records and two probably undescribed species of heterobranch sea slugs placed in four genera, three families, and two orders are reported from Kuwait, northwestern Arabian / Persian Gulf with details and photographs. The present study increases the heterobranch diversity in Kuwaiti waters from 35 to 40 species. The range of habitats in Kuwait provides a vital opportunity for further investigation to understand the actual faunal diversity.

## Keywords

Nudibranchs, diving, intertidal, Kuwait, Arabian Gulf

## Introduction

Heterobranch sea slugs are one of the most colourful marine invertebrates, usually devoid of shells but in a few species, it is found externally and internally (e.g., Cephalaspidea, Aplysiida, Pleurobranchida), occurring in reefs, rocky habitats, and soft substrata

(Yonow 2008; Mehrotra et al. 2021). The Arabian / Persian Gulf (APG) is a shallow marginal sea with a very wide range of temperature (10–48 °C) and salinity (42–65‰) and also highly impacted by anthropogenic activities (Sheppard et al. 2010). Kuwait lies in the northwestern APG, receiving freshwater input from Shatt-Al-Arab in Iraq, and has diverse habitats such as mud flats, sandy beaches, rocky shores, salt marshes, seagrass meadows, and coral reefs (Al-Yamani et al. 2004). The marine biodiversity of these productive habitats is unique and adapted to live in these extreme environmental conditions (salinity > 41 ppt and sea water temperature, 14 to > 30 °C) which falls beyond the physiological threshold for many organisms found elsewhere (Edmonds et al. 2021). Anthropogenic activities such as coastal development, pollution, etc. has immense impact on the fauna and flora in this marginal environment (Sheppard et al. 2010; Burt 2014).

The heterobranch fauna of APG are rather poorly documented with sporadic reports from Kuwait, Saudi Arabia, United Arab Emirates (UAE), and Iran (Glayzer et al. 1984; Jones 1986; Gosliner and Behrens 2004; Al-Yamani et al. 2012; Nithyanandan 2012; Yonow 2012; Gosliner et al. 2015; Rezai et al. 2016; Al-Kandari et al. 2020; Amini-Yekta and Dekker 2021). In Kuwaiti waters to date, 35 species of heterobranchs were recorded belonging to eighteen families and two orders (Al-Yamani et al. 2012; Nithyanandan 2012). In the present study new records of heterobranchs are documented from an offshore island and artificial marine habitats in Kuwaiti waters during the years 2012–2014.

## Materials and methods

The Sabah Al-Ahmad Sea City (**SAASC**) is the largest coastal township development in Kuwait (Jones and Nithyanandan 2012a) covering an area up to 70 $km^2$, with a network of artificial lagoons and habitats ranging from intertidal to subtidal zone (ca. 10 m depth). Heterobranchs were recorded from various artificial marine habitats (rock culverts, bridge piers, etc.) of SAASC (Fig. 1) by SCUBA diving while conducting routine underwater surveys for benthic monitoring during the years 2012–2014. Heterobranchs were photographed at 3–5 m depth using a digital camera (Panasonic LUMIX DMC-TZ7) with a waterproof casing. Due to the low density of animals observed, no attempts were made to collect reference specimens. No live measurements of the individuals were carried out. One individual was photographed from the rocky intertidal habitats of Failaka island during an extensive intertidal benthic survey in the winter of 2014. All morphological features described in this study are based on detailed examination of numerous photographs using Adobe Photoshop CS6. The classification adopted in this study is based on Bouchet et al. (2017) and, for nomenclature, the World Registry of Marine Species (WoRMS 2021) was followed. Identification of recorded individuals were based on Yonow (2008), Gosliner et al. (2015), and recent literature listed in WoRMS (2021).

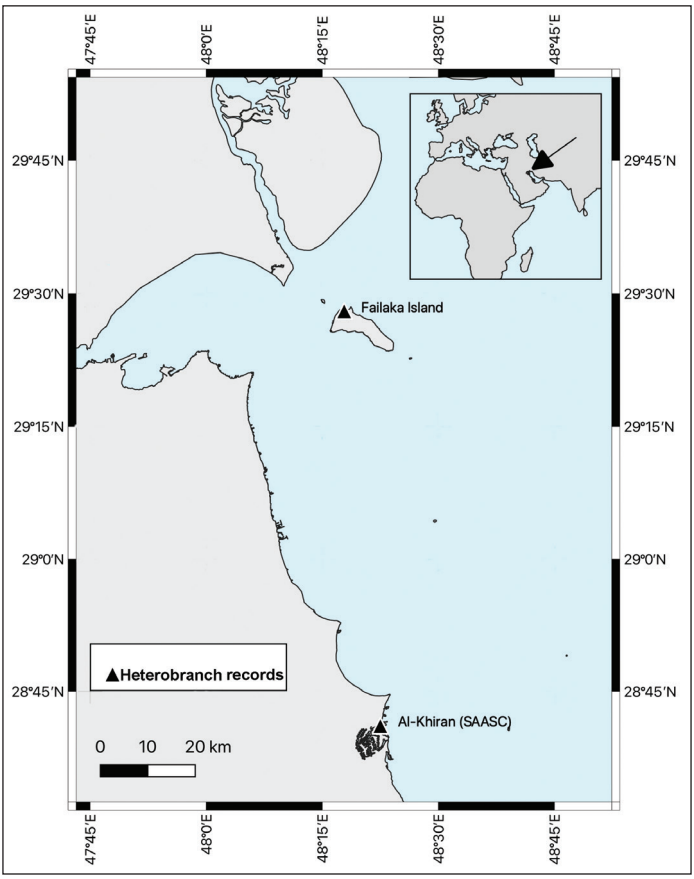


**Figure 1.** Map showing heterobranch record sites in Kuwait.

## Taxonomic account

**Clade TECTIPLEURA Schrödl, Jörger, Klussmann-Kolb & Wilson, 2011**
**Super Order EUOPISTHOBRANCHIA Jörger, Stöger, Kano, Fukuda, Knebelsberger & Schrödl, 2010**
**Order CEPHALASPIDEA P. Fischer, 1883**
**Family AGLAJIDAE Pilsbry, 1895 (1847)**
**Genus *Chelidonura* A. Adams, 1850**

***Chelidonura livida* Yonow, 1994**
Figure 2

*Aglaja cyanea* (*nigra*): Engel and van Eeken 1962 (part): 17, E55/342 (Red Sea).
*Chelidonura africana*: Yonow 1990: 289, pl. 4 (Red Sea; misidentification).
*Chelidonura livida* Yonow, 1994a: 141–147, Fig. 1 (Eilat, Red Sea): Yonow 2008: 78–79, includes five figures (Gulf of Eilat, Red Sea).

**Photographic record.** SAASC Al-Khiran, 13 June 2012, one individual photographed at 3 m depth in sandy substrate, R. Dinesh Kumar.

**Description.** The individual has a black body colour, prominent electric blue spots scattered over the dorsum, head, and parapodia (Fig. 2). White flecks interspersed with electric blue spots are found on the head and along the edges of the parapodia. The caudal flaps are unequal with the left longer than the right, and with an electric blue spot at the base of the left caudal flap (see Fig. 2). The blue spots on the anterior portion of the propodium form a coalescent line which is partly visible in this individual (Fig. 2).

**Distribution.** Israel (Yonow 1994a, 2008), Abu Dhabi (Hardy 2001), Mayotte Island (http://seaslugs.free.fr/nudibranche/a_cheli_livida.htm), Tanzania and Mozambique (Gosliner et al. 2008; Tibiriçá and Malaquias 2017), and Kuwait (this study).

**Remarks.** Yonow (1994a) described *Ch. livida* from Eilat, Israel, in the north-eastern Red Sea. In *Ch. livida*, both sides of the mouth bear whitish or yellowish sensory bristles which is visible in the frontal view or if viewed from above (Yonow 1994a); however, it is not clearly visible in the photograph of the individual presented in this study due to the angle at which it was photographed (Fig. 2). The head shield has two short processes on its lateral side, which is bit longer in the left compared to the right side and tubular when the animal is in relaxed state (Yonow 1994a). This was clearly observed in the individual recorded in this study (Fig. 2). The individual recorded from Mozambique (Tibiriçá and Malaquias 2017: fig. 2f) has prominent electric blue rings that are scattered over the dorsum and parapodial margin. The caudal flaps are rather thin, the right one short and the left one elongated with a prominent electric blue spot. However, the individual observed in this study has short and thick caudal flap with a thin, pointed tip and a blue spot at its base (Fig. 2). The species possesses a highly reduced internal shell. This is a new record to both Kuwait and the APG, this record denoting a range extension into the northern APG from its type locality in the Red Sea.

**Figure 2.** *Chelidonura livida* Yonow, 1994. Photograph R. Dinesh Kumar.

**Clade Nudipleura Wägele & Willan, 2000**
**Order Nudibranchia Cuvier, 1817**
**Family Chromodorididae Bergh, 1891**
**Genus *Goniobranchus* Pease, 1866**

***Goniobranchus bombayanus* (Winckworth, 1946)**
Figure 3

*Glossodoris bombayana* Winckworth, 1946: 155–156, fig. 1 (Bombay, India).
*Goniobranchus naiki* Valdés, Mollo & Ortea, 1999: 468–471, fig. 1 (Mandapam, southern India); Gosliner et al. 2015: 228, one figure.

**Photographic record.** SAASC, Al-Khiran, 23 March 2013, one individual photographed at 5 m depth on a concrete wall adjacent to tidal gates, Don Christopher Pereira.

**Description.** The individual photographed has a translucent white body with conspicuous deep purple spots scattered over the dorsum (Fig. 3). The foot is covered by the dorsum. On the mantle margin, yellow spots are arranged in a row merging with the purple spots. These yellow spots appear as a tubercle projecting from the centre of few purple spot on the dorsum and are confluent with purple spots in the margin. Rhinophores and gills bear rows of faint opaque white spots.

**Distribution.** Known only from Mandapam, southern India (Valdés et al. 1999), Mumbai and Gulf of Kutch, northwestern India (Winckworth 1946; Apte and Desai 2017), and Kuwait (this study).

**Figure 3.** *Goniobranchus bombayanus* (Winckworth, 1946) (arrow indicates the white foot with no spots or markings). Photograph Don Christopher Pereira.

**Remarks.** Johnson and Gosliner (2012), in considering the monophyletic nature of the genus *Chromodoris*, suggested a revision in the classification by moving some Indo-Pacific chromodorids to the genus *Goniobranchus*. According to WoRMS (2021) *Goniobranchus naiki* Valdez, Mollo & Ortea, 1999 from Mandapam, southern India is a junior synonym of *G. bombayanus* (Winckworth, 1946). In *G. naiki*, Valdés et al. (1999) and Gosliner et al. (2015) indicated the occurrence of translucent white spots on the dorsum; in the individual recorded during this study only faint opaque spots were observed (Fig. 3). In *G. bombayanus* the posterior portion of the foot extends beyond the mantle as a white tail with no dark spots (Winckworth 1946), which is also visible in the photographed individual (Fig. 3, arrowed). A new record to Kuwait and the APG.

***Goniobranchus* sp. 1**

Figure 4

**Photographic record.** SAASC, Al-Khiran, 23 March 2013, one individual photographed at 3.5 m depth on a rock culvert, R. Dinesh Kumar.

**Description.** The individual has a white body with dark purple spots scattered over the dorsum and mantle margin (Fig. 4). A row of orange-yellow mantle glands covers the mantle margin. Rhinophores have a white base and bright orange lamellae gradually extending from the anterior surface up to 1/4 of the dorsal side, and the gills are white with a bright orange midrib.

**Distribution.** Kuwait (this study) and Abu Dhabi, UAE Coast (http://medslugs.de/E/Ind-NW/Goniobranchus_sp_10/Goniobranchus_sp_10_01.htm)

**Remarks.** Very similar to *G. kitae* (Gosliner 1994; see below) and *G. tumuliferus* (Collingwood, 1881) (see Gosliner et al. 2015 and Mehrotra et al. 2021). However, the individual observed in this study differs from both *G. kitae* and *G. tumuliferus*

**Figure 4.** *Goniobranchus* sp. 1. Photograph R. Dinesh Kumar.

by having orange rhinophores with a white base, an orange midrib in the gills, purple spots on the elongated foot, and yellow at the tip of the elongated foot (Fig. 4). Probably an undescribed species.

### *Goniobranchus* sp. 2

Figure 5

**Photographic record.** Failaka Island, 22 December 2014, one individual found in rocks in sandy mud intertidal areas at the lowest tide mark, Dr. Valeriy Skryabin.

**Description.** The individual has a white translucent body with dark red / purple spots scattered over the dorsum; a few of the dark red / purple spots have a tubercle-like projection in the middle giving a conical impression (Fig. 5, arrowed). A scattered row of spots extends around the margin of the mantle and the foot. Rhinophores are translucent with white lamellae. Gills are also translucent with a white midrib. The edge of the mantle has a submarginal bright yellow band and an interior ring of opaque white glands.

**Distribution.** Kuwait (this study).

**Remarks.** The individual recorded has a submarginal ring of translucent white glands just inside the prominent bright orange band similar to *G. tumuliferus* (Collingwood, 1881; see also Gosliner et al. 2015: 229). However, in *G. tumuliferus* the rhinophores and tentacles have opaque white tips (Gosliner et al. 2015; Mehrotra et al. 2021), which was not observed in the individual recorded during this study. The translucent white glands with dark red / purple spots interrupting the bright orange band is a character combination of what has been observed in *Goniobranchus kitae* Gosliner, 1994 from Madagascar and *G. bimaensis* (Bergh, 1905) from the Indo-West Pacific. Probably an undescribed species.

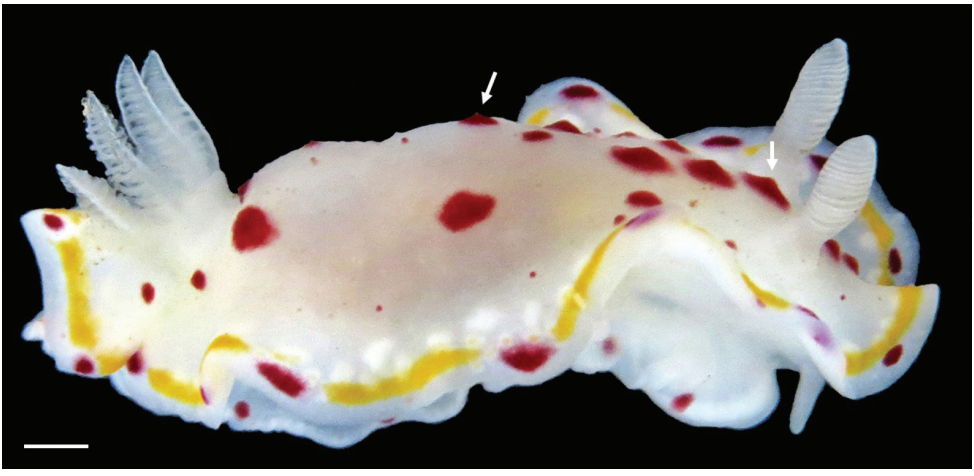

**Figure 5.** *Goniobranchus* sp. 2 (arrows indicate tubercle-like projections in the dark red/purple spots which give the impression of a conical projection). Photograph Dr. Valeriy Skryabin. Scale bar: 1 mm.

## Genus *Hypselodoris* Stimpson, 1855

### *Hypselodoris infucata* (Rüppell & Leuckart, 1830)

Figure 6A, B

*Doris infucata* Rüppell & Leuckart, 1828–1830: tab X, 34, fig. 3 (northern African Red Sea).

**Photographic record.** SAASC, Al Khiran, 2 July 2013, two individuals photographed at 3 m depth on a rock culvert, R. Dinesh Kumar.

**Description.** The two individuals in the photographs have a slender white body with blue, yellow, and black spots scattered all over. At the mantle margin, triangular dark blue-green and pale blue patches alternate (Fig. 6A), and bright yellow spots are

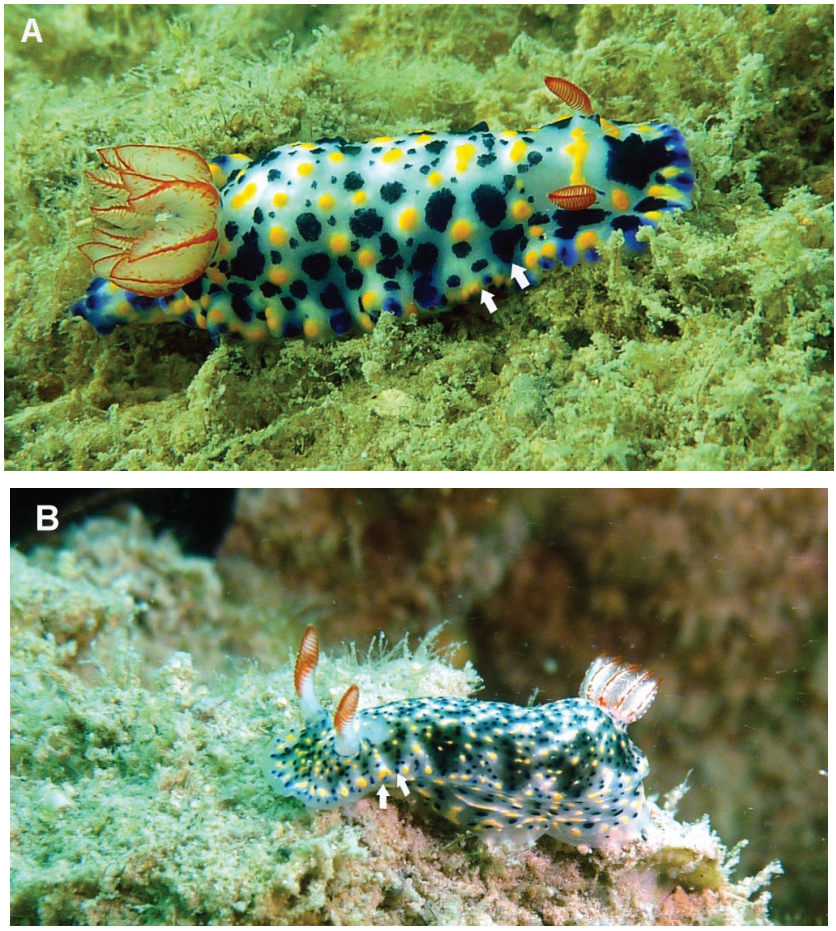


**Figure 6. A** *Hypselodoris infucata* (Rüppell & Leuckart, 1830) **B** colour morph. Arrows indicate alternate dark blue-green and pale blue triangles, a diagnostic feature of this species. Photograph R. Diniesh Kumar.

scattered on both the dorsum and foot. The rhinophores are bright orange-red and the core is white. The oral tentacles are bright orange-red at the midrib and tip (Fig. 6A). A row of prominent dark blue blotches occurs on the either side at the edge of dorsum.

**Distribution.** Indo-West Pacific species and a Lessepsian migrant (Rudman 1977; Yonow 2008), Oman, South Africa, Philippines, Australia (Debelius 1996), Madagascar, Bali, Indonesia, Papua New Guinea, and Hawaii (Johnson and Valdés 2001; Gosliner et al. 2008), Gulf of Kutch and Lakshadweep, India (Apte 2009; Apte et al. 2010), Larak and Lavan islands, Iran (Rezai et al. 2016), Mozambique (Tibiriçá et al. 2017), Pakistan (Gul, 2019), Thailand (Mehrotra et al. 2021), and Kuwait (this study).

**Remarks.** This species exhibits a high degree of variability in colour pattern and the bright yellow spots observed in the individual during the present study was similar to a specimen recorded from Eilat, northern Red Sea (Ben Tov 2003). A second colour morph (Fig. 6B) was also recorded with triangular blue grey patches on the either side of the dorsum as illustrated in Yonow (2008). *Hypselodoris infucata* can be easily confused with *H. kanga* Rudman, 1977 due to morphological similarities (Rudman 2007; Mehrotra et al. 2021). In *H. infucata* the gills are rather simple with a bright red line on the outer and inner edges, whereas in *H. kanga*, they are triangular with three lines and, distinctively, with white or yellow spots in-between (Rudman 2007). Bluish purple lines usually occur in the dorsum of *H. kanga* (Mehrotra et al. 2021); however, individuals observed in this study only have dark blue or black spots. *Hypselodoris infucata* differs externally from another congener, *H. roo* Gosliner & Johnson in Epstein et al. 2018, in not having a white spot at the base of the rhinophores on the posterior side and a broad posterior portion of the notum (Epstein et al. 2018). A new record to Kuwait.

***Hypselodoris* sp.**

Figure 7

**Photographic record.** SAASC, Al-Khiran, 23 March 2013, one individual on an unidentified sponge photographed at 3.5 m depth, R. Dinesh Kumar.

**Description.** The individual photographed has a bluish grey body with yellow and black spots. The margin of the mantle is thin; yellow and black spots extend onto the foot. A prominent row of black blotches is present on the either side of the dorsum. Rhinophores are tipped red-orange, with a translucent white base (Fig. 7). Gills are orange-red at the tips and the midribs are interrupted with white bands. A circular row of blue spots extends onto the base of the slightly elevated gill pocket.

**Distribution.** Kuwait (this study).

**Remarks.** The individual in this study has similarities in colour pattern with two recently described species, *H. confetti* (Johnson & Gosliner in Epstein et al. 2018) and *H. roo*. In *H. confetti*, the gills have purple lines and red-orange tips and in *H. roo* the gills are bright orange-red at tips with two red lines on the exterior side and

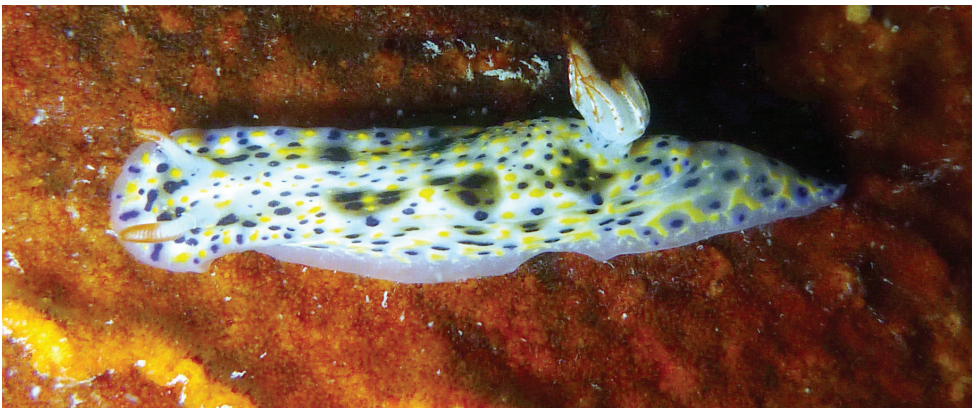

**Figure 7.** *Hypselodoris* sp. on an unidentified sponge. Photograph R. Dinesh Kumar.

one on the interior. However, the individual in this study has gills with orange-red midribs and tips (Fig. 7). The bases of the rhinophores are purple in *H. confetti* and red in *H. roo* with a prominent opaque white spot on the posterior side (Epstein et al. 2018), which is clearly absent in the individual recorded in this study as it only has orange-red tipped rhinophores with white bases (Fig. 7). In *H. roo*, the posterior portion of the notum has a tapering shape, which was also observed in this individual (Fig. 7). A new record to Kuwait and the APG.

**Family Facelinidae Bergh, 1889**
**Genus *Caloria* Trinchese, 1888**

***Caloria indica* (Bergh, 1896)**
Figure 8

*Learchis indica* Bergh, 1896: 385–394, figs 1–4 (Ambon, Indonesia).

**Photographic record.** SAASC, Al-Khiran, 18 November 2014, one individual on sand and rock mixed substratum photographed at 3.5 m depth, Don Christopher Pereira.

**Description.** The body is slender, translucent white, with a marking of white lines on the dorsum up to the rhinophores. Orange markings are prominent on the anterior part in front of the cerata and along the sides between the cerata. The rhinophores are smooth, white in colour, orange at the base with a prominent orange band at the middle. The oral tentacles also appear white, long, and slender, with basal orange markings. The cerata are fusiform with white, brown, and blue bands and a translucent white tip. The tail is white, long, and pointed.

**Distribution.** Indo-West and Central Pacific, Hawaii, Japan, Australia, Indonesia, India, South Africa, Tanzania (Gosliner 1987; Yonow 2008; Gosliner et al. 2015),

**Figure 8.** *Caloria indica* (Bergh, 1896). Photograph Don Christopher Pereira.

India (Sreeraj et al. 2012), Maldives (Yonow 1994b), Thailand (Mehrotra et al. 2021), Myanmar (Sanpanich and Duangdee 2019), Papua and New Guinea (Baine and Harasti 2007), Christmas Island, Fiji, New Caledonia, Oman, Seychelles, and Solomon Islands (Gosliner et al. 2008), and now Kuwait (this study).

**Remarks.** Inhabits coral reef areas (Mehrotra et al. 2021). Feeds on hydroids (Yonow 2008; Gosliner et al. 2015). A new record to Kuwait and the APG.

## Discussion

Kuwait's rich and unique marine biodiversity is poorly documented and more coordinated biodiversity assessments for sustainable management are essential (e.g., Edmonds et al. 2021). The offshore and inshore coral reef habitats are important for several invertebrate and vertebrate species (Papathanasopoulou and Zogaris 2015). Post-gulf war economic development of Kuwait has led to innovative coastal development projects (e.g., Sabah Al Ahmad Sea City) which has increased the extent of both the shoreline and coastal habitats, enhancing marine biodiversity and fisheries (Jones and Nithyanandan 2012b; Nithyanandan 2012; Myers and Nithyanandan 2016; Nithyanandan et al. 2016).

In this study five new records of heterobranch sea slugs to Kuwait and the APG and two potentially new species are reported. Furthermore, this study increases the total number of heterobranch fauna of Kuwait to 40 species, which is 28% of the number reported from both the APG and Gulf of Oman (Amini-Yekta and Dekker 2021).

The occurrence of diverse habitats such as sand, mud flats, rocks, coral reefs, seagrass beds, etc. provides many more opportunities to examine and expand knowledge of the heterobranch diversity in Kuwaiti waters. Harsh environmental conditions in the APG waters of Kuwait potentially governs the impoverished biodiversity of marine biota. Extensive coastal development in the Arabian Peninsula with wide range of artificial marine substrates such as breakwaters, jetties etc. serves as viable benthic habitats attracting colonisation of marine biota (Burt and Bartholomew 2019). In Kuwait, availability of a wide range of benthic substrates both in natural habitats (Al-Kandari et al. 2020) and massive coastal development such as SAASC (Jones and Nithyanandan 2012a) serve as important areas for nudibranch diversity. The colonisation of benthic invertebrates such as sponges, hydroids, etc. in SAASC (Jones and Nithyanandan 2012a; Nithyanandan 2012), which are key prey items for sea slugs (McDonald and Nybakken 1997), could potentially attract them to these artificial habitats. A recent intensive study on sea slug diversity from Thailand indicates the importance of understanding habitat diversity (both natural and artificial) and ecology which drives the functional diversity (Mehrotra et al. 2021).

Historically in Kuwaiti waters efforts were only laid to understand the diversity of heterobranchs (Glayzer et al. 1984; Jones 1986; Al-Yamani et al. 2012; Nithyanandan 2012). Thus, a huge knowledge gap exists in understanding habitat diversity, food preferences, predator-prey interactions, and animal associations in heterobranchs from this marginal environment, which are key factors in driving its diversity and ecology. In the near future, intensive surveys and collecting efforts should incorporate these objectives which could not only help in documenting the diversity of heterobranchs in Kuwait and in the rest of the Arabian / Persian Gulf but also their valuable ecological functions.

## Acknowledgements

MN is thankful to La Ala Al Kuwait Real Estate Co. K.S.C. for the diving and logistic facilities provided during the field work in Sabah Al Ahmad Sea City, Al-Khiran, Kuwait, and to the divers Dinesh Kumar Raja and Don Christopher Pereira for their underwater photographs of heterobranchs. Our sincere thanks to Dr. Nathalie Yonow, University of Swansea, UK, for confirming the identification of heterobranchs reported in this study and her valuable comments. MAK is grateful to Kuwait Petroleum Company (KPC) and Kuwait Institute for Scientific Research for their financial assistance through a project (FM075C) to conduct the intertidal surveys in Failaka Island, where *Goniobranchus* sp. 2 was recorded. We also extend our thanks to Mr. Yusuf Bohadi, Kuwait University, for his assistance in preparing the map (Fig. 1), Dr**.** Valeriy Skryabin for his assistance in photography, and Dr. Ravinesh, Department of Aquatic Biology, University of Kerala, India, for providing relevant literature. We are grateful to the referees for insightful comments.

## References

Adams A (1850) Monograph of the family Bullidae. In: Sowerby II GB (Ed.) Thesaurus Conchyliorum, vol. 2. Privately published, London, 553–608. [pls 119–125]

Al-Kandari M, Oliver PG, Chen W, Skryabin V, Raghu M, Yousif A, Al-Jazzaf S, Taqi A, Al Hamad A (2020) Diversity and distribution of the intertidal Mollusca of the state of Kuwait, Arabian Gulf. Regional Studies in Marine Science 33: e100905. https://doi.org/10.1016/j.rsma.2019.100905

Al-Yamani FY, Bishop J, Ramadhan E, Al-Husaini M, Al-Ghadban AN (2004) Oceanographic Atlas of Kuwait's Waters. Kuwait Institute for Scientific Research, 203 pp.

Al-Yamani FY, Skryabin V, Botlachova N, Revkov N, Makarov M, Grinstov V, Kolesnikova E (2012) Illustrated atlas on the zoobenthos of Kuwait. Kuwait Institute for Scientific Research, 383 pp.

Amini-Yekta F, Dekker H (2021). An updated checklist of marine gastropods of Persian Gulf and Gulf of Oman. Zootaxa 4957: 1–071. https://doi.org/10.11646/zootaxa.4957.1.1

Apte D (2009) Opisthobranch fauna of Lakshadweep islands, India with 52 new records to Lakshadweep and 40 new records to India: Part 1. Journal of Bombay Natural History Society 106: 162–175.

Apte D, Bhave V, Parasharya D (2010) An annotated and illustrated checklist of the Opisthobranch fauna of Gulf of Kutch, Gujarat, India with 21 new records for Gujarat and 13 new records for India: part 1. Journal of Bombay Natural History Society 107: 14–23.

Apte D, Desai D (2017) Field guide to the sea slugs of India. Bombay Natural History Society, 456 pp.

Baine M, Harasti D (2007) The marine life of Bootless Bay, Papua New Guinea. Motupore Island Research Centre (MIRC), School of Natural and Physical Sciences, University of Papua New Guinea, 146 pp.

Ben Tov I (2003) [Mar 26] *Hypselodoris infucata* from the Red Sea. Sea Slug Forum. Australian Museum, Sydney. http://www.seaslugforum.net/find/9458 [Accessed on 10.06.2021]

Bergh R (1889) Malacologische Untersuchungen. Theil 3, Heft 16. In: Semper C (Ed.) Reisen im Archipel der Philippinen. Kreidel, Wiesbaden, 815–872. [pls 82–84]

Bergh R (1891) [October] Die cryptobranchiaten Doridien. Zoologische Jahrbücher, Abtheilung für Systematik, Geographie und Biologie der Thiere 6: 103–144.

Bergh LSR (1896) Eolidiens d'Amboine. Revue Suisse de Zoologie 4: 385–394. https://doi.org/10.5962/bhl.part.35506

Bergh LSR (1905) Die Opisthobranchiata der Siboga-expedition. Siboga-Expeditie 50: 1–248. [pls 1–20]

Bouchet P, Rocroi JP, Hausdorf B, Kaim, A, Kano Y, Nützel A, Parkhaev P, Schrödl M, Strong EE (2017) Revised Classification, Nomenclator and Typification of Gastropod and Monoplacophoran Families. Malacologia 61: 1–526. https://doi.org/10.4002/040.061.0201

Burt JA (2014) The environmental costs of coastal urbanization in the Arabian Gulf. City 18: 760–770. https://doi.org/10.1080/13604813.2014.962889

Burt JA, Bartholomew A (2019) Towards more sustainable coastal development in the Arabian gulf: Opportunities for ecological engineering in an urbanized seascape. Marine Pollution Bulletin 142: 93–102. https://doi.org/10.1016/j.marpolbul.2019.03.024

Collingwood C (1881) On some new species of nudibranchiate Mollusca from the eastern seas. Transactions of the Linnean Society of London, Zoology, series 2, 2: 123–140. https://doi.org/10.1111/j.1096-3642.1881.tb00300.x

Cuvier G (1817) Le règne animal distribué d'après son organisation, tome 2 contenant les reptiles, les poissons, les mollusques, les annélides. Deterville, Paris, [xviii +] 532 pp.

Debelius H (1996) Nudibranchs and sea snails: Indo-Pacific field guide. IKAN-Unterwasserarchiv, Frankfurt, 321 pp.

Edmonds NJ, Al-Zaidan AS, Al-Sabah AA, Le Quesne, WFJ, Devlin MJ, PI Davison, Lyons BP (2021) Kuwait's marine biodiversity: Qualitative assessment of indicator habitats and species. Marine Pollution Bulletin 163: e111915. [15 pp.] https://doi.org/10.1016/j.marpolbul.2020.111915

Engel E, van Eeken CJ (1962) Red sea Opisthobranchia from the coast of Israel and Sinai. Bulletin of Sea Fisheries Research Station, Israel 30: 15–34.

Epstein HE, Hallas JM, Johnson RF, Lopez A, Gosliner TM (2018) Reading between the lines: revealing cryptic species diversity and colour patterns in *Hypselodoris* nudibranchs (Mollusca: Heterobranchia: Chromodorididae). Zoological Journal of the Linnean Society 48: 1–74. https://doi.org/10.1093/zoolinnean/zly048

Fischer P (1883) Manuel de conchyliologie et de paléontologie conchyliologique. Savy, Paris, 417–608.

Glayzer B, Glayzer DT, Smythe KR (1984) The marine Mollusca of Kuwait, Arabian Gulf. Journal of Conchology 31: 311–330.

Gosliner, TM (1987) Nudibranchs of southern Africa: a guide to opisthobranch molluscs of southern Africa. Sea Challengers, California Academy of Sciences, San Francisco, 136 pp.

Gosliner TM (1994) New species of *Chromodoris* and *Noumea* (Nudibranchia: Chromodorididae) from the western Indian Ocean and southern Africa. Proceedings of the California Academy of Sciences 48: 239–252.

Gosliner TM, Behrens DW (2004) Two new species of dorid nudibranchs (Gastropoda, Opisthobranchia) from the Indian Ocean. Proceedings of the California Academy of Sciences 55: 1–10.

Gosliner TM, Behrens DW, Valdés A (2008) Indo-Pacific Nudibranchs and Sea Slugs. A field guide to the world's most diverse fauna. Sea Challengers Natural History Books and the California Academy of Sciences, California, 426 pp.

Gosliner TM, Valdés A, Behrens DW (2015) Nudibranch and sea slug identification, Indo-Pacific. New World Publications, Inc. Jacksonville, Florida, 408 pp.

Gul S (2019) New records of nudibranchs (Gastropoda: Heterobranchia) from the coast of Pakistan (Northern Arabian Sea). The Festivus 51: 114–124.

Hardy P (2001) (May 15) *Chelidonura livida* from United Arab Emirates. Sea Slug Forum, Australian Museum, Sydney. http://www.seaslugforum.net/find/4261 [Accessed on 10.06.2021]

Sea Slugs [Sea Slugs of the Mediterranean Sea and elsewhere] (2017) Goniobranchus sp. 10 Genus: Pease, 1866. [Photo & copyright by Stewart Clarke] http://medslugs.de/E/Ind-NW/Goniobranchus_sp_10/Goniobranchus_sp_10_01.htm

South-west Indian Ocean Seaslug site (2008) Chelidonura livida Yonow, 1994 [Photo Sylvain Le Bris]. http://seaslugs.free.fr/nudibranche/a_cheli_livida.htm

Jones DA (1986) A field guide to the sea shores of Kuwait and the Arabian Gulf, University of Kuwait. Blandford Press, Dorset, 192 pp.

Jones DA, Nithyanandan M (2012a) Recruitment of marine biota onto hard and soft artificially created subtidal habitats in Sabah Al-Ahmad Sea City, Kuwait. Marine Pollution Bulletin 72: 351–356. https://doi.org/10.1016/j.marpolbul.2012.11.001

Jones DA, Nithyanandan M (2012b) Taxonomy and distribution of the genus *Eurydice* Leach, 1815 (Crustacea, Isopoda, Cirolanidae) from the Arabian region, including three new species. Zootaxa 3314: 43–57. https://doi.org/10.11646/zootaxa.3314.1.4

Johnson RF, Gosliner T (2012) Traditional Taxonomic Groupings Mask Evolutionary History: A Molecular Phylogeny and New Classification of the Chromodorid Nudibranchs. PLoS ONE 7: e33479. https://doi.org/10.1371/journal.pone.0033479

Johnson RF, Valdés A (2001) The *Hypselodoris infucata*, *H. obscura* and *H. saintvincentius* species complex (Mollusca, Nudibranchia, Chromodorididae), with remarks on the genus *Brachychlanis* Ehrenberg, 1831. Journal of Natural History 35: 1371–1398. https://doi.org/10.1080/002229301750384310

Jörger KM, Stöger I, Kano Y, Fukuda H, Knebelsberger T, Schrödl M (2010) On the origin of Achochlidia and other enigmatic euthyneuran gastropods, with implications for the systematics of Heterobranchia. BMC Ecology and Evolution 10: e323. https://doi.org/10.1186/1471-2148-10-323

McDonald G, Nybakken JW (1997) List of the worldwide food habits of nudibranchs. Veliger 40(2): 1–426. https://escholarship.org/uc/item/0g75h1q3

Mehrotra R, Caballer Gutiérrez MA, Scott CM, Arnold S, Monchanin C, Viyakarn V, Chavanich C (2021) An updated inventory of sea slugs from Koh Tao, Thailand, with notes on their ecology and a dramatic biodiversity increase for Thai waters. ZooKeys 1042: 73–188. https://doi.org/10.3897/zookeys.1042.64474

Myers A, Nithyanandan M (2016) The Amphipoda of Sea City, Kuwait. The Senticaudata (Crustacea). Zootaxa 4072: 401–429. https://doi.org/10.11646/zootaxa.4072.4.1

Nithyanandan M (2012) New and rare nudibranch records from Kuwait, Arabian Gulf (Mollusca: Opisthobranchia). Marine Biodiversity Records 5: e115. https://doi.org/10.1017/S1755267212000954

Nithyanandan M, Jones DA, Esseen M (2016) Fishery resources of Sabah Al-Ahmad Sea City waterways: A potential contributor for Kuwait's fisheries. Aquatic Ecosystem Health & Management 19: 452–460. https://doi.org/10.1080/14634988.2016.1255104

Papathanasopoulou N, Zogaris S (2015) Coral reefs of Kuwait. KUPEC, Biodiversity East, Cyprus, 273 pp.

Pease WH (1866) Remarks on Nudibranchiata inhabiting the Pacific islands, with descriptions of two new genera. American Journal of Conchology 2: 204–208.

Pilsbry HA (1895–1896) Order Opisthobranchiata. In: Tyron GW, Pislbry HA (Eds) Manual of Conchology 16: 1–1262. [54 pls]

Rezai H, Sei Ali M, Parviz TK, Hamid Reza B, Keivan K (2016) Nudibranchs from the Northern Persian Gulf. Journal of the Persian Gulf (Marine Science) 23/24: 71–78.

Rudman WB (1977) Chromodorid opisthobranch Mollusca from East Africa and the tropical West Pacific. Zoological Journal of the Linnean Society 61: 351–397. https://doi.org/10.1111/j.1096-3642.1977.tb01033.x

Rudman WB (2007) Comment on color variations of *Hypselodoris infucata* from Tulamben by Mike Krampf, Sea Slug Forum, Australian Museum, Sydney. http://www.seaslugforum.net/find/18901 [Accessed on10.06.2021]

Rüppell E, Leuckart FS (1828–1830) Mollusca [in] Atlas zu des Reise im Nordlichen Afrika von Eduard Rüppell. 1. Abth. Zoologie. 5. Neue wirbellose Thiere des Rothen Meers. H.L. Brönner, Frankfurt, 1–22, pls 1–12 [1828], 23–47 [1830].

Sanpanich K, Duangdee T (2019) A survey of marine mollusc diversity in the Southern Mergui archipelago, Myanmar. Phuket Marine Biological Center Research Bulletin 75: 45–60.

Schrödl J, Klussmann K, Wilson NG (2011) Bye-bye Opisthobranchia. A review on the contribution of Mesopsammic sea slugs to Euthyneuran systematics. Thalassas, An International Journal of Marine Sciences 27: 101–112.

Sheppard C, Al-Husiani M, Al-Jamali F, Al-Yamani F, Baldwin R, Bishop J, Benzoni F, Dutrieux E, Dulvy NK, Durvasula SR, Jones DA, Loughland R, Medio D, Nithyandandan M, Pilling GM, Pohkarpov I, Price ARG, Purkis S, Riegl B, Saburova M, Namin KS, Taylor O, Wilson S, Zainal K (2010) The Persian/Arabian Gulf: A young sea in decline. Marine Pollution Bulletin 60: 13–38. https://doi.org/10.1016/j.marpolbul.2009.10.017

Sreeraj CR, Chandrakasan S, Raghunathan C (2012) An annotated checklist of opisthobranch fauna (Gastropoda: Opisthobranchia) of the Nicobar Islands, India. Journal of Threatened Taxa 4: 2499–2509. https://doi.org/10.11609/JoTT.o2783.2499-509

Stimpson W (1855) Descriptions of some of the new marine Invertebrata from the Chinese and Japanese Seas. Academy of Natural Sciences, Philadelphia, 22 pp. https://doi.org/10.5962/bhl.title.51444

Tibiriçá Y, Malaquias MAE (2017) The bubble snails (Gastropoda, Heterobranchia) of Mozambique: an overlooked biodiversity hotspot. Marine Biodiversity 47: 791–811 https://doi.org/10.1007/s12526-016-0500-7

Tibiriçá Y, Pola M, Cervera JL (2017) Astonishing diversity revealed: annotated and illustrated inventory of Nudipleura (Gastropoda: Heterobranchia) from Mozambique. Zootaxa 4359: 1–133. https://doi.org/10.11646/zootaxa.4359.1.1

Trinchese S (1888) Descrizione del nuovo genere Caloria. Memorie della Reale Accademia delle Scienze dell'Istituto di Bologna 9: 291–295.

Valdés Á, Mollo E, Ortea J (1999) Two new species of *Chromodoris* (Mollusca, Nudibranchia, Chromodorididae) from southern India, with a redescription of *Chromodoris trimarginata* (Winckworth, 1946). Proceedings of the California Academy of Sciences 51: 461–472.

Wägele H, Willan RC (2000) Phylogeny of the Nudibranchia. Zoological Journal of the Linnean Society 130: 83–181. https://doi.org/10.1111/j.1096-3642.2000.tb02196.x

Winckworth R (1946) *Glossodoris* from Bombay. Proceedings of the Malacological Society of London 26: 155–160.

WoRMS Editorial Board (2021) World Register of Marine Species. https://www.marinespecies.org [Accessed on 14.06.2021]

Yonow N (1990) Red Sea Opisthobranchia 3: the orders Sacoglossa, Cephalaspidea and Nudibranchia: Doridacea (Mollusca: Opisthobranchia). Fauna of Saudi Arabia 11: 286–299.

Yonow N (1994a) A new species and a new record of *Chelidonura livida* from the Red Sea (Cephalaspidea: Aglajidae). Journal of Conchology 35: 14–147.

Yonow N (1994b) Opisthobranchs from the Maldive Islands, including descriptions of seven new species (Mollusca: Gastropoda). Revue française d'aquariologie (1993) 20: 97–129.

Yonow N (2008) Sea Slugs of the Red Sea. Pensoft Publications, Sofia/Moscow, 304 pp.

Yonow N (2012) Opisthobranchs from the western Indian Ocean, with descriptions of two new species and ten new records (Mollusca, Gastropoda). ZooKeys 197: 1–129. https://doi.org/10.3897/zookeys.197.1728

ZooKeys 1048: 109–143 (2021)
doi: 10.3897/zookeys.1048.68454
https://zookeys.pensoft.net

RESEARCH ARTICLE

A peer-reviewed open-access journal
ZooKeys
Launched to accelerate biodiversity research

# The millipede genera *Amblyiulus* Silvestri, 1896 and *Syrioiulus* Verhoeff, 1914 in the Caucasus, with notes on their distributions (Diplopoda, Julida, Julidae)

Aleksandr P. Evsyukov[1], Sergei I. Golovatch[2], Dragan Ž. Antić[3]

**1** *Don State Technical University, Department of Biology and General Pathology, Rostov-on-Don, Russia* **2** *Institute for Problems of Ecology and Evolution, Russian Academy of Sciences, Moscow, Russia* **3** *University of Belgrade, Faculty of Biology, Institute of Zoology, Belgrade, Serbia*

Corresponding author: Aleksandr P. Evsyukov (aevsukov@mail.ru)

Academic editor: Pavel Stoev | Received 8 May 2021 | Accepted 10 June 2021 | Published 13 July 2021

*http://zoobank.org/FC201D04-9877-4583-92C2-84CC80BB75A5*

**Citation:** Evsyukov AP, Golovatch SI, Antić DŽ (2021) The millipede genera *Amblyiulus* Silvestri, 1896 and *Syrioiulus* Verhoeff, 1914 in the Caucasus, with notes on their distributions (Diplopoda, Julida, Julidae). ZooKeys 1048: 109–143. https://doi.org/10.3897/zookeys.1048.68454

## Abstract

In the Caucasus, the genera *Amblyiulus* Silvestri, 1896 and *Syrioiulus* Verhoeff, 1914 are shown to include two and four species, respectively: *Amblyiulus georgicus* Lohmander, 1932, from Georgia and Armenia, *A. hirtus* **sp. nov.**, from Azerbaijan and Dagestan, Russia, *Syrioiulus adsharicus* (Lohmander, 1936), from Georgia, *S. continentalis* (Attems, 1903), from Azerbaijan and Iran, *S. taliscius* (Attems, 1927), from Azerbaijan, and *S. armeniacus* **sp. nov.**, from Armenia. All these six species are described, illustrated, and keyed, and their distributions are mapped and discussed, based on the literature data and abundant new samples.

## Keywords

Faunistic records, key, map, new species, Pachyiulinae, Pachyiulini, taxonomy

## Introduction

The very large family Julidae, of the basically Holarctic order Julida dominates the millipede faunas of Europe and the Mediterranean, marginally extending into the Oriental realm as well (Enghoff et al. 2015; Kime and Enghoff 2017). The subfamily Pachyiulinae, often referred to as the tribe Pachyiulini, encompasses between 15 and 20 genera, or 16–22 genera or subgenera, according to Antić et al. (2018) and

Vagalinski (2020), respectively, and is characterised by the anterior gonopods being devoid of flagella, with a distinct sternum, both being fused mediobasally, and the posterior gonopods showing a mesomeral process, if any, only as an anterior branch of the opisthomere (Attems 1940; Tabacaru 1978). This group is monophyletic (Enghoff et al. 2013), temperate trans-Palaearctic, mostly restricted to the Mediterranean and ranges from Macaronesia in the west, through the entire Mediterranean, Central Asia, and central China, to Japan in the east. In the Caucasus proper, including the near-Caspian part of the Republic of Azerbaijan, but excluding the one in Iran (= both parts forming the Hyrcanian biogeographic province), this subfamily/tribe is currently known to be represented by three genera only.

The genus *Pachyiulus* Berlese, 1883 contains ca. 15 species of mostly very large julids which are largely confined to Southern and Southeastern Europe, the Near East, and the Caucasus (Enghoff et al. 2015). The Caucasus actually supports a single native species, *P. krivolutskyi* Golovatch, 1977, recently revised (Evsyukov 2016) and endemic to the western Caucasus (= Colchidan biogeographic province) within both Georgia and Russia (Kokhia and Golovatch 2020). One more congener, the eastern Mediterranean and synanthropic *P. flavipes* (C.L. Koch, 1847), has been introduced to the western Caucasus (Lohmander 1936), also being a very common, "tramp" species across Crimea (e.g., Golovatch 2008; albeit perhaps erroneously referred to as *P. varius* (Fabricius, 1781)).

The remaining two known genera of this tribe/subfamily which inhabit the Caucasus are *Amblyiulus* Silvestri, 1896 and *Syrioiulus* Verhoeff, 1914. The diagnoses and species compositions of these two genera, the main focus of the present contribution, remained unclear and confused for a long time, sometimes the latter genus being treated even as a synonym of the former (Tabacaru 1978, 1995). Mauriès (1982), in contrast to Tabacaru (1978), elevated *Syrioiulus* to a full genus and defined it primarily through a deeply bipartite posterior gonopod. He considered *Syrioiulus*, together with the monotypic *Promeritoconus* Verhoeff, 1943, from Turkey, and the species-rich genus *Amblyiulus*, as a single eastern Mediterranean lineage in the subfamily Pachyiulinae that is distinguished by the presence of eyes and, with a few exceptions only, 1+1 frontal setae, the development of apicoventral lobes on the male mandibular stipites, and of subequally high posterior gonopodal mesomeral process and opisthomere. Most, but not all, of the species from the Levant, Sporades (Greece), Caucasus, Iran and even Japan were thereby formally transferred to *Syrioiulus*. Some others from the same regions remained in or newly reassigned to *Amblyiulus*.

Enghoff (1992), in his review of *Dolichoiulus* Verhoeff, 1900, mentioned *Syrioiulus* only in passing. He, in his own outline of the pachyiuline generic classification, rediagnosed *Amblyiulus* and put the main emphasis on the structure of the posterior gonopods which show three apical processes, not two as is characteristic of several other genera, including *Syrioiulus*. Furthermore, he clearly illustrated the gonopods of *A. barroisi* (Porat, 1893), the type species of *Amblyiulus*.

The situation has become fully clarified only very recently, when first Golovatch (2018) and then Vagalinski (2020) confirmed the distinctions between *Amblyiulus* and *Syrioiulus* as lying solely in posterior gonopod conformation, also refining their

diagnoses and scopes. Both these genera appear to be very similar, but differ clearly in the structure of the posterior gonopods: each of these being strongly divided into two branches ("bipartite"), i.e., a frontal (= mesomeral) and a caudal (= opisthomere) branch in *Syrioiulus* spp., vs. "tripartite", with a third branch, a flagelliform rod, in *Amblyiulus* spp. (Golovatch 2018). A further refined account of the main differences between both these genera compared is given below.

Considering the above distinctions, *Amblyiulus* in the Caucasus appears to comprise only one described species: *A. georgicus* Lohmander, 1932. In addition, both Bababekova (1969, 1996) and Rakhmanov (1972) listed in Azerbaijan a dubious species, *A. faliocius* Attems, likely a misspelling of *taliscius*. The genus *Syroiulus* in the Caucasus presently includes three old species, all valid: *S. adsharicus* (Lohmander, 1936), *S. continentalis* (Attems, 1903), and *S. taliscius* (Attems, 1927). Vagalinski (2020), in his review and a provisional checklist of *Syrioiulus* species, emphasised the still-poor distinctions of *Syrioiulus* as opposed to a few pachyiuline genera other than *Amblyiulus*.

## Materials and methods

All material has been shared between the collections of the Zoological Museum of the Moscow State University, Russia (**ZMUM**), the Senckenberg Museum of Natural History in Görlitz, Germany (**SMNG**), and the Institute of Zoology, University of Belgrade, Serbia (**IZB**). The specimens are stored in 70% ethanol. Some parts of males (antennae, gonopods, legs, etc.) and females (vulvae and leg pairs 2) were dissected and mounted in glycerol on temporary microscopic slides. Photographs were taken using a Zeiss StereoDiscovery V.20 microscope and processed with Zeiss ZEN software. Line drawings were executed using a camera lucida attached to a Radical light-transmission microscope. Scanning electron micrographs were taken with a Zeiss CrossBeam 340 (Rostov-on-Don State Technical University, Rostov-on-Don, Russia) or a JEOL JSM-6510LV (**SMNG**) scanning electron microscope (**SEM**). For some SEM micrographs, the gonopods were glued to a small sticky plastic triangle, placed on an SEM-stub, air dried for two days in a glass filled with Silica gel and finally coated with gold. After examination, material was removed from stubs and returned to alcohol. Live animals were photographed in situ using a Canon PowerShot SX120 IS digital camera.

The distribution map was created using Google Earth Pro 7.3.3 and processed in Adobe Photoshop CS6.

A "body ring formula" indicates the number of podous (including the gonopod-bearing segment/ring) and apodous segments/rings in an individual. This formula is p+a+T where p is the number of podous body rings, a the number of apodous body rings, and T represents the telson (Enghoff et al. 1993). Only adults have been analysed in the present study. For morphological descriptions, we largely used the terminology from Minelli (2015), for descriptions of the gonopods, that of Enghoff (1992) with changes in Vagalinski (2020).

The biogeographic regionalisation of the Caucasus follows the botanical one by Menitsky (1991).

No type material of the previously described species has been revised (mostly stored in the Zoological Institute, Russian Academy of Sciences, St. Petersburg) because of the 2020–2021 COVID pandemic, and the descriptive accounts and illustrations available in the literature are sufficiently complete and clear to allow a safe species identification. Colouration is largely described from preserved material. In the catalogue sections, D stands for a description or descriptive notes, R for new or repeated records, while M is a mere mention.

### Refined characteristics of *Amblyiulus* vs. *Syrioiulus*

As shown below in the descriptions of individual species, the use of SEM allows for the distinctions between both genera concerned to be further refined. It is the opisthomere, not the entire posterior gonopod, that is bifid in *Syrioiulus*: a solenomere (with a distinct fovea or a deep saddle-like structure on top) and an anterior process (an anterior, lamellar branch adjacent to the solenomere) (Figs 7D, 10D, 12D–F, 14D). Using standard light microscopy, this anterior process often remains unnoticed, since it is very tightly appressed to the solenomere. In contrast, a third, anteromesal or lateral process/rod of the opisthomere is characteristic of *Amblyiulus* (Figs 3D, F, 5A, D–F, I, J).

As a result, it is only the structure of the opisthomere of the posterior gonopods that allows for the genera *Amblyiulus* and *Syrioiulus* to be more or less confidently diagnosed and separated. At the same time, species of *Syrioiulus* are mostly very similar in gonopodal conformation (Figs 7A–C, E, F, 10A–C, E, F, 12A–C, I, J, 14A–C, E–G), but they differ well in somatic characteristics, such as the presence or absence of eyes, frontal setae, and hairs on the rings (see also Key below). Similarly, within the genus *Pachyiulus*, several species were synonymised based solely on shared gonopodal characters (Mauriès et al. 1997), but later some have been revalidated on the basis of somatic features such as colouration (Frederiksen et al. 2012).

## Taxonomic part

### Genus *Amblyiulus* Silvestri, 1896

**Type species.** *Julus barroisi* Porat, 1893, by original designation.

**Diagnostic remarks.** Here we follow Tabacaru's (1978) opinion that the genera of the subfamily/tribe Pachyiulinae/-ini are best to be diagnosed using a complex of characters, both gonopodal and somatic. In the latest review of this tribe (Mauriès 1982), all genera are divided into three groups depending on the structure of the apical part of the opisthomere, viz., the presence/absence of a fovea and the presence/absence of a pseudoflagellum. He mistakenly assigned the genus *Amblyiulus* to group 3 (along with many other genera like *Dolichoiulus*), which have neither a fovea nor a pseudoflagellum.

However, in accordance with our and earlier descriptions (e.g., Golovatch 2018), *Amblyiulus* has a fovea, however small, on the top of the solenomere. By the presence of a fovea and the absence of a pseudoflagellum, the genera *Parapachyiulus* Golovatch, 1979 and *Dangaraiulus* Golovatch, 1979 also join this group (Golovatch 1979, 2018). According to a number of other characters, such as the presence of frontal setae, apicoventral lobes on the male mandibles, and the mesomeral process being as high as the opisthomere, *Amblyiulus* belongs to Mauriès' subgroup 3aa, together with the genera *Syrioiulus* and *Promeritoconus*. However, it seems noteworthy that sometimes frontal setae can be absent, while male mandibular stipites can remain unmodified.

The promere in *Amblyiulus* is narrowed in the basal third, in contrast to that in *Promeritoconus*, which is narrowed apically; in the apical part it may have one or two denticles, but sometimes none. The head can be with or without frontal setae. The eyes are mostly absent. The opisthomere of the posterior gonopod is tripartite: a solenomere, an anterior process, and an anteromesal or lateral rod, vs. bipartite in *Syrioiulus*.

**Species included.** *Amblyiulus barroisi* (Porat, 1893), *Amblyiulus cedrophilus* (Attems, 1910), *Amblyiulus festae* (Silvestri, 1895), *Amblyiulus georgicus* Lohmander, 1932, *Amblyiulus hirtus* sp. nov., and possibly several others, but their identity requires verification (Golovatch 2018).

### *Amblyiulus georgicus* Lohmander, 1932

Figs 1A, 2, 3, 15A, 16

*Amblyiulus georgicus* Lohmander, 1932a: 180–182, figs 10–12 (D).
*Amblyiulus georgicus*—Lohmander 1936: 170 (M); Kobakhidze 1965: 395 (M); Lokšina and Golovatch 1979: 385 (M).
*Syrioiulus georgicus*—Mauriès 1984: 43 (M); Kokhia and Golovatch 2020: 207 (M).

**Material examined.** Armenia: 3 ♂♂, 5 ♀♀, 2 juv. (ZMUM), SW of Shnokh halfway between Alaverdi and Bagratashen, ca. 1500 m a.s.l., *Carpinus* forest, litter, 24.V.1987; 2 ♀♀ (ZMUM), Odzun W of Alaverdi, 1500–1550 m a.s.l., *Quercus*, *Fagus*, *Carpinus*, etc. forest, litter and under stones with ants, 23–24.V.1987; all leg. S. Golovatch, K. Eskov.

**Diagnosis.** Differs from *A. hirtus* sp. nov., apparently the most similar and geographically the closest congener known to date, by the following combination of somatic and gonopodal characteristics. Head without frontal setae; collum and metazonae of body rings without setae. Male mandibular stipites expanded. Promere wide, with two apical denticles. Solenomere with a membranous lobe notched apically. Rod of opisthomere relatively short. See also Key below.

**Redescription.** Length of adults 27–30 mm (♂♂) or 28–31 mm (♀♀), width 1.6–1.7 mm (♂♂) or 1.7–1.9 mm (♀♀). Number of body rings in adults, 65–67+2+T (♂♂) or 67–69+2+T (♀♀). Body subcylindrical (typical of Julidae), metazonae brownish grey, prozonae yellowish grey (Fig. 1A). Head, a few postcollum rings and telson

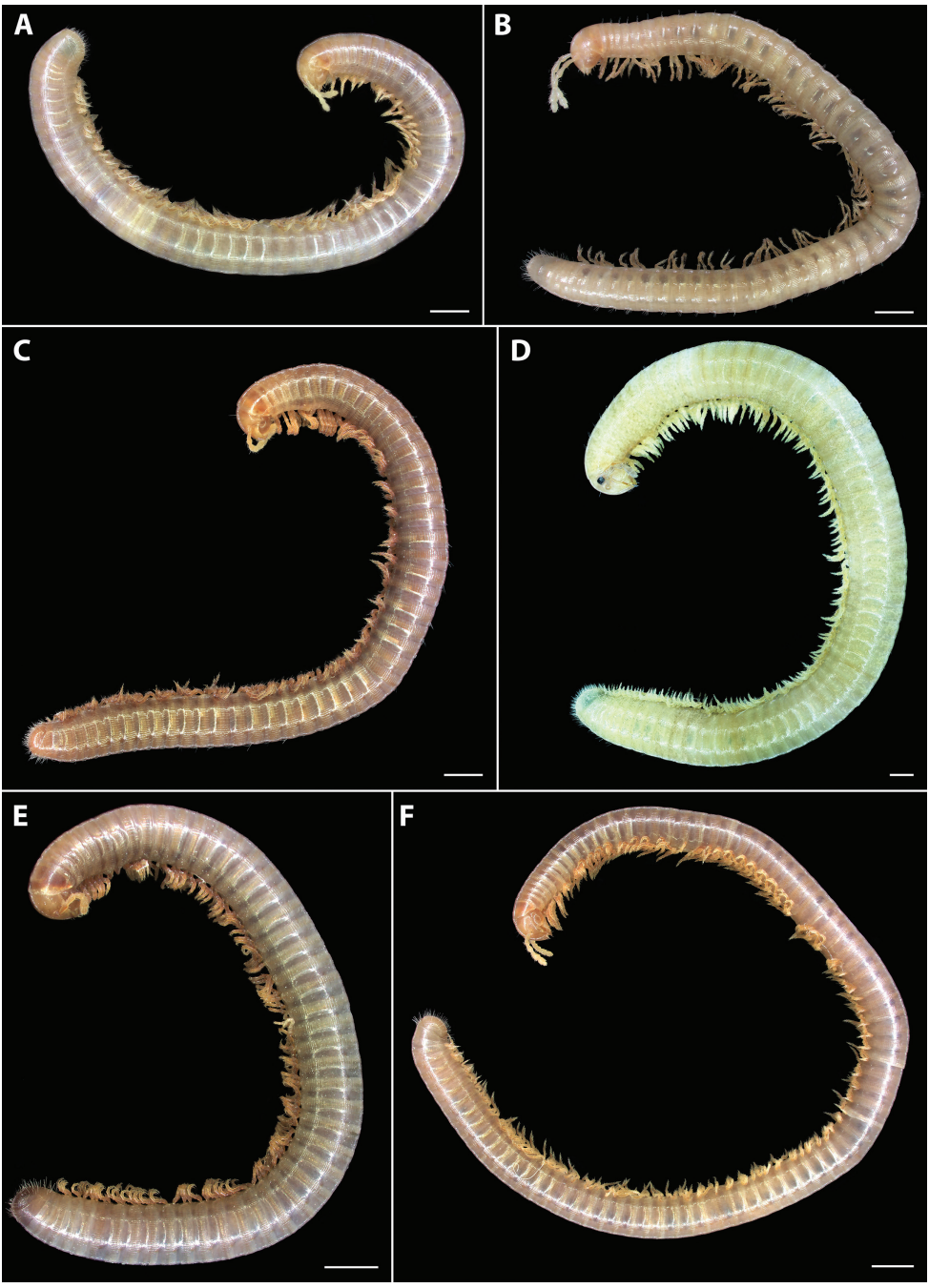


**Figure 1.** Habitus of *Amblyiulus* and *Syrioiulus* species, males, lateral views **A** *A. georgicus* Lohmander, 1932 from Shnokh, Armenia (ZMUM) **B** *A. hirtus* sp. nov., paratype from Bash-Layski, Azerbaijan (ZMUM) **C** *S. adsharicus* (Lohmander, 1936) from Adigeni, Georgia (ZMUM) **D** *S. continentalis* (Attems, 1903) from Istisu, Azerbaijan (ZMUM) **E** *S. taliscius* (Attems, 1927) from Avrora, Azerbaijan (ZMUM) **F** *S. armeniacus* sp. nov., paratype from Shikahoh, Armenia (ZMUM). Scale bars: 1.0 mm.

lighter than other body rings. Collum more vividly red-brown. Antennae, mouthparts, and legs yellow (Fig. 2A–C). Eyes absent. Metazonae with weak and irregular striations, 14–16 striae between dorsal axial line and ozopore (Fig. 2D). Ozopores relatively large, with a stria in front and lying behind suture without touching it (Fig. 2H).

Antennae relatively long, in situ reaching segment 4. Head without frontal setae, but with 8+8–9+9 labral and 2+2 supralabral setae (Fig. 2A–C). Gnathochilarium with four setae on each lamella lingualis, stipites with a group of several short setae in medial part and three long setae at anterolateral margin (Fig. 2I). Collum and metazonae without setae at posterior margin (Figs 1A, 2A–G). Epiproct undeveloped (Fig. 2E, F). Hypoproct subtriangular, with several long setae (Fig. 2G). Telson and anal valves sparsely setose, setae being long (Fig. 2E–G).

**Male.** Mandibular stipites expanded, slightly swollen in distal part (Fig. 2A). Leg pair 1 small, unciform, with a group of setae on each coxa and at base of telopodite; telopodite relatively long (Fig. 2J). Leg pair 2 with pads on postfemur and tibia (Fig. 2K). Penes short, bifurcate on top. Ventral edge of male segment 7 with elongated and rounded lamellae bordering the gonopodal aperture (Fig. 2L).

Gonopods (Fig. 3). Promere spoon-shaped, relatively wide, constricted in basal third; mesal ridge in apical part forming a small mesal denticle (Fig. 3B, E). Lateral denticle large, well-developed. Mesomeral process simple, flattened, ribbon-shaped, notched on top (Fig. 3A, C, F). Opisthomere tripartite (Fig. 3D). Solenomere long, slightly curved, with caudomesal lamella notched apically; apical part with a fovea and a pointed membranous process. Anterior process of opisthomere appressed to solenomere, with a rounded apex. Anterolateral part of opisthomere with a helicoid rod.

**Female.** First two leg pairs unmodified. Vulva rounded, operculum and bursa equal in height (Fig. 15A). Operculum at apical margin oblique, undivided. Bursa asymmetric, lateral valve higher than mesal one. Each valve with two rows of long setae. Median field of bursa very short, narrow; emargination of median field suboval.

**Remarks.** This species was described from Borjom (= Borjomi), Georgia (Lohmander 1932a). The above samples represent the first formal records of this species from Armenia. It seems to populate high-montane deciduous forests in the western part of the Caucasus Minor (= Lesser Caucasus) (Fig. 16).

### *Amblyiulus hirtus* sp. nov.

http://zoobank.org/38675EEE-B4FE-4B8B-BDF2-3E77DAADE5BE
Figs 1B, 4, 5, 15B, 16

**Material examined.** ***Holotype*** ♂ (ZMUM), **Azerbaijan**, NW above Bash-Layski ca. 20 km NNW of Sheki, 1250 m a.s.l., *Fagus*, *Carpinus*, *Acer*, etc. forest, litter, 3.V.1987, leg. S. Golovatch, K. Eskov. ***Paratypes*****:** 5 ♂♂, 3 ♀♀ (ZMUM), same collection data as holotype.

**Non-type material. Azerbaijan:** 2 ♂♂, 6 ♀♀ (ZMUM), SW of Kuba, 750 m a.s.l., *Fagus*, *Quercus*, *Carpinus*, etc. forest, litter and under bark, 23.IV.1987, leg.

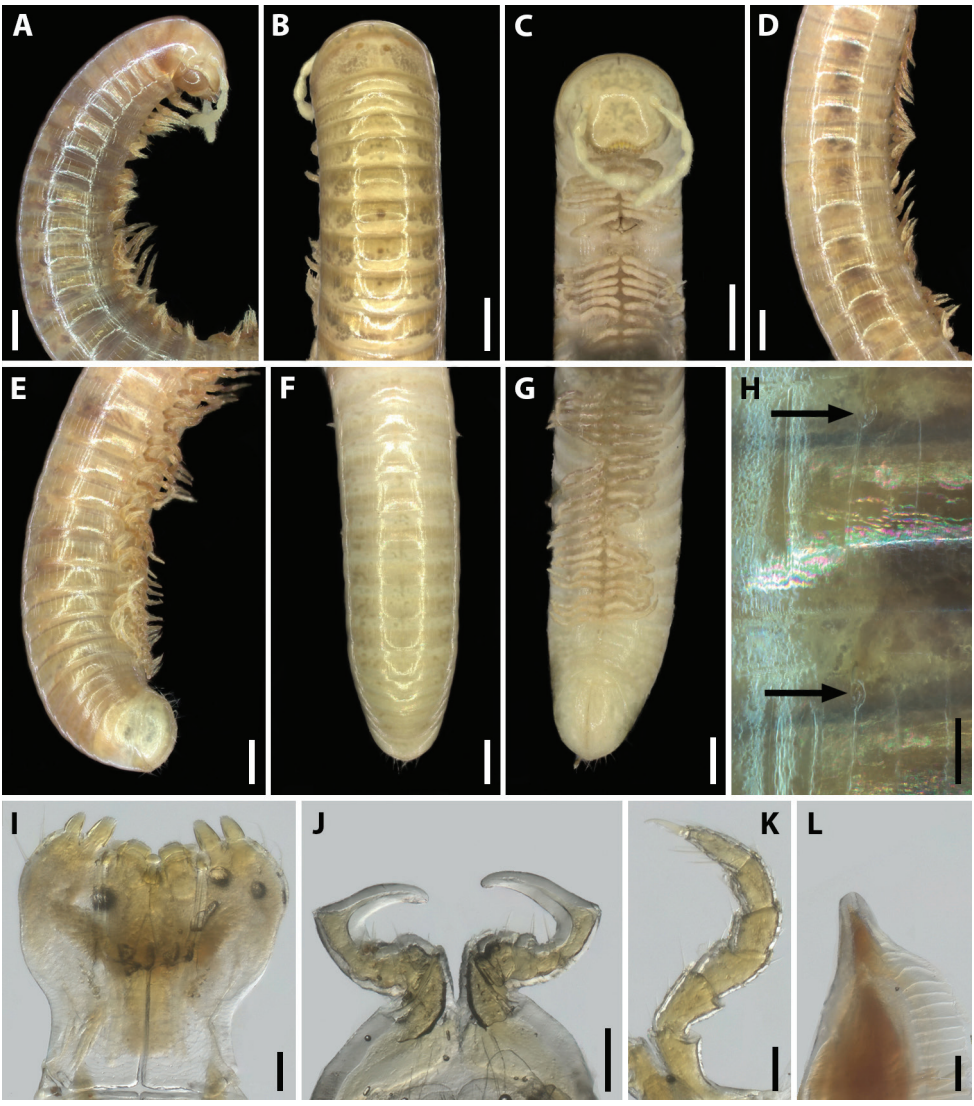


**Figure 2.** *Amblyiulus georgicus* Lohmander, 1932, ♂ from Shnokh, Armenia (ZMUM) **A–C** anterior part of body, lateral, dorsal and ventral views, respectively **D** midbody part, lateral view **E–G** posterior part of body, lateral, dorsal and ventral views, respectively **H** ozopores on midbody rings, lateral view **I** gnathochilarium, ventral view **J** leg pair 1, caudal view **K** leg 2, caudal view **L** ventral edge of pleurotergum 7, lateral view. Scale bars: 0.5 mm (**A–G**); 0.1 mm (**H–L**).

S. Golovatch, K. Eskov; **Russia, Dagestan:** 1 ♂, 2 ♀♀ (ZMUM), Kurush, 2550 m a.s.l., S slope, subalpine and alpine meadows, 20.VIII.1990, leg. G. Magomedov.

**Diagnosis.** Assigned to the genus *Amblyiulus* primarily because of the presence of a rod on the posterior gonopod opisthomere. Differs from *A. georgicus*, perhaps the most similar congener known to date, by the following combination of somatic and

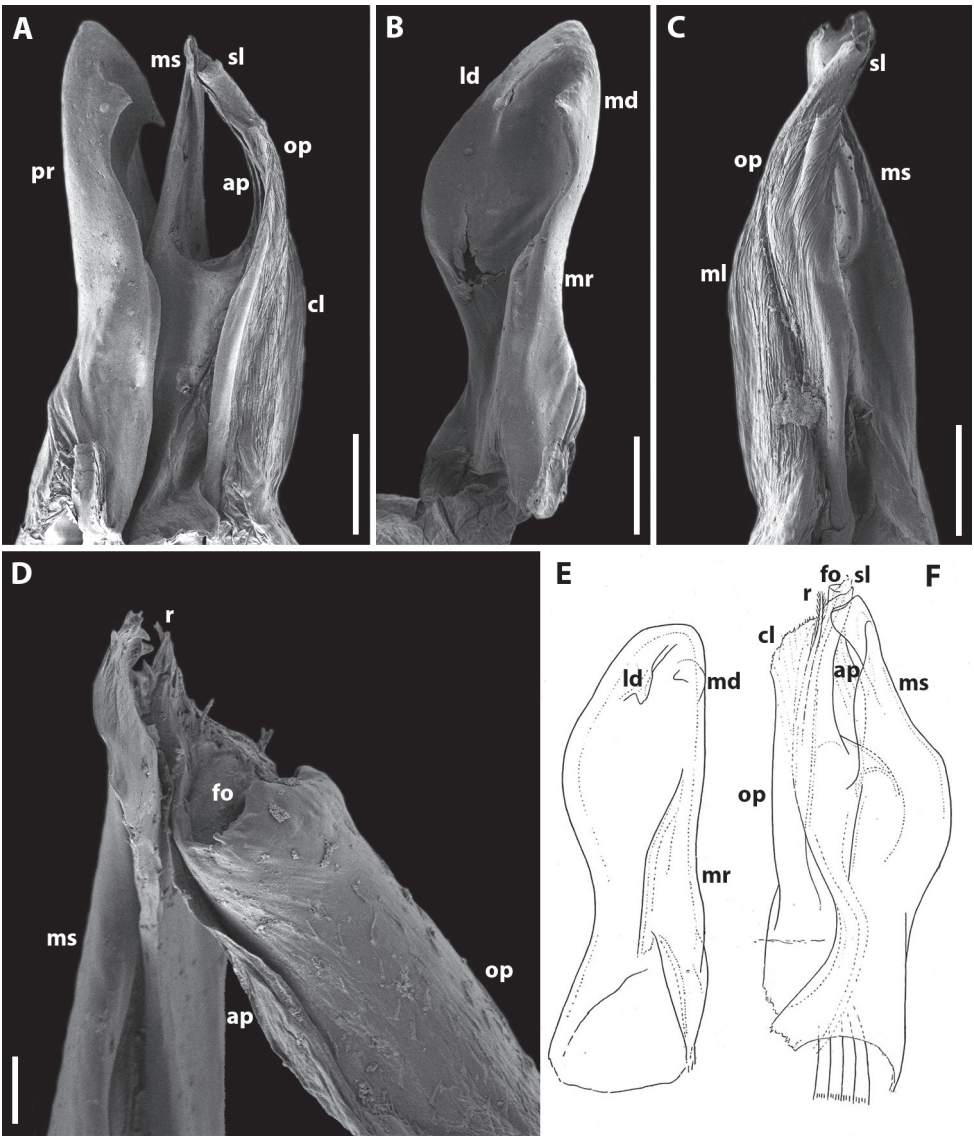


**Figure 3.** *Amblyiulus georgicus* Lohmander, 1932, ♂ from Shnokh, Armenia (ZMUM) (**A–D**) or holotype ♂, after Lohmander (1932) (**E, F**). **A** gonopod, mesal view **B** promere, caudal view **C** posterior gonopod, caudal view **D** end of solenomere, mesal view **E** promere, caudal view **F** posterior gonopod, lateral view. Abbreviations: **ap** anterior process **cl** caudomesal lamella **fo** fovea **ld** lateral denticle **md** mesal denticle **mr** mesal ridge **ms** mesomeral process **op** opisthomere **pr** promere **r** rod **sl** solenomere. Scale bars: 0.1 mm (**A–C**); 0.01 mm (**D**); not to scale (**E, F**).

gonopodal characters. Head with frontal setae; collum and metazonae of body rings each with a posterior whorl of setae. Promere narrow, with two side ridges. Solenomere apically with small filament-like processes. Rod of opisthomere relatively long.

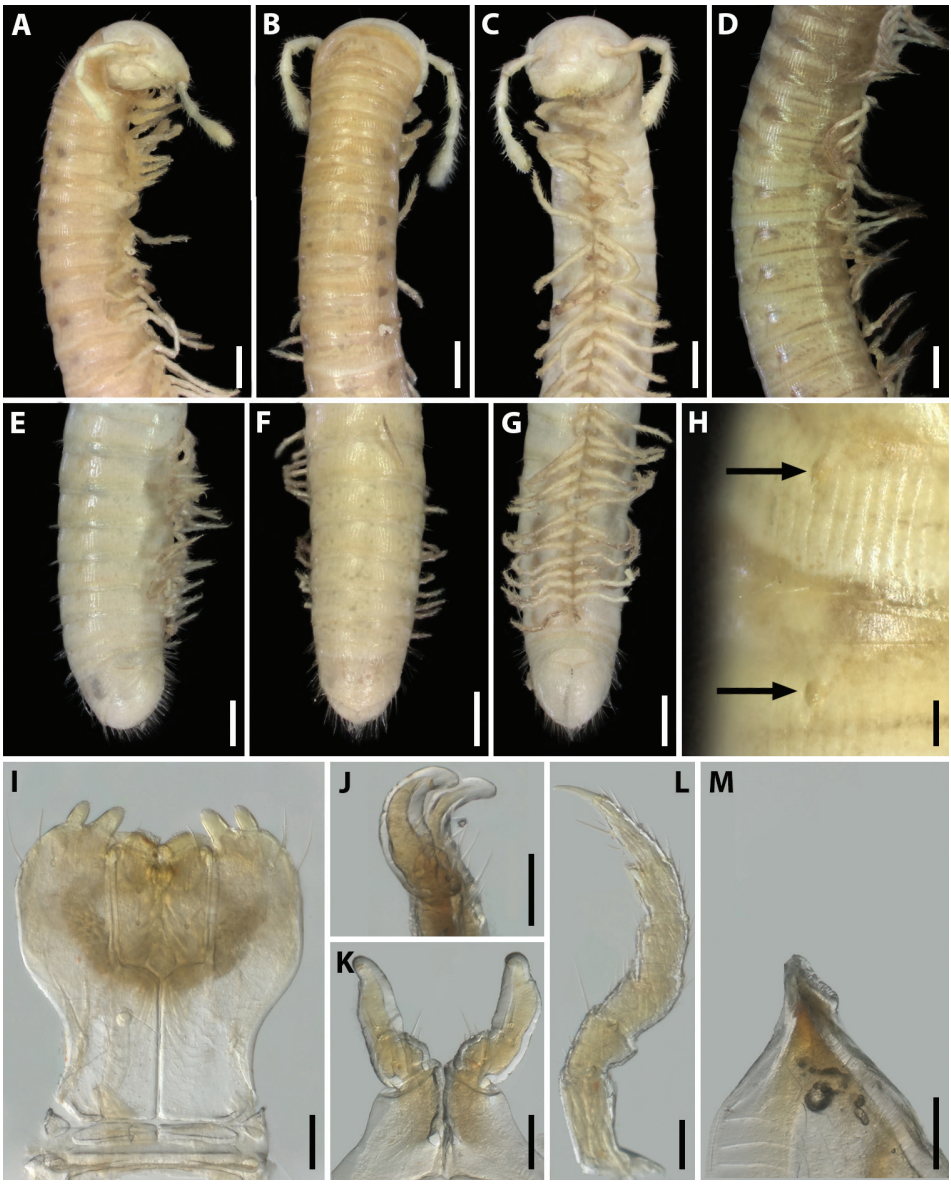


**Figure 4.** *Amblyiulus hirtus* sp. nov., paratype ♂ from Bash-Layski, Azerbaijan (ZMUM) **A–C** anterior part of body, lateral, dorsal and ventral views, respectively **D** midbody part, lateral view **E–G** posterior part of body, lateral, dorsal and ventral views, respectively **H** ozopores on midbody rings, lateral view **I** gnathochilarium, ventral view **J, K** leg pair 1, lateral and caudal views, respectively **L** leg 2, caudal view **M** ventral edge of pleurotergum 7, lateral view. Scale bars: 0.5 mm (**A–G**) or 0.1 mm (**H–M**).

**Name.** To emphasise the presence of metazonal setae; adjective.

**Description.** ***Holotype*:** length 27 mm, width 1.3 mm, number of body rings 51+2+T. Paratypes: length 25–30 mm, width 1.2–1.4 mm, number of body rings in

adults, 45–67+1–3+T (♂♂); or length 27–28 mm, width 1.1–1.3 mm, number of body rings, 46–55+2–3+T (♀♀). Body subcylindrical (typical of Julidae), metazonae and prozonae yellowish grey (Fig. 1B). Head, a few postcollum rings and telson slightly lighter than other body rings. Collum slightly more vividly reddish. Antennae, mouthparts, and legs yellow (Fig. 4A–C). Eyes absent. Metazonae with weak, dense, and regular striations, 21–23 striae per quarter of metazonal surface, i.e., that between dorsal axial line and ozopore (Fig. 4A–G). Ozopores relatively large, with a stria in front, lying behind suture without touching it (Fig. 4H).

Antennae relatively long, in situ reaching ring 4. Head with 1+1 frontal, 8+8–9+9 labral and 2+2 supralabral setae (Fig. 4A–C). Gnathochilarium with three thick setae on each lamella lingualis; stipites without setae in medial part, but with three long setae at anterolateral margin (Fig. 4I). Collum and each following metazona with a whorl of setae at posterior margin (Fig. 4A). Epiproct poorly developed, triangular, with several setae (Fig. 4E, F). Hypoproct subtriangular, covered with long setae (Fig. 4G). Telson and anal valves densely setose, setae being long.

**Male.** Mandibular stipites unmodified (Fig. 4A). Leg pair 1 small, unciform, with a group of setae on coxa and at base of telopodite; telopodites curved anteriad, not anteromesad as in other species of Julidae (Fig. 4J, K). Leg pair 2 with a large pad on tibia and a small one on postfemur (Fig. 4L). Penes short and bifurcate. Ventral edge of male pleurotergum 7 with small subtriangular lamellae bordering the gonopodal aperture (Fig. 4M).

Gonopods (Fig. 5) with anterior and posterior pair equal in height. Promere spoon-shaped, relatively narrow, constricted in basal third; with two ridges: mesal ridge prominent all along; lateral ridge short, located only in apical part of promere (Fig. 5B, H). Mesomeral process simple, flattened, ribbon-shaped, with a small membranous lobe on top (Fig. 5A, C, G, I). Opisthomere tripartite (Fig. 5A, C, E, F). Solenomere long, slightly curved, with a caudomesal lamella notched apically; apical part with a fovea and short filament-like processes (Fig. 5A, C, G, I). Solenomere sometimes with an additional filiform process apically (see Remarks under *Syrioiulus taliscius*). Anterior process notched apically (Fig. 5A, C, E). Rod of solenomere relatively long, consisting of filament-like structures, lateral in position (Fig. 5A, D–G, I).

**Female.** First two leg pairs unmodified. Vulva rounded, operculum higher than bursa (Fig. 15B) and bilobed apically. Bursa asymmetric, lateral valve higher than mesal one. Each valve with two rows of long setae. Median field of bursa very short, narrow; emargination of median field suboval.

**Remarks.** This species seems to be endemic to the eastern part of the Caucasus Major within both northeastern Azerbaijan and the Republic of Dagestan, Russia (Fig. 16).

It is the presence of a laterally positioned rod that brings both *A. georgicus* and *A. hirtus* sp. nov. particularly close together. However, the rod in these two species is located laterally, whereas that in *A. barroisi* anteromesally (Enghoff 1992: fig. 11; Golovatch 2018: fig. 10C). These differences seem to be quite important, but because those three species share not only the presence of a rod, but also a small, but discernible fovea on top of the solenomere, for the time being it seems best to regard the trio as members of *Amblyiulus*.

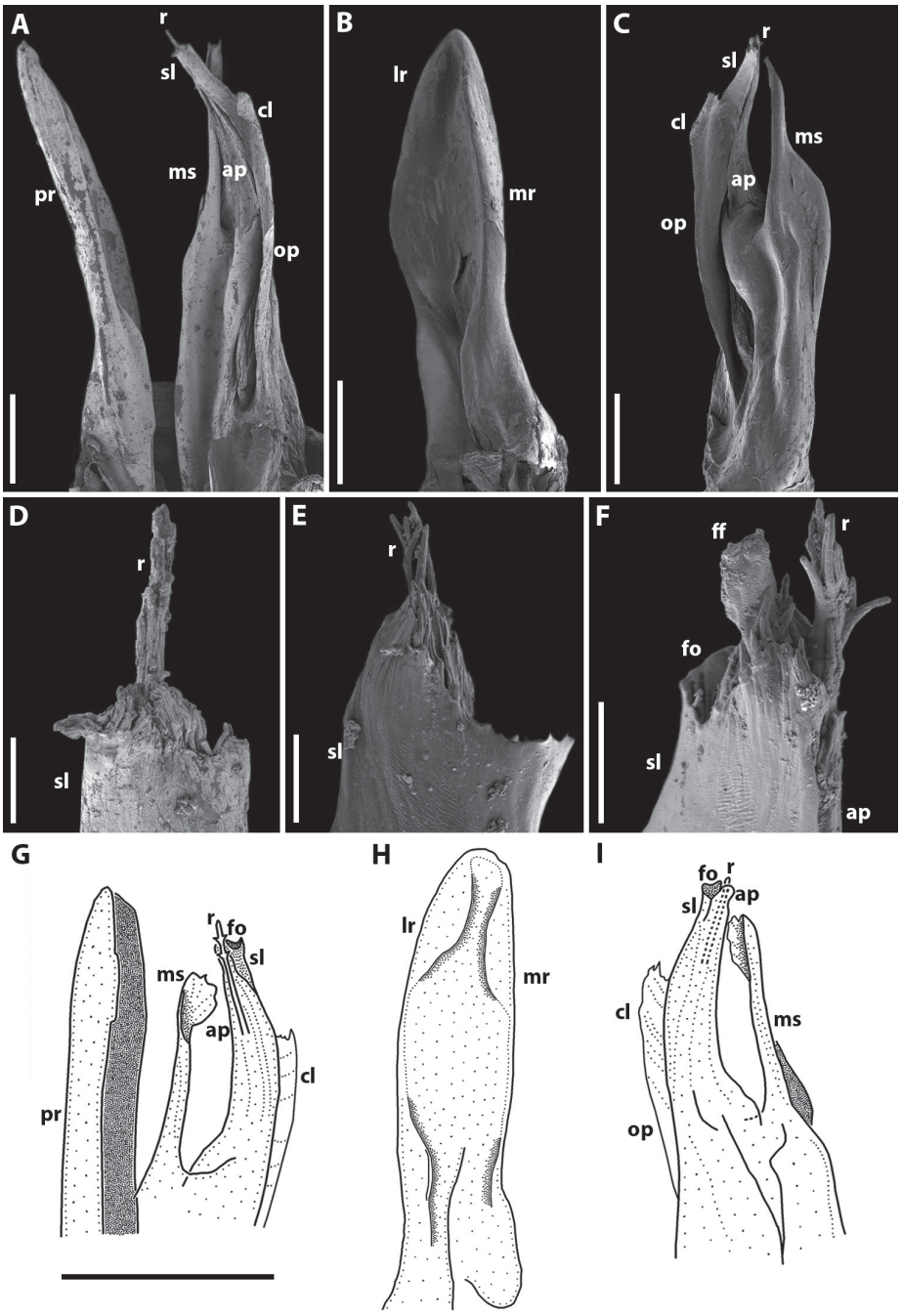


**Figure 5.** *Amblyiulus hirtus* sp. nov., paratype ♂ from Bash-Layski, Azerbaijan (ZMUM) **A, G** gonopod, mesal and lateral views, respectively **B, H** promere, subcaudal and caudal views, respectively **C, I** posterior gonopod, lateral and mesal views, respectively **D, E** end of solenomere, mesal and submesal views, respectively **F** end of opisthomere, mesocaudal view. Abbreviations: **ap** anterior process **cl** caudomesal lamella **ff** filiform process **fo** fovea **lr** lateral ridge **mr** mesal ridge **ms** mesomeral process **op** opisthomere **pr** promere **r** rod **sl** solenomere. Scale bars: 0.1 mm (**A–C**); 0.01 mm (**D–F**); 0.2 mm (**G–I**).

## Genus *Syrioiulus* Verhoeff, 1914

**Type species.** *Dolichoiulus polyzonus* Attems, 1910, by subsequent designation of Jeekel (1971).

**Diagnosis.** All characters as in *Amblyiulus*, except as follows. Promere usually with two denticles in apical part. Head with or without frontal setae. Eyes present or absent. Opisthomere of posterior gonopod bipartite: a solenomere (with a distinct fovea on top) and an anterior process, vs. tripartite in *Amblyiulus*.

**Species included.** *Syrioiulus adsharicus* (Lohmander, 1936), *Syrioiulus andreevi* Mauriès, 1984, *Syrioiulus aharonii* (Verhoeff, 1914), *Syrioiulus armeniacus* sp. nov., *Syrioiulus continentalis* (Attems, 1903), *Syrioiulus discolor* (Lohmander, 1932), *Syrioiulus incarnatus* (Lohmander, 1932), *Syrioiulus lohmanderi* Vagalinski, 2020, *Syrioiulus persicus* (Golovatch, 1983), *Syrioiulus polyzonus* (Attems, 1910), *Syrioiulus taliscius* (Attems, 1927), and several others provisionally listed by Vagalinski (2020).

### *Syrioiulus adsharicus* (Lohmander, 1936)

Figs 1C, 6, 7, 15C, 16

*Amblyiulus* (*Heteropachyiulus*) *adsharicus* Lohmander, 1936: 156–159, figs 131, 132 (D).
*Amblyiulus adsharicus*—Kobakhidze 1964: 191 (M); Lokšina and Golovatch 1979: 385 (M); Talikadze 1984: 143 (M); Kokhia and Golovatch 2018: 40 (M).
*Syrioiulus adsharicus*—Vagalinski 2020: 89 (M); Kokhia and Golovatch 2020: 207 (M).

**Material examined. Georgia:** 10 ♂♂, 16 ♀♀, 5 juv. (ZMUM), 15 km W of Adigeni, *Abies*, *Picea*, *Fagus*, *Acer*, etc. forest, 1500–1700 m a.s.l., litter, logs, under stones, 14–15.V.1983, leg. S. Golovatch; 4 ♂♂, 5 ♀♀ (ZMUM), near Adigeni, 9.VI.1977, leg. V. Dolin.

**Diagnosis.** Differs from all congeners by the following combination of somatic and gonopodal characters. Head with frontal setae. Collum and each metazona of following body rings with a whorl of long setae at caudal margin. Ommatidia present, but only a few ommatidia, all unpigmented and very small. Solenomere with small denticles apically. Anterior process of opisthomere with small filament-like spines apically.

**Redescription.** Length of adults 17–30 mm (♂♂) or 18–31 mm (♀♀), width 1.2–1.4 mm (♂♂) or 1.3–1.7 mm (♀♀). Number of body rings in adults, 50–63+1–2+T (♂♂) or 52–60+1–2+T (♀♀). Body subcylindrical (typical of Julidae), metazonae brownish grey, prozonae violet grey (Figs 1C, 6A, C). Head, collum and body rings from yellow to greyish yellow. Antennae, mouthparts and first leg pairs yellow, other pairs brown (Fig. 6A, C–H). Eyes present, unpigmented, very small, composed of 3–7 ommatidia, unequal numbers on opposite sides of head (Fig. 6B). Metazonae with weak striations, 17–19 striae per quarter of metazonital surface, i.e., that between dorsal axial line and ozopore (Fig. 6E). Ozopores small, lying behind suture and touching it (Fig. 6I).

Antennae relatively long, in situ reaching segment 4. Head with 1+1 frontal, 11+11–13+13 labral and 2+2 supralabral setae (Fig. 6C, D). Gnathochilarium with four long setae on each lamella lingualis, stipites with a medial group of 7–10 short

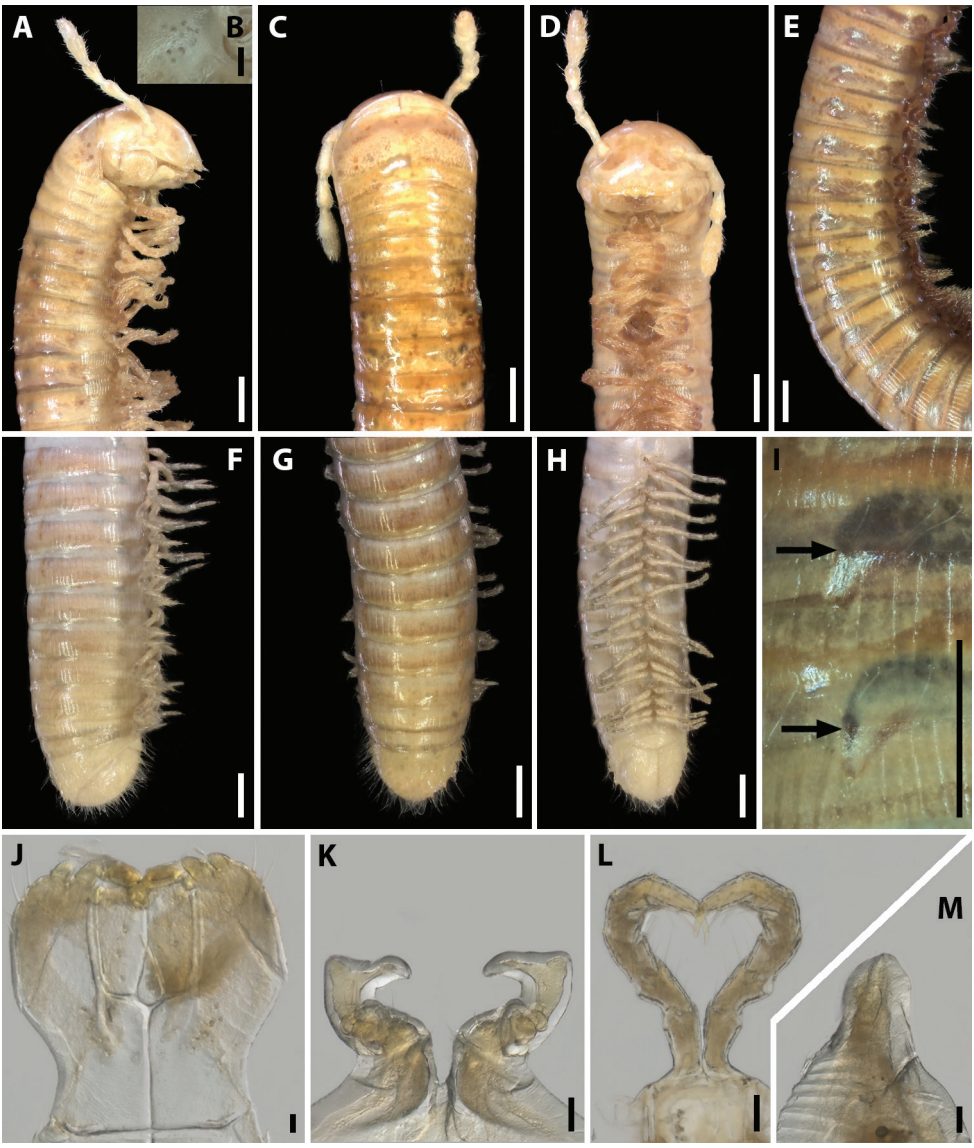


**Figure 6.** *Syrioiulus adsharicus* (Lohmander, 1936), ♂ from Adigeni, Georgia (ZMUM) **A, C, D** anterior part of body, lateral, dorsal and ventral views, respectively **B** Eye, lateral view **E** midbody part, lateral view **F–H** posterior part of body, lateral, dorsal and ventral views, respectively **I** ozopores on midbody rings, lateral view **J** gnathochilarium, ventral view **K** leg pair 1, caudal view **L** leg pair 2, caudal view **M** ventral edge of pleurotergum 7, lateral view. Scale bars: 0.5 mm (**A, C–I**); 0.1 mm (**B**); 0.05 mm (**J–M**).

setae, three long and two short setae at anterolateral margin (Fig. 6J). Collum and each metazona of following rings with a whorl of long setae at posterior margin (Fig. 6A, E, F–H). Epiproct undeveloped (Fig. 6F, G). Hypoproct subtriangular, with long setae (Fig. 6H). Anal valves densely setose, setae being long.

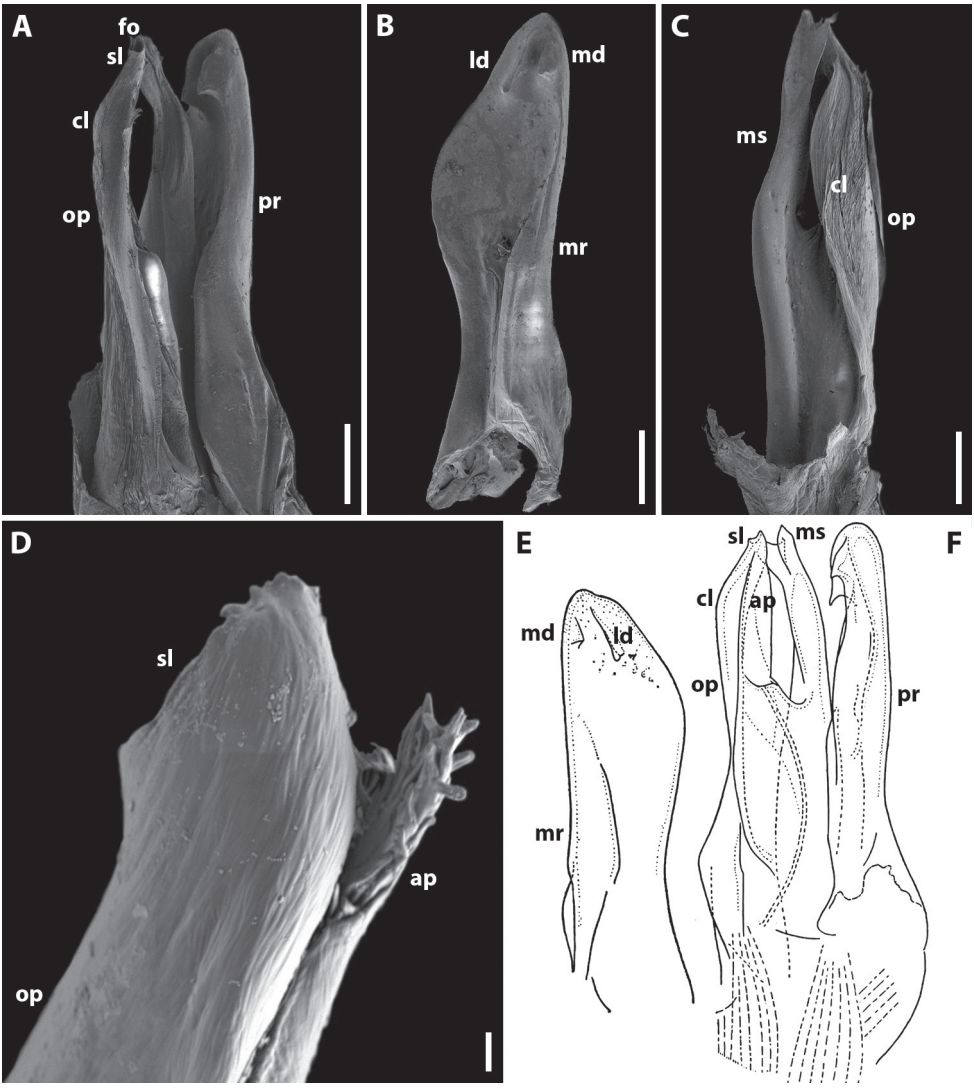


**Figure 7.** *Syrioiulus adsharicus* (Lohmander, 1936), ♂ from Adigeni, Georgia (ZMUM) (**A–D**) or holotype ♂, after Lohmander (1936) (**E, F**) **A, F** gonopod, mesal view **B, E** promere, caudal view **C** posterior gonopod, lateral view **D** end of solenomere, lateral view. Abbreviations: **ap** anterior process **cl** caudomesal lamella **fo** fovea **ld** lateral denticle **md** mesal denticle **mr** mesal ridge **ms** mesomeral process **op** opisthomere **pr** promere **sl** solenomere. Scale bars: 0.1 mm (**A–C**); 0.03 mm (**D**); not to scale (**E, F**).

**Male.** Mandibular stipites expanded, slightly swollen (Fig. 6A). Leg pair 1 small, unciform, telopodites curved anteromesad (as in most other Julidae), with a group of setae on each coxa and at base of telopodite (Fig. 6K). Leg pair 2 with pads on postfemur and tibia (Fig. 6L). Penes short, bifurcate. Ventral edge of male pleurotergum 7 with relatively wide and apically rounded lamellae bordering the gonopodal aperture (Fig. 6M).

Gonopods (Fig. 7) with anterior and posterior pair equal in height. Promere spoon-shaped, constricted in basal third; a mesal ridge along basal 2/3 extent; two apical denticles well-developed, mesal one vertical and with a weakly bifurcate apex, lateral one short, wide and rounded apically (Fig. 7B, E). Mesomeral process simple, flattened, ribbon-shaped, bifurcate (Fig. 7C, F). Opisthomere bipartite (Fig. 7D, C). Solenomere long, erect, with small denticles apically, bearing a fovea at apex; caudomesal lamella wide with a notched apical margin (Fig. 7A, C, F). Anterior process apically with small filament-shaped spines (Fig. 7D).

**Female.** First two leg pairs unmodified. Vulva elongated, covered with long setae (Fig. 15C). Operculum relatively low, deeply divided. Bursa asymmetric, lateral valve higher than mesal one. Median field of bursa narrow; emargination of median field narrow and elongated.

**Remark.** This species was originally described from Batumi, "Bortschacha" (Lohmander 1936). Our new record from near Adigeni is evidence of the species likely to be endemic to the southern part of the Colchidan biogeographic province, all within Georgia (Fig. 16).

### *Syrioiulus continentalis* (Attems, 1903)

Figs 1D, 8A, B, 9, 10, 15D, 16

*Pachyiulus* (*Dolichoiulus*) *continentalis* Attems, 1903: 147, 148, figs 82–84 (D).
*Amblyiulus continentalis*—Lohmander 1932b: 40, 41, figs 33–35 (D); 1936: 156 (R); Rakhmanov 1971: 1412 (R); 1972: 116 (R); Samedov et al. 1972: 1245; Lokšina and Golovatch 1979: 385 (M); Bababekova 1996: 90 (M).
*Syrioiulus continentalis*—Mauriès 1982: 441 (M); 1984: 43 (M); Vagalinski 2020: 89 (M).

**Material examined. Azerbaijan:** 3 ♂♂, 1 ♀ (ZMUM), Talysh Mts, Zuvand, Joni, 1500 m a.s.l., 28–29.V.1976, leg. V.G. Dolin; 1 ♂ (ZMUM), Lenkoran, Hyrcan forest, Khan Bulan River near Alexeevka, 22.IV.1985, leg. E.B. Kupriyanova; 7 ♂♂, 5 ♀♀, 2 juv. (ZMUM), Lenkoran, Hyrcan Nature Reserve, litter, 26.I.–4.II.1985, leg. A. Druk; 2 ♂♂, 4 ♀♀ (ZMUM), same locality, 21.IX.1987, leg. S. Zonstein; 2 ♂♂, 2 juv. (IZB); 1 ♂, 1 ♀, 1 juv. (SMNG), Lənkəran rayon, Hyrcan Nature Reserve, Daştatük 1.3 km Xanbulan Reservoir, *Parrotia* forest, diverse bushes, under leaves, 110 m a.s.l., 38.6747°N, 48.7622°E; 1 ♂ (IZB); 1 ♂ (SMNG), same locality, SW of Aşağı Apu, *Quercus* forest, within leaves and rotten wood, 180 m a.s.l., 38.6726°N, 48.7362°E, all leg. F. Walther, H. Reip, D. Antić; 3 ♂♂, 2 ♀♀, 1 juv. (IZB); 5 ♂♂, 3 ♀♀ (SMNG), Lerik rayon, Hyrcan Nature Reserve, road Lənkəran–Lerik at km 32, small side valley, forest of *Parrotia* with some *Quercus*, thick leaf layer, 400 m a.s.l., 38.7638°N, 48.5819°E; 1 juv. (IZB), Astara rayon, Hyrcan Nature Reserve, SW of Zünqüləş, beginning of a small valley, *Parrotia* and *Alnus* bushes, in leaves, 60 m a.s.l., 38.4493°N, 48.7623°E; 2 ♂♂, 1 juv. (IZB); 2 ♂♂, 1 ♀ (SMNG), same locality, end of small valley, steep slope, *Parrotia*, *Quercus*, *Acer* trees, under leaves and rotten tree


**Figure 8.** Live colouration of two *Syrioiulus* species from Hyrcan Nature Reserve, Azerbaijan **A, B** *S. continentalis* (Attems, 1903) **C, D** *S. taliscius* (Attems, 1927). Pictures by D.Ž. Antić, not taken to scale.

trunks, 130 m a.s.l., 38.4480°N, 48.7597°E, all leg. F. Walther, H. Reip, D. Antić; 2 ♂♂ (ZMUM), Azfilial, 100 m a.s.l., 31.V.–1.VI.1996; 1 ♂ (ZMUM), Apo below Bilasar, 350 m a.s.l., 8–9.VI.1996; 2 ♂♂, 1 ♀, 1 juv. (ZMUM), Astara Distr., Istisu ca. 8 km WSW of Astara, *Quercus*, *Acer*, *Carpinus*, etc. forest, 10–30 m a.s.l., litter, under stones and bark, 10.X.1983; 2 ♀♀ (ZMUM), Istisu ca. 8 km SW of Masally, *Quercus*, *Acer*, *Carpinus* etc. forest, 80–140 m a.s.l., under bark and stones, 19–20.X.1983; 2 ♀♀ (ZMUM), Istisu W of Astara, 100 m a.s.l., 2–6.VI.1996, all leg. S. Golovatch.

**Diagnosis.** Differs from all congeners by the following combination of somatic and gonopodal characters. Head with frontal setae. Collum and each metazona of following body rings with a whorl of long setae at caudal margin. Eyes present. Solenomere with a group of small spines on top. Anterior process of opisthomere subtriangular apically. This species is clearly distinguished in the field from all other millipedes by its characteristic greyish yellow colouration with a yellow stripe dorsally, and its particularly strong odour clearly resembling that of *Pachyiulus krivolutskyi* from the western Caucasus (= Colchis).

**Redescription.** Length of adults 28–45 mm (♂♂) or 26–46 mm (♀♀), width 2.0–2.3 mm (♂♂) or 2.2–2.7 mm (♀♀). Number of body rings in adults, 46–66+1–2+T (♂♂) or 49–66+1–2+T (♀♀). Body subcylindrical, metazonae from greyish yellow to yellow, prozonae light yellow (Figs 1D, 8A, B); live specimens dorsally with a

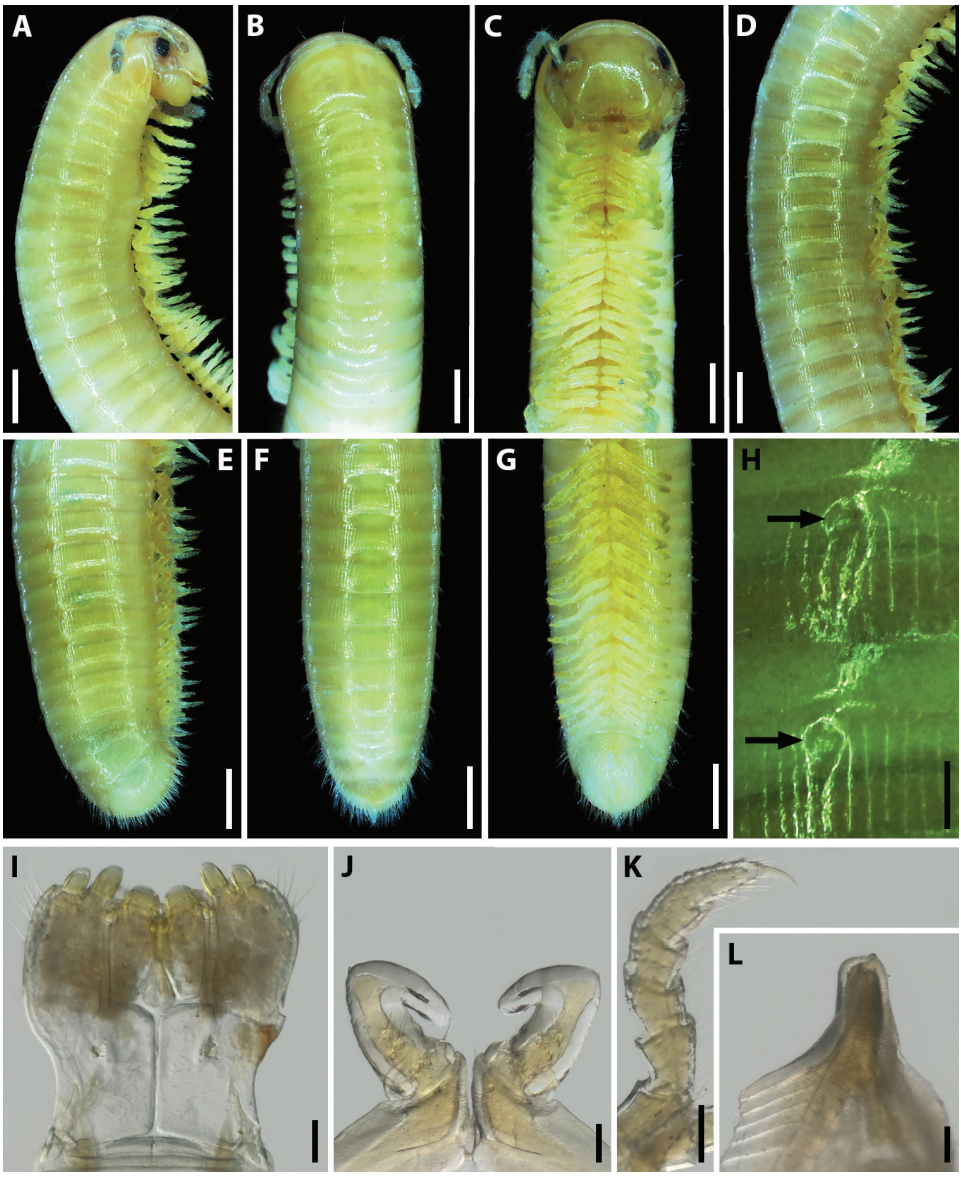


**Figure 9.** *Syrioiulus continentalis* (Attems, 1903), ♂ from Istisu, Azerbaijan (ZMUM) **A–C** anterior part of body, lateral, dorsal and ventral views, respectively **D** midbody part, lateral view **E–G** posterior part of body, lateral, dorsal and ventral views, respectively **H** ozopores on midbody rings, lateral view **I** gnathochilarium, ventral view **J** leg pair 1, caudal view **K** leg 2, caudal view **L** ventral edge of pleurotergum 7, lateral view. Scale bars: 1.0 mm (**A–G**); 0.1 mm (**H–L**).

darker, vivid yellow stripe (Fig. 8B). Head, collum and telson slightly lighter than other body rings (Fig. 8A, B). Antennae grey, mouthparts and legs light yellow (Fig. 9A–G). Eyes present, black, oval, each composed of 19–23 ommatidia (Fig. 9A, C). Striations

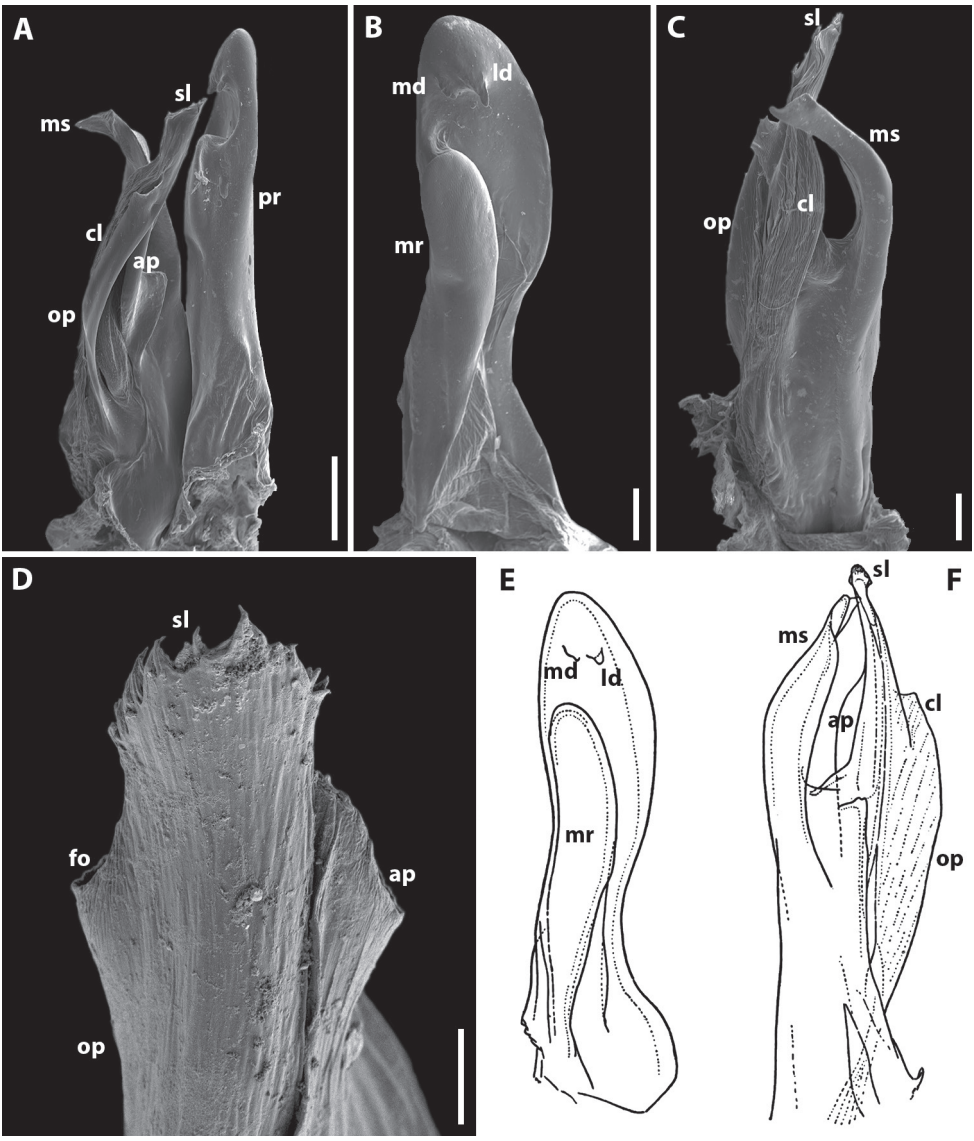


**Figure 10.** *Syrioiulus continentalis* (Attems, 1903), ♂ from Hyrcan Nature Reserve (**A–C**) (SMNG), from Istisu (**D**) (ZMUM) or after Lohmander (1932b) (**E, F**) **A** gonopod, mesal view **B, E** promere, caudal view **C, F** posterior gonopod, lateral view **D** end of solenomere, lateral view. Abbreviations: **ap** anterior process **cl** caudomesal lamella **fo** fovea **ld** lateral denticle **md** mesal denticle **mr** mesal ridge **ms** mesomeral process **op** opisthomere **pr** promere **sl** solenomere. Scale bars: 0.1 mm (**A–C**); 0.01 mm (**D**); not to scale (**E, F**).

on metazonae deep, not reaching the caudal margin, 28–32 striae per quarter of metazonal surface, i.e., between dorsal axial line and ozopore (Fig. 9D). Ozopores large, lying behind suture without touching it (Fig. 9H).

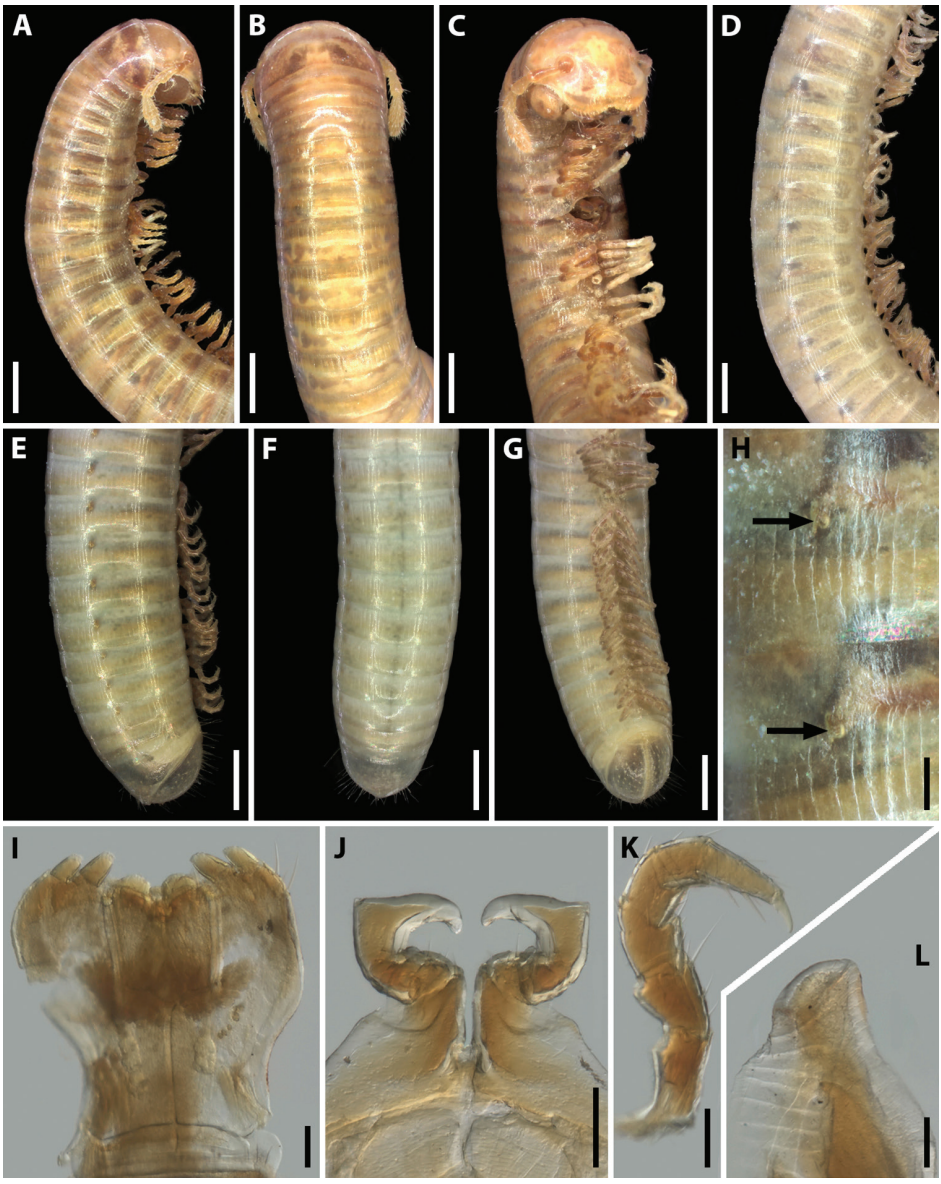


**Figure 11.** *Syrioiulus taliscius* (Attems, 1927), ♂ from Avrora, Azerbaijan (ZMUM) **A–C** anterior part of body, lateral, dorsal and ventral views, respectively **D** midbody part, lateral view **E–G** posterior part of body, lateral, dorsal and ventral views, respectively **H** ozopores on midbody rings, lateral view **I** gnathochilarium, ventral view **J** leg pair 1, caudal view **K** leg 2, caudal view **L** ventral edge of pleurotergum 7, lateral view. Scale bars: 0.5 mm (**A–G**); 0.1 mm (**H–L**).

Antennae relatively long, in situ reaching segment 3. Head with 1+1 frontal, 8+8–9+9 labral and 2+2–4+4 supralabral setae (Fig. 9A–C). Gnathochilarium with three long setae on each lamella lingualis, groups of several small setae in median part

of stipites and six or seven long setae at anterolateral margin (Fig. 9I). Collum and each following metazona with a whorl of long and thick setae at posterior margin (Fig. 9A–F). Epiproct undeveloped (Fig. 9E, F). Hypoproct subtriangular, with long setae (Fig. 9G). Telson and anal valves densely setose, setae being long.

**Male.** Mandibular stipites expanded, with swollen lobes (Fig. 9A). Leg pair 1 small, unciform, telopodites directed anteromesad, with a group of long setae on each coxa; telopodite setose in basal part (Fig. 9J). Leg pair 2 with pads on postfemur and tibia (Fig. 9K). Penes short, bifurcate. Ventral edge of male pleurotergum 7 with narrow elongated lamellae bordering the gonopodal aperture (Fig. 9L).

Gonopods (Fig. 10) with anterior (promere) part higher than posterior (opisthomere) one. Promere spoon-shaped, constricted in basal third; mesal ridge wide along 2/3 extent; with denticles in apical part: mesal denticle small and broadly rounded, lateral one well-expressed and long (Fig. 10B, E). Mesomeral process simple, slightly curved, flattened apically (Fig. 10A, C, F). Opisthomere bipartite (Fig. 10D). Solenomere elongated, with an apical membranous lobe, subtriangular at apex, with a fovea and a group of small spines on top; caudomesal lamella wide (Fig. 10A, C, D, F). Anterior process of opisthomere subtriangular apically (Fig. 10D).

**Female.** First two leg pairs unmodified. Operculum of vulva without setae on caudal surface, apical margin relatively flat (Fig. 15D). Bursa subsymmetrical, lateral valve slightly larger than mesal one. Each valve with two rows of long setae. Median field of bursa narrow; emargination of median field suboval.

**Remarks.** Probably one of the most common and apparently the largest species of the genus. The unusually strong odour and the chemical composition of the repugnatorial secretion are similar to those of *Pachyiulus krivolutskyi* (Makarov et al., pers. obs.). This species inhabits various deciduous forests in Azerbaijan, also occurring in northern Iran (Lohmander 1932b), endemic to the Hyrcanian biogeographic province (Fig. 16).

***Syrioiulus taliscius* (Attems, 1927)**
Figs 1E, 8C, D, 11, 12, 15E, 16

*Amblyiulus taliscius* Attems, 1927: 243, 244, figs 336–338 (D).
*Amblyiulus taliscius*—Lohmander 1932b: 182 (M); 1936: 170 (M); Rakhmanov 1972: 116 (R); Lokšina and Golovatch 1979: 385 (M); Bababekova 1996: 90 (M).
*Syrioiulus taliscius*—Mauriès 1982: 441 (M); 1984: 43 (M); Vagalinski 2020: 92 (M).

**Material examined. Azerbaijan:** 4 ♂♂, 14 ♀♀, 1 juv. (ZMUM), Talysh, Joni, 1500 m a.s.l., 28–29.V.1976, leg. V.G. Dolin; 2 ♂♂ (ZMUM), Lenkoran, Hyrcan Nature Reserve, Telman, 28.IV.1984; 1 ♂, 1 ♀ (ZMUM), same locality, Gaftoni, 9.V.1984, all leg. H. Aliev; 1 ♀ (ZMUM), Hyrcan forest, Khan Bulan River near Alexeevka, 22.IV.1985, leg. E.B. Kupriyanova; 3 ♂♂, 12 ♀♀ (ZMUM), same locality, Avrora, Moscow-Forest, 50 m a.s.l., 1.VI.1996; 3 ♂♂, 3 ♀♀, 1 juv. (ZMUM), same locality, Apo below Bilasar, 350 m a.s.l., 8–9.VI.1996, all leg. S. Golovatch; 1 ♂ (SMNG),

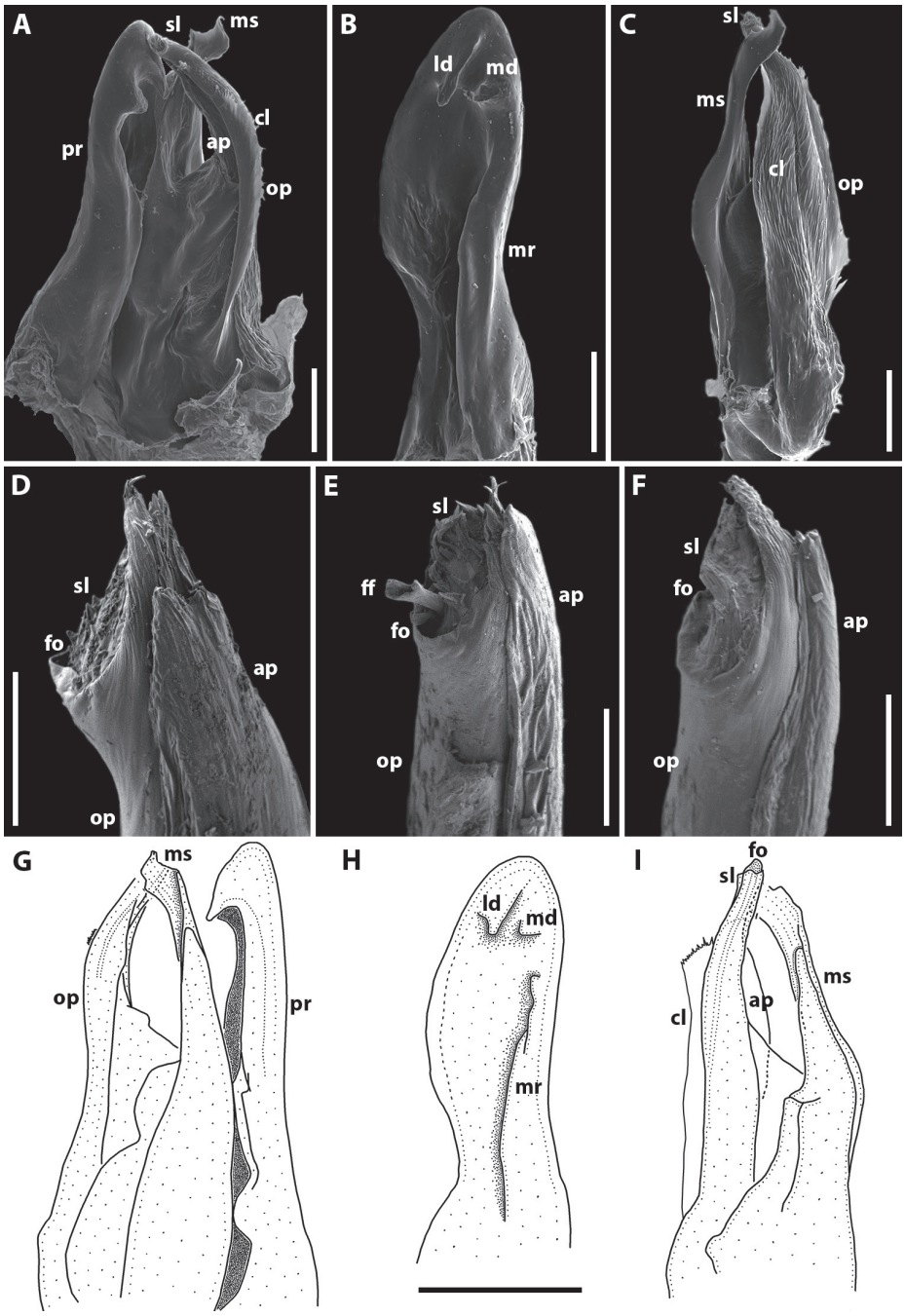


**Figure 12.** *Syrioiulus taliscius* (Attems, 1927), ♂ from Hyrcan Nature Reserve (**A–C**) (SMNG), from Avrora (**D, G, H**) (ZMUM) or from Apo, Azerbaijan (**E, F**) (ZMUM) **A, G** gonopod, mesal and lateral views, respectively **B, H** promere, caudal view **C, I** posterior gonopod, caudolateral and mesal views, respectively **D–F** end of solenomere, mesal views. Abbreviations: **ap** anterior process **cl** caudomesal lamella **fo** fovea **ld** lateral denticle **md** mesal denticle **mr** mesal ridge **ms** mesomeral process **op** opisthomere **pr** promere **sl** solenomere. Scale bars: 0.1 mm (**A–C**); 0.02 mm (**D–F**); 0.2 mm (**G–I**).

Lənkəran rayon, Siyablı, *Parrotia*, *Zelkova*, *Quercus* coppice, steep slope, 110 m a.s.l., 38.7170°N, 48.7253°E; 1 ♂ (IZB), Lerik rayon, Hyrcan Nature Reserve, road Lənkəran–Lerik at km 32, small side valley, forest of *Parrotia* with some *Quercus*, thick leaf litter, 400 m a.s.l., 38.7638°N, 48.5819°E; 7 ♀♀ (IZB), 7 ♀♀ (SMNG), Astara rayon, Hyrcan Nature Reserve, SW of Zünqüləş, end of small valley, steep slope, *Parrotia*, *Quercus*, *Acer* trees, under leaves and rotten tree trunks, 130 m a.s.l., 38.4480°N, 48.7597°E; 2 ♂♂, 1 ♀, 1 juv. (IZB); 2 ♂♂, 2 ♀♀, 1 juv. (SMNG), Lənkəran rayon, Hyrcan Nature Reserve, Daştatük 1.3 km Xanbulan Reservoir, *Parrotia* forest, divers bushes, under leaves, 110 m a.s.l., 38.6747°N, 48.7622°E; 3 ♂♂, 2 ♀♀, 1 juv. (IZB); 5 ♂♂ (1 SEM), 3 ♀♀ (1 SEM), 1 juv. (SMNG) Lənkəran rayon, Hyrcan Nature Reserve, SW of Aşağı Apu, *Quercus* forest, within leaves and rotten wood, 180 m a.s.l., 38.6726°N, 48.7362°E, all leg. F. Walther, H. Reip, D. Antić; 1 ♂ without gonopods (ZMUM), Shemakha Distr., farm Guseinzade, foothills, *Vitis*, summer 1982, leg. A. Ismailov; 1 ♀ (ZMUM), Zakataly Distr., Geyam, cornfield, 17.IV.1986, leg.?; 7 ♂♂, 5 ♀♀ (ZMUM), Baku, City parks, 18–21.V.1981; 1 ♂ (ZMUM), Belokani near Zakatali, 600 m a.s.l., village garden, 24.V.1981; 1 ♀ (ZMUM), above Akhsu 120 km W Baku, 900 m a.s.l., *Quercus* shrub, 22.V.1981, all leg. S. Golovatch and J. Martens; 1 ♀ (ZMUM), ca. 14 km W of Ismailly, Galyhjakh, under bark, 1.V.1987; 1 ♀ (ZMUM), Altyagach, 1050–1100 m a.s.l., *Quercus*, *Fagus*, *Carpinus*, etc. forest, litter, 20 and 26.IV.1987, all leg. S.Golovatch and K. Eskov; 3 ♂♂, 5 ♀♀, 1 juv. (IZB); 3 ♂♂, 5 ♀♀ (SMNG), İsmayıllı rayon, Topçu 7.8 km towards Vəndam, flat area with old *Fagus* forest, under leaves and dead wood, 630 m a.s.l., 40.9193°N, 48.0027°E; 1 ♂ (SMNG), İsmayıllı rayon, Xanəgah 2 rkm towards İsmayıllı, flat area with old *Fagus* forest, with channels, under leaves, 650 m a.s.l., 40.8233°N, 48.1518°E; 1 ♀ (SMNG), İsmayıllı rayon, S of Zərgəran, slope with *Corylus*, *Clematis* and some *Prunus* trees, stone heaps overgrown by moss, mainly in thick leaf litter and under stones, 880 m a.s.l., 40.7310°N, 48.3680°E, all leg. F. Walther, H. Reip, D. Antić.

**Diagnosis.** Differs from all congeners by the following combination of somatic and gonopodal characters. Head without frontal setae. Collum and metazonae of following body rings without setae. Eyes absent. Solenomere in apical part with a group of small spines. Anterior process of opisthomere subtriangular apically.

**Redescription.** Length of adults 26–33 mm (♂♂) or 26–34 mm (♀♀), width 1.2–1.3 mm (♂♂) or 1.2–1.4 mm (♀♀). Number of body rings in adults, 50–65+1–2+T (♂♂) or 49–70+1–2+T (♀♀). Body subcylindrical (typical of Julidae), live specimens with brownish grey pro- and metazonae (Fig. 8C, D), after storage in alcohol prozonae grey, metazonae yellow (Fig. 1E). Head, collum, a few postcollum rings, last body rings, telson and anal valves yellow (Figs 1E, 8C, D). Antennae, mouthparts, and legs light yellow (Fig. 11A–G). Eyes absent. Striations of metazonae deep, not reaching the caudal margin, 23–25 striae per quarter of metazonital surface, i.e., that between dorsal axial line and ozopore (Fig. 11D). Ozopores small, lying behind suture without touching it (Fig. 11H).

Antennae relatively long, in situ reaching segment 3. Head without frontal setae, 9+9–12+12 labral and 2+2 supralabral setae (Fig. 11A–C). Collum and metazonae without setae (Fig. 11A–G). Gnathochilarium with 3–4 long setae on each lamella

lingualis, stipites with a medial curved row of 4–5 thick setae and three long setae at anterolateral margin (Fig. 11I). Epiproct undeveloped (Fig. 11E, F). Hypoproct rounded, with several setae (Fig. 11G). Telson covered with long setae, anal valves densely setose.

**Male.** Mandibular stipites unmodified (Fig. 11A). Leg pair 1 small, unciform, telopodites directed anteromesad (as in most Julidae), with long setae on each coxa and in basal part of telopodite (Fig. 11J). Leg pair 2 with pads on postfemur and tibia (Fig. 11K). Penes short, bifurcate. Ventral edge of male pleurotergum 7 with wide curved lamellae bordering the gonopodal aperture (Fig. 11L).

Gonopods (Fig. 12) with anterior and posterior parts both equal in height. Promere spoon-shaped, constricted in basal third; mesal ridge relatively narrow along 2/3 extent; with denticles in apical part: mesal denticle small and broadly rounded, lateral one well-expressed and long (Fig. 12B, H). Mesomeral process simple, slightly curved, with a wide subquadrate lamella apically (Fig. 12A, C, G, I). Opisthomere bipartite. Solenomere elongated, with a caudomesal, notched, membranous lobe, in apical part with a fovea and a group of small spines (Fig. 12A, C–F). Fovea may be equipped with a filiform process (Fig. 12E). Anterior process subtriangular apically.

**Female.** First two leg pairs unmodified. Operculum of vulva without setae on caudal surface, apical margin poorly divided (Fig. 15E). Bursa mostly symmetric, lateral valve slightly larger than mesal one. Each valve with two rows of long setae. Median field of bursa narrow; emargination of median field suboval.

**Remarks.** This species was described from the Talysh Mts, Lenkoran, Azerbaijan (Attems 1927). In the Caucasus, this is probably one of the most common and widespread congeners. Like *S. continentalis*, it inhabits various deciduous forests, but it can only be considered as subendemic to the Hyrcanian biogeographic province (Fig. 16).

### *Syrioiulus armeniacus* sp. nov.

http://zoobank.org/64FB28BD-A6C0-43AD-A61E-647AA4964982
Figs 1F, 13, 14, 15F, 16

**Material examined.** ***Holotype*** ♂ (ZMUM), **Armenia**, Kafan Distr., Shikahoh Nature Reserve, Shikahoh, 900–950 m a.s.l., *Quercus*, *Fagus*, *Carpinus* forest by spring, litter, logs and under stones, 28.IV.1983, leg. S. Golovatch. ***Paratypes*:** 14 ♂♂, 24 ♀♀ (ZMUM), same collection data as holotype.

**Non-type material. Armenia:** 4 ♂♂, 3 ♀♀ (ZMUM), Shikahoh Nature Reserve, Nerkin And, old *Platanus* stand along river, litter, in rotten wood, under stones, 30.IV.1983; 1 ♂, 1 ♀ (ZMUM), near Kajaran, Megri Mt. Ridge, N of Tashtun Pass, 2000 m a.s.l., *Quercus* forest on steep slope, litter, logs, 27.IV.1983; 5 ♂♂, 3 ♀♀, 2 juv. (ZMUM), Megri Distr., SSE of Lichk, Megri River valley, *Quercus* forest, litter, under stones and in rotten wood, 25.IV.1983; 2 ♂♂, 16 ♀♀, 2 juv. (ZMUM), above Kuris, 1500 m a.s.l., *Quercus* and *Carpinus* forest, litter, under bark and stones along spring, 26.IV.1983; 12 ♂♂, 11 ♀♀, 1 juv. (ZMUM), ca. 4 km NNW of Megri,

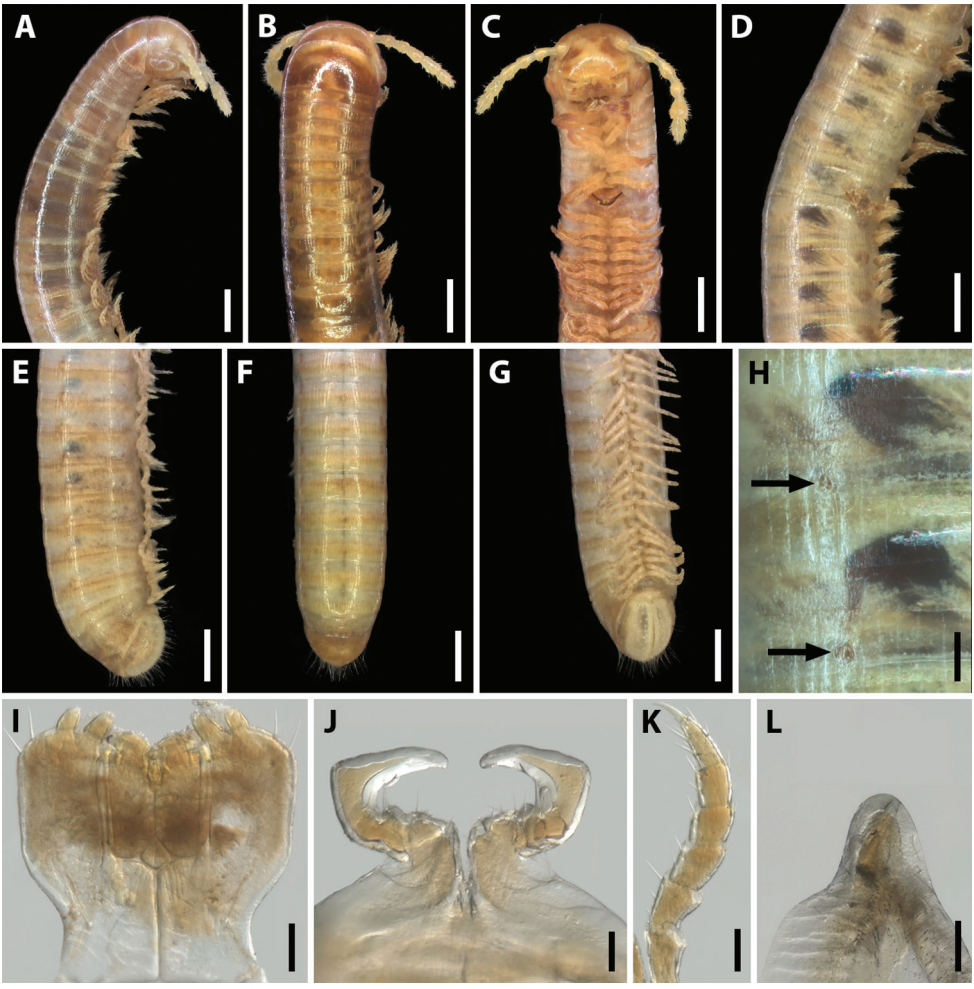


**Figure 13.** *Syrioiulus armeniacus* sp. nov., paratype ♂ from Shikahoh, Armenia (ZMUM) **A–C** anterior part of body, lateral, dorsal and ventral views, respectively **D** midbody part, lateral view **E–G** posterior part of body, lateral, dorsal and ventral views, respectively **H** ozopores on midbody rings, lateral view **I** gnathochilarium, ventral view **J** leg pair 1, caudal view **K** leg 2, caudal view **L** ventral edge of pleurotergum 7, lateral view. Scale bars: 0.5 mm (**A–G**); 0.1 mm (**H–L**).

Legvaz, *Juglans* and *Quercus* shrub with *Paliurus* and *Rosa*, litter and under stones, 1000 m a.s.l., 24–25.IV.1983; 5 ♂♂, 2 ♀♀ (ZMUM), 6 km N of Shvanidzor, sparse *Quercus* forest, 1200–1300 m a.s.l., litter, under stones and bark, 24.IV.1983; 5 ♂♂, 6 ♀♀, 2 juv. (ZMUM), environs of Megri, xeriphytous bare canyon, under stones, sparse *Juniperus* and *Paliurus*, ca. 1000 m a.s.l., 24.IV.1983, all leg. S. Golovatch; 2 ♀♀ (ZMUM), Odzun W of Alaverdi, 1500–1550 m a.s.l., *Quercus*, *Fagus*, *Carpinus* etc. forest, litter and under stones with ants, 23–24.V.1987, leg. S. Golovatch and K. Eskov; 1 ♀ (ZMUM), Nurkus, 7.VII.1985, leg. V.A. Zakharyan.

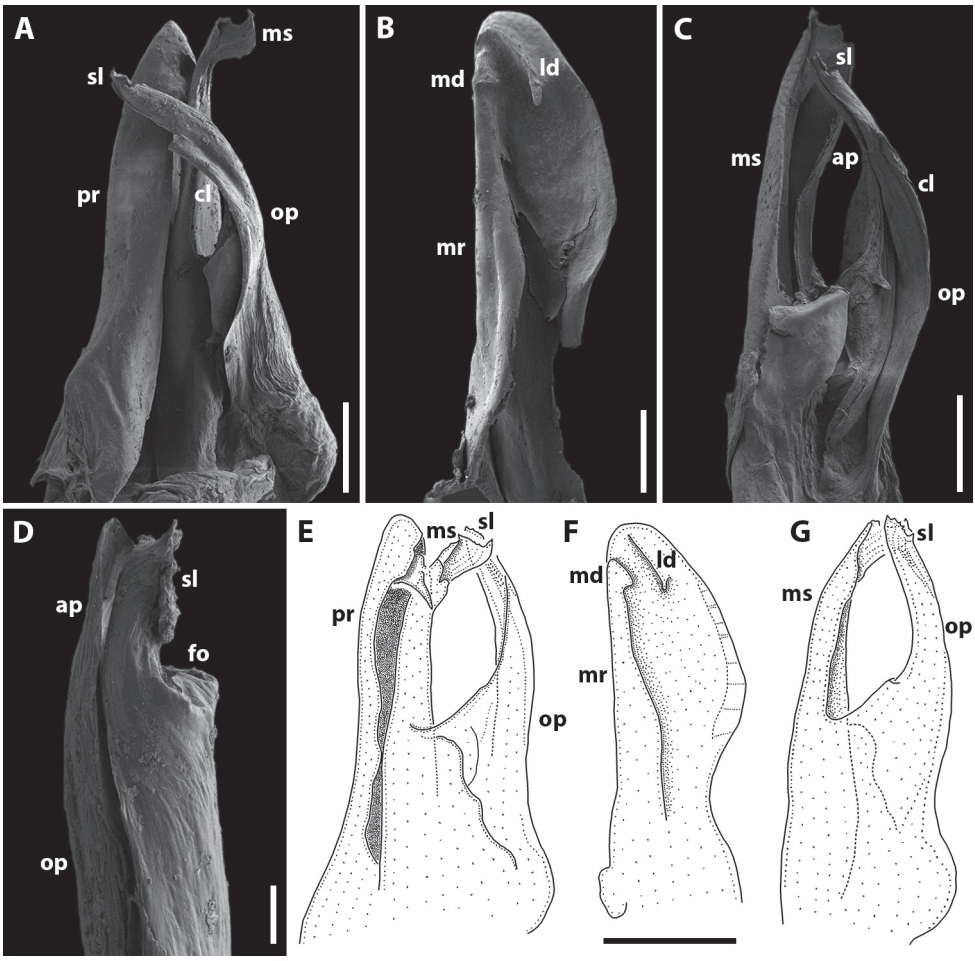


**Figure 14.** *Syrioiulus armeniacus* sp. nov., paratype ♂ from Shikahoh, Armenia (ZMUM) **A, E** gonopod, mesocaudal and mesal views, respectively **B, E** promere, caudal views **C, G** posterior gonopod, mesal views **D** end of solenomere, mesal view. Abbreviations: **ap** anterior process **cl** caudomesal lamella **fo** fovea **ld** lateral denticle **md** mesal denticle **mr** mesal ridge **ms** mesomeral process **op** opisthomere **pr** promere **sl** solenomere. Scale bars: 0.1 mm (**A–C**); 0.01 mm (**D**); 0.2 mm (**E–G**).

**Diagnosis.** This new species belongs to the genus *Syrioiulus* because of the presence of only two apices on the opisthomere. Differs from all regional congeners by the following combination of somatic and gonopodal characters. Head with frontal setae. Collum and metazonae of following body rings without setae. Eyes absent. Solenomere with a pointed process apically. Anterior process rounded on top.

**Name.** The new species is named after its terra typica; adjective.

**Description.** Holotype: length 25 mm, width 1.2 mm, number of body rings 50+2+T. Paratypes and non-type material: length 17–33 mm, width 1.2–1.6 mm, number of body rings, 50–68+1–2+T (♂♂); or length 20–29 mm, width 1.2–1.6 mm,

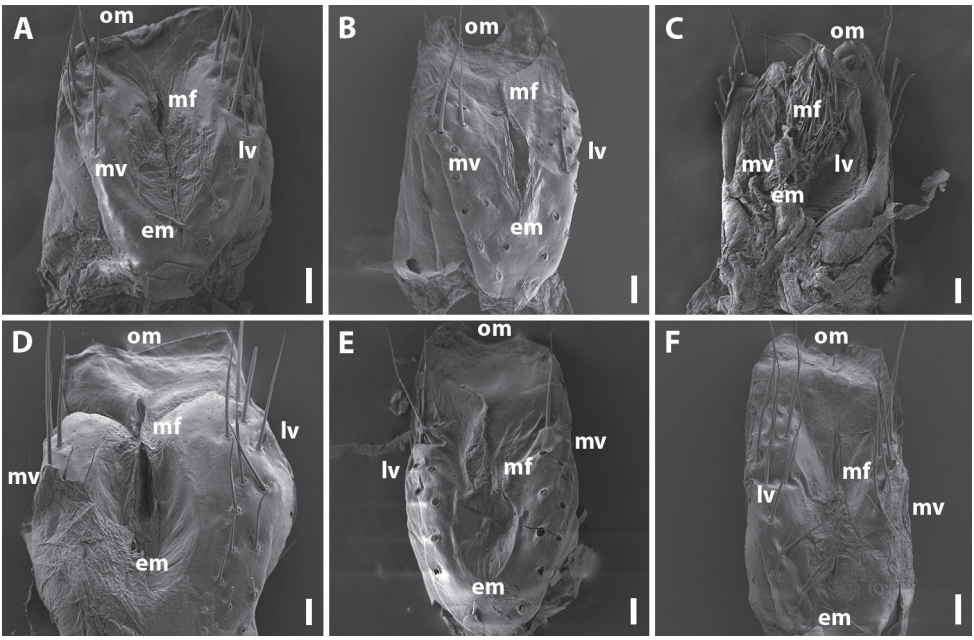


**Figure 15.** Vulvae of *Amblyiulus* and *Syrioiulus* species from the Caucasus, caudal views **A** *A. georgicus* Lohmander, 1932 from Shnokh, Armenia (ZMUM) **B** *A. hirtus* sp. nov., paratype from Bash-Layski, Azerbaijan (ZMUM) **C** *S. adsharicus* (Lohmander, 1936) from Adigeni, Georgia (ZMUM) **D** *S. continentalis* (Attems, 1903) from Istisu, Azerbaijan (ZMUM) **E** *S. taliscius* (Attems, 1927) from Avrora, Azerbaijan (ZMUM) **F** *S. armeniacus* sp. nov., paratype from Shikahoh, Armenia (ZMUM). Abbreviations: **em** emargination of median field **lv** lateral valve **mf** median field **mv** median valve **op** operculum. Scale bars: 0.03 mm.

number of body rings, 46–55+2–3+T (♀♀). Body subcylindrical, metazonae brownish yellow, prozonae brownish grey (Figs 1F, 13A–G). Head, collum and telson slightly lighter than body rings (Fig. 1F). Antennae, mouthparts, and legs yellow (Fig. 13A, C–E, G). Eyes absent. Metazonae with weakly developed, dense, and regular striations, 20–23 striae per quarter of metazonital surface, i.e., that between dorsal axial line and ozopore (Fig. 13D). Ozopores relatively large, situated between striae in touch with one of them, lying behind suture without touching it (Fig. 13H).

Antennae relatively long, in situ reaching segment 3. Head with 1+1 frontal, 9+9–10+10 labral and 2+2 supralabral setae (Fig. 13A–C). Gnathochilarium with three thick setae on each lamella lingualis; stipites with a group of 6–9 setae in medial part and three long setae in anterolateral part (Fig. 13I). Collum and metazonae without setae (Fig. 13A, B). Epiproct poorly developed, triangular, with several long setae (Fig. 13E, F). Hypoproct subtriangular, covered with long setae (Fig. 13G). Telson and anal valves densely setose.

**Male.** Mandibular stipites modified, slightly swollen in distal part (Fig. 13A). Leg pair 1 small, unciform, telopodites directed anteromesad (typical of Julidae), with a group of setae on coxa and telopodite (Fig. 13J). Leg pair 2 with small pads on

postfemur and tibia (Fig. 13K). Penes short, bifurcate. Ventral edge of male pleurotergum 7 with wide curved lamellae bordering the gonopodal aperture (Fig. 13L).

Gonopods (Fig. 14) with anterior and posterior parts both equal in height. Promere spoon-shaped, bowl being relatively wide, constricted in basal third; mesal ridge well-developed all along, with a small mesal denticle in apical part; lateral denticle large, rounded on top (Fig. 14B, F). Mesomeral process simple, flattened, ribbon-shaped, widened apically, with a group of small teeth (Fig. 14A, C, E, G). Opisthomere bipartite. Solenomere long, slightly curved; its apical part with a fovea and a pointed process (Fig. 14A, C, D, G). Anterior process as high as solenomere, rounded at tip (Fig. 14D).

**Female.** First two leg pairs unmodified. Vulva rounded, operculum higher than bursa (Fig. 15F). Operculum slightly divided at apical margin. Bursa asymmetric, lateral valve higher than mesal one. Each valve with two rows of long setae. Median field of bursa narrow; emargination of median field elongated and suboval.

**Remark.** This species seems to be endemic to the Caucasus Minor within Armenia, but most likely it also occurs in the adjacent parts of eastern Azerbaijan and northwestern Iran (Fig. 16).

**Pachyiulini gen. sp. 1**
Fig. 16

**Material examined.** 1 ♀ (ZMUM) **Russia**, Stavropol Area, Kochubeevsky Distr., Nevinnomyssk, mouth of Bolshoy Zelenchuk River, floodplain forest, 17.IV.2016, leg. R.B. Zuev, A.V. Aulova.

**Brief description.** Body grey, head and collum dark yellow, antennae and legs yellow. The following somatic characteristics seem to be the most important: absence of eyes, presence of frontal setae, presence of caudal whorls of setae on metazonae, absence of an epiproct, and setose anal valves.

**Remark.** Unfortunately, the only female does not allow a closer generic allocation.

**Pachyiulini gen. sp. 2**
Fig. 16

**Material examined. Georgia:** 1 ♀ (ZMUM), Ajaria, Kintrish Nature Reserve, Zeraboseli, 450–600 m a.s.l., 1–3.VI.1981, leg. S. Golovatch, J. Martens; 1 ♀ (ZMUM), same locality, 800 m a.s.l., *Rhododendron* thicket, litter, 13.X.1981, leg. S. Golovatch; 1 ♀ (ZMUM), same locality, valley of Khekpara River, 12.X.1984, leg. E. Kvavadze.

**Brief description.** Body greyish yellow. Head, collum, a few postcollum rings and telson slightly lighter than other body rings. Ommatidia and frontal setae absent. Collum and each metazona of following rings with a whorl of long setae at posterior margin. Epiproct undeveloped. Anal valves densely setose.

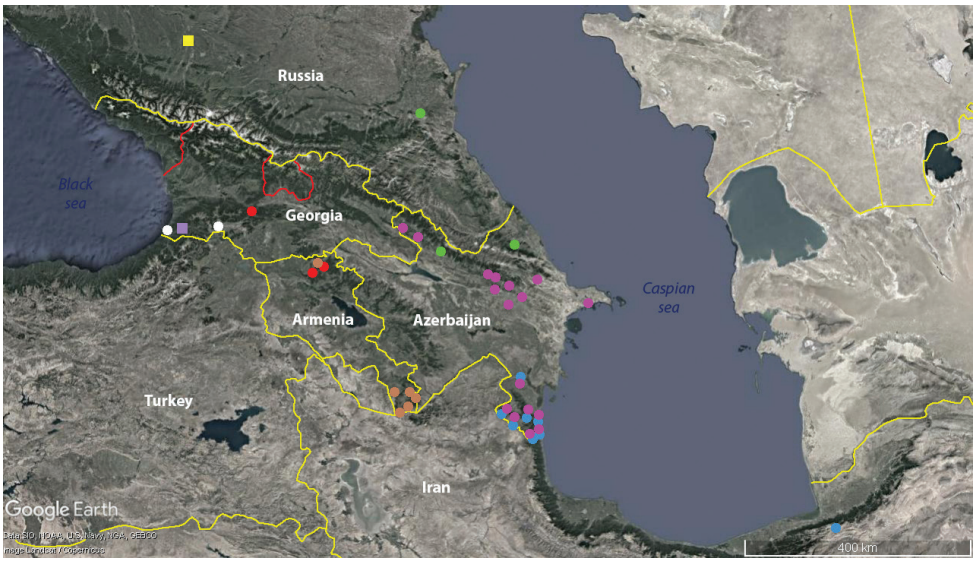


**Figure 16.** Distributions of *Amblyiulus* and *Syrioiulus* species in the Caucasus: red circle *A. georgicus* Lohmander, 1932; green circle *A. hirtus* sp. nov.; white circle *S. adsharicus* (Lohmander, 1936); blue circle *S. continentalis* (Attems, 1903); pink circle *S. taliscius* (Attems, 1927); brown circle *S. armeniacus* sp. nov.; yellow square Pachyiulini gen. sp. 1; purple square Pachyiulini gen. sp. 2.

**Remarks.** These specimens differ from *Syrioiulus adsharicus* in the absence of frontal setae and ommatidia. The absence of males makes it impossible to definitively identify the above samples. At least the taxonomic significance of frontal setae must not be overestimated, as they may be present or absent even within the same species, e.g., *S. aharonii* (see Golovatch 2018).

Since the two unidentified species may well prove to represent *Amblyiulus* or *Syrioiulus*, we map their records in Figure 16, but omit them from the key below.

## Key to *Amblyiulus* and *Syrioiulus* species known to occur in the Caucasus (based on males)

1 Opisthomere of gonopod with a rod (Fig. 3D, F, G, I) ... (genus *Amblyiulus*) **2**
– Opisthomere of gonopod without rod ..... (genus *Syrioiulus*) **3**
2 Head without frontal setae, collum and metazonae of body rings without setae (Fig. 2A–C). Promere relatively wide, with two apical denticles (Fig. 3B, E) ..... ***A. georgicus***
– Head with 1+1 frontal setae, collum and metazonae of body rings with whorls of setae at caudal margin (Fig. 4A–C). Promere narrow, without apical denticles (Fig. 5B, H)..... ***A. hirtus* sp. nov.**
3 Eyes present ..... **4**
– Eyes absent ..... **5**

4 Larger: width > 2.0 mm. Eyes well-developed, black, oval, each composed of 19–23 ommatidia (Fig. 9A) ..... ***S. continentalis***
– Smaller: width < 1.3 mm. Eyes present, but very small and unpigmented, each composed of 3–7 ommatidia (Fig. 6B) ..... ***S. adsharicus***
5 Head without frontal setae (Fig. 11A–C) ..... ***S. taliscius***
– Head with 1+1 frontal setae (Fig. 13A–C) ..... ***S. armeniacus* sp. nov.**

## Discussion

Two allopatric species of *Amblyiulus*, both likely endemic, are found to populate the Caucasus. *Amblyiulus georgicus* inhabits western and central Transcaucasia, while *A. hirtus* sp. nov. seems to be confined to northeastern Transcaucasia and the eastern Caucasus, i.e., occurring on both macro slopes of the Caucasus Major (Fig. 16).

The genus *Syrioiulus* is more diverse and widespread, but presently it seems to be restricted to Transcaucasia. Thus, *S. adsharicus* has a rather narrow distribution in the southwestern parts of the Colchidan biogeographic province. Two most widespread species, *S. continentalis* and *S. taliscius*, are often sympatric to even syntopic within the Hyrcanian biogeographic province, but the latter species also occurs in the Caucasus Minor and the eastern part of the Caucasus Major. *Syrioiulus armeniacus* sp. nov. inhabits the Caucasus Minor within southern and central Transcaucasia (Fig. 16).

As regards the vertical distributions, most species of *Amblyiulus* and *Syrioiulus* in the Caucasus are confined to montane forests, as are probably all *Syrioiulus* species known from Hyrcania, including the Iranian *S. astrabadensis* (Lohmander, 1932b), *S. discolor* (Lohmander, 1932b), *S. incarnatus* (Lohmander, 1932b), *S. lohmanderi* Vagalinski, 2020, *S. persicus* (Golovatch, 1983) and *S. zarudnyi* (Lohmander, 1932b) (Enghoff and Moravvej 2005; Vagalinski 2020). Within the Republic of Azerbaijan, however, *S. taliscius* inhabits not only lowland to foothill woodlands (50–1100 m a.s.l.), but also drier steppe- or bush-clad slopes, being inclined to synanthropisation as well (parks in Baku City). The same generally applies to both *S. continentalis* and *S. armeniacus* sp. nov., as they also populate xerophytic environments. *Amblyiulus hirtus* sp. nov. has been encountered in mid-montane deciduous forests, as well as subalpine and alpine meadows up to 2550 m a.s.l.

Only two species of *Syrioiulus*, *S. continentalis* and *S. taliscius*, are endemic or subendemic, respectively, to the Hyrcanian biogeographic province within the Republic of Azerbaijan and Iran, while the remaining *Amblyiulus* and *Syrioiulus* spp., however provisionally, are formally strictly endemic to the Caucasus sensu lato, including Hyrcania (Fig. 16). Generally, the problem concerning the origins of the *Amblyiulus* and *Syrioiulus* species could be approached through analysing the distribution areas of both these genera. However, because their species compositions are far from settled, including new congeners and records certainly ahead, their exact ranges cannot be outlined at the moment. Based on the highest species diversity estimates, one of the

main centres of *Amblyiulus* and *Syrioiulus* speciation could have lain in the Middle East, whence members of both genera might have reached the Caucasus sensu lato. The roles that both Colchis and, especially, Hyrcania, two major, relictual, meso- to hygrophilous biogeographic provinces of, and refugia in, the region concerned, could have played in the evolution and secondary speciation seem paramount. It is hardly random that most pachyiuline species in the Caucasus are encountered in the Caucasus Minor, the immediate northern peninsular continuation of Asia Minor.

Both unidentified species seem to be endemic to the Caucasus, with Pachyiulini gen. sp. 1 being confined to Ciscaucasia, and Pachyiulini gen. sp. 2 to deciduous forests in southern Colchis, occurring sympatrically with *Syrioiulus adsharicus* (Fig. 16).

The above picture is definitely very far from final, but it agrees well with the biogeography of the Caucasus (e.g., Abdurakhmanov 2017). Given that the Pachyiulini in the faunas of Turkey (Enghoff 2006) and Iran (Vagalinski 2020) are likewise quite poorly known, each amounting to only a handful of species, there can hardly be any doubt that future progress in the study of pachyiulines in the Caucasus region and adjacent countries will reveal numerous novelties. In addition, given the presence in Crimea of a troglobitic species, *Syrioiulus kovali* (Golovatch, 2008), finding cave species of Pachyiulini in the Caucasus could also be expected (Golovatch 2008; Golovatch et al. 2017; Turbanov et al. 2018). The present taxonomy and distributions as outlined above must be clarified and refined through future research, both morphology- and molecular-based.

## Acknowledgements

We are most grateful to all collectors who rendered us their material for treatment. We are also greatly obliged to both Igor Zabiyaka (Don StateTechnical University, Rostov-on-Don, Russia) for taking SEM pictures. DA is grateful to Hans Reip and Frank Walther (both Germany) for their help during the field trip in Azerbaijan in March 2015, as well as again to Hans Reip and Karin Voigtländer (Germany) for their help in the preparation of some samples used here for SEM. AE was supported by RFBR, Project No. 20-54-18008, SG by the Presidium of the Russian Academy of Sciences, Programme No. 41 "Biodiversity of Natural Systems and Biological Resources of Russia", while DA by the project "Biogeography of the land molluscs of the Caucasus region" funded by VolkswagenStiftung, and the Serbian Ministry of Education, Science, and Technology (Grant 173038) for making his field trip to Azerbaijan possible, as well as by the SYNTHESYS Project (DE-TAF-5619) financed by European Community Research Infrastructure Action under the FP7 "Capacities" Program which allowed him short visits to the Senckenberg Museum of Natural History in Görlitz (Germany) in 2016. We are most thankful to Henrik Enghoff (Copenhagen, Denmark) and Boyan Vagalinski (Sofia, Bulgaria), the reviewers who provided constructive criticism and thus considerably improved our paper. Pavel Stoev (Sofia, Bulgaria) very helpfully served as the managing editor.

## References

Abdurakhmanov GM (2017) [Biogeography of the Caucasus]. KMK Scientific Press, Moscow, 718 pp. [in Russian]

Antić DŽ, Rađa T, Akkari N (2018) Revision of the genus *Hylopachyiulus* Attems, 1904, with a description of a new species from Croatia (Diplopoda, Julida, Julidae). Zootaxa 4531(2): 225–241. https://doi.org/10.11646/zootaxa.4531.2.4

Attems C (1903) Beiträge zur Myriopodenkunde. Zoologische Jahrbücher, Abtheilung für Systematik, Ökologie und Geographie der Thiere 18(1): 63–154. https://www.biodiversitylibrary.org/item/39593#page/7/mode/1up

Attems C (1910) Description de Myriapodes nouveaux recueillis par M. Henri Gadeau de Kerville pendant son voyage zoologique en Syrie. Bulletin de la Société des Amis des Sciences naturelles de Rouen 46(5): 61–67. [for 1911]

Attems C (1927) Über palaearktische Diplopoden. Archiv für Naturgeschichte 92(1–2): 1–256.

Attems C (1940) Beiträge zur Kenntnis der Iuliden. Annalen des Naturhistorischen Museums in Wien 50: 294–327. [for 1939] https://www.jstor.org/stable/41768871?refreqid=excelsior%3A091e80c6182689ffb777e81754a42426&seq=1

Bababekova LA (1969) [To the study of the myriapod fauna (Diplopoda) of the Lenkoran zone]. In: Ghilarov MS (Ed.) Problems of Soil Zoology. Materials of the III All-Union Conference, Moscow, 1969, 21–22. [in Russian]

Bababekova LA (1996) [The subphylum of tracheates – Tracheata]. In: Aliev SV, Kasyimov AG (Eds) Animal life of Azerbaijan. Vol. 2: The phylum of arthropods. Elm Publishers, Baku, 89–97. [in Russian]

Berlese A (1883) Acari, Myriopoda et Scorpiones hucusque in Italia reperta. Acari, Miriapodi e Scorpioni Italiani. Fascicolo VI. Acari, Myriapoda et Scorpiones huscque in Italia reperta 6. Padova. https://doi.org/10.5962/bhl.title.69269

Enghoff H (1992) *Dolichoiulus* – a mostly Macaronesian multitude of millipedes. With the description of a related new genus from Tenerife, Canary Islands (Diplopoda, Julida, Julidae). Entomologica Scandinavica, Supplement 40: 1–158.

Enghoff H (2006) The millipedes of Turkey (Diplopoda). Steenstrupia 29(2): 175–198.

Enghoff H, Moravvej SA (2005) A review of the millipede fauna of Iran (Diplopoda). Zoology in the Middle East 35: 61–72. https://doi.org/10.1080/09397140.2005.10638104

Enghoff H, Dohle W, Blower JG (1993) Anamorphosis in millipedes (Diplopoda) – the present state of knowledge with some developmental and phylogenetic considerations. Biological Journal of the Linnean Society 109: 103–234. https://doi.org/10.1111/j.1096-3642.1993.tb00305.x

Enghoff H, Petersen G, Seberg O (2013) The aberrant millipede genus *Pteridoiulus* and its position in a revised molecular phylogeny of the family Julidae (Diplopoda: Julida). Invertebrate Systematics 27: 515–529. https://doi.org/10.1071/IS13016

Enghoff H, Golovatch SI, Short M, Stoev P, Wesener T (2015) Diplopoda – taxonomic overview. In: Minelli A (Ed.) The Myriapoda. 2. Brill, Leiden – Boston: 363–453.

Evsyukov AP (2016) The millipede *Pachyiulus krivolutskyi* Golovatch, 1977, the easternmost species of the eastern Mediterranean genus *Pachyiulus* Berlese, 1883, endemic to the west-

ern Caucasus (Diplopoda: Julida: Julidae). Russian Entomological Journal 25(4): 299–306. https://doi.org/10.15298/rusentj.25.3.12.

Fabricius JC (1781) Classis V. Unogata. In: Johann Christian Fabricii species insectorum. Carol Ernest Bohnii, Hamburgi et Kilonii, 528–533.

Frederiksen SB, Petersen G, Enghoff H (2012) How many species are there of *Pachyiulus*? A contribution to the taxonomy of Europe's largest millipedes (Diplopoda: Julida: Julidae). Journal of Natural History 46(9–10): 599–611. https://doi.org/10.1080/00222933.2011.651636

Golovatch SI (1977) [New or little known Julida (Diplopoda) of the Sataplia Reserve (SSR Georgia)]. Bulletin of the Moscow Society of Naturalists, Biological series 82(4): 46–51. [in Russian]

Golovatch SI (1979) [The composition and zoogeographic relationship of the diplopod fauna of Middle Asia. Part 2]. Zoologicheskii zhurnal 58(9): 1313–1325. [in Russian, a summary in English]

Golovatch SI (1983) A contribution to the millipede fauna of Iran (Diplopoda). Annalen des Naturhistorischen Museums in Wien 85B: 157–169. https://www.jstor.org/stable/41766661?refreqid=excelsior%3A5eb142deb52b42c7863cd6bf33059830&seq=1

Golovatch SI (2008) On three remarkable millipedes (Diplopoda) from the Crimea, Ukraine. International Journal of Myriapodology 1: 97–110. https://doi.org/10.1163/187525408X316767

Golovatch SI (2018) The millipede subfamily Pachyiulinae in Israel, with the description of a new species (Diplopoda, Julida, Julidae). Zoologicheskii zhurnal 97(7): 791–805. https://doi.org/10.1134/S0044513418070073

Golovatch SI, Turbanov IS, VandenSpiegel D (2017) Contributions to the cave millipede fauna of the Crimean Peninsula (Diplopoda), with the description of a new species. Arthropoda Selecta 26(2): 103–111. https://kmkjournals.com/journals/AS/AS_Index_Volumes/AS_26/AS_26_2_103_111_Golovatch_et_al

Jeekel CAW (1971) Nomenclator generum et familiarum Diplopodorum: A list of the genus and family-group names in the class Diplopoda from the 10th edition of Linnaeus, 1758, to the end of 1957. Monografieën van de Nederlandse Entomologische Vereniging 5: 1–412. [for 1970]

Kime RD, Enghoff H (2017) Atlas of European millipedes 2: Order Julida (Class Diplopoda). European Journal of Taxonomy 346: 1–299. https://doi.org/10.5852/ejt.2017.346

Kobakhidze DN (1964) Myriopods (Myriopoda). [Animal Life of Georgia 2: Athropods]. Tbilisi: SSR Georgia Academy of Sciences Publishers: 186–195. [in Georgian]

Kobakhidze DN (1965) [A list of millipedes (Diplopoda) of SSR Georgia]. Fragmenta Faunistica 11(21): 390–398. [in Russian, summaries in Polish and German]

Koch CL (1847) System der Myriapoden mit den Verzeichnissen und Berichtigungen zu Deutschlands Crustaceen, Myriapoden und Arachniden. In: Panzer GWF, Herrich-Schäffer GAW (Hrgb.) Kritische Revision der Insectenfaune Deutschlands, III. Bändchen, Regensburg, 1–196. https://doi.org/10.5962/bhl.title.49866

Kokhia MS, Golovatch SI (2018) A checklist of the millipedes of Georgia, Caucasus (Diplopoda). ZooKeys 741: 35–48. https://doi.org/10.3897/zookeys.741.20042

Kokhia MS, Golovatch SI (2020) Diversity and distribution of the millipedes (Diplopoda) of Georgia, Caucasus. ZooKeys 930: 199–219. https://doi.org/10.3897/zookeys.930.47490

Lohmander H (1932a) Neue transkaukasische Diplopoden. 4. Aufsatz über Diplopoden aus Sowjet-Union. Zoologischer Anzeiger 98(7/8): 171–182.

Lohmander H (1932b) Neue Diplopoden aus Persien. Göteborgs Kungliga Vetenskaps- och Vitterhets-Samhälles Handlingar 5, Ser. B 3(2): 1–44.

Lohmander H (1936) Über die Diplopoden des Kaukasusgebietes. Göteborgs Kungliga Vetenskaps- och Vitterhets-Samhälles Handlingar, Ser. 5B, 5(1): 1–196.

Lokšina IE, Golovatch SI (1979) Diplopoda of the USSR fauna. Pedobiologia 19: 381–389.

Mauriès J-P (1982) *Dolichoiulus tongiorgii* (Strasser), Diplopode halophile nouveau pour la faune de France. Remarques sur la classification des Pachyiulini (Myriapoda, Diplopoda, Iulida). Bulletin du Muséum national d'Histoire naturelle, Série 4, 4(3–4): 433–444.

Mauriès J-P (1984) Deux espèces nouvelles de Diplopodes cavernicoles des Cyclades: *Hyleoglomeris beroni* (Glomerida) et *Syrioiulus andreevi* (Iulida). Biologia Gallo-Hellenica 11(1): 37–49.

Mauriès J-P, Golovatch SI, Stoev P (1997) The millipedes of Albania: recent data, new taxa; systematical, nomenclatural and faunistical review (Myriapoda, Diplopoda). Zoosystema 19(2–3): 255–292.

Menitsky YL (1991) The project, "A synopsis of the Caucasian flora". A map of the floristic districts. Botanicheskii zhurnal 76(11): 1513–1521. [in Russian] http://arch.botjournal.ru/?t=issues&id=19911111&rid=pdf_0005139

Minelli A [Ed.] (2015) The Myriapoda. V. 2. Treatise on Zoology – Anatomy, Taxonomy, Biology. Leiden & Boston, Brill, 482 pp. https://doi.org/10.1163/9789004188273

Porat CO (1893) Myriopodes récoltés en Syrie par le Docteur Théodore Barrois. Revue biologique du nord de la France 6(2): 62–79.

Rakhmanov RR (1971) [Distribution and ecology of *Amblyiulus continentalis* (Diplopoda, Julidae) in the Lenkoran zone of Azerbaijan]. Zoologicheskii zhurnal 50(9): 1412–1413. [in Russian, a summary in English]

Rakhmanov RR (1972) [Millipedes of the Lenkoran zone of Azerbaijan]. In: Ghilarov MS (Ed.) Problems of Soil Zoology. Materials of the IV All-Union Conference, Baku 1972. Nauka Publishers, Moscow, 116–116. [in Russian]

Samedov NG, Bababekova LA, Rakhmanov RR (1972) [Distribution of myriapods (Myriapoda) in various types of soil of Lenkoran]. Zoologicheskii zhurnal 51(8): 1244–1247. [in Russian, a summary in English]

Silvestri F (1895) Viaggio del Dr. E. Festa in Palestina, nel Libano e regioni vicine. XIII. Chilopodi e diplopodi. Bollettino del Museo di zoologia e di anatomia comparata della Reale Università di Torino 10(199): 1–3. https://doi.org/10.5962/bhl.part.8049

Silvestri F (1896) I Diplopodi. Parte I. Sistematica. Annali del Museo civico di storia naturale di Genova, serie 2, 16: 121–254. http://biodiversitylibrary.org/page/7697911

Tabacaru I (1978) Sur la systématique des Pachyiulinae. Description d'une nouvelle espèce de *Geopachyiulus*. Travaux de l'Institut de Spéologie "Emile Racovitza" 17: 67–80.

Tabacaru I (1995) Diplopodes d'Israël. 1. *Libanaphe adonis galilaensis* n. ssp. avec une liste révisée des Diplopodes signalés en Israël. In: Por FD, Decu V, Negrea S, Dimentman C (Eds) Soil Fauna of Israel. Volume 1. Editura Academiei Române, Bucharest, 19–28. [156 pp.]

Talikadze DA (1984) [On the millipede fauna (Diplopoda) of the Colchidan Province of the Caucasus]. Zoologicheskii zhurnal 63(1): 142–145. [in Russian, a summary in English]

Turbanov IS, Golovatch SI, VandenSpiegel D (2018) New interesting records of three cavernicolous millipede species from the Crimean Peninsula. Arthropoda Selecta 27(3): 201–209. https://doi.org/10.15298/arthsel.27.3.02

Vagalinski B (2020) A new species of *Syrioiulus* Verhoeff, 1914 from Iran, with remarks on the taxonomy of the genus (Diplopoda: Julida: Julidae). Revue suisse de Zoologie 127(1): 83–94. https://doi.org/10.35929/RSZ.0008

Verhoeff KW (1901) Beiträge zur Kenntniss paläarktischer Myriopoden. XVII. Aufsatz: Diplopoden aus dem Mittelmeergebiet. Archiv für Naturgeschichte 67(1): 79–102. [for 1900] https://doi.org/10.5962/bhl.part.7278

Verhoeff KW (1914) Einige Chilognathen aus Palästina (Über Diplopoden 68. Aufsatz.). Verhandlungen der Zoologisch-botanischen Gesellschaft in Wien 64: 61–75.

Verhoeff KW (1943) Über Diplopoden aus der Türkei. III. Zoologischer Anzeiger 143(9–10): 216–242.

ZooKeys 1048: 145–175 (2021)
doi: 10.3897/zookeys.1048.67564
https://zookeys.pensoft.net

RESEARCH ARTICLE

A peer-reviewed open-access journal
ZooKeys
Launched to accelerate biodiversity research

# A new Palaearctic species of the subgenus *Lunatipula* (Diptera, Tipulidae) from the West Caucasus with a survey of the *caucasica* species group

Vladimir I. Lantsov[1], Valentin E. Pilipenko[2]

**1** *Tembotov Institute of Ecology of Mountain Territories of Russian Academy of Sciences, I. Armand str., 37a, Nalchik 360051, Russia* **2** *Lomonosov Moscow State University, GSP-1, Leninskie Gory, Moscow 119991, Russia*

Corresponding author: Vladimir I. Lantsov (lantsov@megalog.ru)

Academic editor: Netta Dorchin | Received 19 April 2021 | Accepted 14 June 2021 | Published 13 July 2021

*http://zoobank.org/578795FD-41BF-4807-B001-6F7B5AC4D4B9*

**Citation:** Lantsov VI, Pilipenko VE (2021) A new Palaearctic species of the subgenus *Lunatipula* (Diptera, Tipulidae) from the West Caucasus with a survey of the *caucasica* species group. ZooKeys 1048: 145–175. https://doi.org/10.3897/zookeys.1048.67564

## Abstract

The *caucasica* species group in the subgenus *Lunatipula* is redefined and now consists of five species native to the Caucasus. *Tipula* (*L.*) *eleniya* **sp. nov.** is described as new to science, and variations in the male terminalia in two populations are noted. Two subspecies (*quadridentata quadridentata* and *quadridentata paupera*) are elevated to species rank. Detailed photo's complement the descriptions of all five species (*caucasica*, *eleniya*, *paupera*, *quadridentata*, *talyshensis*), and data on ecology and distribution patterns are included as well as identification keys to males and females. *Tipula caucasica* is recorded from the West Caucasus and *Tipula quadridentata* is recorded from Dagestan (Russia) for the first time. Parallel evolution is traced in the male terminalia of the new species and in several non *caucasica* species group of Palaearctic *Lunatipula.*

## Keywords

Crane flies, male and female terminalia, new species, Russia, *Tipula eleniya*

## Introduction

There are 502 species in the subgenus *Lunatipula* Edwards in the world fauna (Oosterbroek 2021). This is the dominant taxon of crane flies in the Caucasus (Savchenko 1964, 1983), comprising at least 53 known species, which is ca. 32% of the total spe-

cies of the family in this region (164). Riedel (1920) pioneered the work on crane flies of the Caucasus and neighboring regions, especially on the subgenus *Lunatipula*. He provided information on seven species of *Lunatipula*, three of which were described as new to science: *Tipula* (*Lunatipula*) *caucasica* Riedel, *Tipula* (*Lunatipula*) *armata* Riedel (synonym of *zaitzevi* Savchenko, 1952), and *Tipula* (*Lunatipula*) *aurita* Riedel. Savchenko (1954, 1957, 1964, 1968) made subsequent invaluable contributions to the knowledge of the regional fauna of the subgenus by describing 57 species, of which 32 were from the Caucasus and only two of these were subsequently synonymized (Oosterbroek 2021). The species group *caucasica* was first proposed by Savchenko (1964) to comprise four species endemic to the Caucasus. A number of subsequent studies have been published since on the diversity and ecology of some species of the subgenus *Lunatipula* from the Caucasus (Lantsov 1998, 2002, 2007, 2018). In this study we present new data on the taxonomic status, morphology, and distribution of the *caucasica* species group, provide a key to all currently known species, and describe *Tipula eleniya* Lantsov & Pilipenko as new to science. It was found in the Western Caucasus (Krasnodarskiy kray) at altitudes of 1200–2000 m. The new species is characterized by a projection on the inner gonostylus of the male, the structure of this shape is not known in any of the 502 known species, including the 360 Palaearctic species.

## Materials and methods

All crane flies were collected by sweep-net and then pinned. The genitalia were macerated in warm 10% KOH for ca. one hour to remove soft tissue, and then rinsed in distilled water. Cleared genitalia are preserved in glycerol in micro vials pinned with their respective specimens. Specimens were studied with an Olympus SZ61 stereo microscope. A Nikon d7000 digital camera equipped with combined Tamron 70–300 / 4–5.6 and EL-Nikkor 50/2.8 lenses or Mitutoyo M Plan Apo 10X Microscope objective lens was used to capture partially focused images of each specimen or structure. These were stacked using the Helicon Focus (version 7.6.4) software (http://www.heliconsoft.com/heliconsoft-products/helicon-focus). Photographs of lateral and dorsal view and details of the structure of head, pronotum and scutum were made with a Canon 5D Mark IV digital camera equipped with a Canon MP-E 65mm f/2.8 1–5 × macro lens and Canon Macro Twin-Lite MT-26EX-RT flash. Adobe Photoshop CC 2019 software was used to edit the pictures. Measurement were made with an MBS–10 microscope with a scale installed in the focal plane of the 8× eyepiece (divisions of scale: 0.1 mm at 8 × 1 magnification, 0.05 mm at 8 × 2 magnification, 0.025 at 8 × 4 magnification).

For citing label data on type specimens, a slash / separates each label. Square brackets [ ] are used to indicate additional information not on the original label. Original spelling is retained, including punctuation. In some cases, holotypes were marked by a red label without text and some paratypes were not initially marked. In such cases, specimens with locality labels corresponding to those in the publications of Savchenko (1964) or Savchenko and Kandybina (1987), were provided with a red label with the word “Holotype” or a white label with the word “Paratype,” and pinned with the

specimen. These type specimens are deposited in the Zoological Institute of Russian Academy of Science, St. Petersburg, Russia. The holotype and paratypes of the *Tipula* (*Lunatipula*) *caucasica* were unavailable for this study.

We generally follow the terminology of Cumming and Wood (2017) except that for head morphology we follow Crampton (1943) and Savchenko (1983), and regarding wing venation, we follow Savchenko (1983). Veins are indicated by capitals; cells are indicated by lowercase letters.

All measurements of the new species were made on pinned material.

Species distributions are given according to Oosterbroek (2021).

The original descriptions and measurements by Riedel (1920) and Savchenko (1964) were taken into account in the redescriptions of the species.

Abbreviations for institutional and private collections used herein: **IEMT** Tembotov Institute of Ecology of Mountain Territories of Russian Academy of Sciences, Nalchik, Russia; **VPMC** private collection of Valentin E. Pilipenko, Moscow, Russia; **ZISP** Zoological Institute Russian Academy of Sciences, St. Petersburg, Russia. All specimens from the *caucasica* species group deposited in ZISP and collected before 1964 have been identified by E.N.Savchenko unless specifically noted.

## Taxonomy

### Family Tipulidae Latreille, 1802

**Genus *Tipula* Linnaeus, 1758**

**Subgenus *Lunatipula* Edwards, 1931**

**The *caucasica* species group. Diagnosis** (after Savchenko 1964 with additions)**.** Medium sized grey species. Rostrum with nasus, wings with more or less distinct bluish tint in transmitted light; metakatepisternum with setae; abdomen slate or brownish grey with lateral intermittent dark brown stripe on tergites. Males with tergite 9 transverse with two or three concave notches at apex; inner gonostylus posteriorly simple; sternite 8 with paired appendages composed of short wide base with bristles and an elongate glabrous spine bent medially; no dense brush of setae between bases of paired appendages (except for *T. quadridentata*). Caucasian endemics. Savchenko included the following species in the *caucasica* group: *caucasica*, *quadridentata quadridentata*, *quadridentata paupera*, *talyshensis.*

***Tipula* (*Lunatipula*) *caucasica* Riedel, 1920**

Figs 1, 2, 12A–C, 13A, 14A,F

*Tipula* (*Lunatipula*) *caucasica* Riedel 1920: 17 (type locality: Georgia, Mts'chet, prope Tiflis); Savchenko 1964: 390; Oosterbroek, Theowald 1992:104; Lantsov 2020: 294; Oosterbroek 2021.

**Material examined.** Georgia • 1 male, 3 females; "ущ. Бани-Хеви бл. Боржоми, Аджаро-Имеретинск. хр. [Gorge Bani-Khevi near Borjomi, Adjaro-Imeretinsk. Ridge]; 26 Jun. 1958; Kurnakov leg.; ZISP • 1 male; "Цхра-Цхаро близ Бакуриани" [Tskhra-Tskharo near Bakuriani]; 29 Jun. 1958; Kurnakov leg.; ZISP •1 male; "Леберде, Менгрелия, Грузия" [Leberde, Mengrelia, Georgia]; 17 Jul. 1959; Savenko leg.; ZISP • 1 male; "Аджаро-Имеретинск. хр. Горы у Саирме, Грузия" [Adjaro-Imeretinsk. Ridge, mountains near Sairme, Georgia]; 23 May 1958; Kurnakov; ZISP • 2 males, 1 female; "ущ. Цваниат-Хеви Аджаро-Имеретинск. хр. Грузия" [Tsvaniat-Khevi Gorge, Adjaro-Imeretinsk. Ridge, Georgia]; 23 Jun. 1958; Kurnakov leg; / "Высокотравье у верхн. границы леса у ручья" [High grass at the edge of the border of the forest by the stream]; ZISP • 2 males; "с. Отхара, Гудаутск. р-н, Абхазия, бер. речки, кусты." [village Otkhara, Gudautsk. District, Abkhazia, river bank, bushes]; 30 Jun. 1958; Kurnakov; ZISP •2 males; "Абхазия, с. Отхара предгорья Бзыбского хр." [Abkhazia, village Otkhara foothills of the Bzybsk Ridge]; 20 May 1958; Kurnakov; / "Дубово-грабовый лес, кусты Asalia" [Oak-hornbeam forest, bushes Asalia"]; ZISP; Azerbaijan • 1 male; "Белоканы, хр. Ахкемал. Азерб. 200 м" [Belokany, Akhkemal Ridge. Azerb.[aidjan] alt. 200 m]; 15 Jun. 1964; Pastukhov leg.; ZISP; Russia – **Krasnodarskiy kray** • 1 male; Sotshi prov. Pontica; 6 May 1932; B.Rohdendorf leg.; / "T.caucasica Ried det. Lacksch." [terminalia in Canada balsam pinned with specimen]; ZISP • 1 female, Khosta, Caucasian Reserve, Tiso-samshitovaya rosha [Yew-and-Boxwood Tree Grove]; 43°31'656"N, 39°52'467"E; alt. 54 m; collected at light, 8 May 2018; V. Lantsov leg.; IEMT • 2 males, 2 females; same collection data as for preceding, 43°31'688"N, 39°52'561"E; alt. 35 m; 8 May 2018; V. Lantsov leg. / Lime-beech (*Tilia begoniifolia* and *Fagus orientalis*) forest with yew (*Taxus baccata*) and hornbeam (*Carpinus betulus*) in tree layer and butcher's-broom (*Ruscus colchicus* – dominant and *Ruscus aculeatus*) in ground layer [one of the females was collected in the same community in a damp place near a yew log]; IEMT • 2 males, 2 females, same collection data as for preceding, 43°31'780"N, 39°52'518"E; alt. 98 m; 9 May 2018; V. Lantsov leg.; / Hornbeam – ash (*Carpinus orientalis*, *Fraxinus excelsior*) forest with addition of yew (*Taxus baccata*) and lime (*Tilia begoniifolia*) with blackberry (*Rubus sanctus*) and fig (*Ficus carica*) in shrub layer and with butcher's-broom (*Ruscus colchicus*) in ground layer; ZISP • 4 males, 4 females, same collection data as for preceding, 43°31'775"N, 39°52'423"E; alt. 101 m; 9 May 2018; V. Lantsov leg.; / Hornbeam (*Carpinus orientalis*) forest with butcher's-broom (*Ruscus colchicus*) and fern (*Asplenium scolopendrium*) in ground layer; ZISP • 1 male and 1 female (in copula), 1 female; same collection data as for preceding, 43°31'913"N, 39°52'463"E; alt. 153 m; 9 May 2018, V. Lantsov leg. / Ash-lime (*Fraxinus excelsior* + *Tilia begoniifolia*) forest with hornbeam (*Carpinus betulus*) and with black berry (*Rubus anatolicus*) and miscellaneous herbs in ground layer; IEMT • 2 males, 1 female, same collection data as for preceding, 43°31'825"N, 39°52'653"E; alt. 99 m; 10 May 2018, V. Lantsov leg.; IEMT • 1 male, same collection data as for preceding, 43°31'656"N, 39°52'467"E; alt. 54 m; V. Lantsov leg.; ZISP • 2 males, 1 female, same collection data as for preceding,43°32'257"N, 39°52'682"E; alt. 94 m; 10 May 2018, V. Lantsov leg.; / beech (*Fagus orientalis*) forest

with addition of yew (*Taxus baccata*) and hornbeam (*Carpinus betulus*) with bunch grass (*Calamagrostis arundinacea*) in ground layer; IEMT • 6 males, 3 females; Krasnodar Territory, environs Shakhe River higher than Salokh-Aul; 5–8 Jun. 2011; V. Pilipenko leg.; VPMC; Russia – **Dagestan** • 1 female, "Хочал-Даг, альп. обл. Дагст. [Дагестан]" [Hochal-Dag, alp. Region Dagst. [Dagestan]]; 29 Jun. 1909 Mlokosevich leg.; ZISP • 1 female; Tlyaratinsky district, near village Salda, stream on the right bank of the river Dzhurmut; 41°58'388"N, 46°30'446"E; alt. 1792 m; 2 Jul. 2016, V. Lantsov leg.; / "Oak (*Quercus iberica*) sparse forest with *Populus tremula* and *Acer platanoides* in tree layer, *Rosa canina*, *Spiraea crenata* and *Cotoneaster integerrimus* in shrub, and clover (*Trifolium canescens*) and miscellaneous herbs in ground layer; ZISP • 2 males, 1 female; near village Betelda, stream on the left bank of the river Dzhurmut; 41°56'853"N, 46°32'424"E; alt. 1850 m; 3 Jul. 2016, V. Lantsov leg.; / Willow (*Salix caprea*) shrub with herbaceous layer (*Epilobium montanum*) (dominant), *Cardamine seidlitziana*, *Mentha caucasica*, *Veronica anagallis-aquatica* and *Myosoton aquaticum* community near spring above the flood plain of the left bank of the river; ZISP • 2 males; near village Genekolob, on the high left bank of the river Dzhurmut; 41°57'392"N, 46°31'276"E; alt. 2011 m; 4 Jul. 2016, V. Lantsov leg.; / Oak (*Quercus iberica*) forest with mountain-ash (*Sorbus aucuparia*), wayfaring tree (*Viburnum lantana*) in shrub layer [the lower border of a forest and a forb-cereal meadow]; ZISP • 2 males; same collection data as for preceding, 41°57'449"N, 46°31'228"E; alt. 1977 m; 4 Jul. 2016, V. Lantsov leg.; ZISP • 2 males, between the villages of Gerel and Genekolob, the right bank of the river Dzhurmut, 41°55'619"N, 46°34'468"E; alt. 1925 m; 5 Jul. 2016, V. Lantsov leg.; / Above the floodplain terrace with a rare herbaceous birch (*Betula raddeana*) forest with willow (*Salix caprea*) (coppice forest); ZISP.

**Diagnosis.** Dark stripes medially on lighter background extending entire length of scutum. Inner gonostylus posteriorly with wedge-shaped projection directed anteriorly. Tergite 9 at apex with three rounded notches, middle one usually deepest and widest.

**Redescription.** Adult male (Fig. 1A, B). General color grey. Body length 14–17 mm, wing 14–17.5 mm.

***Head.*** Light grey, sometimes bluish (Figs 1B, 13A). Rostrum whitish dorsally, flanks rusty or brownish with whitish bristles; nasus distinct, with long, whitish yellow setae; palpus grey. Frons with rows of brown setae along inner edge of eye. Vertex with faint dark median line, posteriorly with dark grey striation, with group of small rusty setae arranged fan-like on either side of glabrous medial area. Genae rusty; wide dark median stripe ventrally on rostrum, continuing along gula midline. Pharyngeal foramen framed with long, rusty hair-like setae. Postgenae light grey.

***Antenna*** (Fig. 1B) 13-segmented, if bent backwards just reaching wing base. Scape light brown or grey, depending on angle of rotation to light source, with slightly pronounced silvery pruinescence and brown horizontal striations. Pedicel yellow, sometimes brownish at base. Flagellomeres brownish, thickened at base, verticils subequal in length to corresponding flagellomeres.

***Thorax*** (Fig. 1B). Grey or blue-grey. Pronotum with dark grey median stripe. Katepisternum, anepisternum and meron grey, glabrous. Scutum with four longitu-

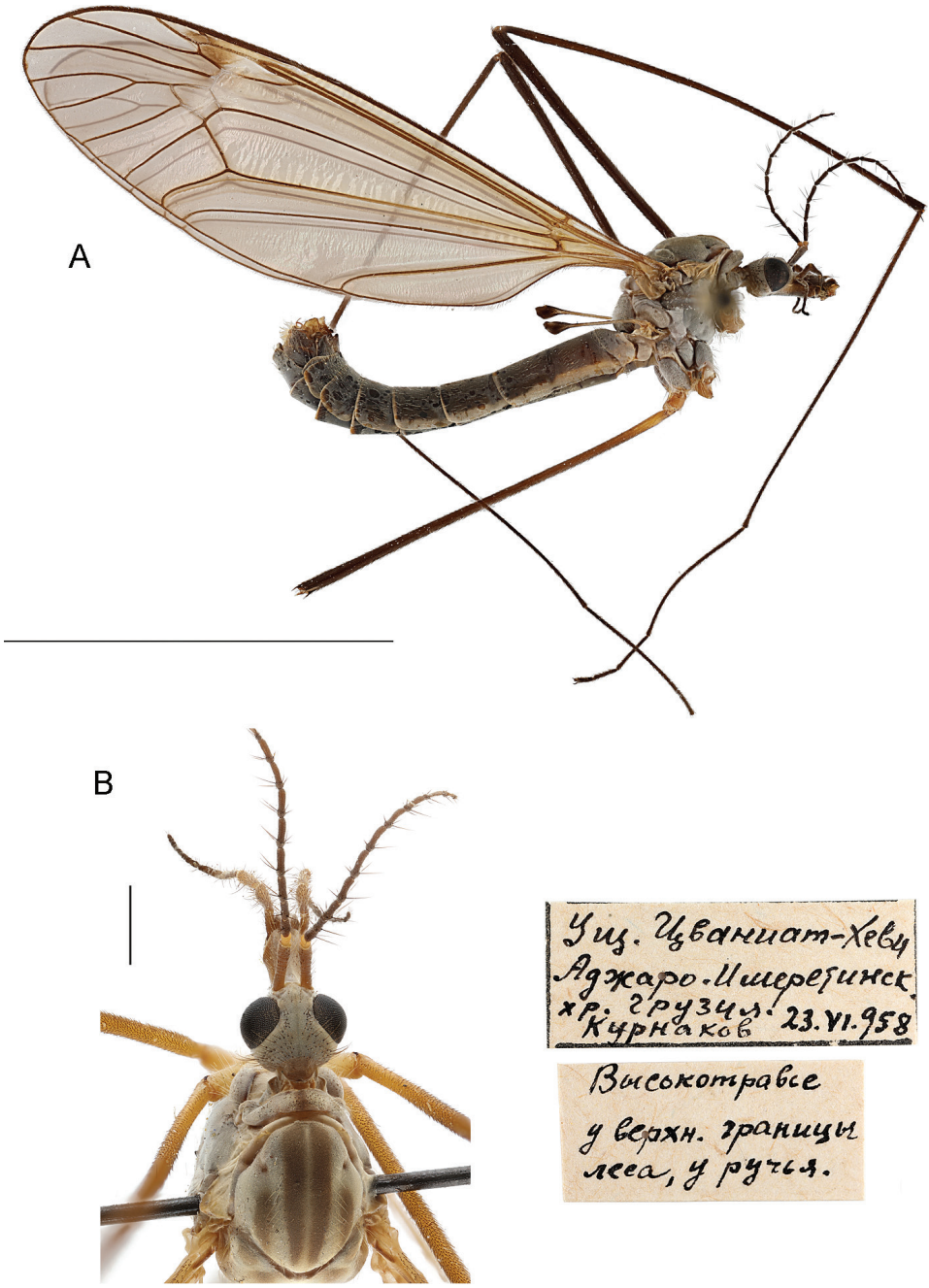


**Figure 1.** *T.* (*Lunatipula*) *caucasica* male habitus **A** general lateral view **B** head and thorax, dorsal view. Scale bars: 10 mm (**A**), 1 mm (**B**).

dinal wide brownish stripes on lighter background; medial stripes extending length of scutum. Scutal lobes, scutellum and mediotergite grey with light bristles in dark brown sockets.

***Wings*** (Fig. 1A) greyish with a bluish tinge in transmitted light, stigma brown; narrow whitish area (lunule) extending to base of discal cell.

***Halteres*** (Fig. 1A) with light brown or dark-yellow stem, lighter yellow at base, covered with short small pale setae; knob dark brown to black.

***Legs*** with coxae light grey with long light hairs. Coxae may appear darker when specimen is rotated. Trochanters yellow. Femora yellow at base, rest of femora, tibiae, and tarsi dark brown.

***Abdomen*** (Figs 1A, 2A). Grey or dark grey; tergites with dark lateral stripe narrowly interrupted with whitish at posterior margins, lateral margins with wider whitish edge.

***Terminalia*** (Figs 2, 14A, F). Hypopygium (Fig. 2B, C) not much thicker than rest of abdomen, brown with moderately dense grey pruinescence, with golden yellow hairs. Gonocoxite (Fig. 2C, G) with broad tooth ventrally. Tergite 9 (Figs 2C, E, F; 14A) transverse, lateral corner broadly rounded, at apex with three rounded notches, middle one usually deepest and widest, bounded laterally by two large dentate projections with blunt apices, clearly visible when viewed from above (Figs 2F, 14A) (Riedel 1920; Savchenko 1964). When viewed from behind, three pairs of very short projections are visible (Fig. 2E). Outer gonostylus (Figs 2G, 14F) very small, wineglass shaped, elongated distally. Inner gonostylus posteriorly, with wedge-shaped projection (Figs 2G, 14F). Paired appendage of sternite 8 (Fig. 2D) with base ~ 2 × as long as wide, with thin rigid yellow setae along edge, not obscuring gap in middle; long, glabrous red-brown spine arising from base, bent, and intersecting medially. Paired appendage of sternite 9 (Fig. 2K, L) with thick pubescent apex. Gonocoxal fragment (Fig. 2I) flattened at the base. Semen pump and aedeagus as in Figure 2J.

**Female.** Body length 17–21.5 mm, wing 15.5–18 mm. Antennae with scape and pedicel brownish yellow. Legs stocky, black to brown, yellow at base, femora grey. Wings with noticeable bluish tint; whitish area (lunule) of wings barely reaching base of discal cell. Female terminalia (Fig. 12A–C) comparatively short. Tip of cercus upcurved, length of cercus ~ 0.8 mm. Hypogynial valve only slightly longer than width at base; length of hypogynial valve 0.2 mm. Sternite 9 and furca as in Figure 12A, C.

**Comparison with closely related species.** This species differs from other species of the *caucasica* group primarily by the presence of a large, anteriorly directed sharp wedge-shaped projection located posteriorly on the inner gonostylus.

**Elevation.** Adults were collected at altitudes ranging from sea level (Black Sea coast at 35 m) to 2011 m (in Dagestan).

**Flight period.** From end of April to the beginning of July.

**Habitat.** Specimens were captured in diverse forest habitats (see above) predominantly in mesophytic moderately moist deciduous or mixed communities with *Fagus orientalis*, *Taxus baccata*, *Carpinus orientalis*, *Quercus iberica*, *Populus tremula*, *Acer platanoides*, etc., sometimes in communities near springs with *Salix caprea*.

**Distribution.** Endemic to the Caucasus. It was recently noted for Russia (Dagestan) for the first time (Lantsov 2020). Currently known from the West Caucasus (first record), East Caucasus and Transcaucasus.

**Remarks.** According to Riedel (1920), a series of type specimens, four males, two females. "Mts'chet prope Tiflis [Georgia, Tbilisi], 6. 5. 1913 (Mus. Caucas. Ph. Za-

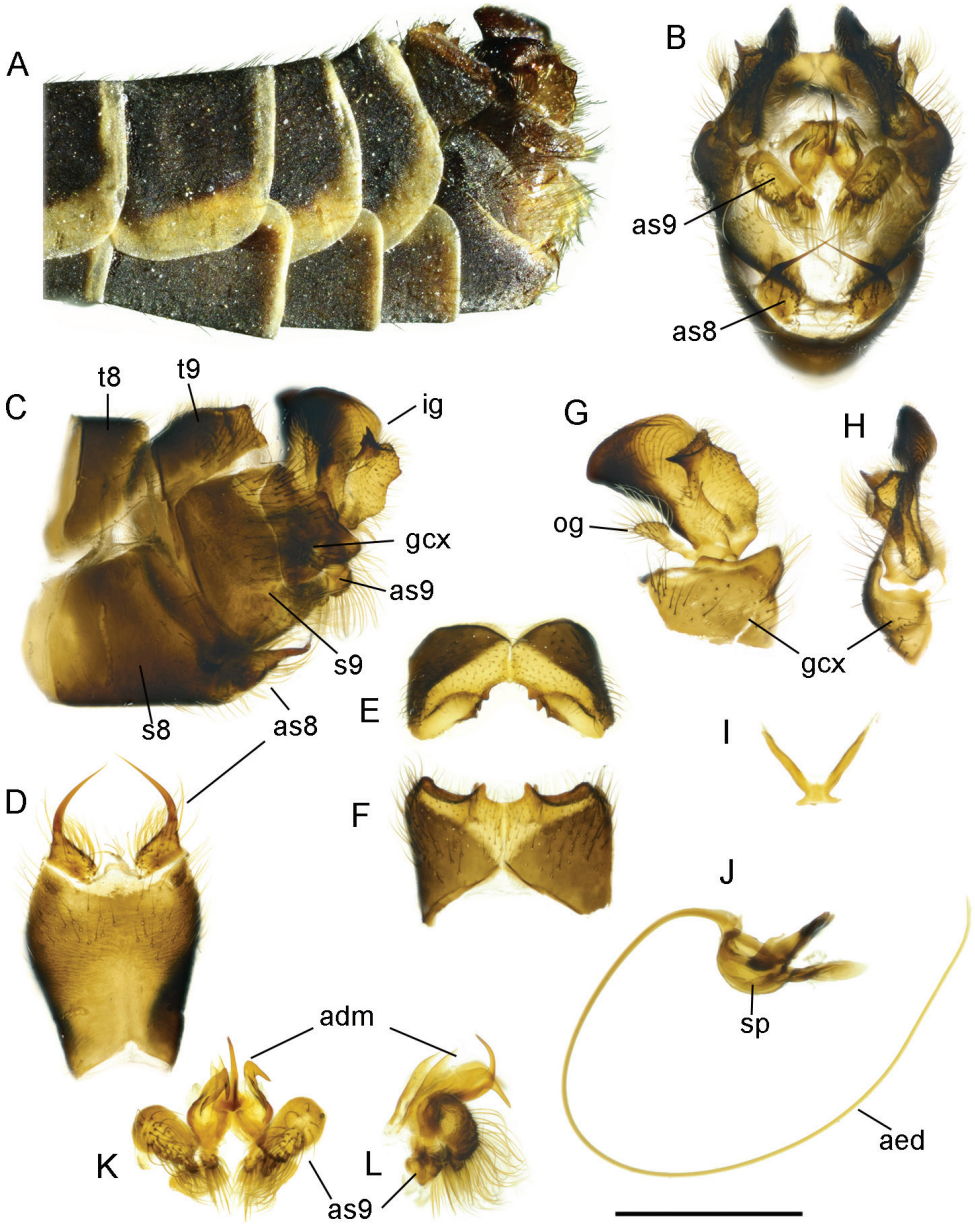


**Figure 2.** *T.* (*Lunatipula*) *caucasica* **A** terminal segments of male abdomen, lateral view (dry) **B–L** male terminalia (after KOH 10% treatment) **B** hypopygium, caudal view **C** hypopygium, lateral view **D** sternite 8, ventral view **E** tergite 9, caudal view **F** tergite 9, dorsal view **G** inner and outer gonostylus, lateral view **H** inner and outer gonostylus, caudal view **I** gonocoxal fragment, dorsal view **J** semen pump and aedeagus, lateral view **K** adminiculum and paired apical appendages of sternite 9, caudal view **L** adminiculum and paired apical appendages of sternite 9, lateral view. Abbreviations: adm–adminiculum; as 8–paired appendages of sternite 8; as 9–apical appendages of sternite 9; ig–inner gonostylus; gcx–gonocoxite; og–outer gonostylus; s8–sternite 8; s9–sternite 9; t9–tergite 9. Scale bar: 1 mm.

itzev)" were deposited in the "Museum Caucasicum in Tiflis". In the author's publication, neither the holotype nor the paratypes are indicated. Presumably, they are not indicated on the material itself. Because this material turned out to be inaccessible to the authors of this article – it is not yet known whether this material has survived at all – there was no opportunity to designate lectotype and paralectotypes.

***Tipula (Lunatipula) eleniya* sp. nov.**
http://zoobank.org/2847C4F8-9727-4FC3-BECD-C552B75382C8
Figs 3, 4, 5, 13B, 14B, G

**Material examined.** ***Holotype*:** Russia • 1 male; Krasnodarskiy Kray, Sochi env. Psekhako Mt., 43°41'28"N, 40°22'E; alt. ~ 2000 m; 14–18 Jun. 2008; K. Tomkovich leg.; ZISP. Holotype in good condition; however, left antenna, front right and left hind legs missing. ***Paratypes*:** Russia • 1 male; same data as for holotype • 2 males; Krasnodarskiy Kray, Kamyshanova Polyana env. [Biological station of Krasnodar State University], 44°16'91"N, 40°04'46"E; alt. 1200 m; 26 Jul. 2018; V..Pilipenko leg.; ZISP.

**Diagnosis.** Male. General coloration grey with silver pruinescence. Tergite 9 with deep rounded notches either side of slightly grooved cone-shaped projection. Sternite 8 with a pair of small appendages, each bearing a long medially curved spine, broad base of appendages with fringe of long whitish hairs. Outer gonostylus small, triangular, slightly thickened distally, covered with long setae. Inner gonostylus with small rod-like outgrowth in middle of outer edge.

**General description.** Adult (Fig. 3A). Male body length 15.7 mm, wing length 16.2 mm, haltere 2.5 mm, nasus 0.13 mm, rostrum 0.8 mm, scape 0.6 mm, pedicel 0.15 mm, 1st flagellomere 0.5 mm. Length (mm) of leg segments, fore (1), mid (2), and hind (3); successively femur, tibia, 1st and 2nd tarsomeres: 1 (9.7; 10.4; 8.5; 3.8), 2 (9.8; 10.5; 9.0; 4.5) and 3 (10.0; 13.0; 9.0; 4.5). Length (mm) of 3rd, 4th, and 5th tarsomeres of all three pairs of legs, approximately the same: 1.0; 0.6; 0.5 mm, respectively.

**Description.** ***Head*** (Figs 3, 13B) grey with silvery pubescence. Rostrum grey dorsally, ventrally yellow-brown with sparse light rusty setae in black sockets. Nasus distinct, appearing triangular in dorsal aspect, covered with long, sparse procumbent setae. Frons and gula bare. Vertex (Fig. 13B) framed by rows of sparse setae alongside eye, glabrous in center with indistinct narrow longitudinal dark grey line. Genae, including lateral part of rostrum, with very sparse fine pale bristles. Tempora and postgenae with sparse black setae.

***Antennae***, bent backwards, reaches base of abdomen. Scape grey with silvery pruinescence, pedicel dirty yellow brown. Flagellomeres dark brown with verticils on slightly thickened bases, longest verticils subequal to length of respective flagellomere.

***Thorax*** (Fig. 3A, B) grey with silvery pruinescence, and short sparse whitish hairs. Pronotum dark brown with a weak dark stripe medially, and short sparse whitish bristles. Scutum (Fig. 3B) with four brownish grey longitudinal stripes, lateral stripe

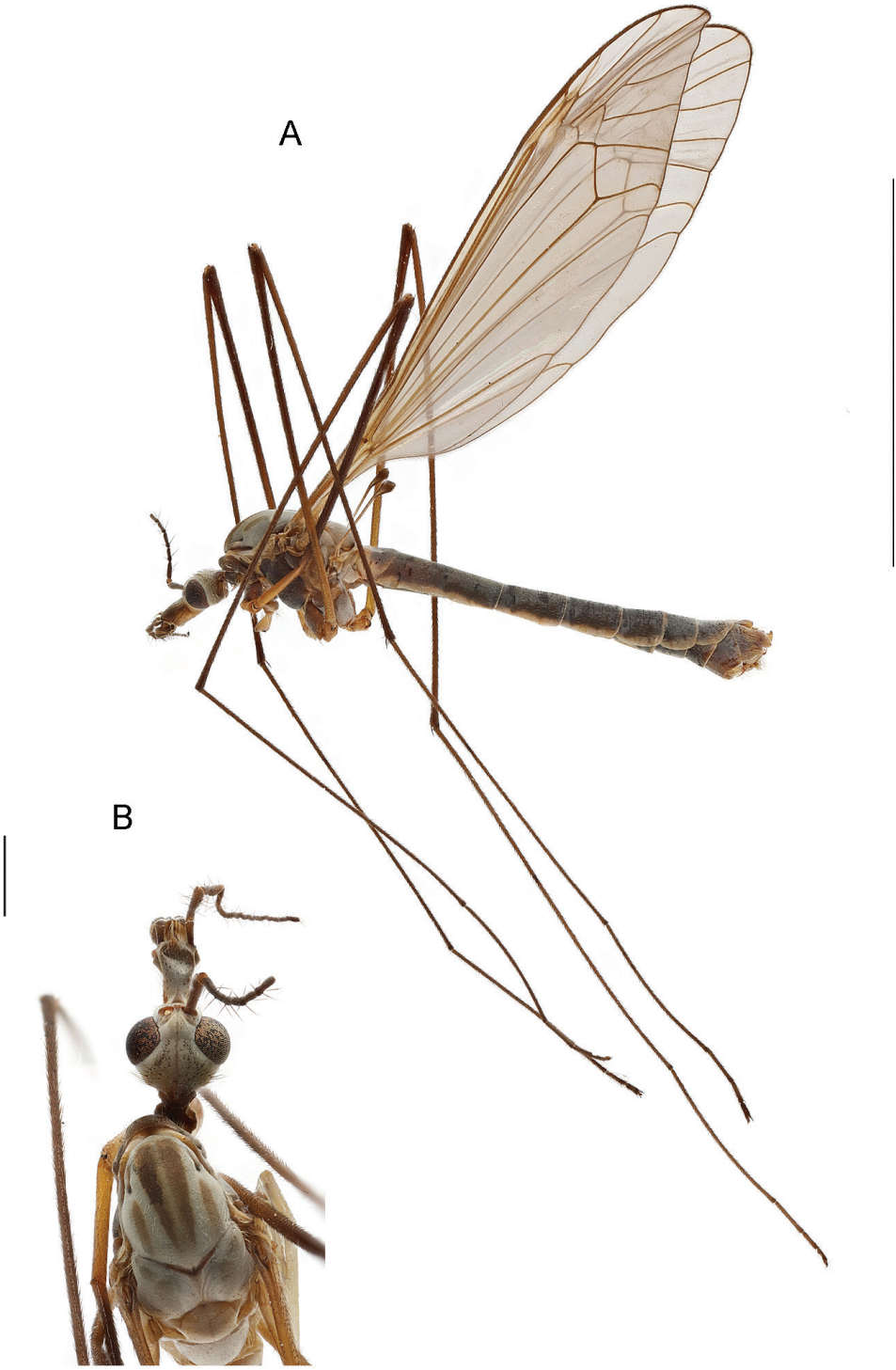


**Figure 3.** *T.* (*Lunatipula*) *eleniya* sp. nov., male habitus. Holotype **A** general lateral view **B** head and thorax, dorsal view. Scale bars: 10 mm (**A**), 1 mm (**B**).

shorter, medial stripes narrowly separated by dirty yellow area. Katepisternum, anepisternum, katepimeron, anepimeron and meron grey, bare, with silvery pruinescence; scutellum and mediotergite light grey with silvery pruinescence; scutal lobes with wide dark grey stripe, bordered by sparse whitish setae and with long yellow setae anterolaterally at wing base. Scutellum framed anteriorly with brown, with sparse yellow setae laterally, and with vague narrow dark grey medial line. Mediotergite light grey with sparse yellow setae and with silvery pruinescence. Laterotergite grey with silvery pruinescence and sparse erect short brown setae.

***Wings*** (Fig. 3A) with typical venation for the subgenus, transparent with brownish tin, (viewed in transmitted light). Stigma dirty yellow. Oblique lunule proximal to stigma. Setae on costal and subcostal veins; group of short black macrotrichia distally on *R* and base of $R_1$. Distal section of $R_5$, $R_{4+5}$, *r-m*, base of pentagonal discal cell lighter and weakened. Stem of cell $m_1$ approximately half length of cell. Apex of vein $Cu_1$ sharply curved at wing margin.

***Halteres.*** Stem grey with base covered with short white setae, knob dark grey.

***Legs.*** Coxae light grey with silvery pruinescence; laterally with long sparse whitish yellow setae; medially with very short yellowish setae. Trochanters yellow with long yellow setae. Femora brown, narrowly yellow at base, covered with adpressed short brown setae; tibiae brownish; tarsal segments dark brown with short, adpressed brown setae. Tibial spur formula 1-2-2. Tarsal claws with a small tubercle at the base (magnification 10 × 4.5); with short but clearly visible arolium between ones.

***Abdomen*** (Figs 3A, 4A). Tergites and sternites grey with silvery pruinescence, and sparse fine short golden setae. Tergites with lateral dark grey intermittent stripe, no distinct dorsal stripe. Tergites laterally and distally edged with whitish-yellow, proximal segments with thinner distal edge, becoming wider on caudal segments.

***Terminalia*** (Figs 4, 5, 14B, G). Hypopygium grey to dark grey, moderately thickened, with silvery pruinescence (Fig. 4A–C). Tergite 9 with two deep rounded notches flanking a median cone-shaped projection, the apex of which has a small groove (Figs 4E, F; 5G–L, 14B). The dorsolateral edges of the tergite 9 convex, curved inward. Sternite 8 (Fig. 4D) with a pair of small appendages bearing long medially curved spine, base of appendages with fringe of long whitish hairs not obscuring gap between. Appendages of sternite 9 (Fig. 4K, L) abundantly pubescent. Outer gonostylus (Figs 4G, 5A–F, 14G) small, triangular, slightly thickened distally, covered with long bristles. Inner gonostylus (Figs 4G, H; 5A–F, 14G) with small rod-shaped outgrowth in middle of outer edge (Figs 4G, 14G), twice as long as wide at base, slightly narrower medially, tip obliquely truncate. Posterior part of inner gonostylus a wide triangular plate with short sparse brown bristles in inner surface, long whitish setae in outer one. Gonocoxite (Figs 4G, 5A–C) with two wide dentate outgrowths, ventral one longer, pointed, dorsal one rounded; long yellowish setae laterally on gonocoxite. Gonocoxal fragment (Fig. 4I) with short forked extension at base. Semen pump and aedeagus as in Figure 4J.

**Female** unknown.

**Variation.** Three variants exist of the small rod-like outgrowth of the inner gonostylus: variant I (holotype – Sochi env., Psekhako Mt, alt. 2000 m) (Fig. 5A, D), variant II (paratype) (Fig. 5B, E) and variant III (paratype) (Fig. 5C, F). (variants II and

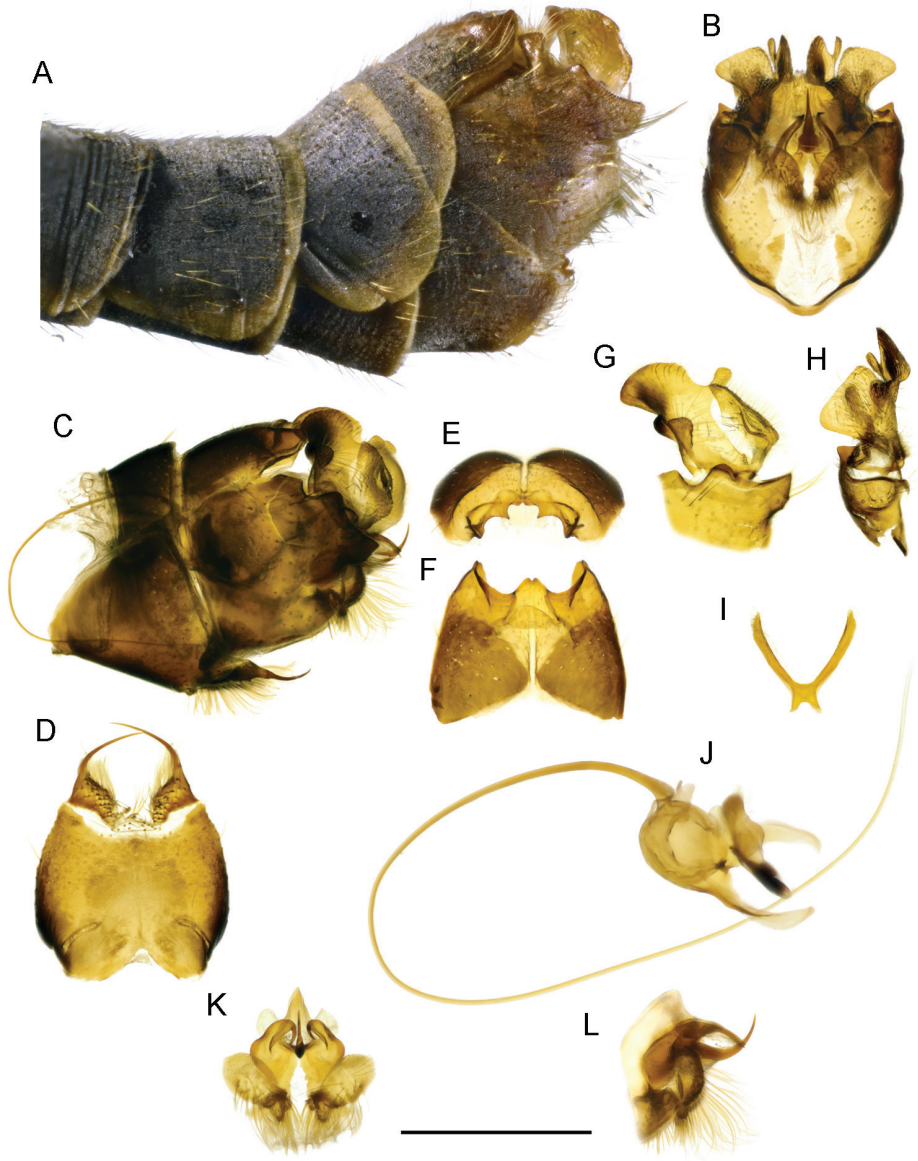


**Figure 4.** *T.* (*Lunatipula*) *eleniya* sp. nov. **A** terminal segments of male abdomen, lateral view (dry) **B–L** male terminalia (after KOH 10% treatment) **B** hypopygium (without sternite 8), caudal view **C** hypopygium, lateral view **D** sternite 8, ventral view **E** tergite 9, caudal view **F** tergite IX, dorsal view **G** inner and outer gonostylus, lateral view **H** inner and outer gonostylus, caudal view **I** gonocoxal fragment, dorsal view **J** semen pump and aedeagus, lateral view **K** adminiculum and paired apical appendages of sternite 9, caudal view **L** adminiculum and paired apical appendages of sternite 9, lateral view. Scale bar: 1 mm.

III from Kamyshanova polyna env., alt. 1200 m). There are also some differences in the shape of tergite 9 (Fig. 5G–L). Given the paucity of material, and the minor differences observed, the authors consider this to be intraspecific variability.

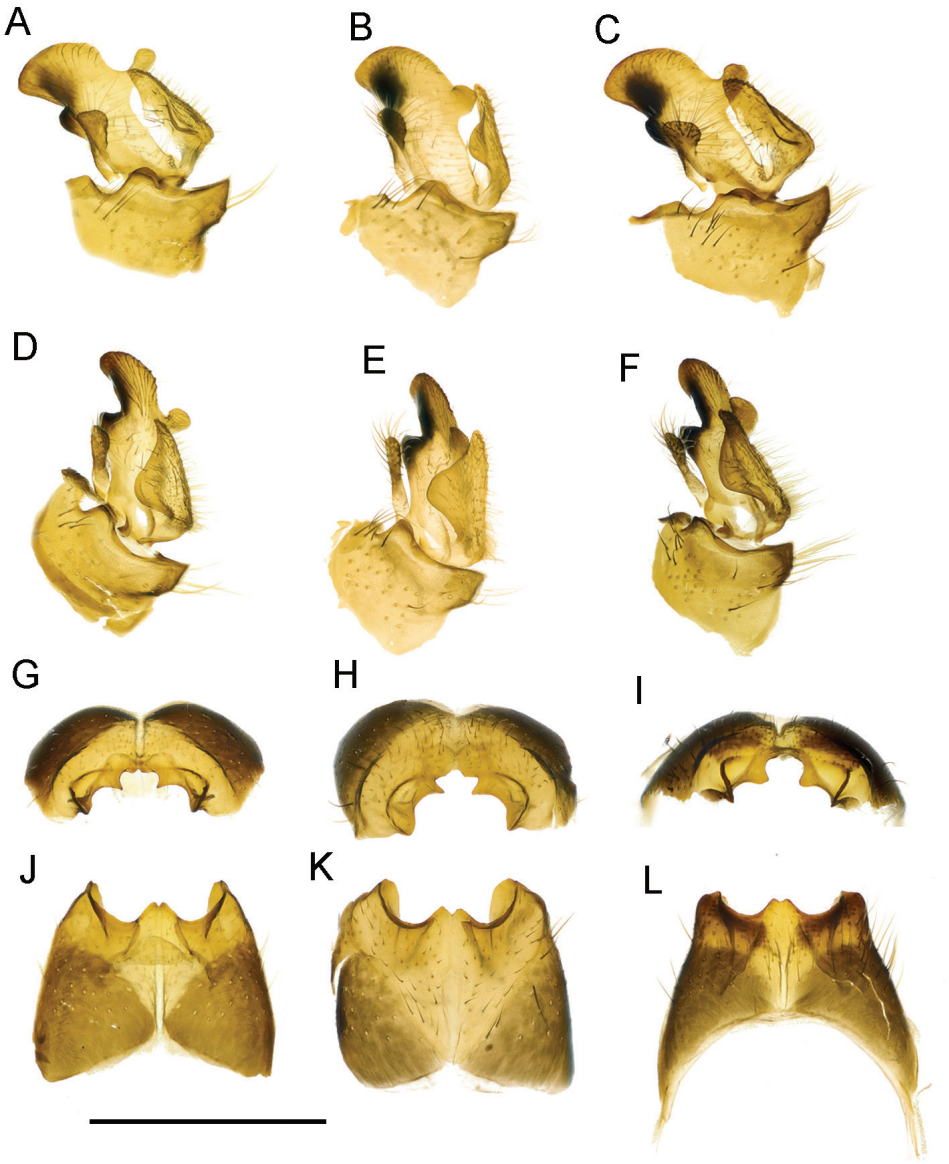


**Figure 5.** *T.* (*Lunatipula*) *eleniya* sp. nov., variation in the structure of the male terminalia **A, D, G, J** variant I (holotype) **B, E, H, K** variant II (paratype) **C, F, I, L** variant III (paratype) **A–C** inner and outer gonostylus, lateral view **D–F** inner and outer gonostylus, latero-caudal view **G–I** tergite 9, caudal view **J–L** tergite 9, dorsal view. Scale bar: 1 mm.

**Comparisons to similar species.** The new species is readily separable from all other species of the subgenus by the presence of an outgrowth medially, on the outer edge of the inner gonostylus (Figs 4G; 5A–F; 14G).

**Elevation.** Adults were collected at altitudes ranging from 1200–2000 m.

**Flight period.** Adults are active from middle of June through the end of July.

**Habitat.** Mixed moderately moist mesophytic plants, shady communities that include common hornbeam (*Carpinus betulus*), oriental beech (*Fāgus orientālis*), Nordman fir (*Abies nordmanniana*), ash vulgaris (*Fraxinus excelsior*), field maple (*Acer campestre*), colchis holly (*Ilex colchica*), etc.

**Distribution.** Endemic to the Caucasus: currently known from the West Caucasus.

**Etymology.** *Tipula* (*Lunatipula*) *eleniya* sp. nov. is named after the mother of the first author, Elena Nikolaevna Lantsova.

### *Tipula (Lunatipula) paupera* Savchenko, 1964

Figs 6, 7, 13C, 14C, I

*Tipula* (*Lunatipula*) *quadridentata paupera* Savchenko 1964: 393 (type locality: Georgia, Zagor Pass, Svanetiya); Oosterbroek, Theowald 1992: 118; Oosterbroek 2021.

**Material examined.** ***Holotype*:** Georgia •1 male; "Загор [Загар Сванетия], Груз. ССР" [Zagor Pass Svanetiya, Gruz. SSR. Georgian Soviet Socialist Republic]; alt. 2623 m; 19 Jul. 1957; R. Savenko leg.; ZISP. / "*Tipula 4-dentata paupera* ssp. n. det. Savchenko" / "Holotypus" [Holotype not initially marked; red label] / "*Tipula* (*Lunatipula*) *paupera* Sav., stat. nov. Lantsov, Pilipenko, 2020" [white label]. Thorax (prescutum, scutum, scutellum) smeared, obscuring coloration. Preservation of legs: forelegs both with only trochanters; midlegs: left with part of femur, right only with femur; hind legs: right missing. Wings slightly crumpled. ***Paratypes*.** Georgia •1 male; "ур. Лаедиль (Корулдаш [Корулдаши] – Загар)" [Laedil [territory] (Koruldash [Koruldashi] – Zagar)]; 5 Aug. 1957; Savenko leg.; ZISP. / "Paratypus" [Paratype not initially marked; red label] / "*Tipula* (*Lunatipula*) *paupera* Sav., stat. nov. Lantsov, Pilipenko, 2020" [white label] • 2 males; "Спуск с перевала Басса в Накру [в долину р. Накра], Ставропольский кр." [Descent from the Bassa Pass to Nakra [to the valley of the river Nakra], Stavropol kr. [Stavropol Territory – in error, Georgia, Svanetiya]; 5 Aug. 1956; L. Arens leg.; ZISP. / "Paratypus" [Paratype not initially marked; red label] / "*Tipula* (*Lunatipula*) *paupera* Sav., stat. nov. Lantsov, Pilipenko, 2020" [white label].

**Diagnosis.** Male. Gonocoxite with two elongate, pointed teeth, one dorsally and one ventrally. Tergite 9 with two projections posteriorly, separated by deep wide notch. Paired appendages of sternite 8 widely spaced, base shorter than wide, gap between not masked by setae. Apical appendages of sternite 9 elongate, narrow distally, with dense bundle of relatively short golden yellow setae at tip.

**Redescription.** Adult male (Fig. 6A, B). General color light grey. Body length 15.5 mm, wings 16.5 mm.

***Head*** (Figs 6B, 13C). Rostrum dorsally light grey to whitish with silvery pruinescence, dark brown procumbent setae, base of rostrum dorsally light beige, laterally dirty rusty, yellow. Nasus well defined with longer whitish procumbent setae. Palpus

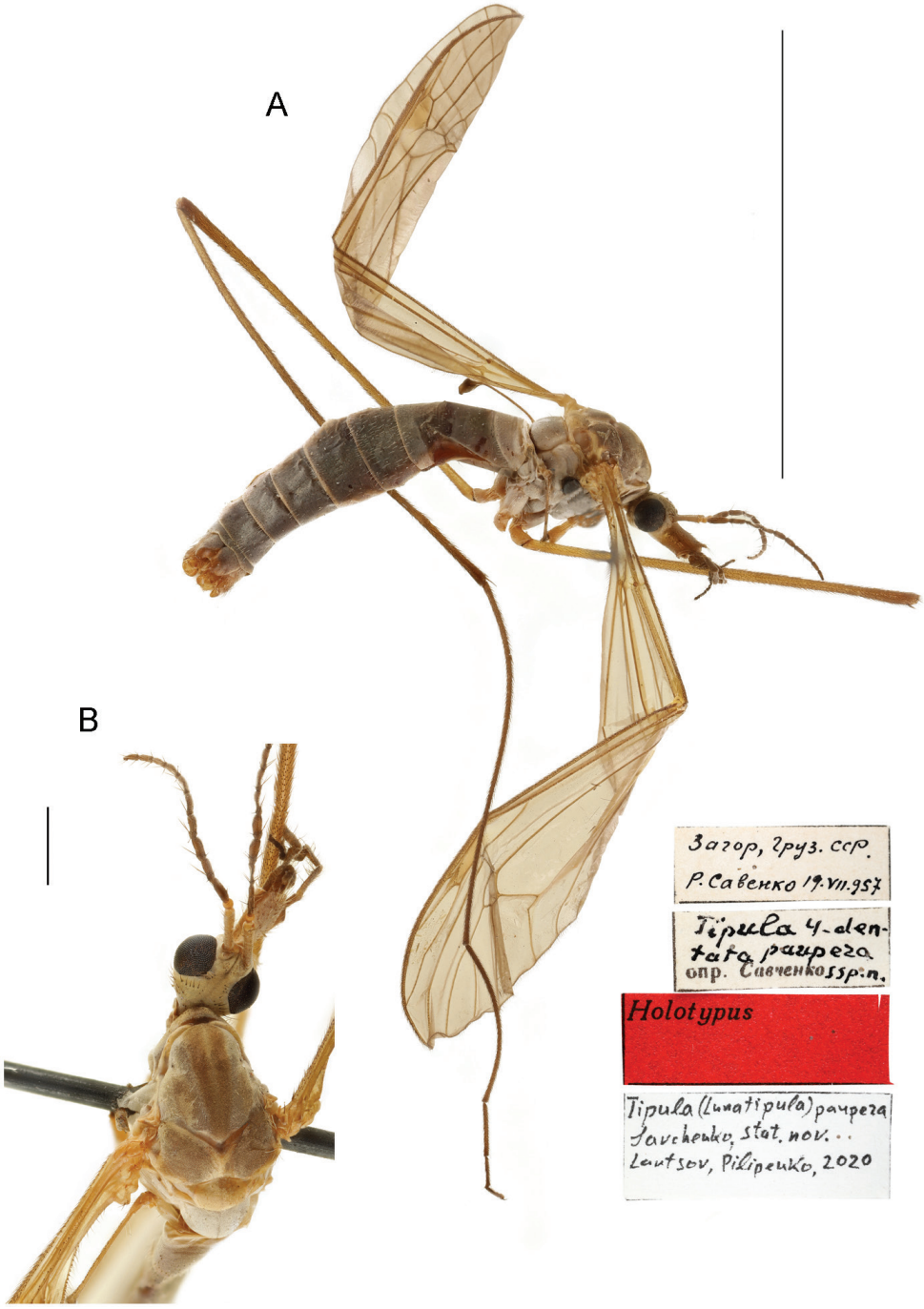


**Figure 6.** *T.* (*Lunatipula*) *paupera*, male habitus **A** general lateral view **B** head and thorax, dorsal view. Scale bars: 10 mm (**A**), 1 mm (**B**).

dark brown. Vertex (Fig. 13C) light sandy color with soft silvery pruinescence, dark grey thin median line extending to occiput; nine or ten short brown setae, behind antenna, four or five longer brown setae alongside eye. Row of long brown setae on temporal region and around occipital foramen. Gula and gena (including rostrum ventrally) yellowish-sandy to light brown, with medially enfolded region ventrally marked by moderately broad, light brown median line; gena near eyes light yellow; postgena yellow to sandy.

***Antennae*.** Scape light grey with silvery pruinescence, pedicel yellow with subtle brown ring at base. Flagellomeres brown.

***Thorax*** (Fig. 6A, B). Pronotum grey with dark broad median stripe with blurred edges. Scutum with four brown stripes, central pair more pronounced, widener anteriorly with dirty yellow between. Scutal lobes brown with silvery pruinescence. Scutellum and mediotergite with thin fuzzy grey median line; scutellum yellow to light grey; mediotergite light grey with silvery pruinescence and scattered whitish short bristles. Katepisternum, anepisternum, katepimeron, anepimeron and meron light grey with silvery pruinescence, glabrous.

***Wings*.** Transparent, without noticeable marble pattern, with light brown stigma. Longitudinal veins with macrotrichia.

***Halteres*.** Stem light brown to dirty yellow, knob brown.

***Legs*.** Coxae light grey with silvery pruinescence and long, whitish bristles; trochanters light brown; femora yellow at base, light brown with darkened tips, with adpressed dark brown bristles.

***Abdomen*** (Figs 6A, 7A). Grey with short whitish bristles. Posterior and lateral margins of tergites with thin whitish edging.

***Terminalia*** (Figs 7, 14C, I). Hypopygium not thickened. Tergite 9 and gonocoxites with silvery pruinescence. Gonocoxite (Figs 7G, 14I) with two teeth. Tergite 9 (Figs 7E, F; 14C) distally with projection on either side of deep, wide central notch. Paired appendages of sternite 8 (Fig. 7D) widely separated, basal section shorter than width, gap between not masked by setae. Appendage of sternite 9 (Fig. 7K, L) with dense bundle of relatively short golden-yellow setae at tip. Gonocoxal fragment as in Figure 7I, semen pump and aedeagus as in Figure 7J.

**Female.** Unknown.

**Status.** The species was described and treated as a subspecies of *T. quadridentata*. It is elevated here to species rank because of the presence of a number of differences of the species from *T. quadridentata* and all other species of the *caucasica* species group (see below).

**Comparison with closely related species.** This species differs from all other species of the *caucasica* group by the number and arrangement of setae dorsally on the head (Fig. 13C), the deep median notch at the apex of tergite 9 (Figs 7F, 14C), and the more widely spaced appendages of sternite 8 (Fig. 7D). It differs from *T. eleniya* sp. nov., *T. quadridentata*, and *T. caucasica* in the shape and presence of the dense bun-

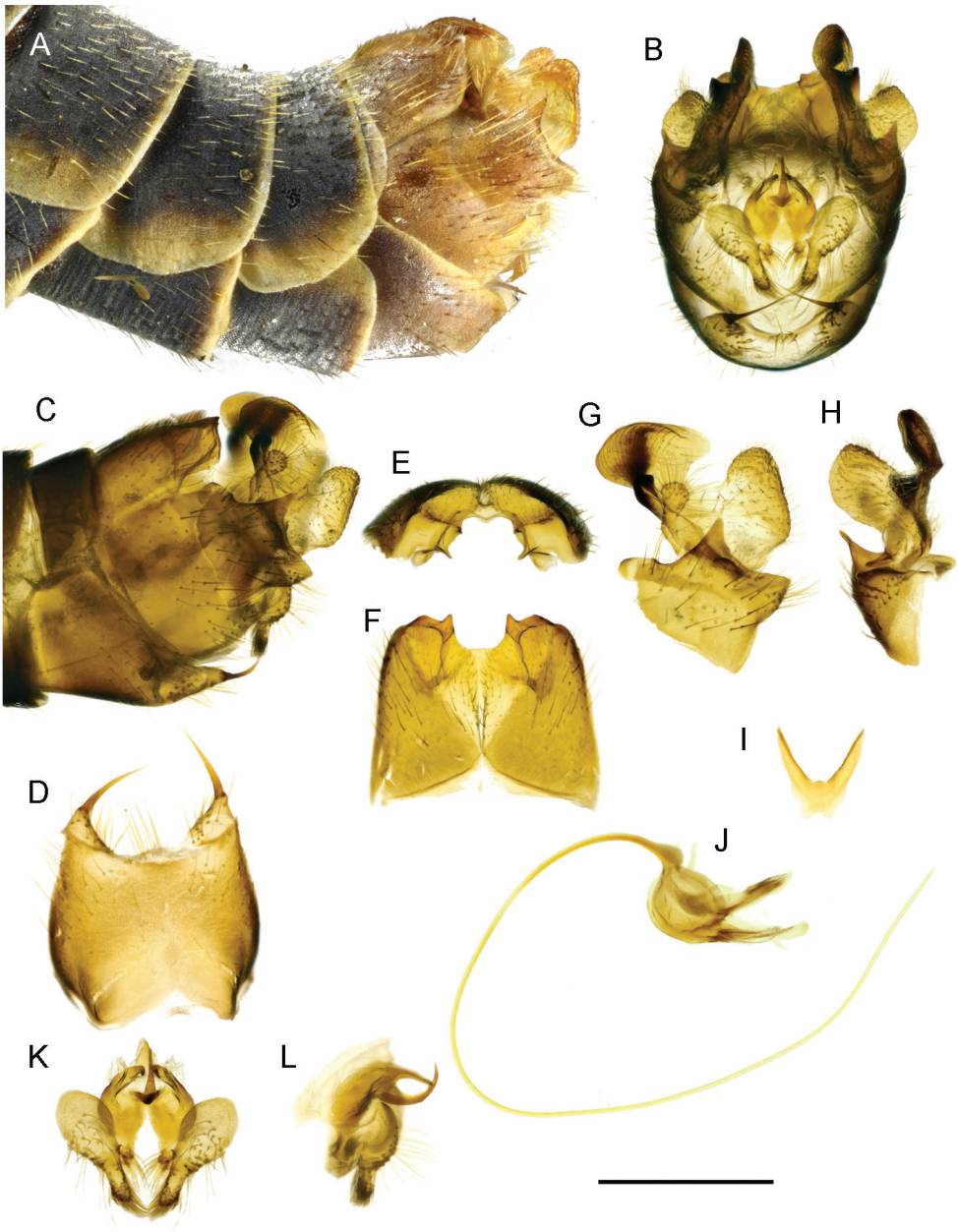


**Figure 7.** *T.* (*Lunatipula*) *paupera* **A** terminal segments of male abdomen, lateral view (dry) **B–L** male terminalia (after KOH 10% treatment) **B** hypopygium, caudal view **C** hypopygium, lateral view **D** sternite 8, ventral view **E** tergite 9, caudal view **F** tergite 9, dorsal view **G** inner and outer gonostylus, lateral view **H** inner and outer gonostylus, caudal view **I** gonocoxal fragment, dorsal view **J** semen pump and aedeagus, lateral view **K** adminiculum and paired apical appendages of sternite 9, caudal view **L** adminiculum and paired apical appendages of sternite 9, lateral view. Scale bar: 1 mm.

dle of short setae on the appendages of sternite 9 (Fig. 7K). This species is similar to *T. quadridentata* in having two teeth on the gonocoxite (Figs 7G, 14I, J).

**Elevation.** The holotype was probably collected at 2623 m (height of Zagar Pass) and one of the paratypes was collected "on the descent from the Bassa Pass", the height of which is 3057 m. It can be assumed that this species occurs in high-mountainous habitats.

**Flight period.** Adults were collected from the last third of July to early August.

**Habitat.** Data absent.

**Distribution.** Endemic to the Caucasus-currently known from the southern slopes of the Greater Caucasus (Georgia).

### *Tipula (Lunatipula) quadridentata* Savchenko, 1964

Figs 8, 9, 12D–F, 13D, 14D,J

*Tipula* (*Lunatipula*) *quadridentata quadridentata* Savchenko 1964: 392 (type locality: Russia, near Stavropol); Oosterbroek and Theowald 1992: 118; Oosterbroek 2021.

**Material examined.** ***Holotype.*** Russia • 1 male; "околицы Ставрополя, байрачн. [ый] лес" [near Stavropol, bairak forest] [small forest in steppe ravines]; 25 May 1954; [S.] Medvedev leg.; ZISP. / "южн. скл. под пологом [леса]" [southern slopes under the canopy forest] / "T. (Lunatipula) quadridenta sp. n., опр. Е.Савченко" [det. E. Savchenko]. The specimen is very badly damaged and glued together. The head is glued to the thorax; the abdomen is broken in half and glued together; two legs of uncertain position are glued to the specimen, one without coxa and trochanter, and the other missing the last four tarsal segments. **Paratypes.** Russia •1 male; "Старый лес к югу от Ставрополя" [Old forest south of Stavropol]; 25 May 1954;[S.] Medvedev leg.; ZISP. / "ниж. часть сев. склона" [lower part of northern slope] • 1 female, "Георгиевское лесничество Туапсинск. р-н" [Georgievskoe forestry Tuapse District]; 21 May 1954; K. Arnoldi leg.; ZISP •1 male, same collection data as for preceding; 22 May 1954 • 3 males, 2 females; "г. Лысая, 800–900 м, Туапсинск. р-н" [mount Lysaya, alt. 800–900 m, Tuapse District]; 26 May 1954; K. Arnoldi leg.; ZISP; / "вершинная луговина и опушка леса 800–900 m" [summit meadow and forest edge, alt. 800–900 m].

**Additional material.** Russia • 9 males, 8 females; "курорт "Горячий Ключ" хр. Котх.[ский] Краснодар.[ский] кр. дуб.[овый] лес" [Goryachiy Klyuch resort Koth[skiy] Ridge, Krasnodar.[sky] District oak. Forest]; 18 May 1956; Gilyarov leg.; ZISP / "T. (Lunatipula) quadridentata sp. n. опр. Е.Н.Савченко" • 1 female, "м. [мыс] Пенай, к югу от Новороссийска" [m. (cape) Penay, south of Novorossiysk] 24. V. [1]956; Gilyarov leg.; ZISP • 1 male, 1 female; "окр. ст. Смоленской, Сиверского р-на, Краснодар. кр." [near Smolensk station, Siversky Region, Krasnodar District] 20 May 1963; Savchenko leg.; / "опуш.[ка] смеш.[анного] предгорн.[ого] леса" [edge of mixed foothill forest]; ZISP • 1 male; "окр. ст. Кривенковской, Туапс.[инского] р-на Краснодар.[ского] края" [around village Krivenkovskaya, Tuapse Region of

Krasnodar District]; 25 May 1963; Savchenko leg.; / "опушка листв.[енного] леса у реки, вдоль горн.[ого] потока" [the edge of the foliage forest near the river, along the mountain stream]; ZISP • 1 male; Khosta, Krasnodarskiy Kray, Caucasian Reserve, Tiso-samshitovaya rosha [Yew-and-Boxwood Tree Grove]; 43°32'014"N, 39°52'621"E; alt. 135 m; 10 May 2018; V. Lantsov leg.; / Fern-butcher community on the rocky slopes of the right side of the gorge of the Khosta River**;** IEMT • 1 male; Khosta, Krasnodarskiy Kray, Caucasian Reserve, Tiso-samshitovaya rosha [Yew-and-Boxwood Tree Grove]; 43°31'656"N, 39°52'467"E; alt. 54 m; 12 May 2018, V. Lantsov leg.; / collected on light; IEMT • 2 males (in alcohol); North Caucasus, Krasnodarskiy Kray, near village Mezmay; 44°11'291"N, 39°58'090"E; alt. 808 m; 15 May 2018; V. Lantsov leg.; / Beech (*Fagus orientalis*), fruit tree (*Pyrus* sp. and *Malus* sp.) forest with *Fraxinus excelsior* in under growth, *Sambucus nigra*, *Cornus mas*, *Rosa canina*, *Crataegus* sp., in shrub layer and sedge *Carex pendula*, cereals and herbs in ground layer [a leveled area of the light part of the forest, possibly a site of a wild pear-apple orchard 50–70 years old]; IEMT • 1 male; Krasnodar Territory, Apsheron District, environs of village Mezmay, Guam Gorge, left slope, 44°12'409"N, 39°55'056"E, alt. 547 m; 24 May 2019; V. Lantsov leg.; / Landslide foot, community with butterbur [*Petasites albus*] as dominant along the banks of the stream**,** open places at the edge of the forest; ZISP • 8 males (in alcohol); Krasnodar Territory, Seversky District, in vicinity of village Thamaha, 3 May 2016; S. Kustov leg.; ZISP • 7 males, 1 female (in alcohol ); Krasnodar Territory, Seversky District, environs of village Plancheskaya, 3 May 2016. S. Kustov leg.; ZISP • 5 males (in alcohol); Krasnodar Territory, environs of village Bolshoy Utrish; 1 May 2008; E. Hachikov. leg.; ZISP • 3 males (in alcohol); Krasnodar Territory, municipality Anapa, environs of village Sukko, Kvashin's Gorge, Dolgaya Niva territory; 44°47'20"N, 37°28'33"E; alt. 67 m; 6–8 May 2016; S. Kustov, V. Gladun. leg.; ZISP • 5 males (in alcohol ); Krasnodar Territory, river Shakhe Gorge; 43°52'46"N, 39°50'00"E; 2 May 2012; V. Pilipenko leg.; VPMC • 3 males; (in alcohol); Khosta, Krasnodarskiy Kray, Caucasian Reserve, Tiso-samshitovaya rosha [Yew-and-Boxwood Tree Grove]; 43°32'014"N, 39°52'621"E; 8 May 2012; V. Pilipenko leg.; VPMC • 4 males (in alcohol); Krasnodar Territory, 13 km to the N from Sochi, Sukhoy Canyon; 43°32'N, 39°56'E; 5 May 2014; V. Pilipenko leg.; VPMC; RUSSIA – Dagestan • 5 males; Makhachkala, Tarki Distr.; 42°56'57"N, 47°29'41"E; alt. 220 m; 1 May 2019., V. Pilipenko leg.; cemetery on the hillside; VPMC • 1 male, 1 female; same locality; 10 May 2019., V. Pilipenko leg.; VPMC • 1 male, Tarki-Tau Mt.; 42°56'28"N, 47°28'08"E; alt. 450 m; 2 May 2019; V. Pilipenko leg.; oak forest; VPMC.

**Diagnosis.** Tergite 9 with four widely spaced teeth and with three rounded notches distally; caudal margin of gonocoxite with two dentate projections. Paired appendages of sternite 8 with wide base bearing thick yellow setae distally covering gap between. Cercus long and straight; hypogynial valve only slightly longer than width at base.

**Redescription.** Adult male (Fig. 8A, B). General body coloration grey. Body length 15–16 mm, wings 15.5–17 mm.

***Head*** (Figs 8B, 13D). Vertex dirty grey with longitudinal thin dark grey midline. Rostrum grey dorsally with long brown setae mixed with shorter white setae, but gla-

brous at base, laterally and ventrally dirty yellow (nearly rusty). Nasus well developed, with long, whitish procumbent setae. Frons light grey and yellow with group of 2–4 small brown setae behind each antenna . Gula grey, glabrous with narrow brown stripe. Gena light grey near eyes.

***Antennae*.** Framing around antennal sockets yellow. Scape light brown, pedicel yellow, flagellomeres brown; verticils not longer than corresponding flagellomeres.

***Thorax*** (Fig. 8A, B). Dark grey with silvery pruinescence. Pronotum dark grey; katepisternum dorsally with groups of whitish setae. Scutum with 4 brownish stripes (Fig. 8B), spaces between stripes grey with long whitish bristles. Mediotergite grey with whitish bristles.

***Wings*** (Fig. 8A)**.** Transparent, without noticeable marble pattern, with light brown pterostigma. Longitudinal veins with macrotrichia.

***Halteres*.** Stem light brown to yellowish, knob brown.

***Legs*.** Femora light brown with procumbent dark brown bristles. Tarsal claws without noticeable tooth at base.

***Abdomen*** (Figs 8A, 9A). Dark grey with short whitish bristles. Tergites with distal and lateral whitish edging.

***Terminalia*** (Figs 9, 14D, J). Hypopygium not thickened. Tergite 9 and gonocoxite with silver pruinescence. Upper margin of gonocoxite with two dentate projections. Tergite 9 (Figs 9E, F; 14D) at apex with four widely spaced teeth and with three rounded notches, narrower middle notch bounded by small flat projection bearing sharp thorn beneath; small backwards projecting spine beneath tergite 9. Outer and inner gonostyli (Figs 9G, H; 14J) without significant features. Paired appendages of sternite 8 (Fig. 9D) large, wide base with fringe of thick yellow setae hiding gap between (apparent on pinned specimens). Paired apical appendages of sternite 9 as in Figure 9K, L. Gonocoxal fragment (Fig. 9I) with characteristic small V-shaped fork at base. Semen pump and aedeagus as in Figure 9J.

**Female.** Body length 17.5–19.5 mm, wings 16–18.5 mm. Scape and pedicel brownish yellow. Terminalia (Fig. 12D–F). Cercus long and straight. Hypogynial valve (Fig. 12E) only slightly longer than wide at base. Sternite 9 and furca as in Figure 12D, F.

**Comparison with closely related species.** This species differs from other species of the *caucasica* species group (in the male) by tergite 9 with four widely spaced teeth and with three small notches at the apex and a small spine beneath (Figs 9E, F; 14D). Paired appendages of sternite 8 is broadest, with thick yellow bristles that cover the gap between; in the other species this gap is not obscured. *Tipula quadridentata* is similar to *T. paupera* by having two teeth on the edge of the gonocoxite and similar coloring of the antenna. The outer gonostylus is somewhat larger than in *T. caucasica*. The gonocoxal fragment is similar to that of *T. talyshensis* (Figs 9I, 11I). The female has a parallel-sided, straight cercus whereas it is upturned at the tip in *T. caucasica* and broader at base in *T. talyshensis*.

**Elevation.** Adults were collected at altitudes ranging from sea level (54 m in Tisosamshitovaya rosha) to 800–900 m (in Mount Lysaya, Tuapse district).

**Flight period.** Adults were collected from throughout the month of May.

**Habitat.** Specimens are found in moderately humid woody deciduous communities.

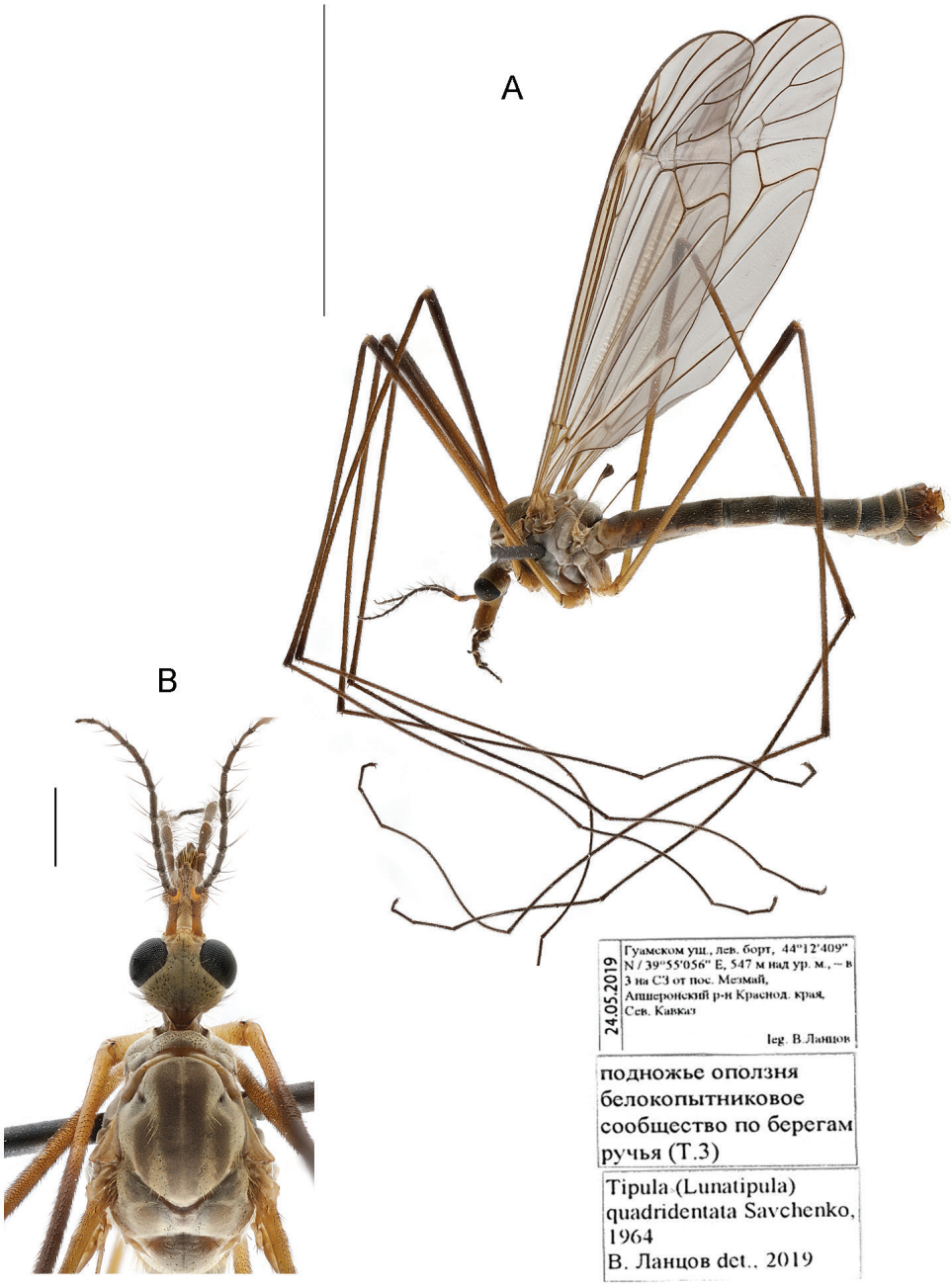


**Figure 8.** *T.* (*Lunatipula*) *quadridentata*, male habitus **A** general lateral view **B** head and thorax, dorsal view. Scale bars: 10 mm (**A**), 1 mm (**B**).

**Distribution.** Endemic to the Caucasus; currently known from the West Caucasus (northern and southern slopes; Krasnodar and Stavropol Territory) and from the East Caucasus (Dagestan; first record).

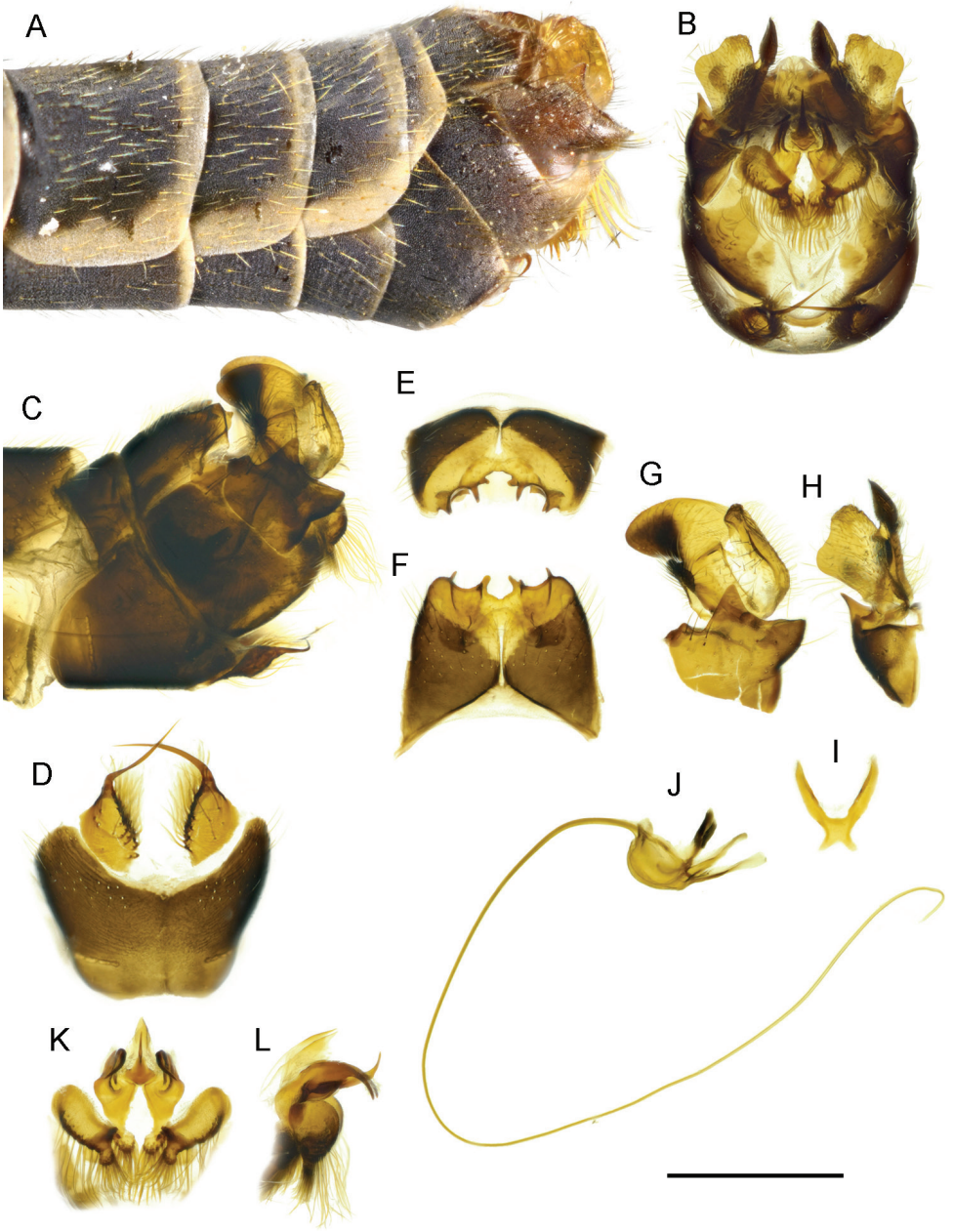


**Figure 9.** *T.* (*Lunatipula*) *quadridentata* **A** terminal segments of male abdomen, lateral view (dry) **B–L** male terminalia (after KOH 10% treatment) **B** hypopygium, caudal view **C** hypopygium, lateral view **D** sternite 8, ventral view **E** tergite 9, caudal view **F** tergite 9, dorsal view **G** inner and outer gonostylus, lateral view **H** inner and outer gonostylus, caudal view **I** gonocoxal fragment, dorsal view **J** semen pump and aedeagus, lateral view **K** adminiculum and paired apical appendages of sternite 9, caudal view **L** adminiculum and paired apical appendages of sternite 9, lateral view. Scale bar: 1 mm.

***Tipula (Lunatipula) talyshensis* Savchenko, 1964**
Figs 10, 11, 12G–I; 13E, 14E, K

*Tipula* (*Lunatipula*) *talyshensis* Savchenko 1964: 391 (type locality: Azerbaijan, Lerik region); Oosterbroek, Theowald 1992: 121; Oosterbroek 2021.

**Material examined.** ***Holotype*:** Azerbaijan •1 male, "р-н Лерик, Азербайдж. ССР 26. VI. [1]954 Джафаров" [Lerik region, Azerbaijan. SSR. [Azerbaijanskaya Soviet Socialist Republic] [alt. ~1115 m, 38°46'31"N, 48°24'55"E]; 26 Jun. 1954; Jafarov; / "*Tipula talyshensis* det. Savchenko sp. n." [white label] / [Original red label without text] / "Holotypus" [red label]; ZISP. Holotype in good condition (Fig. 10A, B), however, some legs missing: fore legs – left missing, right up to femur; mid legs – left present, right missing; hind legs – left and right up to femur. ***Paratypes*.** Azerbaijan •2 males, 2 females; same data as for holotype [printed on white paper] / "Paratypus" [Paratype not initially marked; red label]; ZISP.

**Diagnosis.** Male. Tergite 9 at apex with a denticle on either side of wide, shallow, flat median notch. Paired apical appendages of sternite 9 narrower distally, bearing tassel of long golden setae. Female. Hypogynial valve several times longer than width at base.

**Redescription.** Adult male (Fig. 10A, B). General body coloration grey. Body length 15–20 mm, wings 18–19.5 mm.

***Head*** (Fig. 13E). Vertex light grey with indistinct median grey line, glabrous in middle and around eye with rows of setae between. Rostrum dorsally dark grey, whitish at base, ventrally light brown with grey median stripe. Nasus with long, whitish procumbent setae. Tempora and genae light grey to whitish (color depending on angle of inclination) with faint silvery pruinescence.

***Antennae*.** Scape dark grey with rusty bristles, pedicel yellowish with indistinct brown line in middle, flagellum brown.

***Thorax*** (Fig. 10A, B). Pronotum grey with whitish setae. Scutum (Fig. 10B) with four brownish stripes on grey, short whitish setae between central and side stripes. Scutal lobe grey with faint silvery pruinescence, anterolaterally with group of whitish setae. Pleura and coxae grey with silvery pruinescence; katepisternum dorsally with sparse whitish setae, anepisternum and meron glabrous. Scutellum and mediotergite grey with whitish setae, scutellum with dark grey median line visible as specimen is rotated.

***Wings*** (Fig. 10A). Translucent, grey, with light brown pterostigma. Longitudinal veins *C*, *Sc*, and *R* and bases of $A_1$ and $A_2$ with macrotrichia.

***Halteres*.** Stem yellowish with light setae, knob brown.

***Legs*.** Coxae grey with silvery pruinescence and long, whitish setae. Femora light brown with procumbent dark brown setae. Claws of fifth tarsal segment without spine at base.

***Abdomen*** (Figs 10A, 11A). Dark grey with short whitish setae. Posterior margins of tergites without noticeable light edging, lateral margins with wide whitish to yellowish edging.

***Terminalia*** (Figs 11, 14E, K). Hypopygium (Fig. 11A, B, C) not thickened. Tergite 9 (Figs 11E, F; 14E) trapezoidal, apex with rather wide, shallow median notch

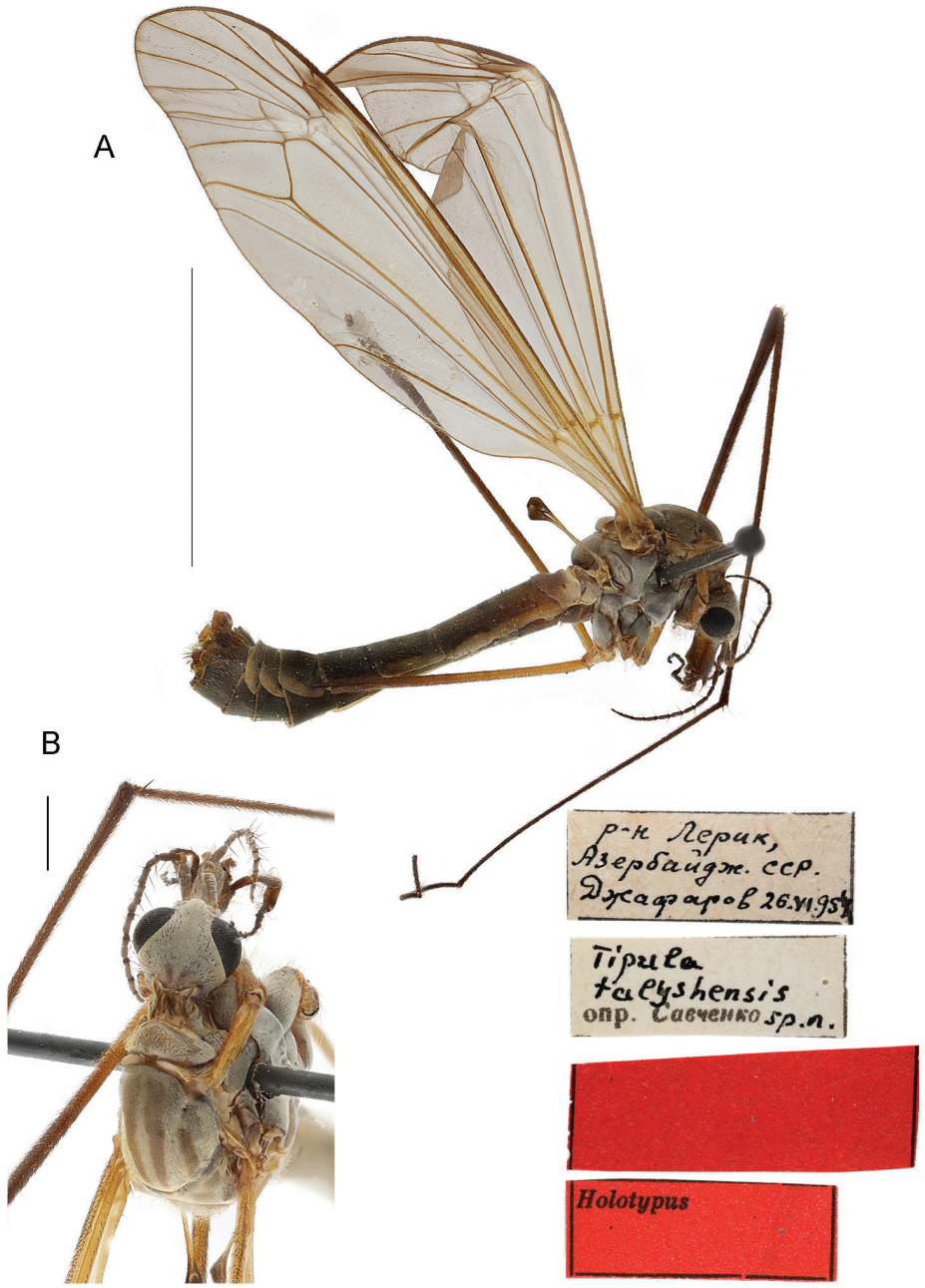


**Figure 10.** *T.* (*Lunatipula*) *talyshensis*, male habitus **A** general lateral view **B** head and thorax, dorsal view. Scale bars: 10 mm (**A**), 1 mm (**B**).

bounded by a denticles. Gonocoxites (Figs 11G, 14K) with large ventral tooth, dorsal tooth truncated at apex. Outer gonostylus without significant features (Fig. 11G). Inner gonostylus as in Figures 11G, H; 14K. Paired appendages of sternite 8 (Fig. 11D)

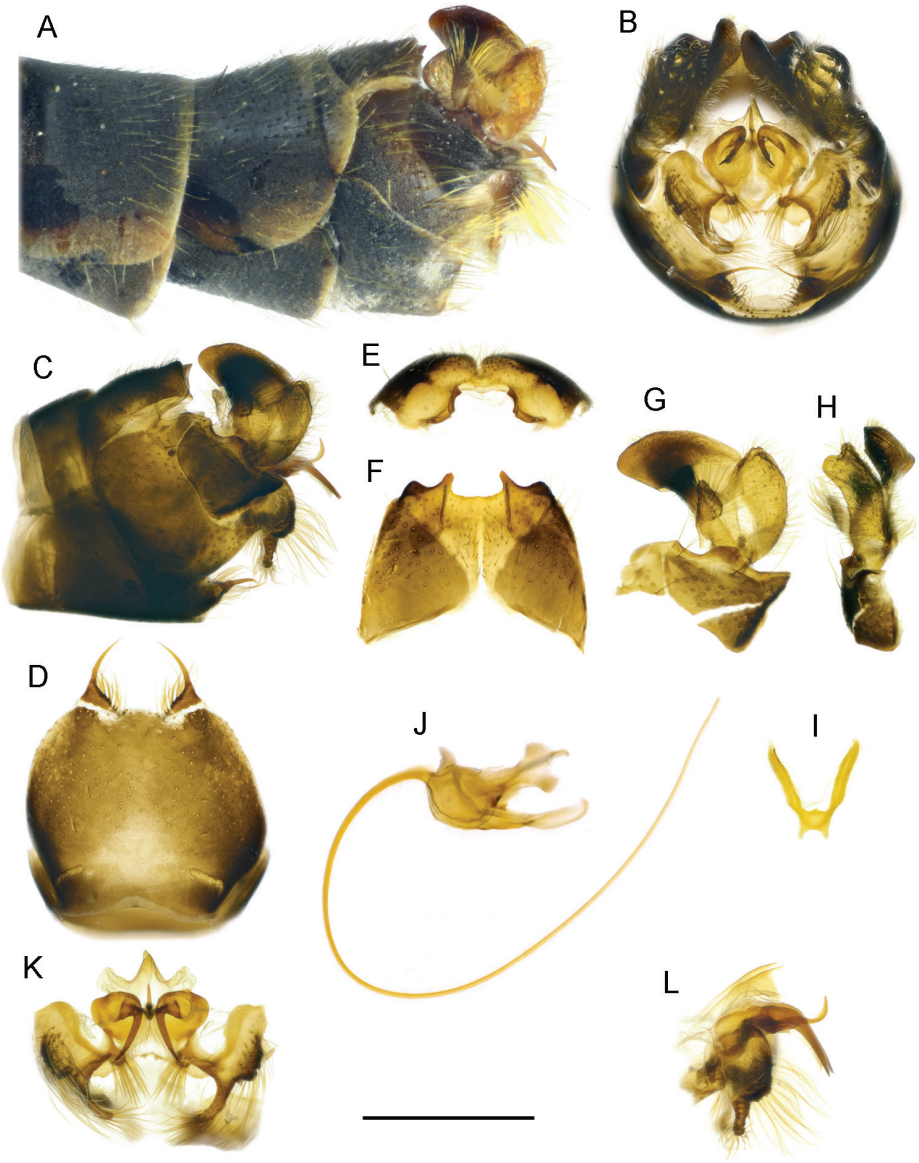


**Figure 11.** *T.* (*Lunatipula*) *talyshensis* **A** terminal segments of male abdomen, lateral view (dry) **B–L** male terminalia (after KOH 10% treatment) **B** hypopygium, caudal view **C** hypopygium, lateral view **D** sternite 8, ventral view **E** tergite 9, caudal view **F** tergite 9, dorsal view **G** inner and outer gonostylus, lateral view **H** inner and outer gonostylus, caudal view **I** gonocoxal fragment, dorsal view **J** semen pump and aedeagus, lateral view **K** adminiculum and paired apical appendages of sternite 9, caudal view **L** adminiculum and paired apical appendages of sternite 9, lateral view. Scale bar: 1 mm.

relatively small, with fringe of hairs along inner edge. Apical appendages of sternite 9 (Fig. 11K, L) narrowed distally, bearing tassel of long golden setae. Gonocoxal fragment, semen pump and aedeagus as in Figure 11I, J, respectively.

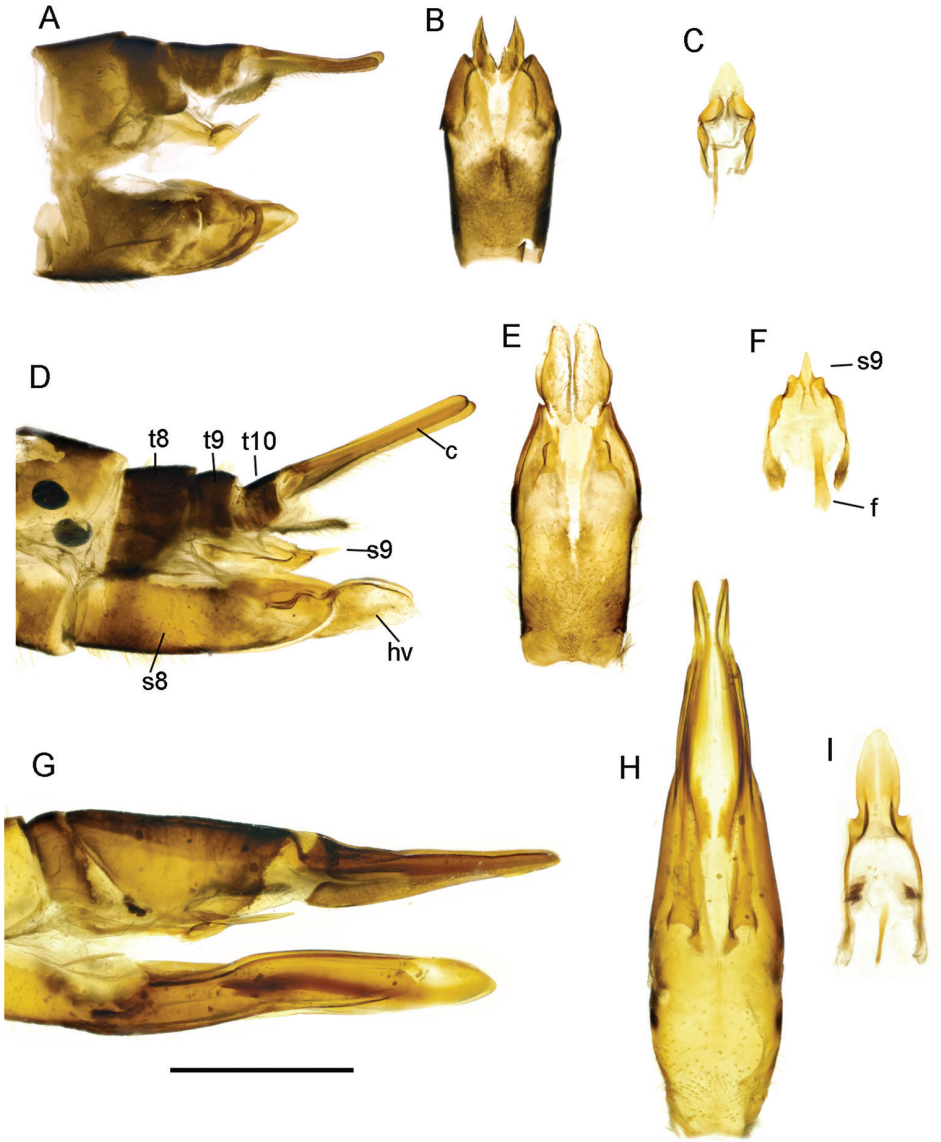


**Figure 12.** Female terminalia of *caucasica* species group **A–C** *T.* (*Lunatipula*) *caucasica* **D–F** *T.* (*Lunatipula*) *quadridentata* **G–I** *T.* (*Lunatipula*) *talyshensis* **A, D, G** ovipositor, lateral view **B, E, H** ovipositor ventral view **C, F, I** sternite 9 and furca, lateral view. Abbreviations: c–cerci; f–furca; hv–hypogynial valve; s–sternite; t–tergite. Scale bar: 1 mm.

**Female.** Adult female body length 18–25 mm, wings 18–18.5 mm. Similar to male. Cercal hypogynial valve (Fig. 12G, H) several times longer than wide at base. Sternite 9 and furca as in Figure 12I.

**Comparison with closely related species.** This species differs from other species of the *caucasica* group by the broad shallow notch at the apex of tergite 9, the tassel of golden setae at the tip of the apical appendage of sternite 9, and by the small size of the

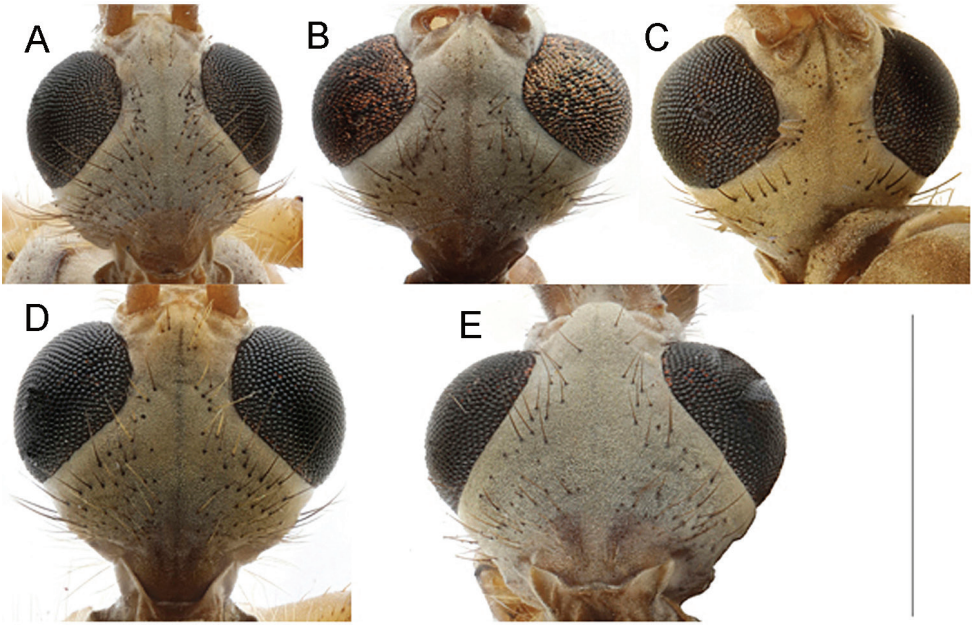


**Figure 13.** Heads of *caucasica* species group, dorsal view **A** *T.* (*Lunatipula*) *caucasica* **B** *T.* (*Lunatipula*) *eleniya* sp. nov. **C** *T.* (*Lunatipula*) *paupera* **D** *T.* (*Lunatipula*) *quadridentata* **E** *T.* (*Lunatipula*) *talyshensis.* Scale bar: 1 mm.

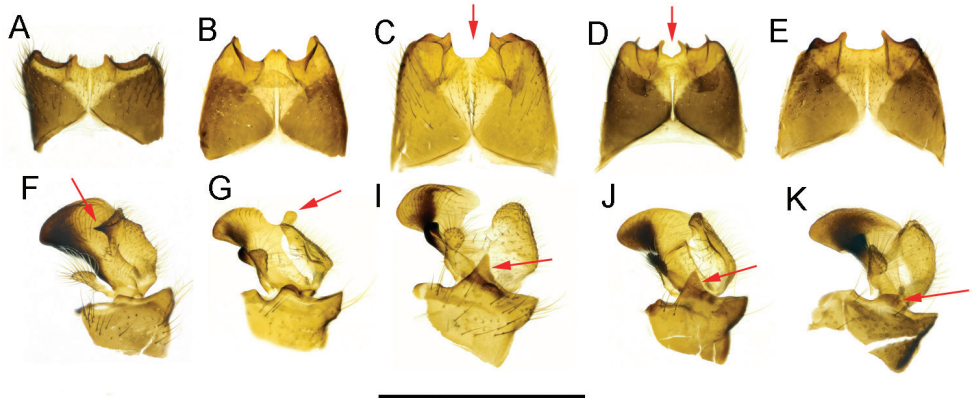


**Figure 14.** Comparisons of some components of male terminalia of the *caucasica* species group **A, F** *T.* (*Lunatipula*) *caucasica* **B, G** *T.* (*Lunatipula*) *eleniya* sp. nov. **C, I** *T.* (*Lunatipula*) *paupera* **D, J** *T.* (*Lunatipula*) *quadridentata* **E, K** *T.* (*Lunatipula*) *talyshensis* **A–E** tergite 9, dorsal view **F–K** inner and outer gonostylus, lateral view. Arrows point to central notch at apex of tergite 9 (**C, D**), to the wedge-shaped projection posteriorly on inner gonostylus (**F**), to the rod-like outgrowth behind anterior beak of inner gonostylus (**G**), to the anterior (dorsal) margin of gonocoxite (**I, J, K**). Scale bar: 1 mm.

paired appendages of sternite 8. The unusually long hypogynial valve of the female distinguishes this species from that of *T. caucasica* and *T. quadridentata*, the other known females of the *caucasica* group.

**Elevation.** Adults were collected at altitudes ~ 1115 m.

**Flight period.** Adults were collected on 26 June.

**Habitat.** No data.

**Distribution.** Endemic to the Caucasus – currently only known from Talysh (Azerbaijan).

## Key to males and females of the *caucasica* species group

**Males**

1 Inner gonostylus with rod-like outgrowth behind anterior beak (Fig. 14G).... ..... ***T. eleniya* sp. nov.**

– Without such an outgrowth behind anterior beak on the inner gonostylus (Fig. 14F, I–K) ..... **2**

2 Wedge-shaped projection posteriorly on inner gonostylus (Fig. 14F) ..... ..... ***T. caucasica* Riedel, 1920**

– Without such a wedge-shaped projection posteriorly on inner gonostylus....**3**

3 Anterior (dorsal) margin of gonocoxite with sharp dentate projection in addition to smaller more ventral tooth (Fig. 14 I, J). Adminiculum and paired apical appendage of sternite 9 as in Figure 7K or 9K..... **4**

– Anterior (dorsal) margin of gonocoxite with only traces of a projection at most (Fig. 14K). Apical appendage of sternite 9 narrowed distally, bearing tassel of long golden setae (Fig. 11K, L) ..... ***T. talyshensis* Savchenko, 1964**

4 Tergite 9 at apex with four projections, central notch between middle projections small and shallow (dorsal view) (Fig. 14D). Paired appendage of sternite 8 with thick yellow setae on base covering space between. Setal arrangement on vertex as in Figure 13 D. Adminiculum and paired apical appendages of sternite 9 as in Figure 9K..... ***T. quadridentata* Savchenko, 1964**

– Tergite 9 at apex with only two projections, central notch between quite wide and deep (dorsal view) (Fig. 14C). Gap between paired appendage of sternite 8 usually exposed, not masked by setae. Arrangement of setae on vertex as in Figure 13C. Adminiculum and paired apical appendage of sternite 9 as in Figure 7K..... ***T. paupera* Savchenko, 1964**

**Females (known for three species of the *caucasica* group only)**

1 Hypogynial valve long, more than three times longer than width at base (Fig. 12G, H) ..... ***T. talyshensis* Savchenko, 1964**

– Hypogynial valve short, length approximately equal to width at base (Fig. 12A, B, D, E) ..... **2**

2 Cercus upcurved distally (Fig. 12A) ..... ***T. caucasica* Riedel, 1920**

– Cercus straight (Fig. 12D) ..... ***T. quadridentata* Savchenko, 1964**

## Discussion

All species belonging to the *caucasica* species group are morphologically quite distinct including *T. quadridentata* and *T. paupera*, previously considered as subspecies. Their status as separate species is beyond doubt: each is distinguishable by the structure of tergite 9 as well as additional distinctive features mentioned in the descriptions and comparisons above, as well as in the keys. For *T. caucasica*, this is a characteristic wedge-shaped projection posteriorly on the inner gonostylus (Fig. 14F); for *T. eleniya*, it is a unique rod-shaped outgrowth of the inner gonostylus (Fig. 14G); *T. talyshensis* differs by the unique structure of the paired appendage of sternite 9 (Fig. 11K). The inner gonostyli of *T. quadridentata*, *T. paupera*, and *T. talyshensis* are similar in lateral view (Fig. 14I, J, K), but these species differ in size, shape, and coverage of the paired appendages of sternite 8 (Figs 7D, 9D, 11D). *T. eleniya*, *T. quadridentata*, and *T. talyshensis* are similar in the structure of the gonocoxal fragment, semen pump, and aedeagus (Figs 4I, J; 9I, J; 11I, J). The color and arrangement of the setae on the vertex of the head in *T. paupera* distinguishes it from all other species of the group (Fig. 13C). The variability seen in the outgrowth of the inner gonostylus of *T. eleniya* (Fig. 5) probably indicates the plasticity of this species and confirms the need for additional studies.

Females of only three of the five species of the *caucasica* species group are known, and they differ sufficiently in the structures of the cerci, hypogynial valves, and sternite 9 (Fig. 12), as reflected in the identification key. Of interest would be the immature stages of the species of the *caucasica* species group, about which nothing is yet known.

Zoogeographically, the *caucasica* species group belongs to the Caucasian subgroup, a part of the eastern Mediterranean group, which is, in turn, a part of the Mediterranean species complex (Savchenko 1983). These species are narrow-range endemics to the Caucasus. Ecologically, they are confined to mesophytic habitats within the forest belt, occurring in a fairly wide range of altitudes and can be classified as species characteristic of deciduous forest and mixed communities.

### Parallel morphology in the subgenus *Lunatipula* in the structure of internal gonostylus in Palaearctic species

The inner gonostylus of *T.* (*L.*) *eleniya* was compared with those of the 502 known species including the 360 Palaearctic species of the subgenus *Lunatipula.* No direct matches were found, but outgrowths of various shapes on the middle of the inner gonostylus were found in some Palaearctic species: two species from Turkey (*Tipula* (*Lunatipula*) *auriculata* Mannheims, 1963 and *Tipula* (*Lunatipula*) *horsti* Theischinger, 1982), one from China (*Tipula* (*Lunatipula*) *oreada* Alexander, 1933), and two from Kyrgystan (*Tipula* (*Lunatipula*) *milkoi* Pilipenko, 2005 and *Tipula* (*Lunatipula*) *zarnigor* Savchenko, 1954). The latter species has also been recorded in Tajikistan and northeastern Afghanistan (Oosterbroek 2021). The species belong to the same sub-

genus, but are classified in different species groups and are geographically dispersed in this regard, it can be assumed that these various outgrowths to be independently derived and therefor examples of parallel evolution.

## Acknowledgements

The authors express their sincere gratitude to the staff of The Laboratory of Insect Taxonomy (Diptera Department) of the Zoological Institute of Russian Academy of Sciences (St. Petersburg, Russia) – Nikolai Parmonov, Galina Suleimanova, Emilia Narchuk, and Olga Ovchinnikova for the opportunity to work with material from the collection of the institute. The authors would like to express their sincere gratitude to Vladimir Neymorovets (All-Russian Research Institute of Plant Protection, St. Peterburg, Russia) for making the general color photographs of the crane flies. The authors sincerely thank Fenja Brodo (Ottawa, Canada) for valuable advice and assistance in the revision of the English text. We are very grateful for Konstantin Tomkovich (Moscow) for the gift of material collected in the Caucasus Reserve. The authors are sincerely thankful to Nelli Tsepkova (Tembotov Institute of Ecology of Mountain Territories of Russian Academy of Sciences, Nalchik) for providing the geobotanical data in the field and to Nadya Matveyeva (Komarov Botanical Institute of the Russian Academy of Sciences, St. Petersburg) for her professional comments concerning English names of plant communities. This study has been partly supported by the Russian Science Foundation (project no. 18-04-00961). The research was carried out as part of the Scientific Project of the State Order of the Government of Russian Federation to Lomonosov Moscow State University No. 12103230063-3.

## References

Crampton GC (1943) The external morphology of the Diptera. Bulletin Connecticut State Geological and Natural History Survey 64: 10–165. [reprinted 1966.].

Cumming JM, Wood DM (2017) Adult morphology and terminology. In: Kirk-Spriggs AH, Sinclair BJ (Eds) Manual of Afrotropical Diptera (Vol. 1). South African National Biodiversity Institute, Pretoria, 107–151.

Lantsov VI (1998) New for the Caucasus and North Caucasus species of crane-flies (Diptera, Tipulidae). Fauna of the Stavropol region 8: 41–44. [in Russian]

Lantsov VI (2002) Fauna structure and chorology of crane-flies (Diptera, Tipulidae) of Teberdinsky State Nature Biosphere Reserve. Biological diversity of the Caucasus (Transactions of II regional conference) Suchum, 18–23 September 2001: 108–121. [in Russian]

Lantsov VI (2007) Crane-flies (Diptera, Tipulidae) of high altitude landscapes of the Caucasus. In: Mountain ecosystems and their components. Materials of I international conference, 13–18 August 2007, Nalchik 2: 94–99. [in Russian]

Lantsov VI (2018) Habitats of the Northern Caucasus crane fly *Tipula* (*Lunatipula*) *sublunata* (Diptera: Tipulidae). In: Materials of XVIII All-Russia Conference on Soil Zoology. Moscow, 118–119. [in Russian]

Lantsov VI (2020) Biological diversity of crane flies (Diptera, Tipuloidea) in the natural landscapes of Dagestan (North-East Caucasus, Russia) // XI All-Russian Dipterological Symposium (with international participation). Voronezh. August 24–29, 2020. Proceedings of conference / Responsible editors: O.G.Ovchinnikova, I.V.Shamshev. St.Petersburg: Russian Entomological Society, LEMA, 292–296. https://doi.org/10.47640/978-5-00105-586-0_2020_292

Oosterbroek P (2021) Catalogue of the Craneflies of the World. http://ccw.naturalis.nl/detail.php [latest update 7 May 2021]

Riedel MP (1920) Nematocera Polyneura (Dipt.) aus dem Kaukasus. Zoologische Jahrbucher, Abteilung fur Systematik, Geographie und Biologie der Tiere 43: 13–22.

Savchenko EN (1954) New species of crane-flies (Diptera, Tipulidae) of the fauna of the USSR. Trudy Zoomuzeya, Kievskiy Gosudarctvennyy Universitet 4: 109–132. [in Russian]

Savchenko EN (1957) Two new species of crane-flies (Diptera, Tipulidae) from the North Caucasus. Zoologicheskiy Zhurnal 36: 1493–1499 [in Russian with English summary]

Savchenko EN (1964) Crane-flies (Diptera, Tipulidae), Subfam. Tipulinae, Genus *Tipula* L., 2. Fauna USSR, N.S. 89, Nasekomye Dvukrylye [Diptera] 2(4): 1–503. [in Russian]

Savchenko EN (1968) New or little known species of crane-flies (Diptera, Tipulidae) from the Transcaucasus. Entomologicheskoe Obozrenie 47: 912–936 [in Russian with English summary] (English translation: Entomological Review 47: 557–571.

Savchenko EN (1983) Crane-flies (Family Tipulidae), Introduction, Subfamily Dolichopezinae, Subfamily Tipulinae (start). Fauna USSR, N.S. 127, Nasekomye Dvukrylye [Diptera], 2(1–2): 1–585. [In Russian]

Savchenko EN, Kandybina MN (1987) Tipulidae. In: Kandybina MN, Lantsov VI, Savchenko EN (Eds) A Catalog of the Type-Specimens in the Collection of the Zoological Institute, Academy of Sciences of the USSR. Insecta, Diptera, N 3, Families Tanyderidae, Trichoceridae, Limoniidae, Tipulidae. Zoological Institute of Academy of science of the USSR, Nauka, Leningrad, 21–61 [in Russian]